UNIVERSITÀ DEGLI STUDI DI PAVIA

DOTTORATO IN SCIENZE CHIMICHE E FARMACEUTICHE

XXXI CICLO

Coordinatore: Chiar.mo Prof. Mauro Freccero

NOVEL PHOTOCATALYTIC APPROACHES FOR ECOSUSTAINABLE SYNTHESIS

Tutore

Chiar.mo Prof. Maurizio Fagnoni

Tesi di Dottorato di

LUCA CAPALDO

A.A. 2017- 2018

ACKNOWLEDGMENTS

Come mi è capitato di dire più volte in questi tre anni, il dottorato non è un "corso": è un'avventura. Un'avventura che nessuno potrebbe sognarsi di finire senza un tutor che lo guidi passo dopo passo, dei colleghi che lo stimolino a dare sempre il 110% e una famiglia che lo sproni nei momenti più bui.

Per questo voglio ringraziare dapprima i miei mentori, il *Prof. Maurizio Fagnoni* e il *Prof. Tehshik P. Yoon*. Al primo, che mi ha indirizzato quotidianamente nelle ardue scelte professionali, sarò sempre riconoscente per i miei successi lavorativi. Mi ha sempre consigliato e mostrato pazientemente perché una strada fosse migliore di un'altra, come scegliere un esperimento anziché un altro per verificare un'ipotesi. Il che, dopotutto, è uno dei due insegnamenti più preziosi per un dottorando. As for the latter, I spent only 5 months in his laboratory in Wisconsin, but I had the opportunity to work with incredible scientists! His point of view in Subgroup meetings on Fridays and Group Meeting on Thursdays helped me to understand how much developing a critical thinking, building original ideas and becoming an independent scientist are important in our work; which is the other most important lesson for a Ph.D. student.

Un ringraziamento enorme a *Davide* (per gli amici, *Davidì*), il mio personalissimo lab supervisor, a cui devo un'altra buona fetta della mia crescita come chimico: lo ringrazio non solo per la pazienza, ma anche per le mille opportunità collaborative che mi ha offerto e di cui mi ha reso partecipe.

Anche a *Stefano* (*Steu*), il mio supervisor di tesi magistrale, va un ringraziamento particolare, per avermi dato la possibilità di affinare le mie capacità divulgative e didattiche. Per citarne alcune: Universitiamo, ben 3 PLS e Everyday Light.

Ora, per ringraziare tutte le altre persone che hanno segnato profondamente la mia vita da dottorando, sia in Italia che in America, ci vorrebbe un'altra tesi come Acknowledgment; pertanto mi limiterò a citare quelli preziosi più preziosi. Grazie a:

- *Jian*, my hood mate: thank you for all the discussions we had about life and science and, in particular, for your chemical tips!
- *Steven* and *Niecia*, my coffee mates: thank you for all the talks about Trump and his work that cheered me up during the period of Italian elections... Thank you also for your support in making me hold my nerves in hard times in science.
- *Yukki*, my "hiiiiiiii" mate: thank you for your genuinity, thank you very much for this. Don't you dare lose this peculiarity in your life: that is what makes you stronger than a lot of people (and scientists) in this world! Thank you also for your wonderful drawing!
- All *the Yoon Group*: thank you guys for your tips, your science and your personalities. I really hope that your thirst of science will never fade, for the sake of chemistry!
- *Carlottina*, la mia compagna di "Gestapo": grazie infinite per avermi aiutato a rendere piacevoli anche i momenti più bui in viale Taramelli 10… Un grazie enorme anche per avermi sempre spalleggiato in mille cause e, cosa più importante, aiutato a mantenere l'ordine in laboratorio!
- *Ste* ed *Edo*, i miei colleghi: non so se ringraziarvi di più per le lezioni scientifiche che mi avete dato (che pure sono molte) oppure per le "pirlate" che abbiamo detto/fatto. Dato che ho ringraziato tutti per la scienza fino a qui, vi ringrazio solo ed esclusivamente per le seconde!

Infine, arriviamo alla famiglia, or better families. Indeed, during my stay in the US, I was hosted by Mary, my dear Mary. I actually have no words to describe how nice and kind she was to me, how can I even think to have enough breath to thank such a genuine person?! As I said more than once, she's become my second mum in less than 6 months! We spent nights watching movies, the Bachelor, movies, the Bachelorette and I even learned how to use a lawnmower! We had such a wonderful time in Madison… I really hope to see you soon!

E la mia famiglia: in primis, Giulia. Come potrebbe mancare lei, compagna di mille avventure vissute in 10 anni… Non me ne vogliano le altre persone genuine qui dentro, ma lei di gran lunga le batte tutte. E con genuinità, mi ha sempre aiutato a rimettermi in campo con grinta dopo gli insuccessi e le delusioni che la ricerca sa dare. Perché se c'è una cosa che si impara bene in 3 anni di dottorato è la seguente: il vero ricercatore non è quello che scopre, è quello che non si arrende.

Ma vogliamo parlare di mamma, papà e Andrea? Come sarei potuto arrivare qui senza di loro, proprio non riesco a immaginarmelo. Mi hanno aiutato e motivato per ventisette anni e mi hanno sempre stimolato a farcela da solo, in tutto: a casa, nella vita, ed è forse per questo che oggi do un'enorme importanza all'indipendenza, soprattutto quella di pensiero.

“May it be a light to you in dark places,

when all other lights go out.”

J. R. R. Tolkien

CHAPTER 1

PHOTOCATALYSIS: A VALUABLE TOOL FOR ORGANIC SYNTHESIS

Over the past decades, photochemical synthesis, *i.e.* organic synthesis that uses light as source of energy to break and forge bonds, has vehemently re-emerged as an important theme of research in organic chemistry. There are at least three main features that contribute to maintain this trend: (i) reactivity, (ii) selectivity and (iii) practicality.

i. Reactivity: the open-shell reactive intermediates that are characteristic of photochemical activation (including electronically excited organic molecules, carbon- and heteroatom-centered radicals and radical ions) participate in bond-forming reactions that are often difficult to access using closed-shell intermediates or ground-state pathways.

ii. Selectivity: over the past decades, perhaps the major criticism addressed to photochemistry was the total unpredictability in terms of product distribution and selectivity. However, the recent and deep understanding of photochemical mechanisms as well as the development of stable and controllable light sources have led to beautifully predictable results. As a matter of fact, a unique advantage of photochemical activation arises from the fact that different chemical moieties possess characteristic absorption spectra. Thus, irradiation with controlled wavelengths enables the energy of a photon, typically 40-100 kcal/mol, to target a specific component within a complex reaction mixture. This can provide for excellent functional group tolerance, unique selectivity and opportunities for the invention of novel activation modes.

iii. Practicality: notably, photons do not possess any mass and are made of pure energy, thus no workup is needed in order to remove them from the reaction mixture. Additionally, light is light, which means that no expensive lasers or sci-fi energy sources are needed to trigger photochemical reactions. Actually, there is plenty of examples in the literature that rely on direct sunlight, LEDs and even cheap 19 W

IKEA Compact Fluorescent Lamps! Finally, photochemistry is the perfect bridge to other disciplines, such as engineering: in fact, several approaches are being adopted in order to make photochemistry even more convenient in terms of practicality, for example paving the way to flow photochemistry.

These features make photochemistry of significant contemporary interest for both academic researchers and industrial practitioners.

However, in the case of small organic molecules, electronically excited states are often accessible only upon irradiation with quite short wavelengths of ultraviolet (UV) light. These high-energy photons might cause uncontrolled processes to occur, *e.g.* photodecomposition or polymerization, resulting in a dramatically reduced applicability of this branch of chemistry. This has called for the need of an alternative approach to harness the energy of light in chemical reactions, namely photocatalysis.

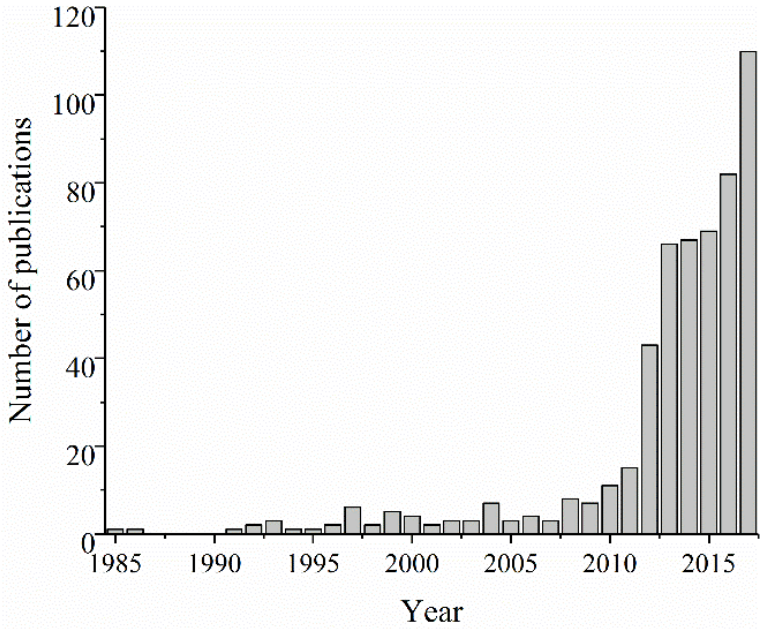

Figure 1.1 Plot of the number of publications concerning "Photocatalysis" refined by "Organic Chemistry". Data obtained from the database "Web of Science".

In these reactions, the substrate does not absorb light directly, instead low-energy light is absorbed by a purposely added molecule (photocatalyst, PC) that converts this energy into chemical energy for substrate activation. The effect of this upgrade is straightforward, not

only as far as stability of the reactants is concerned, but also in terms of predictability, efficiency and environmental sustainability. To quantify the impact that photocatalysis is having on modern organic synthesis, it is sufficient to plot the number of publications per year: the trend clearly shows a surge starting around 2008 (see Figure 1.1).

Photocatalysis has actually been unanimously recognized as a versatile strategy in organic chemistry. As a matter of fact, a substrate can be activated by a photocatalyst either through Single-Electron Transfer (SET) or Hydrogen-Atom Transfer (HAT), depending on the nature of both the substrate and the photocatalyst (see Figure 1.2).

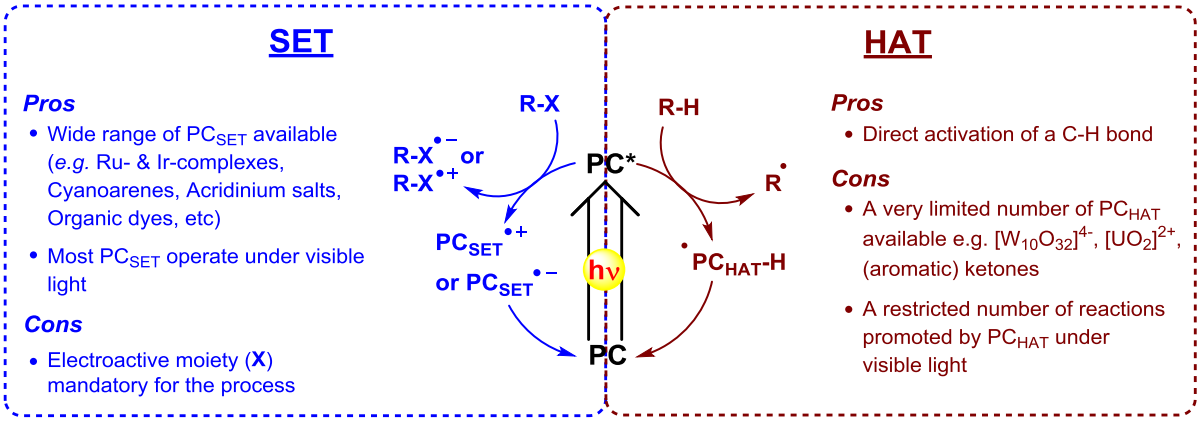

Figure 1.2 Substrate activation paths in photocatalysis: Single-Electron Transfer and Hydrogen-Atom Transfer. PC_{SET}: photocatalyst operating via SET; PC_{HAT}: photocatalyst operating via HAT.

The first mechanism has recently gained a great interest among photochemists around the world (according to REAXYS Database, there are 30,177 synthetic protocols developed via SET at the time of writing) because of the multitude of (visible-light absorbing) PC_{SET} available: Ir- and Ru-polypyridyl complexes,[1] organic dyes, acridinium ions, cyanoarenes and others.[2] However, the presence of an electroactive moiety X, meant to finely tune the redox potential of the substrate and make the photocatalytic SET feasible, is often crucial. This also requires an additional synthetic step to introduce this function on the otherwise inert substrate.

Besides, photocatalytic HAT processes have the great advantage to cleave directly X-H (often, alkyl C-H) bonds in the substrate.[3] However, due to the scarce number of PC_{HAT} studied so far, there has been a frustrated spread of this research field (294 reactions so far). From this perspective, extensive efforts to devise robust and efficient synthetic protocols, as well as new PC_{HAT}, are needed.

Other than these two mechanisms, another one is receiving a great deal of attention due to its versatility, *i.e.* Energy Transfer (ET) or triplet sensitization. In these reactions, the photocatalyst absorbs light to generate a singlet excited state (S_1); then an extremely efficient Inter-System Crossing (ISC) process to a triplet excited state (T_1, lower in energy than S_1) occurs. Roughly speaking, if the T_1 of the photocatalyst is more energetic than that of the substrate, an Energy Transfer may occur, being thermodynamically favorable (see Figure 1.3). Usually, the main mechanism is a double-electron exchange between the substrate and the sensitizer (Dexter mechanism),[4] which is different from Fluorescence Resonance Energy Transfer (Förster mechanism), consisting in a non-radiative dipole-dipole coupling.[5]

An ET allows to take advantage of the intrinsic reactivity of the T_1 of the substrate without a direct absorption of light by the substrate itself. There is no need to stress that the more favored the ISC in the photocatalyst, the more efficient the system, which is the main reason that lies behind the surge and spread of transition-metal-based triplet sensitization, with Ir(III) complexes being undoubtedly the most investigated.[6–12]

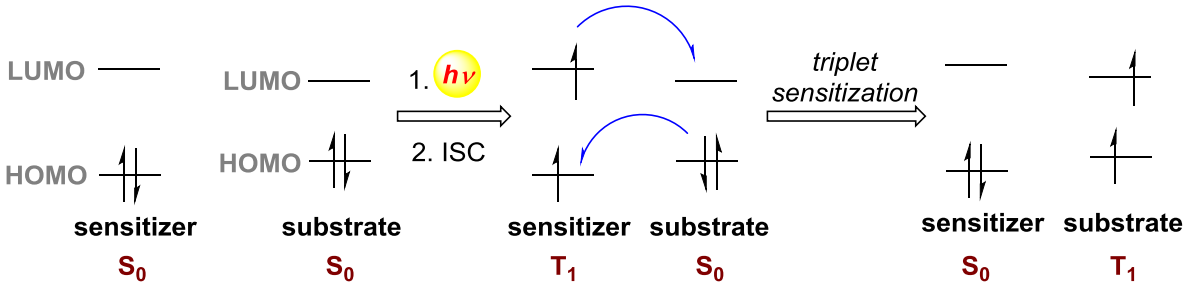

Figure 1.3 Triplet sensitization: frontier orbitals diagram for Dexter mechanism.

Coming to the present project, entitled "*Novel photocatalytic approaches for ecosustainable synthesis*", I decided to address photocatalysis as a synthetic methodology. Accordingly, I planned to study the three mechanisms presented above and evaluate their use in ecosustainable organic synthesis. In fact, photocatalysis has undoubtedly stood out as one of the most important methodologies in green chemistry for several reasons, among which:

- It uses cheap and renewable energy, *i.e.* light, to generate fleeting intermediates to be used in synthesis;
- Solar light can be used to improve the sustainability of the process;
- It is a catalytic approach;
- Atom efficiency of these processes is often very high (especially for HAT and ET).

In other words, in the frame of the abuzzing and growing field of photocatalysis, the present work is meant to further address the need for the development of robust and reliable protocols for the generation of elusive intermediates for organic synthesis relying on all the three activation pathways shown so far: Single-Electron Transfer (SET, see Chapter 2), Hydrogen Atom Transfer (HAT, see Chapter 3) and Energy Transfer (ET, see Chapter 5). Plus, preliminary data about the study of promising catalysts for visible-light photocatalyzed HAT reactions are reported in Chapter 4.

Aim 1. Study of activation manifolds.

Aim 1 was addressed through the development of four independent synthetic protocols:

- Chapter 2:
  a) the generation of benzyl radicals from arylacetic acids (via SET);[13]
  b) the generation of acyl radicals from acylsilanes (via SET);[14]
- Chapter 3:
  a) the use of vinylpyridines as a new class of electrophilic olefins for the Giese reaction (via HAT);[15]

- Chapter 5:
    a) the study of the scope of photocycloadditions between styrenes and vinyl boronate esters (via ET).

Aim 2. Research of catalysts for Visible-light Photocatalyzed HAT.

Aim 2 was addressed through the study of two novel photocatalysts for C-C bond formation via HAT mechanism under visible-light irradiation.

- Chapter 4:
    a) the uranyl cation;
    b) the class of antimony-oxo porphyrins.

It is worth mentioning here that, with the aim of making my Ph.D. experience more complete, I spent five months (January - June 2018) at the University of Wisconsin – Madison in the Prof. Tehshik P. Yoon's research group. During this experience, I had the opportunity to study synthetic strategies for [2+2] photocycloadditions relying on Transition Metal Complexes as photocatalysts via triplet sensitization (see Chapter 5). This experience allowed me to study the Energy Transfer mechanism and the use of transition metals complexes in photocatalysis much more in detail.

References

(1) Prier, C. K.; Rankic, D. a.; MacMillan, D. W. C. *Chem. Rev.* **2013**, *113* (7), 5322–5363.

(2) Romero, N. A.; Nicewicz, D. A. *Chem. Rev.* **2016**, *116* (17), 10075–10166.

(3) Protti, S.; Fagnoni, M.; Ravelli, D. *ChemCatChem* **2015**, *7* (10), 1516–1523.

(4) Dexter, D. L. *J. Chem. Phys.* **1953**, *21* (5), 836–850.

(5) Förster, T. *Ann. Phys.* **1948**, *437* (1–2), 55–75.

(6) Lu, Z.; Yoon, T. P. *Angew. Chem. Int. Ed.* **2012**, *51* (41), 10329–10332.

(7) Skubi, K. L.; Kidd, J. B.; Jung, H.; Guzei, I. A.; Baik, M.-H.; Yoon, T. P. *J. Am. Chem. Soc.* **2017**, *139* (47), 17186–17192.

(8) Scholz, S. O.; Farney, E. P.; Kim, S.; Bates, D. M.; Yoon, T. P. *Angew. Chem. Int. Ed.* **2016**, *55* (6), 2239–2242.

(9) Hurtley, A. E.; Lu, Z.; Yoon, T. P. *Angew. Chem. Int. Ed.* **2014**, *53* (34), 8991–8994.

(10) Blum, T. R.; Miller, Z. D.; Bates, D. M.; Guzei, I. A.; Yoon, T. P. *Science* **2016**, *354* (6318), 1391–1395.

(11) Miller, Z. D.; Lee, B. J.; Yoon, T. P. *Angew. Chem. Int. Ed.* **2017**, *56* (39), 11891–11895.

(12) Farney, E. P.; Yoon, T. P. *Angew. Chem. Int. Ed.* **2014**, *53* (3), 793–797.

(13) Capaldo, L.; Buzzetti, L.; Merli, D.; Fagnoni, M.; Ravelli, D. *J. Org. Chem.* **2016**, *81* (16), 7102–7109.

(14) Capaldo, L.; Riccardi, R.; Ravelli, D.; Fagnoni, M. *ACS Catal.* **2018**, *8* (1), 304–309.

(15) Capaldo, L.; Fagnoni, M.; Ravelli, D. *Chem. Eur. J.* **2017**, *23* (27), 6527–6530.

CHAPTER 2

PHOTOCATALYSIS VIA SINGLE-ELECTRON TRANSFER

This chapter reports two examples of synthetic protocols based on photocatalyzed Single-Electron Transfer.

The first study deals with α-arylacetic acids as precursors of benzyl radicals to achieve the photocatalyzed benzylation of electron-poor olefins. The reaction proceeded smoothly in the presence of catalytic amounts of a W-based catalyst, TBADT (tetrabutylammonium decatungstate, $(Bu_4N)_4[W_{10}O_{32}]$) under UV light (λ_{exc} = 310 nm). The use of a base ($NaHCO_3$), a salt ($NaClO_4$) and a co-catalyst (biphenyl) is mandatory. The reaction tolerates several substituents on the aromatic ring (whether electron-donating or electron-withdrawing) and can be successfully extended to heteroaromatic analogues.

The second study deals with acylsilanes as a source of acyl radicals under photocatalytic conditions: being complementary to studies already present in the literature, our protocol allowed to generate aliphatic acyl radicals under mild conditions both under UV and visible light irradiation as well as under flow and solar conditions. The reaction proceeded smoothly in the absence of additives and the so-obtained acyl radicals were trapped by electrophilic traps to afford Stetter adducts in high yields.

SMOOTH PHOTOCATALYZED BENZYLATION OF ELECTROPHILIC OLEFINS VIA DECARBOXYLATION OF ARYLACETIC ACIDS.[1]

Introduction

Carboxylic acids are versatile organic compounds that have stimulated growing attention in recent years. In particular, the presence of the carboxylic group as "traceless activating agent" makes them suitable for decarboxylative couplings. Besides thermal reactions, requiring the help of a metal catalyst (usually silver),[2,3] decarboxylation can be conveniently achieved photocatalytically through a redox step (SET). Both oxidative and reductive strategies have been reported (see Figure 2.1).

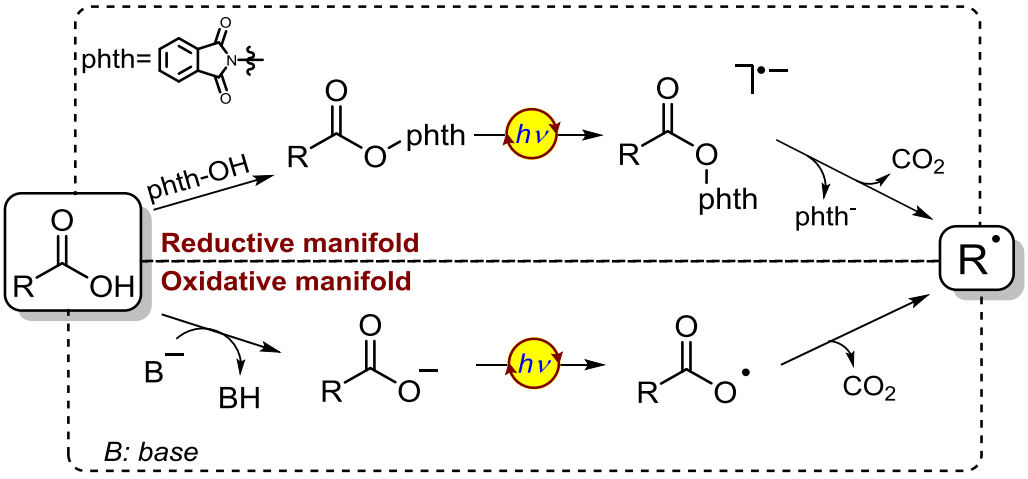

Figure 2.1 Oxidative and reductive strategies can be adopted for the activation of carboxylic acid in photocatalysis.

As for the reductive manifold, they are usually activated as *N*-Hydroxyphthalimide esters (NHP esters): these compounds efficiently fall apart yielding the corresponding phthalimide anion, one molecule of CO_2 and, finally, a C-centered radical.[4–9]

On the other hand, it is possible to activate carboxylic acids through a photocatalyzed oxidative step, especially from the corresponding carboxylate anions, to get the corresponding carboxylyl radicals, which in turn lose CO_2 to yield C-centered radicals.[10–19]

Significantly, an oxidative manifold is more straightforward compared to a reductive one since it does not require any preliminary, time-demanding functionalization of the substrate.

As for the applications of the resulting photogenerated carbon-centered radicals, they were used in several instances to design efficient synthetic protocols. A typical case is the conjugate addition onto electron-poor olefins (Scheme 2.1, *path a*)[2,3,11,20,21] or allyl sulfones[7] forming a new C−C bond. Efficient fluorinating agents (*e.g.*, Selectfluor®) were likewise used for C−F bond formation (*path b*).[22,23] In rare instances, the stability of the radical allowed for a dimerization process (*path c*),[24] while the presence of a reducing agent (*e.g.*, a thiol) led to an overall removal of the carboxylic group (*path d*).[25] More recently, dual catalytic processes combining a photocatalyst (PC) with a transition-metal based catalyst (*e.g.*, based on Ni) have been developed and allowed the formation of C(sp^3)-C(sp^2) bonds (*path e, e'*).[11,15,26–28]

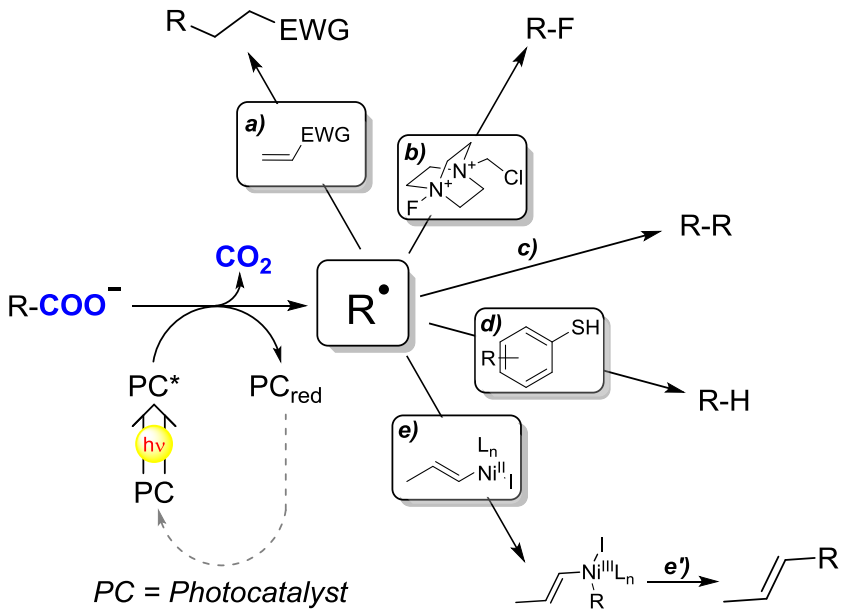

Scheme 2.1 Synthetic applications of a C-centered radical generated via photocatalyzed decarboxylation.

For all these processes, perhaps the most critical step is the decarboxylation of the carboxylyl radical resulting from the photocatalytic oxidation. It is particularly favored when the resulting radical (Scheme 2.1, R•) is stabilized, as in the case of secondary or tertiary alkyl radicals, along with α-amino (from the corresponding amino acids) or α-oxy radicals. Benzyl radicals were generated from phenylacetic acids and used as well, but never in the benzylation of olefins, due to the lack of reactivity of these radicals toward C=C double bonds. Since benzyl radicals can be

classified as nucleophilic radicals, based on their reduction and oxidation potentials,[29] an approach to promote their addition onto C=C would consists in the use of electrophilic olefins.

Apart from photocatalytic applications, the use of arylacetic acids in photochemical processes has been only sparsely reported.[30,31] Under direct irradiation, the photoelimination of CO_2 often took place and triggered the desired process. Early studies demonstrated that the loss of CO_2 is pH dependent. As a matter of fact, the involvement of radical intermediates was postulated when phenylacetic acids were irradiated, while the formation of benzyl anions was claimed when irradiating the corresponding sodium salts.[32,33] Elsewhere, the carboxylic group was used as an electrofugal group in the route to α,n-didehydrotoluenes (DHTs) starting from isomeric (n-chlorophenyl) acetic acids.[34] Notably, the decarboxylation of arylacetic acids is of particular interest in pharmacokinetic studies, since this process is mainly responsible for the in vivo photodecomposition of several nonsteroidal anti-inflammatory drugs (NSAIDs).

As part of the ongoing interest of my research group in photocatalyzed C−C bond formation reactions, I focused on the use of tetrabutylammonium decatungstate (TBADT; $(nBu_4N)_4[W_{10}O_{32}]$) as a convenient, cheap, and robust photocatalyst for the benzylation of electron-poor olefins via decarboxylation of easily available arylacetic acids. In the last few years, we found that TBADT is particularly efficient in hydrogen atom transfer reactions[35–41] and, only to a minor extent, as a photoredox catalyst.[42] Interestingly, its reactive excited state, a relaxed triplet excited state named **wO**, has a remarkable redox potential, $E(\mathbf{wO}/[W_{10}O_{32}]^{5-})$, which can be estimated being around +2.44 V vs SCE.[43] Accordingly, the proposed plan for the benzylation of electrophilic olefins is based on the use of TBADT in the role of photoredox catalyst to be reductively quenched either by arylacetic acids or their more oxidizable equivalents, *i.e.* carboxylates. On one side, the photocatalytic cycle will be closed thanks to the re-oxidation of the reduced form of the photocatalyst by a purposely added electrophilic olefin, thus generating a radical anion of the latter. On the other side, upon loss of CO_2, benzyl radicals will be generated and trapped by the radical

anion of the electrophilic olefins to get the target products, in what actually is a radical-radical anion coupling.

Results and discussion

To evaluate the feasibility of the photocatalytic oxidation of carboxylates, cyclic voltammetry experiments were performed. All the measured potentials E(R-COO•/R-COO$^-$) fall in the +0.9 - +1.4 V vs SCE range, as reported in Table 2.1.

*Table 2.1 Oxidation potentials of phenylacetic acid (**2.1a**) and of carboxylates **2.1a**$^-$**–2.1q**$^-$ studied in the present work.*

Compound	$E_{1/2}$*	Compound	$E_{1/2}$*
2.1a 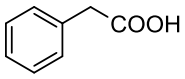	+2.51 V	**2.1i$^-$** 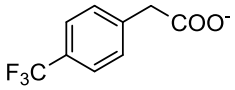	+1.39 V
2.1a$^-$ 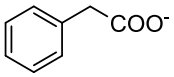	+1.27 V	**2.1j$^-$** 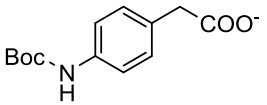	+0.91 V
2.1b$^-$ 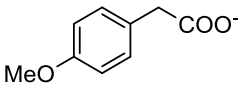	+0.99 V	**2.1k$^-$** 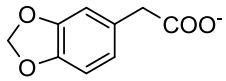	+0.97 V
2.1c$^-$ 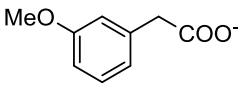	+1.17 V	**2.1l$^-$** 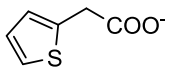	+1.04 V
2.1d$^-$ 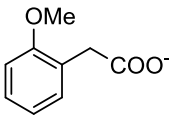	+1.07 V	**2.1m$^-$-o$^-$** 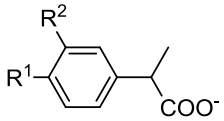	
2.1e$^-$ 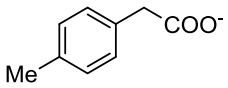	+1.17 V	**2.1m$^-$**, $R^1 = R^2 = H$	+1.07 V
2.1f$^-$ 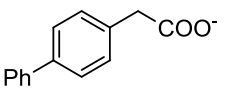	+1.17 V	**2.1n$^-$**, $R^1 = CH_2CH(CH_3)_2$, $R^2 = H$	+1.11 V
2.1g$^-$ 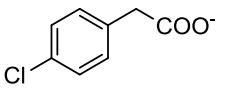	+1.25 V	**2.1o$^-$**, $R^1 = Ph$, $R^2 = F$	+1.04 V
2.1h$^-$ 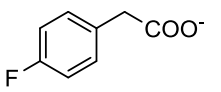	+1.21 V	**2.1p$^-$-q$^-$** 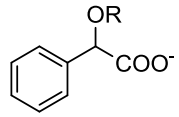	
		2.1p$^-$, R = H	+1.16 V
		2.1q$^-$, R = CH_3	+0.97 V

*[V vs SCE]

In the case of derivatives **2.1a** and **2.1a⁻-2.1q⁻**, typically irreversible or quasi-reversible redox behaviors were observed.[44] For this reason, data reported in Table 2.1 refer to $E_{1/2}$ (half-wave potential) values of the oxidation process, better appreciated when plotting the cyclic voltammogram in the semi-differential mode. In the case of phenylacetic acid **2.1a** in acetonitrile (in the presence of nBu$_4$N$^+$ClO$_4^-$ 0.1 M as the supporting electrolyte), an oxidation wave was registered at + 2.51 V vs SCE, partially superimposed with the anodic oxidation of the solvent. By contrast carboxylate anions **2.1a⁻-2.1q⁻**, obtained upon addition of a base (1 equiv. of a nBu$_4$N$^+$OH$^-$ 1.0 M in MeOH was used), showed much lower oxidation potentials (see Table 2.1).

Then, I undertook the electrochemical investigation for electron-poor olefins **2.2** by performing cyclovoltammetry experiments in acetonitrile (in the presence of nBu$_4$N$^+$ClO$_4^-$ 0.1 M as the supporting electrolyte): a reversible redox behavior was observed. For this reason, the E_0' values are reported (see Table 2.2), in accordance with a previous work by my group.[42] The analysis revealed that the reduction potentials for **2.2a-2.2e** vary from -1.09 V vs SCE (for **2.2b**) to -1.65 V vs SCE (for **2.2e**),[42] with the newly investigated derivative **2.2c** showing a reduction potential at -1.20 V vs SCE (see Table 2.2).

*Table 2.2 Reduction potentials of the electron-poor olefins (**2.2a-2.2e**) studied in the present work.*

Compound		E_0'*	Compound		E_0'*
2.2a	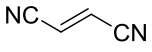	-1.31 V	**2.2d**	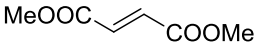	-1.47 V
2.2b	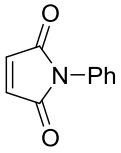	-1.09 V	**2.2e**	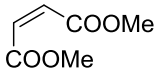	-1.65 V
2.2c	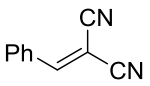	-1.20 V			

*[V vs SCE]

Finally, as for the photocatalyst TBADT, the redox potential of the excited state has only been estimated to lie in the range +2.24-+2.64 vs SCE. Similarly, it is not possible to give a precise value

for the redox potential of the reduced species $[W_{10}O_{32}]^{5-}$, since it is known to disproportionate in solution according to equation (eq. 2.1):[45]

$$2[W_{10}O_{32}]^{5-} \rightarrow [W_{10}O_{32}]^{6-} + [W_{10}O_{32}]^{4-} \quad \text{(eq. 2.1)}$$

However, the following values are commonly accepted: $E([W_{10}O_{32}]^{4-}/[W_{10}O_{32}]^{5-})$ = -0.9 V vs SCE and $E([W_{10}O_{32}]^{5-}/[W_{10}O_{32}]^{6-})$ = -1.4 V vs SCE.[46]

Since the redox value of the substrates and the photocatalyst matched, I moved to the optimization of reaction conditions.

Initial experiments were carried out on the reaction between parent phenylacetic acid (**2.1a**) and fumaronitrile (**2.2a**) to give benzylsuccinonitrile **2.3** (Table 2.3).

When an equimolar (0.05 M) solution of **2.1a** and **2.2a** in acetonitrile in the presence of TBADT (4 mol%) was irradiated for 24 h at 310 nm, the expected product was not detected by GC analysis (*entry 1*). We then thought that the use of water as co-solvent could promote the desired SET and, actually, when shifting to mixed aqueous media, however, small amounts of **2.3** were formed (*entries 2, 3*). The role of additives was next evaluated. Comparable results were obtained in the presence of sodium hydrogen carbonate alone (1 equiv.; *entry 4*), or when it was coupled with sodium perchlorate (1 equiv.; *entry 5*), with the yield never exceeding 20%, despite an almost quantitative consumption of **2.2a** (> 90%). By contrast, the addition of biphenyl had a tremendous effect and raised the formation of **2.3** in up to 83% yield (*entries 6, 7*). Other experiments (*entries 8-10*) demonstrated that the presence of all the three additives ($NaHCO_3$, $NaClO_4$ and biphenyl) was mandatory for the success of the reaction and that a bivalent perchlorate ($Mg(ClO_4)_2$) was less beneficial than $NaClO_4$ (*entry 11*).

Table 2.3 Optimization of reaction conditions.[a]

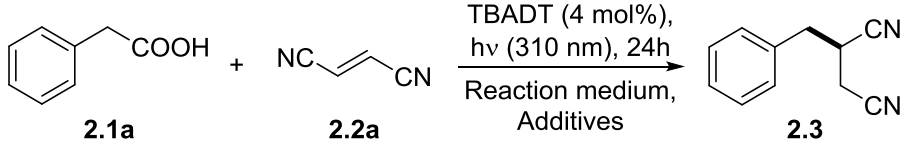

2.1a **2.2a** (0.05 M) **2.3**

Entry	**2.1a** (equiv.)	Reaction medium	Additives	**2.3** Yield (%)[b]
1	1.0	MeCN	-	n.d.
2	1.0	MeCN-H_2O 5/1	-	traces
3	1.0	MeCN-H_2O 2/1	-	14
4	1.0	MeCN-H_2O 2/1	$NaHCO_3$ (1.0 equiv.)	17
5	1.0	MeCN-H_2O 2/1	$NaHCO_3$ (1.0 equiv.) $NaClO_4$ (1.0 equiv.)	20
6	1.0	MeCN-H_2O 2/1	$NaHCO_3$ (1.0 equiv.) $NaClO_4$ (1.0 equiv.) Biphenyl (0.5 equiv.)	52
7	**1.0**	**MeCN-H_2O 2/1**	**$NaHCO_3$ (1.0 equiv.) $NaClO_4$ (1.0 equiv.) Biphenyl (1.0 equiv.)**	**83**
8	1.0	MeCN-H_2O 2/1	$NaHCO_3$ (1.0 equiv.) Biphenyl (1.0 equiv.)	61
9	1.0	MeCN-H_2O 2/1	$NaClO_4$ (1.0 equiv.) Biphenyl (1.0 equiv.)	13
10	1.0	MeCN-H_2O 2/1	Biphenyl (1.0 equiv.)	23
11	1.0	MeCN-H_2O 2/1	$NaHCO_3$ (1.0 equiv.) $Mg(ClO_4)_2$ (1.0 equiv.) Biphenyl (1.0 equiv.)	53
12	1.5	MeCN-H_2O 2/1	$NaHCO_3$ (1.5 equiv.) $NaClO_4$ (1.0 equiv.)	69
13[c]	1.0	MeCN-H_2O 2/1	$NaHCO_3$ (1.0 equiv.) $NaClO_4$ (1.0 equiv.) Biphenyl (1.0 equiv.)	8[d]
14[e]	1.0	MeCN-H_2O 2/1	$NaHCO_3$ (1.0 equiv.) $NaClO_4$ (1.0 equiv.) Biphenyl (1.0 equiv.)	n.d.[f]

[a] *Reaction conditions:* ***2.1a*** *(0.15 mmol),* ***2.2a*** *(0.15 mmol),* $(nBu_4N)_4[W_{10}O_{32}]$ *(TBADT, 4 mol%) in 3 mL of the chosen reaction medium.* [b] *Gas Chromatography (GC) yields are based on the consumption of the olefin (****2.2a****); the consumption of* ***2.2a*** *was always > 90%, except where otherwise noted.* [c] *No TBADT used.* [d] *The formation of by-products has been observed by GC analysis.* [e] *In the absence of light.* [f] *No consumption (< 5%) of the olefin was observed.*

Interestingly, a good yield (69% GC yield, *entry 12*) was likewise observed in the absence of biphenyl when increasing the amount of acid (up to 1.5 equiv.). Blank experiments demonstrated the crucial role of both TBADT and light in the desired process (*entries 13, 14*).

Having the optimized conditions in hand (*entry 7*, Table 2.3), I next evaluated the scope of the reaction (Table 2.4), by investigating different combinations of arylacetic acids **2.1** (see Table 2.1) and electron-poor olefins **2.2** (see Table 2.2). The reaction of phenylacetic acid **2.1a** with fumaronitrile **2.2a** and *N*-phenyl maleimide **2.2b** gave products **2.3** and **2.4** in 80% and 72% isolated yield, respectively. The reaction was next extended to 4-methoxyphenylacetic acid **2.1b**, that gave products **2.5-2.7** in good to excellent yields in the reaction with **2.2a**, **2.2b** and benzylidenemalononitrile **2.2c**. By contrast, the reaction of **2.1b** with dimethyl fumarate **2.2d** gave only a modest yield (40%) of adduct **2.8**, that was increased (61% yield) when using an excess of **2.1b** (1.5 equiv., perchlorate omitted). When repeating the synthesis of **2.8** by using isomeric dimethyl maleate **2.2e** as the radical trap, the process was sluggish giving the desired product in 37% yield (with only 75% consumption of **2.2e**). The reactions of 3-methoxy (**2.1c**) and 2-methoxy (**2.1d**) phenylacetic acids likewise gave adducts **2.9** and **2.10** in 54 and 70% yield, respectively, in the reaction with **2.2a**. Aliphatic (in 4-methylphenylacetic acid **2.1e**) or aromatic (in 4-biphenylacetic acid **2.1f**) groups in the para- position were tolerated and the expected adducts with fumaronitrile were obtained in 52% and 63% yield, respectively (compounds **2.11**, **2.12**). In the latter case, product **2.12** was likewise formed in a good yield (75%) in the absence of biphenyl.

Table 2.4 Benzylation of electron-poor olefins via decarboxylation of arylacetic acids.[a]

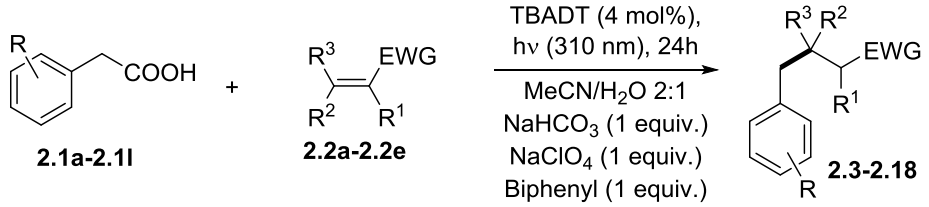

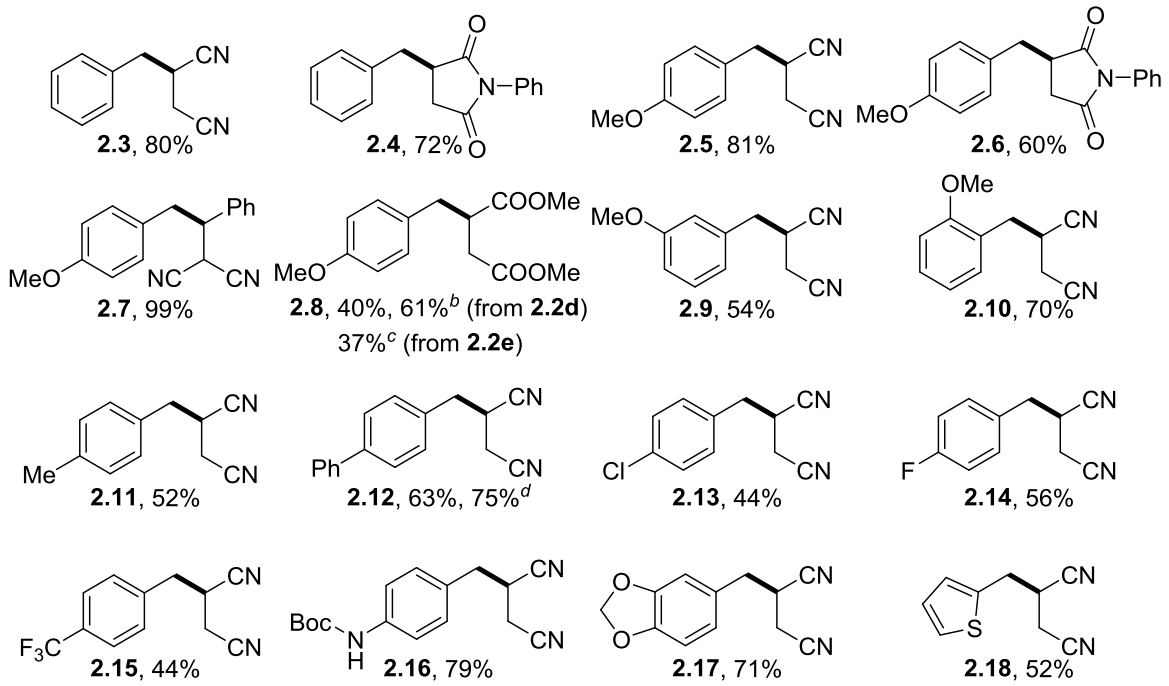

[a] *Reactions carried out on a 0.75 mmol scale (0.05 M); all data are the average of two experiments. Isolated yields by silica gel chromatography.* [b] *Conditions from Table 2.3, entry 8.* [c] *Yield based on 75% consumption of* ***2.2e****.* [d] *Reaction carried out in the absence of biphenyl.*

Electron withdrawing substituted 4-chloro (**2.1g**), 4-fluoro (**2.1h**) and 4-trifluoromethyl (**2.1i**) phenylacetic acids underwent addition onto fumaronitrile to give compounds **2.13**-**2.15** in decent yields (45-55% range). It is worth highlighting here that the nature of the substituent markedly affected the process in terms of yields. In fact, the more electron donating the substituent, the smoother the oxidation of the carboxylate and the subsequent reactivity.

4-Aminophenylacetic acid was also tested, but was not soluble under the optimized reaction conditions. Protection of the amino group as carbamate in 4-(*tert*-butoxycarbonylamino)phenylacetic acid **2.1j** restored the usual reactivity to give adduct **2.16** in good yield (79%) upon reaction with **2.2a**. The reaction could be extended to substrates bearing two substituents on the aromatic ring, as well as to heteroaryl substituted acetic acids, as demonstrated

by (3,4-methylenedioxy)phenylacetic acid **2.1k** and 2-thiopheneacetic acid **2.1l**, that reacted with **2.2a** to give, respectively, compounds **2.17** and **2.18**.

Next, I shifted my attention to 2-arylpropionic acids, as reported in Scheme 2.2a. In particular, parent 2-phenylpropionic acid **2.1m** gave adduct **2.19** in 80% yield as a 1:1 diastereomeric mixture.

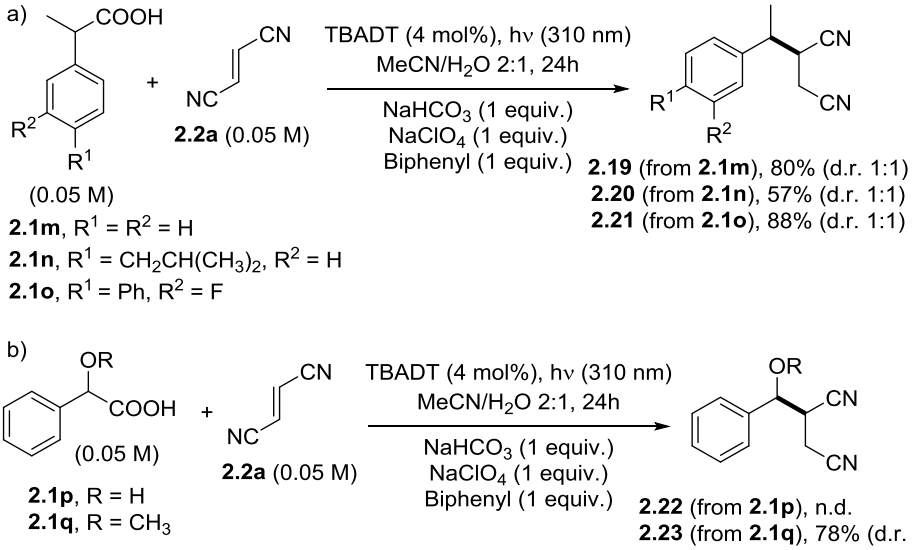

*Scheme 2.2 Reactivity of: a) 2-phenylpropionic acids **2.1m-2.1o** and b) mandelic acid derivatives **2.1p**, **2.1q**.*

Furthermore, since several NSAIDs pertain to this family, I subjected two very well-known drugs to the reaction conditions. Indeed, both ibuprofen (**2.1n**) and flurbiprofen (**2.1o**) gave the expected adducts **2.20** and **2.21** in 57% and 88% isolated yield (as 1:1 diastereomeric mixtures), respectively. Finally, I tested the effect of oxygen-based substituents in the benzylic position (Scheme 2.2b). Thus, when using mandelic acid **2.1p**, benzaldehyde was detected (by GC analysis) as the exclusive product at the expense of the expected adduct **2.22**. However, when employing α-methoxyphenylacetic acid **2.1q**, the usual reactivity was restored, allowing to isolate product **2.23** in 78% yield as a 1:1 diastereomeric mixture in the reaction with **2.2a**. In light of the data presented so far, it can be stated that the present work compares favorably with other decarboxylative photocatalytic strategies employing arylacetic acids and is complementary, since this is one of the rare examples of electron-poor olefins benzylation.[42,47–49] The proposed reaction mechanism is gathered in Scheme 2.3 and is strengthened by the electrochemical investigation reported above.

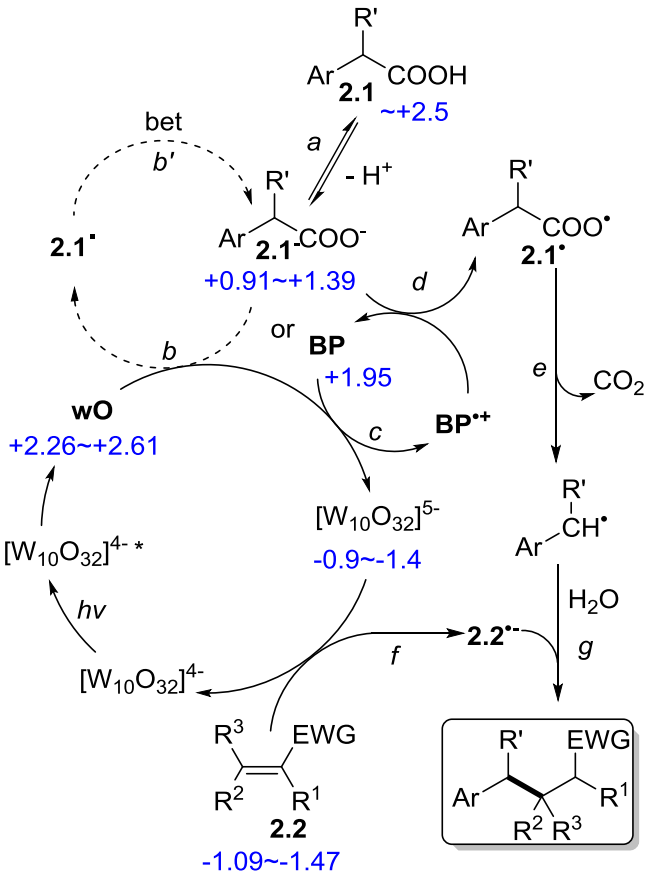

Scheme 2.3 Proposed mechanism. In blue, redox potential of involved species reported vs SCE. BP: biphenyl.

Assuming the average value of the redox potential of **wO** being +2.44 V vs SCE,[43] the occurrence of an electron transfer from **2.1a** (see Table 2.1) to **wO** cannot be excluded. The efficiency of this process, however, is expected to be very low, as also confirmed by the reaction carried out in neat acetonitrile, where no product **2.3** has been detected in the reaction with **2.2a** (Table 2.3, *entry 1*). By contrast, when in the anionic form, the -COO^- group functions as an efficient electroauxiliary moiety,[50] since it lowers the oxidation potential of the substrate with respect to the corresponding unsubstituted derivative and also drives the selectivity. Thus, the reaction takes place significantly only on the easier oxidizable carboxylate anions **2.1**$^-$ (see Scheme 2.3, *path a*). It is worth mentioning here that the reaction medium did not affect the stability of the decatungstate anion, while this does not tolerate strongly basic conditions.[51] Thus, excitation of the $[W_{10}O_{32}]^{4-}$ cluster populates the highly oxidizing **wO** state, capable to accept an electron from the carboxylate anion **2.1**$^-$ (*path b*; dashed arrow). However, this step is not efficient *per se*, as supported by the low

yields observed in *entries 2-5*, Table 2.3. Two main reasons may explain this behavior. Given that both **2.1**$^{-}$ and **wO** are negatively charged, an electrostatic repulsion may hamper *path b*. Moreover, a back electron transfer (bet, *path b'*) may be involved, preventing the otherwise fast decarboxylation (reported to be in the order of 10^{10} s^{-1})[52] of the thus formed $ArCH_2$-$COO^{\bullet}$ radical (**2.1**$^{\bullet}$).

The key point to the success of the present reaction is the use of biphenyl (BP).[53] Thus, BP ($E(BP^{\bullet+}/BP)$ = +1.95 V vs SCE)[54] can be oxidized (in competition with **2.1**$^{-}$) to the corresponding long-lived radical cation $BP^{\bullet+}$ (*path c*). $BP^{\bullet+}$ is then capable of oxidizing **2.1**$^{-}$ to **2.1**$^{\bullet}$ (*path d*), that in turn loses CO_2 to give the corresponding benzyl radical (*path e*). BP has the role of electron transfer agent[55] and it is able to overcome the electrostatic repulsion between **2.1**$^{-}$ and **wO** and to separate **2.1**$^{\bullet}$ from $[W_{10}O_{32}]^{5-}$, preventing bet and leading to a productive oxidation of **2.1**$^{-}$ (in turn triggering decarboxylation). The actual concentration of BP (1 equiv., Table 2.3) must be high enough to prevent any competitive (yet, unproductive) direct oxidation of **2.1**$^{-}$. The presence of $NaClO_4$ is likewise important in favoring the electron transfer process, since it contributes to increase the ionic strength of the reaction medium.[42] Another important point is related to the trapping of $ArR'CH^{\bullet}$. Benzyl radicals are rather stable species, quite difficult to trap and with a marked tendency to dimerize.[24] As previously demonstrated by my group, this limitation can be overcome by having recourse to easily reducible olefins (see above).[42] Indeed, the olefins have a role in the regeneration of the photocatalyst (*path f*) by the concomitant conversion into the corresponding radical anions (**2.2**$^{\bullet-}$). The reduction potential of the deactivated photocatalyst has been estimated to lie in the -0.9 to -1.4 V vs SCE range. This is due to the possible involvement of the highly reducing $[W_{10}O_{32}]^{6-}$ species, in turn obtained via disproportionation of the mono-reduced form $[W_{10}O_{32}]^{5-}$.[42] As a result, the C-C bond forming step occurs via a radical-radical anion coupling (*path g*), leading to the desired product upon addition of a proton (from the aqueous solvent). This behavior has been confirmed in the present system, where the least two reducible olefins used, *viz.* isomeric dimethyl fumarate **2.2d** and dimethyl maleate **2.2e**, both gave product **2.8** in a modest yield, with an

efficiency proportional to their reduction potentials (the more negative the reduction potential, the worse the efficiency).[42] An excess of the acid (**2.1b**$^{-}$), however, ameliorated the performance of the reaction with **2.2d** (61% yield, even in the absence of biphenyl), highlighting that the limitations related to *path b* (see above) can be overcome by increasing the absolute concentration of the electron donor.

As for the employed acids, despite their oxidation potentials span over a quite large range (see Table 2.1), the reaction proceeds satisfactorily, demonstrating the potential of TBADT as photoredox catalyst. The presence of a biphenyl moiety in compound **2.1f** allowed the reaction to proceed even in the absence of the electron transfer agent. Another interesting case is the selective activation of the -COOH group in (3,4-methylenedioxy)phenylacetic acid **2.1k**, despite the presence of the two methylene hydrogen atoms, likewise prone to be activated under TBADT photocatalyzed conditions via a competitive HAT step.[51] Phenylpropionic acids behave quite similarly to the corresponding C2-homologues despite the stability imparted by the methyl group to the resulting benzyl radical. Different is the case of mandelic acid derivatives, where the presence of the benzylic -OH group in **2.1p** completely diverted the reactivity, leading to a formal decarboxylation/oxidation rather than the desired C-C bond formation, as previously observed.[25,56,57] However, when using substrate **2.1q** bearing a α-methoxy substituent, the usual reactivity was restored.

Conclusions

The present work demonstrates that C-C bond forming reactions starting from arylacetic acids and easily reducible olefins are feasible. The success of the protocol is based on the use of TBADT as photoredox catalyst and the -COOH moiety in the role of electroauxiliary group. The reaction requires a fine tuning of the conditions and a mixed aqueous solvent is needed to solubilize all the compounds present in solution. Interestingly, biphenyl, acting as an electron transfer agent, has a fundamental role in improving the performance of the reaction.

ACYL RADICALS FROM ACYLSILANES: PHOTOREDOX-CATALYZED SYNTHESIS OF UNSYMMETRICAL KETONES.[58]

Introduction

Acyl radicals are valuable intermediates for the preparation of ubiquitous functional groups in nature such as unsymmetrical ketones and amides.[59] One common way to generate these intermediates is to start from acyl selenides in the presence of an organotin reagent and a radical initiator.[59] A greener approach consists in the use of aldehydes as starting materials and light to promote the C(sp^2)-H homolytic cleavage of the formyl hydrogen,[60–63] facilitated by the low bond dissociation energy (88.7 kcal/mol for propanal).[64] My group (and others) demonstrated that tetrabutylammonium decatungstate ($(n\text{Bu}_4\text{N})_4[\text{W}_{10}\text{O}_{32}]$, TBADT)[35–37,41,65,66] can be used as the photocatalyst for the generation of acyl radicals via a Hydrogen Atom Transfer (HAT) process.[67–71] This smooth process, however, may fail if the H-atom donor contains other labile C-H bonds, like in the case of piperonal, where the activation of the methylene hydrogens in the benzodioxole ring is exclusive.[51] Additionally, the volatility of some aldehydes (*e.g.* acetaldehyde) may represent a serious drawback of this approach. This calls for alternative strategies for acyl radicals generation and a reasonable choice is photoredox catalysis.[72–74] Unfortunately, this approach appears unsuccessful, due to the electrochemical inertia of aldehydes ($E_{1/2}$ > +2 V vs SCE,[75] $E_{1/2}$ ~ -1.65 V vs SCE for benzaldehyde).[76] Nevertheless, the use of a redox active moiety (an electroauxiliary group)[50,77] in the acyl radical precursor may drive the desired redox reaction with positive effects in terms of conditions mildness and selectivity. In fact, some groups recently studied the formation of acyl radicals from RC(=O)X derivatives under photoredox catalyzed conditions (Scheme 2.4). α-Keto acids were used as a source of acyl radicals (Scheme 2.4, *case a*). These compounds are easily oxidized when in the anionic form ($E_{1/2}$ ~ +1.0 V vs SCE)[17] and Ru(II) complexes,[17] Eosin,[78] Ir(III) complexes,[79–83] and acridinium salts[84] were used to promote the acyl radical formation via oxidation and ensuing elimination of carbon dioxide from the resulting carboxylyl radical. However, most of

the reported examples dealt with aroyl radicals, while only a handful of examples exploiting aliphatic analogues was reported.[17,78–83] Acyl radicals were also formed through the photocatalyzed reduction of *in-situ* prepared (mixed) anhydrides (*case b*[12] and *c*[85]) or acyl chlorides (Scheme 2.4, *case d*[86]).

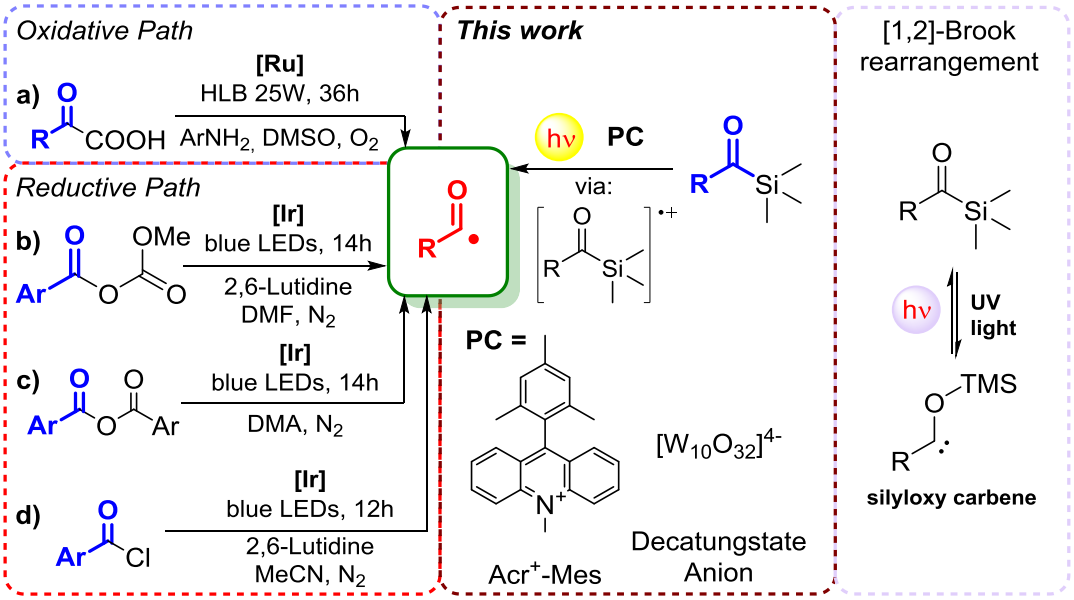

HLB: household light bulb, DMA: *N*,*N*-dimethylacetamide

Scheme 2.4 Photoredox catalyzed generation of acyl radicals. On the right, [1,2]-Brook rearrangement triggered by light is shown.

The existing protocols, however, often made use of expensive transition-metal photocatalysts.[17,78–83] Accordingly, I started thinking that a cheaper and more direct way to generate acyl radicals was needed: an interesting and unexplored class of compounds worth to be tested is that of acylsilanes.[87–89] Remarkably, these compounds can be easily prepared according to several robust procedures. These include the formation of 1,3-dithianes (Brook–Corey strategy) or benzotriazole adducts from aldehydes, the oxidation of (α-hydroxyalkyl)silanes, the silylation of carboxylic acid derivatives (esters, amides or acyl chlorides), the adoption of (silylated) alkynes as starting materials and others.[89–95] Furthermore, they are emerging as interesting building blocks in organic synthesis due to their diverse reactivity modes,[87,95–99] including their application for acyl group transfer reactions.[100–104] Acylsilanes are widely used to install an acyl group onto conjugate acceptors (*e.g.* sila-Stetter reactions with electron-poor olefins), where the presence of cyanide

anion[103] or high amounts (30 mol%) of thiazolium salts and a strong base[100–102] is required. Addition of acylsilanes onto imines furnished the corresponding (protected) α-aminoketones.[100,101]

Even more interestingly, acylsilanes can be readily oxidized ($E_{1/2}$ of decanoyltrimethylsilane = + 1.33 V)[75] and the resulting radical cations easily lose a stable silyl cation and an acyl cation chemistry resulted by oxidation of the corresponding acyl radicals.[75,105]

The proposed plan for the use of acylsilanes as precursors of acyl radicals is based on the fact that they can lose a positively charged trimethylsilyl mojety, affording the desired intermediate.

Results and discussion

To evaluate the feasibility of the mesolytic step, cyclic voltammetry experiments were performed (see Table 2.5, Table S.2.1) to assess the redox potential of the acylsilanes used in this work (**2.24a-2.24d**).

*Table 2.5 Oxidation potentials of acylsilanes (**2.24a-2.24d**) studied in the present work.*

Compound	$E_{1/2}$*	Compound	$E_{1/2}$*
2.24a 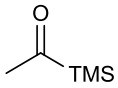	+1.46 V	**2.24c** 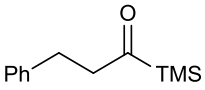	+1.26 V
2.24b 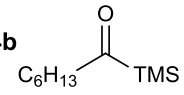	+1.31 V	**2.24d** 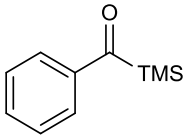	+1.51 V

*[V vs SCE]

Once potentials were determined, a set of catalysts was tested to check the feasibility of the photocatalytic oxidation of acylsilanes (Table 2.6), being aware that, upon direct photoexcitation, acylsilanes could be easily converted into reactive siloxycarbenes through a 1,2-silyl migration (Scheme 2.4, right).[106–112] I started to explore the reactivity of tetrabutylammonium decatungstate (TBADT, $(n\text{Bu}_4\text{N})_4[\text{W}_{10}\text{O}_{32}]$), a polyoxometalate well known to promote (besides HAT reactions)[67–71] Single Electron Transfer (SET) processes, also under sunlight irradiation (see

above).[1,42,113,114] Among visible light photocatalysts, I chose to screen 9-mesityl-10-methylacridinium tetrafluoroborate (Acr^+-Mes; E[*Acr^+-Mes/$Acr^•$-Mes]= +2.06 V vs SCE),[115] 9,10-dicyanoanthracene (E[*DCA/$DCA^{•-}$] = +1.99 V vs SCE),[116] 2,4,6-triphenylpyrylium tetrafluoroborate (TPT, E[*TPT^+/$TPT^•$]>+1.9 V vs SCE), [116] $Ru(bpz)_3[PF_6]_2$ (E[*Ru^{2+}/Ru^+]= +1.3 V vs SCE; bpz = 2,2'-bipyrazine).[117]

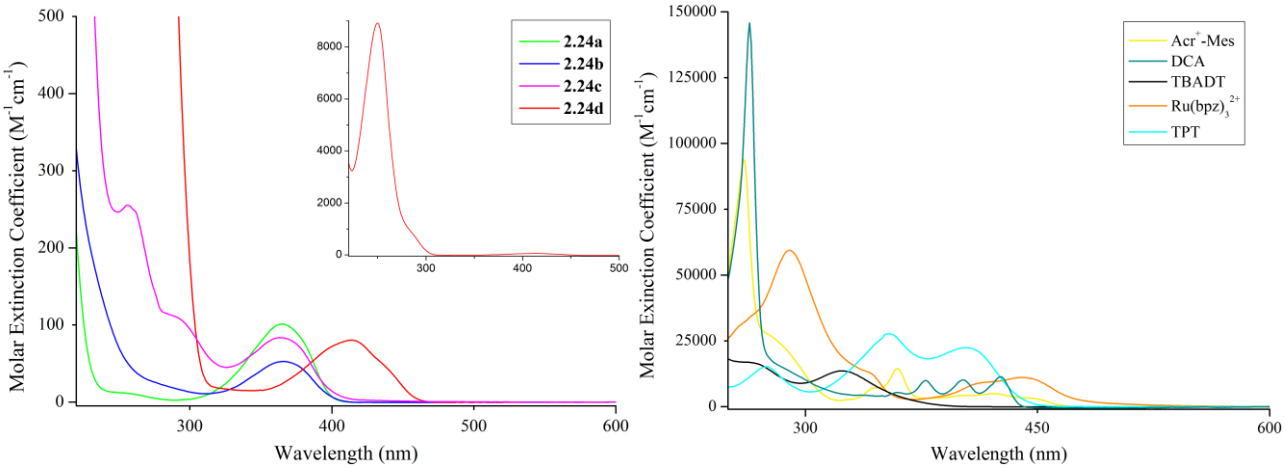

*Figure 2.2 Left: UV-Vis spectra of acylsilanes **2.24a-d** used in this work (from 1 mM solutions in MeCN). The inset shows the full spectrum of **2.24d** (from a 1 mM solution in MeCN). Right: UV-Vis spectra of photocatalysts used in this work from 5×10^{-6} M solutions in MeCN or $CHCl_3$ (only for DCA).*

As a model reaction, I then planned to acylate Michael acceptors for the synthesis of substituted ketones. As mentioned, the crucial point here was the choice of the light source (see Figure 2.2) since the direct absorption of the acylsilanes leads to a competitive carbene chemistry.[106–112] I started the optimization studies from the photocatalyzed addition of acetyltrimethylsilane **2.24a** onto dimethyl maleate **2.2e** (Table 2.6) and TBADT was the first photocatalyst tested. As shown in Table 2.6 (*entries 1-6*), the best yield of dimethyl 2-acetylsuccinate **2.25** (72%, *entry 3*) was found with a 2 mol% loading of the photocatalyst, a slight excess of **2.24a** (1.2 equiv.) in a MeCN/H_2O 5:1 mixture under irradiation for 8 h adopting phosphor-coated lamps with an emission centered at 310 nm. Irradiation at 366 nm or under solar simulated conditions (*entries 5* and *6*) led to lower yields. Blank experiments demonstrated that light and catalyst were both necessary for the desired acylation to occur.

Table 2.6 Optimization of reaction conditions.[a]

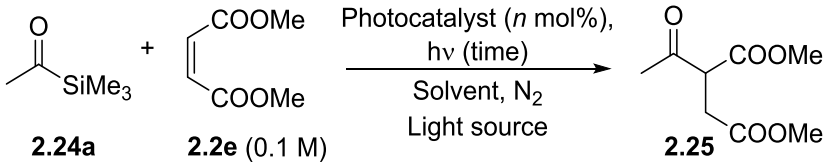

2.24a **2.2e** (0.1 M) **2.25**

Entry	Photocatalyst	**2.24a** (M)	Solvent	Time (h)	Light Source	**2.2e** Consumption (%)	**2.25** Yield (%)[b]
1	TBADT (2 mol%)	0.1	MeCN	8	310 nm	30	62[c]
2	TBADT (2 mol%)	0.1	MeCN/H_2O 5:1	8	310 nm	72	71
3	**TBADT (2 mol%)**	**0.12**	**MeCN/H_2O 5:1**	**8**	**310 nm**	**100**	**72**
4	TBADT (2 mol%)	0.12	MeCOMe/H_2O 5:1	8	310 nm	100	52
5	TBADT (2 mol%)	0.12	MeCN/H_2O 5:1	8	366 nm	65	52
6	TBADT (2 mol%)	0.12	MeCN/H_2O 5:1	8	SolarBox[d]	100	63
7	Acr^+-Mes (5 mol%)	0.12	$CHCl_3$	48	410 nm[e]	< 5	Traces
8	Acr^+-Mes (5 mol%)	0.12	CH_2Cl_2/MeOH 1:1	48	410 nm[e]	23	20
9	Acr^+-Mes (5 mol%)	0.15	MeOH	48	410 nm[e]	68	65
10	Acr^+-Mes (10 mol%)	0.15	MeOH	48	410 nm[e]	85	75
11	**Acr^+-Mes (10 mol%)**	**0.15**	**MeOH**	**48**	**410 nm[e, f]**	**100**	**81**
12	Pyrylium salt (2 mol%)	0.12	MeCN	24	410 nm[e]	< 5	n.d.
13	Pyrylium salt (2 mol%)	0.12	MeCN/H_2O 5:1	24	410 nm[e]	< 5	Dirty reaction
14	$Ru(bpz)_3^{2+}$ (5 mol%)	0.12	MeCN/H_2O 5:1	24	450 nm[e, g]	< 5	n.d.
15	DCA (0.75 mol%)	0.12	MeCN	24	410 nm[e]	19	n.d.
16	DCA (5 mol%)	0.12	$CHCl_3$	24	410 nm[e]	39	9

*[a] Reaction conditions: **2.24a** (0.1-0.15 M), **2.2e** (0.1 M), photocatalyst (n mol%) in 1 mL of the chosen solvent under deaerated conditions. [b] Gas Chromatography (GC) yields referred to the consumption of the limiting reagent (**2.2e**), using n-dodecane as internal standard. [c] A complex mixture containing **2.25** was formed. [d] Irradiation carried out with a solar simulator equipped with a 1.5 kW Xe lamp, 500 $W \cdot m^{-2}$. [e] Irradiation carried out with one LED (1W). [f] Under air equilibrated conditions. [g] Three cycles of freeze-pump-thaw were performed prior to irradiation.*

With the aim to shift the irradiation range to visible light,[72–74] I focused on colored photoorganocatalysts.[116] Accordingly, the same model reaction was investigated by using Acr^+-Mes (5 mol%)[115] upon 410 nm LED irradiation. At the beginning, chloroform was used as the solvent, but the product was formed only in traces (*entry 7*). However, the yield markedly increased when a protic solvent was added (*e.g.* MeOH, *entry 8*), reaching 65% yield in neat MeOH (*entry 9*). A good yield of **2.25** (81% yield, *entry 11*) was obtained by increasing the concentration of the photocatalyst (up to 10 mol%) and by adopting **2.24a** 0.15 M under air equilibrated conditions. Gratifyingly, the acylation occurred with no need of additives (*e.g.* PhSH) usually required to regenerate the photocatalyst (see Table S.2.2 in Experimental Section).[118]

Finally, pyrylium salt (*entries 12* and *13*), $Ru(bpz)_3^{2+}$ (*entry 14*) and DCA (*entries 15* and *16*) were tested, but the desired product **2.25** was not detected, with the only exception of *entry 16* (9% yield at 39% conversion of **2.2e**).

Once chosen the best photocatalysts for the present reaction, *i.e.* TBADT and Acr^+-Mes, whose optimized conditions are reported in *entries 3* and *11*, respectively, I focused on the olefin scope in the reaction with acetylsilane **2.24a**. First, olefins bearing different EWG groups were subjected to TBADT-photocatalyzed acetylation (Table 2.7).

The reaction was satisfactory with unsaturated esters **2.2e** and **2.2f** (up to 69% yield) and afforded the corresponding keto esters **2.25** and **2.26**. The synthesis of **2.25** was repeated also under flow conditions, exploiting a photochemical apparatus made by a PTFE tubing coiled around the cooling system (made of quartz) of a 125 W medium pressure Hg lamp.[119] Remarkably, this apparatus allowed to obtain in 4 h a yield (72%) comparable to that observed under batch conditions (reactor volume: 12 mL, flow rate: 0.05 mL min^{-1}). Noteworthy, compound **2.25** was likewise prepared (73% yield) upon exposure to direct solar light for two days (8 hours per day, see Experimental Section).

Table 2.7 Olefin Scope for the Acetylation of Electron-Poor Olefins.[a,b]

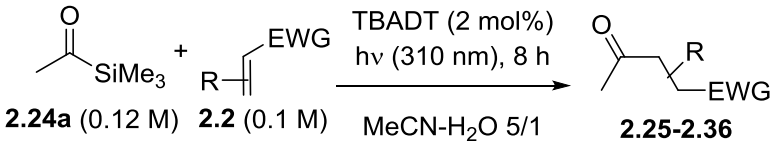

2.24a (0.12 M) **2.2** (0.1 M) **2.25-2.36**

Olefin, **2.2**	Product, yield[b]	Olefin, **2.2**	Product, yield[b]
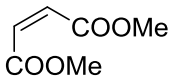 **2.2e**	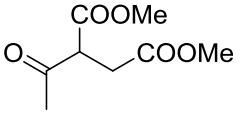 **2.25**, 69, 72[c], 73[d]	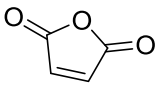 **2.2k**	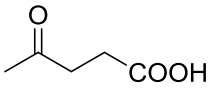 **2.31**, 63[f]
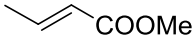 **2.2f**	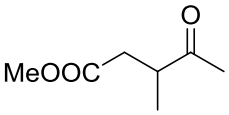 **2.26**, 60	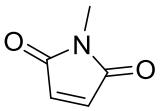 **2.2l**	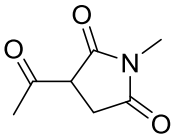 **2.32**, 79
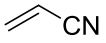 **2.2g**	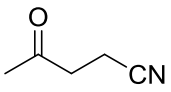 **2.27**, 47[e]	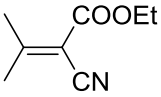 **2.2m**	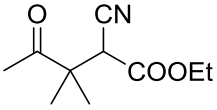 **2.33**, 63
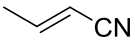 **2.2h**	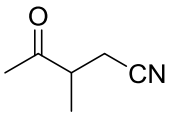 **2.28**, 56	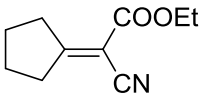 **2.2n**	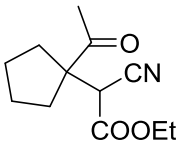 **2.34**, 64
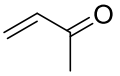 **2.2i**	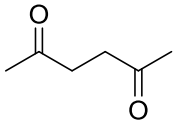 **2.29**, 55	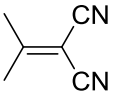 **2.2o**	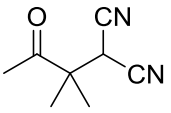 **2.35**, 89
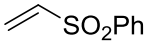 **2.2j**	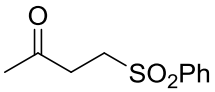 **2.30**, 61	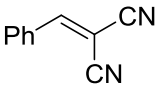 **2.2c**	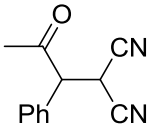 **2.36**, traces

[a] *Reaction conditions (see entry 3, Table 2.6).* [b] *Isolated yield after silica gel chromatography.* [c] *Flow conditions: see text and Experimental Section for details.* [d] *16 h Sunlight irradiation (see Experimental Section).* [e] *0.15 M* ***2.24a****.* [f] *Product* ***2.31*** *was obtained by spontaneous decarboxylation of the resulting acetylsuccinic acid.*

The presence of a methyl group in the β-position of crotonitrile **2.2h** allowed to isolate product **2.28** in a higher yield with respect to **2.27**, despite a higher excess of **2.24a** was used in the reaction with acrylonitrile (**2.2g**). 1,4-Diketone **2.29** and γ-keto sulfone **2.30** were isolated in a good yield (>50%) starting from vinyl ketone **2.2i** and vinyl sulfone **2.2j**, respectively. Anhydride **2.2k** afforded the Stetter adduct that, upon spontaneous ring opening and CO_2 loss, afforded levulinic acid **2.31** in 63% yield. Reaction with maleimide **2.2l** to give product **2.32** worked better (79% yield). 1,1-Disubstituted alkenes **2.2l**-**2.2n** were interesting substrates since in the first two cases the acylation

led to trifunctionalized derivatives **2.33** and **2.34**, again in more than 60% yield. The acylation of **2.2n** gave the best yield in the series (89%), but the acylation of dinitrile **2.2c** led to a complex mixture, where **2.36** was obtained only in traces.

Table 2.8 Selected Examples of Acr$^+$-Mes Visible-Light Photocatalyzed Acetylation of Electron-Poor Olefins.[a]

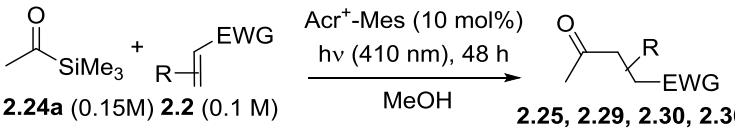

2.24a (0.15M) **2.2** (0.1 M) → **2.25, 2.29, 2.30, 2.36**

Olefin, **2.2**	Product, yield[b]	Olefin, **2.2**	Product, yield[b]
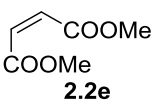 **2.2e**	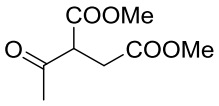 **2.25**, 81, 71[c]	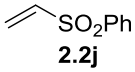 **2.2j**	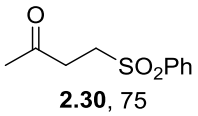 **2.30**, 75
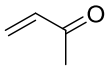 **2.2i**	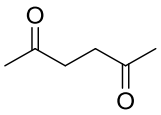 **2.29**, 71	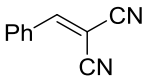 **2.2c**	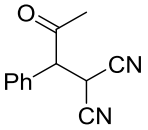 **2.36**, 55

[a] *Reaction conditions (see entry 11, Table 2.6).* [b] *Isolated yield after silica gel chromatography.* [c] *Reaction carried out under direct sunlight irradiation (40 h); yield based on 69% consumption of* ***2.2e****.*

Next, I tested selected reactions reported in Table 2.7 under visible-light by using Acr$^+$-Mes (Table 2.8). Good results were obtained for some selected electron-poor olefins, *i.e.* **2.2e**, **2.2i**, **2.2j** and **2.2c**. Interestingly, this visible-light methodology allowed us to isolate product **2.36** in a good yield (55%) through irradiation with LEDs centered at 410 nm. Nevertheless, I found that when using some Michael acceptors (e.g. **2.2f-h** and **2.2k**), a dirty reaction was observed and the expected ketones were formed in a lower amount (traces in some cases) with respect to the same reactions photocatalyzed by TBADT. We deem that the efficiency of the closure of the photocatalytic cycle is strictly dependent on the reducing ability of the reduced form of the photocatalyst. Being TBADT the more reducing of the two, the closure of the cycle is much more efficient, allowing to obtain products **2.26-2.28**. In the case of the acridinium salt, we think that the closure of the cycle is slower, allowing side reactions (note, for example, that **2.2f-h** undergo polymerization very easily) to occur.

I then measured the quantum yield of formation of product **2.25** by using Acr^{+}-Mes[118] and TBADT[120] as photocatalysts, being 0.24 and 0.60, respectively, at short irradiation time (<20% consumption of **2.2e**). By contrast, the corresponding values determined at full consumption of the olefin were 0.01 and 0.38, respectively.

I also performed dedicated ON-OFF experiments[121] to verify the effect of irradiation on the same reaction system.

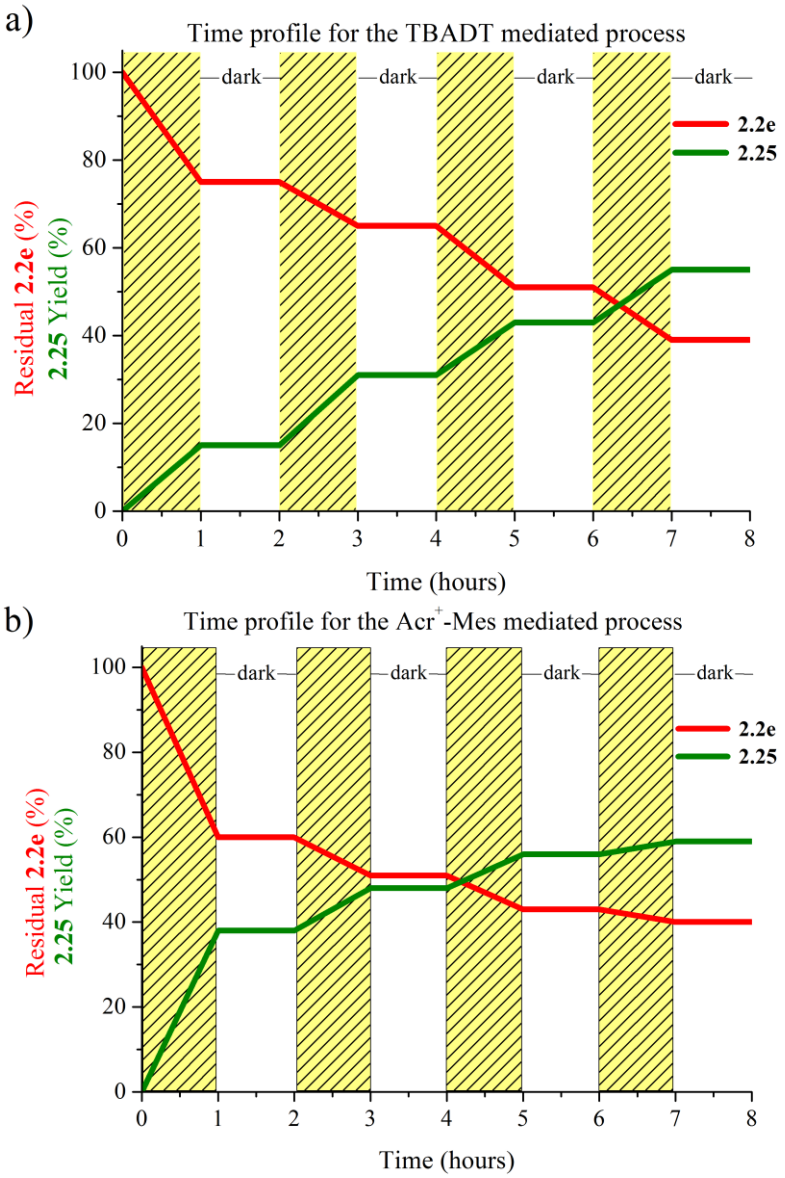

*Figure 2.3 Time profile for the reaction of **2.24a** with **2.2e** to give **2.25** in the presence of: (a) TBADT and (b) Acr^{+}-Mes under optimized reaction conditions (see Table 2.6). Light was switched off during the "dark" periods.*

As reported in Figure 2.3, the reaction stops when light is turned off, both in the case of TBADT and Acr^+-Mes, and an increase in both olefin consumption and product formation is observed only under irradiation.

I then extended the scope of the reaction to other alkanoyl or aroyl silanes by using either TBADT (method A, Table 2.9) or Acr^+-Mes (method B) as the photocatalysts. Heptanoylsilane **2.24b** was used to prepare substituted ketones **2.37-2.39** in satisfying yields. As for acylsilane **2.24c**, the synthesis of ketones **2.40-2.42** was satisfying in the presence of Acr^+-Mes, while TBADT gave lower yields due to the formation of a significant amount of 3-phenylpropanal (50-70%, Table 2.9).

Table 2.9 Acylsilane scope for the Acylation of Electron-Poor Olefins.[a]

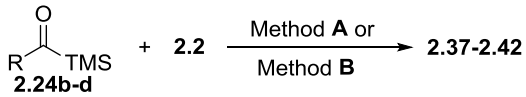

substrate	method	product	yield (%)[b]	substrate	method	product	yield (%)[b]
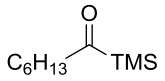 **2.24b**	**A**	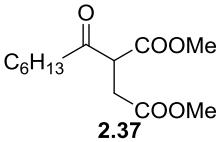 **2.37**	73%	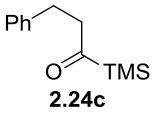 **2.24c**	**A**	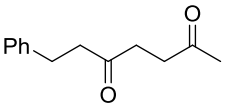 **2.40**	16%[c]
	B		31%		**B**		23%
2.24b	**A**	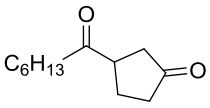 **2.38**	58%	**2.24c**	**A**	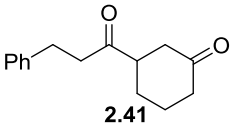 **2.41**	10%[c]
	B		43%		**B**		30%
2.24b	**A**	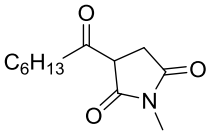 **2.39**	61%	**2.24c**	**A**	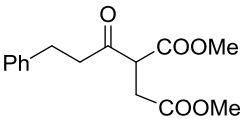 **2.42**	10%[c]
	B		78%		**B**		44%

[a] *Method A:* ***2.24*** *(0.12 M),* ***2.2*** *(0.1 M), TBADT (2 mol%) in 15 ml of MeCN/H_2O 5:1 irradiated at 310 nm. Method B:* ***2.24*** *(0.15 M),* ***2.2*** *(0.1 M), Acr^+-Mes (10 mol%) in 10 ml of MeOH irradiated at 410 nm under aerated conditions (see Table S.2.2 in Experimental Section).* [b] *Isolated yield after silica gel chromatography.* [c] *A 50-70% amount of 3-phenylpropanal detected.*

Next, I tested benzoylsilane **2.24d** but no ketone **2.43** was formed under the two conditions screened (even at 450 nm for Acr^+-Mes) and a direct conversion to benzaldehyde was observed during the irradiation (Table 2.10).

*Table 2.10 Reactivity of acylsilane **2.24d**.*[a]

substrate	method	product	yield (%)
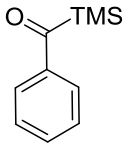 **2.24d**	**A**	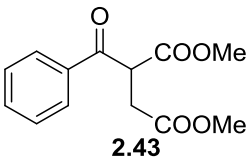 **2.43**	n.d.[b]
	B		n.d.[b]

[a] *For Method A and B see Table 2.9.* [b] *Benzaldehyde formed quantitatively.*

In the last two cases, *i.e.* for **2.24c** and **2.24d**, the formation of the aldehydes has been ascribed to the strong competitive absorption of the starting acylsilanes (see Figure 2.2) causing a direct photochemistry of **2.24c**,**d**.[106–112]

Finally, I tested the reactivity as radical traps of vinyl (hetero)arenes (Table 2.11), which are compounds well known to absorb light in the UV range.

Table 2.11 Functionalization of Vinyl (Hetero)arenes.[a]

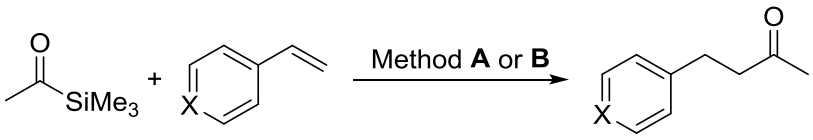

2.24a **2.2** (0.1 M) **2.44-46**

Entry	Method	Olefin **2**	Product, yield[b]
1	**A**	**2.2p**, X = C-H	**2.44**, n.d.
	B		n.d.
2	**A**	**2.2q** X = C-CN	**2.45**, traces[c,d]
	B		75%
3	**A**	**2.2r** X = N	**2.46**, 23%[e]
	B		68%

[a] *Methods A and B: see Table 2.9.* [b] *Isolated yield after silica gel chromatography.* [c] *Consumption of the olefin: 80%.* [d] *Dirty reaction.* [e] *Yield based on 40% consumption of **2.2r**.*

As a matter of fact, their functionalization by means of Method A (TBADT, λ_{exc} = 310 nm) was unsuccessful probably due to lurking polymerization. Conversely, when turning to Method B (Acr^+-Mes, λ_{exc} = 410 nm), reactivity was restored. Thus, 4-vinylbenzonitrile (**2.2q**) and 4-vinylpyridine (**2.2r**) were acylated in 75% and 68% yield, respectively, starting from **2.24a**.

On the basis of the data reported so far, I deem that a similar photocatalytic cycle operates for both TBADT and Acr^+-Mes (Scheme 2.5). I propose that their excited states (PC*) are capable of

oxidizing the acylsilanes tested (**2.24**; see Table 2.5) to the corresponding radical cations **2.24**$^{\bullet+}$. Mesolytic cleavage of the C-Si bond gave the nucleophilic acyl radical, in turn prone to add onto electron-poor olefins (**2.2**). The resulting radical adducts **I**$^{\bullet}$ were then reduced by the reduced form of the photocatalyst to **I**$^{-}$ and protonation finally afforded the desired products (**2.25-2.46**). The formation of an acyl radical intermediate was proved through trapping experiments with TEMPO to give adduct **2.47** (see Table S.2.3 in Experimental Section).[60,122]

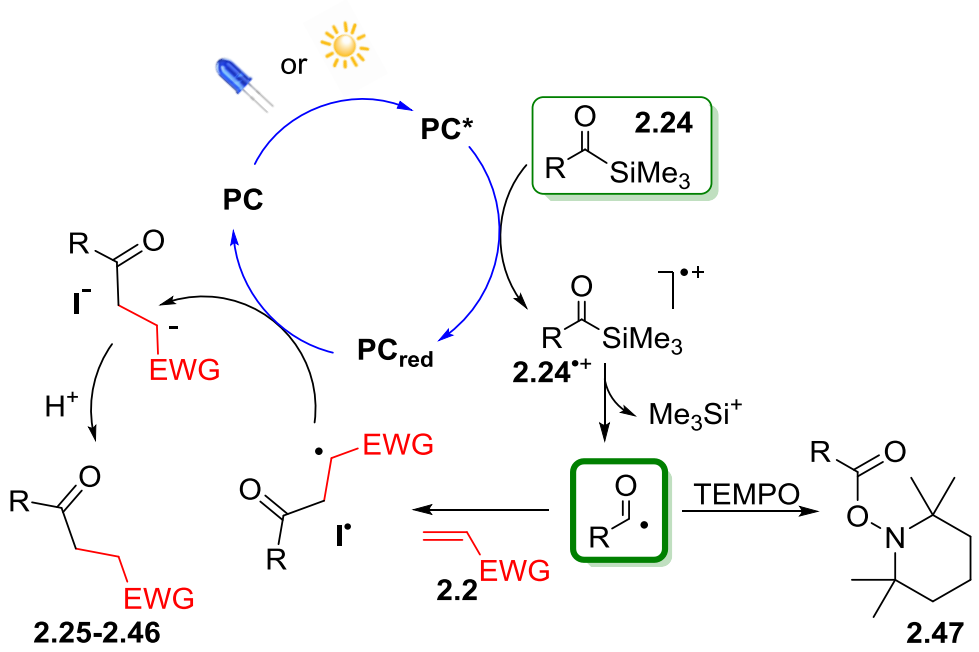

Scheme 2.5 Proposed Mechanism for the Photoredox Catalyzed Synthesis of Unsymmetrical Ketones.

This general scheme is largely documented for the TBADT photocatalyzed functionalization of olefins.[65] However, I assume that the mechanism reported in Scheme 2.5 likewise operates in the case of Acr^{+}-Mes, and no sulfur containing additive (*e.g.* PhSH) was mandatory for the regeneration of the photocatalyst.[116] On the other hand, the capability of dicyanoalkyl radicals to serve as oxidants for Acr-Mes$^{\bullet}$ is documented[123,124] and the feasibility of this electron transfer process was apparent on the basis of the value of the reduction potential of Acr^{+}-Mes ($E_{1/2}$ ~ -0.57 V vs SCE),[125] that is quite similar to the reduction potentials of the cyanomethyl radical ($E_{1/2}$ ~ -0.72 V vs SCE)[126] or $^{\bullet}CH_2COOEt$ ($E_{1/2}$ ~ -0.63 V vs SCE).[126] The occurrence of a chain reaction mechanism can be safely excluded on the basis of the above mentioned redox potentials, since direct oxidation of the

starting acylsilanes by radical adducts is largely endergonic. Moreover, the measured quantum yields in the synthesis of **2.25** were far lower than 1 when using both TBADT and Acr^{+}-Mes photocatalysts.

Conclusions

In conclusion, the first use of acylsilanes in phototoredox catalysis has been reported. The adoption of decatungstate and acridinium salts as photocatalysts allowed for the use of solar/visible light to promote the reaction. Aliphatic acyl radicals were smoothly obtained and used for the acylation of Michael acceptors for the efficient synthesis of unsymmetrical ketones. The present approach is mild and green since the 1,4-difunctionalized derivatives formed may be prepared by simply exposing the reaction vessel to sunlight, thus performing the so-called window-ledge chemistry.

References

(1) Capaldo, L.; Buzzetti, L.; Merli, D.; Fagnoni, M.; Ravelli, D. *J. Org. Chem.* **2016**, *81* (16), 7102–7109.

(2) He, Z.; Tan, P.; Hu, J. *Org. Lett.* **2016**, *18* (1), 72–75.

(3) Wu, S. W.; Liu, J. L.; Liu, F. *Org. Lett.* **2016**, *18* (1), 1–3.

(4) Yang, J.; Zhang, J.; Qi, L.; Hu, C.; Chen, Y. *Chem. Commun.* **2015**, *51* (25), 5275–5278.

(5) Lackner, G. L.; Quasdorf, K. W.; Overman, L. E. *J. Am. Chem. Soc.* **2013**, *135* (41), 15342–15345.

(6) Schnermann, M. J.; Overman, L. E. *Angew. Chem. Int. Ed.* **2012**, *51* (38), 9576–9580.

(7) Hu, C.; Chen, Y. *Org. Chem. Front.* **2015**, *2* (10), 1352–1355.

(8) Schwarz, J.; König, B. *Green Chem.* **2016**, *18* (17), 4743–4749.

(9) Li, C.; Wang, J.; Barton, L. M.; Yu, S.; Tian, M.; Peters, D. S.; Kumar, M.; Yu, A. W.; Johnson, K. A.; Chatterjee, A. K.; Yan, M.; Baran, P. S. *Science* **2017**, *356* (6342), eaam7355.

(10) Zuo, Z.; Ahneman, D. T.; Chu, L.; Terrett, J. A.; Doyle, A. G.; MacMillan, D. W. C. *Science* **2014**, *345* (6195), 437–440.

(11) Zuo, Z.; Cong, H.; Li, W.; Choi, J.; Fu, G. C.; MacMillan, D. W. C. *J. Am. Chem. Soc.* **2016**, *138* (6), 1832–1835.

(12) Bergonzini, G.; Cassani, C.; Wallentin, C. J. *Angew. Chem. Int. Ed.* **2015**, *54* (47), 14066–14069.

(13) Chu, L.; Ohta, C.; Zuo, Z.; MacMillan, D. W. C. *J. Am. Chem. Soc.* **2014**, *136* (31), 10886–10889.

(14) Griffin, J. D.; Zeller, M. A.; Nicewicz, D. A. *J. Am. Chem. Soc.* **2015**, *137* (35), 11340–11348.

(15) Huang, H.; Li, X.; Yu, C.; Zhang, Y.; Mariano, P. S.; Wang, W. *Angew. Chem. Int. Ed.* **2017**,

56 (6), 1500–1505.

(16) Yang, C.; Yang, J. D.; Li, Y. H.; Li, X.; Cheng, J. P. *J. Org. Chem.* **2016**, *81* (24), 12357–12363.

(17) Liu, J.; Liu, Q.; Yi, H.; Qin, C.; Bai, R.; Qi, X.; Lan, Y.; Lei, A. *Angew. Chem. Int. Ed.* **2014**, *53* (2), 502–506.

(18) Le Vaillant, F.; Wodrich, M. D.; Waser, J. *Chem. Sci.* **2017**, *8* (3), 1790–1800.

(19) Le Vaillant, F.; Courant, T.; Waser, J. *Angew. Chem. Int. Ed.* **2015**, *54* (38), 11200–11204.

(20) Chinzei, T.; Miyazawa, K.; Yasu, Y.; Koike, T.; Akita, M. *RSC Adv.* **2015**, *5* (27), 21297–21300.

(21) Maeda, K.; Saito, H.; Osaka, K.; Nishikawa, K.; Sugie, M.; Morita, T.; Takahashi, I.; Yoshimi, Y. *Tetrahedron* **2015**, *71* (7), 1117–1123.

(22) Rueda-Becerril, M.; Mahé, O.; Drouin, M.; Majewski, M. B.; West, J. G.; Wolf, M. O.; Sammis, G. M.; Paquin, J.-F. F. *J. Am. Chem. Soc.* **2014**, *136* (6), 2637–2641.

(23) Ventre, S.; Petronijevic, F. R.; Macmillan, D. W. C. *J. Am. Chem. Soc.* **2015**, *137* (17), 5654–5657.

(24) Manley, D. W.; Walton, J. C. *Org. Lett.* **2014**, *16* (20), 5394–5397.

(25) Cassani, C.; Bergonzini, G.; Wallentin, C. J. *Org. Lett.* **2014**, *16* (16), 4228–4231.

(26) Noble, A.; McCarver, S. J.; Macmillan, D. W. C. *J. Am. Chem. Soc.* **2015**, *137* (2), 624–627.

(27) Oderinde, M. S.; Varela-Alvarez, A.; Aquila, B.; Robbins, D. W.; Johannes, J. W. *J. Org. Chem.* **2015**, *80* (15), 7642–7651.

(28) Huang, H.; Jia, K.; Chen, Y. *ACS Catal.* **2016**, *6* (8), 4983–4988.

(29) Wayner, D. D. M.; McPhee, D. J.; Griller, D. *J. Am. Chem. Soc.* **1988**, *110* (1), 132–137.

(30) Lukeman, M. In *CRC Handbook of Organic Photochemistry and Photobiology*; Griesbeck, A., Oelgemoeller, M., Ghetti, F., Eds.; CRC Press: Boca Raton, 2012; pp 715–726.

(31) Boscà, F.; Marin, M. L.; Miranda, M. A. In *CRC Handbook of Organic Photochemistry and Photobiology*; Horspool, W., Lenci, F., Eds.; CRC Press: Boca Raton, 2004; pp 64-1/64-10.

(32) Epling, G. A.; Lopes, A. *J. Am. Chem. Soc.* **1977**, *99* (8), 2700–2704.

(33) Albini, A.; Fagnoni, M. In *Photochemically-Generated Intermediates in Synthesis*; Wiley: Hoboken, 2013.

(34) Ravelli, D.; Protti, S.; Fagnoni, M. *J. Org. Chem.* **2015**, *80* (2), 852–858.

(35) Murphy, J. J.; Bastida, D.; Paria, S.; Fagnoni, M.; Melchiorre, P. *Nature* **2016**, *532* (7598), 218–222.

(36) Symeonidis, T. S.; Tamiolakis, I.; Armatas, G. S.; Lykakis, I. N. *Photochem. Photobiol. Sci.* **2015**, *14* (3), 563–568.

(37) Yamada, K.; Okada, M.; Fukuyama, T.; Ravelli, D.; Fagnoni, M.; Ryu, I. *Org. Lett.* **2015**, *17* (5), 1292–1295.

(38) Qrareya, H.; Dondi, D.; Ravelli, D.; Fagnoni, M. *ChemCatChem* **2015**, *7* (20), 3350–3357.

(39) Halperin, S. D.; Fan, H.; Chang, S.; Martin, R. E.; Britton, R. *Angew. Chem. Int. Ed.* **2014**, *53* (18), 4690–4693.

(40) Ravelli, D.; Zoccolillo, M.; Mella, M.; Fagnoni, M. *Adv. Synth. Catal.* **2014**, *356* (13), 2781–2786.

(41) Okada, M.; Fukuyama, T.; Yamada, K.; Ryu, I.; Ravelli, D.; Fagnoni, M. *Chem. Sci.* **2014**, *5* (7), 2893–2898.

(42) Montanaro, S.; Ravelli, D.; Merli, D.; Fagnoni, M.; Albini, A. *Org. Lett.* **2012**, *14* (16), 4218–4221.

(43) Waele, V. De; Poizat, O.; Fagnoni, M.; Bagno, A.; Ravelli, D. *ACS Catal.* **2016**, *6* (10), 7174–7182.

(44) Marken, F.; Neudeck, A.; Bond, A. M.; Marken, F.; Neudeck, A.; Bond, A. M. *Cyclic voltammetry*; Scholz, F., Ed.; Springer: Berlin, 2002.

(45) Yamase, T.; Takabayashi, N.; Kaji, M. *J. Chem. Soc. Dalt. Trans.* **1984**, *0* (5), 793.

(46) Renneke, R. F.; Pasquali, M.; Hill, C. L. *J. Am. Chem. Soc.* **1990**, *112* (18), 6585–6594.

(47) Hayamizu, T.; Maeda, H.; Ikeda, M.; Mizuno, K. *Tetrahedron Lett.* **2001**, *42* (12), 2361–

2364.

(48) Cermenati, L.; Albini, A.; Cermenati, L.; Richter, C.; Albini, A. *Chem. Commun.* **1998**, No. 7, 805–806.

(49) Cermenati, L.; Mella, M.; Albini, A. *Tetrahedron* **1998**, *54* (11), 2575–2582.

(50) Tyson, E. L.; Farney, E. P.; Yoon, T. P. *Org. Lett.* **2012**, *14* (4), 1110–1113.

(51) Ravelli, D.; Albini, A.; Fagnoni, M. *Chem. Eur. J.* **2011**, *17* (2), 572–579.

(52) Abel, B.; Assmann, J.; Buback, M.; Grimm, C.; Kling, M.; Schmatz, S.; Schroeder, J.; Witte, T. *J. Phys. Chem. A* **2003**, *107* (45), 9499–9510.

(53) Fagnoni, M.; Mella, M.; Albini, A. *J. Am. Chem. Soc.* **1995**, *117* (30), 7877–7881.

(54) Guirado, G.; Fleming, C. N.; Lingenfelter, T. G.; Williams, M. L.; Zuilhof, H.; Dinnocenzo, J. P. *J. Am. Chem. Soc.* **2004**, *126* (43), 14086–14094.

(55) Jeffrey, J. L.; Petronijević, F. R.; Macmillan, D. W. C. *J. Am. Chem. Soc.* **2015**, *137* (26), 8404–8407.

(56) Itoh, A.; Kodama, T.; Inagaki, S.; Masaki, Y. *Org. Lett.* **2000**, *2* (3), 331–333.

(57) Habibi, M. H.; Farhadi, S. *Tetrahedron Lett.* **1999**, *40*, 2821–2824.

(58) Capaldo, L.; Riccardi, R.; Ravelli, D.; Fagnoni, M. *ACS Catal.* **2018**, *8* (1), 304–309.

(59) Chatgilialoglu, C.; Crich, D.; Komatsu, M.; Ryu, I. *Chem. Rev.* **1999**, *99* (8), 1991–2070.

(60) Moteki, S. A.; Usui, A.; Selvakumar, S.; Zhang, T.; Maruoka, K. *Angew. Chem. Int. Ed.* **2014**, *53* (41), 11060–11064.

(61) Papadopoulos, G. N.; Limnios, D.; Kokotos, C. G. *Chem. Eur. J.* **2014**, *20*, 13811–13814.

(62) Yadav, V. K.; Srivastava, V. P.; Yadav, L. D. S. *Tetrahedron Lett.* **2016**, *57* (23), 2502–2505.

(63) Papadopoulos, G. N.; Kokotos, C. G. *Chem. Eur. J.* **2016**, *22* (20), 6964–6967.

(64) Luo, Y.-R. *Handbook of bond dissociation energies in organic compounds*; CRC Press LLC: Boca Raton, 2000.

(65) Ravelli, D.; Protti, S.; Fagnoni, M. *Acc. Chem. Res.* **2016**, *49* (10), 2232–2242.

(66) Halperin, S. D.; Kwon, D.; Holmes, M.; Regalado, E. L.; Campeau, L. C.; Dirocco, D. A.; Britton, R. *Org. Lett.* **2015**, *17* (21), 5200–5203.

(67) Esposti, S.; Dondi, D.; Fagnoni, M.; Albini, A. *Angew. Chem. Int. Ed.* **2007**, *46* (14), 2531–2534.

(68) Ryu, I.; Tani, A.; Fukuyama, T.; Ravelli, D.; Montanaro, S.; Fagnoni, M. *Org. Lett.* **2013**, *15* (10), 2554–2557.

(69) Capaldo, L.; Fagnoni, M.; Ravelli, D. *Chem. Eur. J.* **2017**, *23* (27), 6527–6530.

(70) Quattrini, M. C.; Fujii, S.; Yamada, K.; Fukuyama, T.; Ravelli, D.; Fagnoni, M.; Ryu, I. *Chem. Commun.* **2017**, *53* (15), 2335–2338.

(71) Abrams, D. J.; West, J. G.; Sorensen, E. J. *Chem. Sci.* **2017**, *8* (3), 1954–1959.

(72) Prier, C. K.; Rankic, D. a.; MacMillan, D. W. C. *Chem. Rev.* **2013**, *113* (7), 5322–5363.

(73) Ravelli, D.; Protti, S.; Fagnoni, M. *Chem. Rev.* **2016**, *116* (17), 9850–9913.

(74) Douglas, J. J.; Sevrin, M. J.; Stephenson, C. R. J. *Org. Proc. Res. Dev.* **2016**, *20* (7), 1134–1147.

(75) Yoshida, J. ichi; Itoh, M.; Matsunaga, S. ichiro; Isoe, S. *J. Org. Chem.* **1992**, *57* (18), 4877–4882.

(76) Nakajima, M.; Fava, E.; Loescher, S.; Jiang, Z.; Rueping, M. *Angew. Chem. Int. Ed.* **2015**, *54* (30), 8828–8832.

(77) Yoshida, J. I.; Kataoka, K.; Horcajada, R.; Nagaki, A. *Chem. Rev.* **2008**, *108* (7), 2265–2299.

(78) Zhou, C.; Li, P.; Zhu, X.; Wang, L. *Org. Lett.* **2015**, *17* (24), 6198–6201.

(79) Cheng, W. M.; Shang, R.; Yu, H. Z.; Fu, Y. *Chem. Eur. J.* **2015**, *21* (38), 13191–13195.

(80) Wang, G. Z.; Shang, R.; Cheng, W. M.; Fu, Y. *Org. Lett.* **2015**, *17* (19), 4830–4833.

(81) Chu, L.; Lipshultz, J. M.; MacMillan, D. W. C. *Angew. Chem. Int. Ed.* **2015**, *54* (27), 7929–7933.

(82) Gu, L.; Jin, C.; Liu, J.; Zhang, H.; Yuan, M.; Li, G. *Green Chem.* **2016**, *18* (5), 1201–1205.

(83) Xiao, T.; Li, L.; Zhou, L. *J. Org. Chem.* **2016**, *81* (17), 7908–7916.

(84) Xu, N.; Li, P.; Xie, Z.; Wang, L. *Chem. Eur. J.* **2016**, *22* (7), 2236–2242.

(85) Bergonzini, G.; Cassani, C.; Lorimer-Olsson, H.; Hörberg, J.; Wallentin, C.-J. *Chem. A Eur. J.* **2016**, *22* (10), 3292–3295.

(86) Li, C. G.; Xu, G. Q.; Xu, P. F. *Org. Lett.* **2017**, *19* (3), 512–515.

(87) Page, P. C. B.; Klair, S. S.; Rosenthal, S. *Chem. Soc. Rev.* **1990**, *19* (2), 147.

(88) Patrocínio, A. F.; Moran, P. J. S. *J. Braz. Chem. Soc.* **2001**, *12* (1), 7–31.

(89) Zhang, H.-J.; Priebbenow, D. L.; Bolm, C. *Chem. Soc. Rev.* **2013**, *42* (21), 8540.

(90) Kirihara, M.; Suzuki, S.; Ishihara, N.; Yamazaki, K.; Akiyama, T.; Ishizuka, Y. *Synthesis* **2017**, *49*, 2009–2014.

(91) Haas, M.; Schuh, L.; Torvisco, A.; Stueger, H.; Grogger, C. *Phosphorus. Sulfur. Silicon Relat. Elem.* **2016**, *191*, 638–640.

(92) Nikolaev, A.; Orellana, A. *Org. Lett.* **2015**, *17* (23), 5796–5799.

(93) Lu, P.; Feng, C.; Loh, T. P. *Org. Lett.* **2015**, *17* (13), 3210–3213.

(94) Cirriez, V.; Rasson, C.; Riant, O. *Adv. Synth. Catal.* **2013**, *355* (16), 3137–3140.

(95) Ruiz, J.; Karre, N.; Roisnel, T.; Chandrasekhar, S.; Grée, R. *Eur. J. Org. Chem.* **2016**, *2016* (4), 773–779.

(96) Ando, M.; Sasaki, M.; Miyashita, I.; Takeda, K. *J. Org. Chem.* **2015**, *80* (1), 247–255.

(97) Marri, G.; Reddy, J. S.; Ruiz, J.; Das, S.; Grée, R. *Eur. J. Org. Chem.* **2015**, *2015* (4), 840–846.

(98) Rong, J.; Oost, R.; Desmarchelier, A.; Minnaard, A. J.; Harutyunyan, S. R. *Angew. Chem. Int. Ed*. **2015**, *54* (10), 3038–3042.

(99) Wu, L.; Li, G.; Fu, Q.; Yu, L.; Tang, Z. *Org. Biomol. Chem.* **2013**, *11* (3), 443–447.

(100) Mattson, A. E.; Bharadwaj, A. R.; Zuhl, A. M.; Scheidt, K. A. *J. Org. Chem.* **2006**, *71* (15), 5715–5724.

(101) Mattson, A. E.; Scheidt, K. A. *Org. Lett.* **2004**, *6* (23), 4363–4366.

(102) Mattson, A. E.; Bharadwaj, A. R.; Scheidt, K. A. *J. Am. Chem. Soc.* **2004**, *126* (8), 2314–

2315.

(103) Degl'Innocenti, A.; Ricci, A.; Mordini, A.; Reginato, G.; Colotta, V. *Gazz. Chim. Ital.* **1987**, *117*, 645–648.

(104) Labarre-Lainé, J.; Beniazza, R.; Desvergnes, V.; Landais, Y. *Org. Lett.* **2013**, *15* (18), 4706–4709.

(105) Yoshida, J. -i.; Matsunaga, S. -i.; Isoe, S. *Tetrahedron Lett.* **1989**, *30*, 5293–5296.

(106) Duff, J. M.; Brook, A. G. *Can. J. Chem.* **1973**, *51*, 2869–2883.

(107) Bourque, R. A.; Davis, P. D.; Dalton, J. C. *J. Am. Chem. Soc.* **1981**, *103* (3), 697–699.

(108) Dalton, J. C.; Bourque, R. A. *J. Am. Chem. Soc.* **1981**, *103* (3), 699–700.

(109) Zhang, H.-J.; Becker, P.; Huang, H.; Pirwerdjan, R.; Pan, F.-F.; Bolm, C. *Adv. Synth. Catal.* **2012**, *354* (11–12), 2157–2161.

(110) Becker, P.; Priebbenow, D. L.; Pirwerdjan, R.; Bolm, C. *Angew. Chem. Int. Ed.* **2014**, *53* (1), 269–271.

(111) Becker, P.; Pirwerdjan, R.; Bolm, C. *Angew. Chem. Int. Ed.* **2015**, *54* (51), 15493–15496.

(112) Ito, K.; Tamashima, H.; Iwasawa, N.; Kusama, H. *J. Am. Chem. Soc.* **2011**, *133* (11), 3716–3719.

(113) Tanielian, C.; Seghrouchni, R.; Schweitzer, C. *J. Phys. Chem. A* **2003**, *107* (8), 1102–1111.

(114) Duncan, D. C.; Fox, M. A. *J. Phys. Chem. A* **1998**, *102* (24), 4559–4567.

(115) Tsudaka, T.; Kotani, H.; Ohkubo, K.; Nakagawa, T.; Tkachenko, N. V; Lemmetyinen, H.; Fukuzumi, S. *Chem. Eur. J.* **2017**, *23* (6), 1306–1317.

(116) Romero, N. A.; Nicewicz, D. A. *Chem. Rev.* **2016**, *116* (17), 10075–10166.

(117) Haga, M.-A.; Dodsworth, E. S.; Eryavec, G.; Seymour, P.; Lever, A. B. P. *Inorg. Chem.* **1985**, *24* (12), 1901–1906.

(118) Romero, N. A.; Nicewicz, D. A. *J. Am. Chem. Soc.* **2014**, *136* (49), 17024–17035.

(119) Fagnoni, M.; Bonassi, F.; Palmieri, A.; Protti, S.; Ravelli, D.; Ballini, R. *Adv. Synth. Catal.* **2014**, *356* (4), 753–758.

(120) Dondi, D.; Fagnoni, M.; Albini, A. *Chem. Eur. J.* **2006**, *12* (15), 4153–4163.

(121) Miyake, Y.; Nakajima, K.; Nishibayashi, Y. *J. Am. Chem. Soc.* **2012**, *134* (7), 3338–3341.

(122) Koutoulogenis, G. S.; Kokotou, M. G.; Voutyritsa, E.; Limnios, D.; Kokotos, C. G. *Org. Lett.* **2017**, *19* (7), 1760–1763.

(123) Hamilton, D. S.; Nicewicz, D. A. *J. Am. Chem. Soc.* **2012**, *134* (45), 18577–18580.

(124) Grandjean, J. M. M.; Nicewicz, D. A. *Angew. Chem. Int. Ed.* **2013**, *52* (14), 3967–3971.

(125) Ohkubo, K.; Mizushima, K.; Iwata, R.; Souma, K.; Suzuki, N.; Fukuzumi, S. *Chem. Commun.* **2010**, *46* (4), 601–603.

(126) Bortolamei, N.; Isse, A. A.; Gennaro, A. *Electrochim. Acta* **2010**, *55* (27), 8312–8318.

CHAPTER 3

PHOTOCATALYSIS VIA HYDROGEN ATOM TRANSFER

Chapter 3 deals with a relatively underrated activation pathway in photocatalysis, *i.e.* Hydrogen Atom Transfer.[1]

Hydrogen atom transfer (HAT) is a chemical transformation consisting of the concerted movement of two elementary particles, namely a proton and an electron, between two substrates in a single kinetic step[2,3] according to Equation (3.1).

$$A_1\text{–}H + A_2 \rightarrow A_1 + A_2\text{–}H \qquad \text{(eq. 3.1)}$$

Conceptually, HAT can be considered a subclass of the larger family of proton-coupled electron transfer (PCET) processes, in which the proton and the electron move together, sharing the starting and the final orbitals.[4]

Significantly, HAT represents a key step in a wide variety of chemical reactions, including the combustion of hydrocarbons and aerobic oxidations, and it is involved in several atmospheric phenomena as well. In biology, several metalloenzymes are known to operate through a HAT step, and the role of such processes in the destructive effects of reactive oxygen species (ROS) in vivo and in the mechanism of action of antioxidants is studied in depth. [2,3,5–7] Besides, photocatalyzed HAT has been used in organic synthesis as a powerful and versatile strategy for the activation of several substrates. In these reactions, no preliminary manipulation of the substrate is needed (for example, introduction of an electroactive moiety), and a C-H bond is selectively broken. This activation may occur either directly (*d*-HAT) or indirectly (*i*-HAT).

As for the former, the excited state of a photocatalyst (PC*) abstracts a H-atom directly from the substrate (Scheme 3.1).[8] The catalytic cycle is then closed by means of a back-HAT step (dashed arrow) to one of the intermediates formed during the process.

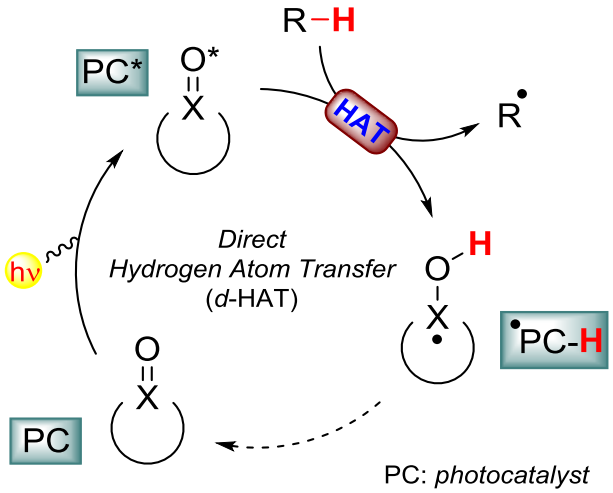

Scheme 3.1 Typical reaction mechanism involving a direct HAT approach.

So far, the number of available photocatalysts able to perform this chemistry has been quite limited[8] and actually restricted to the families of aromatic ketones[9–11] and polyoxometalates (particularly, the decatungstate anion $[W_{10}O_{32}]^{4-}$).[12,13]

On the other hand, as for *i*-HAT, PC* can be exploited to generate a thermal H-abstractor by interaction with a suitable species Y-W(H), according to three different mechanisms (Scheme 3.2).

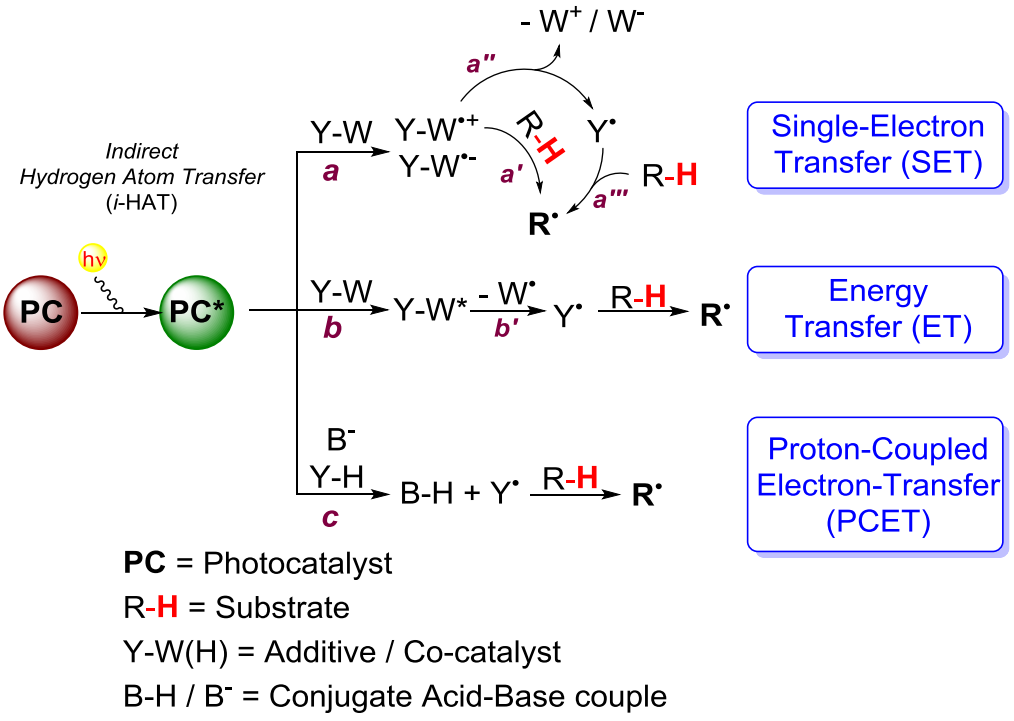

Scheme 3.2 Typical reaction mechanisms involving an indirect HAT approach.

The first possibility is to take advantage of the intrinsic capability of excited states to act as oxidants or reductants. Accordingly, PC* can promote a single electron transfer step (SET; *path a*), thus converting Y-W to the corresponding radical ion (either $Y\text{-}W^{\bullet+}$ or $Y\text{-}W^{\bullet-}$). This intermediate could be engaged directly in a HAT step with the substrate R-H (*path a'*)[14,15] or undergo the loss of a charged moiety (W^+ or W^-) to give a H-abstractor species $Y^\bullet$ (*paths a''* and *a'''*).[16–19] An alternative option involves an energy transfer step (ET; *path b*) between PC* and Y-W. The resulting excited species Y-W* then undergoes homolytic fragmentation, generating a thermal H-abstractor ($Y^\bullet$, *path b'*) prone to activate R-H via HAT.[20] Finally, PC* can promote a PCET with an additive Y-H, also involving a suitable base (B^-). As a result, radical $Y^\bullet$ is formed, in turn able to promote the desired HAT step (*path c*).[21]

As already mentioned in Chapter 2, my group has a pluriannual expertise in the use of the decatungstate anion $[W_{10}O_{32}]^{4-}$ in the role of PC_{HAT} (λ_{exc}=323 nm): upon absorption of a photon, this compound can promote an efficient homolytic cleavage of C-H bonds in a variety of organic derivatives. Accordingly, we achieved the smooth C-H functionalization of aldehydes, amides, ethers and acetals, as well as alkanes, by trapping these radicals with electron-poor olefins such as unsaturated esters, nitriles and ketones, along with maleimide and maleic anhydride (Giese or Stetter reaction)[12] or, more recently, with heterocycles (Minisci reaction).[22]

Accordingly, I decided to take advantage of this peculiar reactivity of TBADT to design a new synthetic protocol via *d*-HAT based on the use of vinylpyridines in the role of electron-poor olefins in a photocatalyzed Giese addition.

VINYLPYRIDINES AS BUILDING BLOCKS FOR THE PHOTOCATALYZED SYNTHESIS OF ALKYLPYRIDINES[23]

Introduction

My group has sought for a long time a way to use vinylaromatics in a synthetic protocol based on photocatalyzed HAT, however any attempt to use them in the functionalization of a vast array of organic derivatives was unsuccessful, mainly due to the lurking photochemical polymerization,[24,25] often triggered by direct absorption of light (see Chapter 1). Moreover, the excited state of TBADT is strongly electrophilic in character and shows a preference for the abstraction of nucleophilic hydrogens, thus generating nucleophilic radicals. Due to this polarity, only electrophilic C=C double bonds can efficiently trap them while, when moving to electron-rich styrene, trapping is highly disfavored.

In light of this, I reasoned that a more electron deficient vinylaromatic would allow to overcome the mismatched polarity. Remarkably, I found out that vinylpyridines were not only good radical traps because of their inherent electron-poor behavior, but also a convenient starting point for the synthesis of valuable compounds, *i.e.* alkylpyridines, well known for their antibiotic, antimycotic and cytotoxic activity (Figure 3.1).[26]

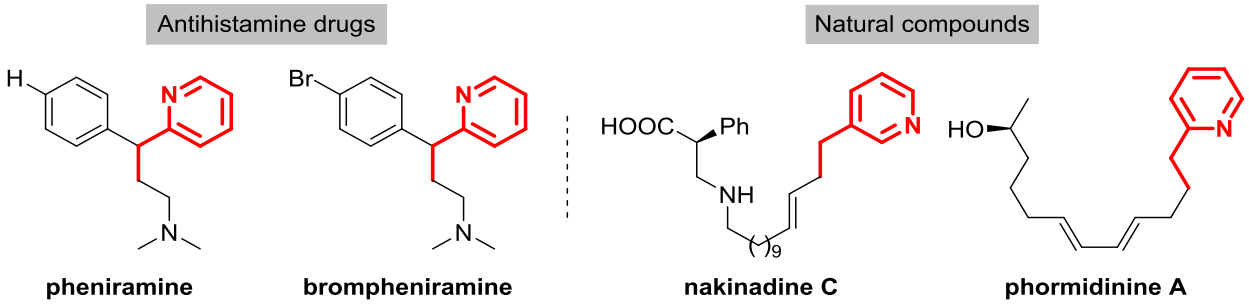

Figure 3.1 Alkylpyridine motif is present in several bioactive compounds such as antihistamine drugs and natural compounds.

Additionally, substituted alkylpyridines were recently investigated for their peculiar umami flavor[27,28] or as polar surfactants.[29]

From a synthetic standpoint, vinylpyridines are useful substrates for the preparation of alkylpyridines via direct addition of nucleophiles onto the double bond. Different strategies are known for the C-alkylation of ethenylpyridines via addition of C-nucleophiles (benzyl anions[30] or enolate anions[31–33]), under reductive conditions,[34] under acid-catalyzed,[35] NHC-catalyzed[36] or metal-catalyzed[37–39] conditions. Recently, an interesting organocatalytic enantioselective addition of aldehydes onto vinylpyridines has been likewise described.[40]

Another mild approach involves the addition of carbon-centered radicals onto the double bond. A dated example is the functionalization of 4-vinylpyridine by photodecomposition of alkylmercury halides (Scheme 3.3, *path a*).[41] In another instance, the thermal generation of radicals was achieved starting from alkyl halides, through a Zn-promoted reaction (*path b*).[42] Quite surprisingly, only a few examples were reported for the functionalization of vinylpyridines by means of photoredox catalysis (*path c*), contrary to the several examples published on styrenes.[43,44] Actually, only α-carbonyl,[45] α-oxy[46] and α-amino radicals[47,48] were smoothly generated and used for the preparation of alkylpyridines (*path c*). Carbon-centered radicals obtained by a photocatalyzed proton-coupled electron transfer on *N*-arylamide derivatives were likewise trapped by 2-vinylpyridine.[49]

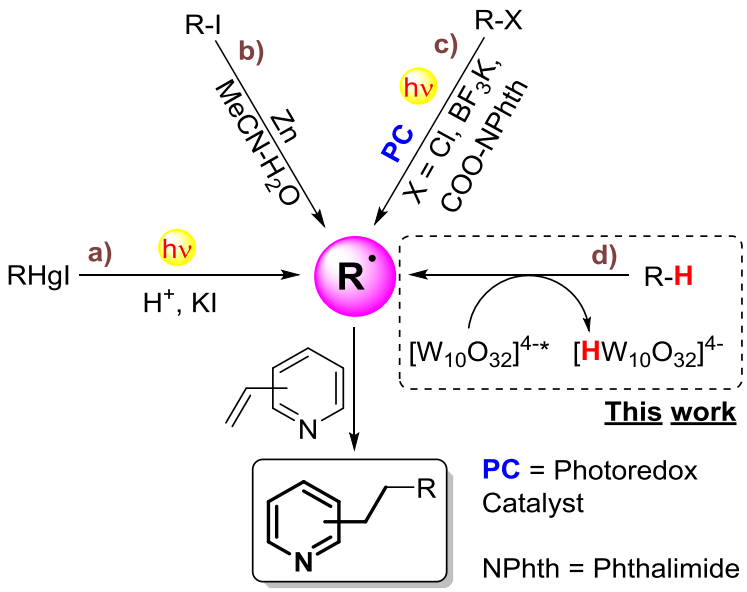

Scheme 3.3 Generation of carbon-based radicals (R•) by cleavage of a R-X (paths a-c) and a R-H bond (this work, path d) for the synthesis of alkylpyridines.

In all the radical-based strategies discussed so far, an X group must be present in the radical precursor to promote the cleavage of the C-X bond and the ensuing radical formation. By contrast, the direct generation of radicals by cleavage of a C-H bond still represents a harsh challenge and has not been exploited for vinylpyridines derivatization so far.

I surmised that the formation of carbon-centered radicals could be attained by a homolytic C-H cleavage via a hydrogen atom transfer (HAT)[1,8] by using a decatungstate salt (TBADT, $(nBu_4N)_4[W_{10}O_{32}]$) as the photocatalyst (Scheme 3.3, *path d*).[12,50–56]

Results and discussion

To test the feasibility of the combination of a photocatalytic HAT approach with vinylpyridines, I started by choosing a model reaction. I tested the addition of cyclohexane (**3.1g**) onto 4-vinylpyridine (**2.2r**) to give 4-(2-cyclohexylethyl)pyridine (**3.9**) as a model reaction (Table 3.1).

Table 3.1 Optimization of reaction conditions.

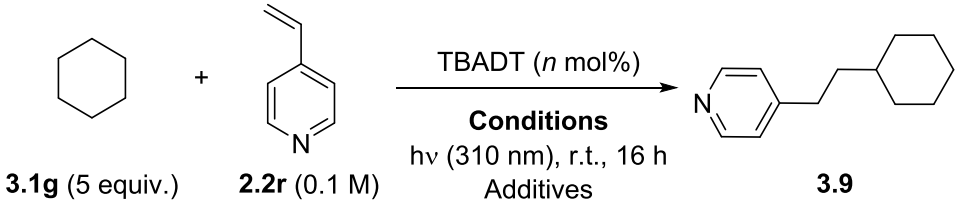

Entry	**TBADT** (mol %)	Solvent	Additive	Yield[a]
1	-	MeCN	-	traces[b]
2	1	MeCN	-	50%
3	**2**	**MeCN**	**-**	**68%**
4	4	MeCN	-	49%
5	2	MeCN/H_2O 9:1	-	12%
6	2	MeCN/CH_2Cl_2 9:1	-	18%
7	2	MeCN	PTSA	n.d.[c]
8	2	MeCN	MSA	n.d.[c]
9	2	MeCN	BA	45%[d]

PTSA: p-toluenesulfonic acid; MSA: methanesulfonic acid; BA: benzoic acid
*[a] GC yields based on **2.2r** conversion have been reported, adopting dodecane as external standard. A quantitative **2.2r** conversion took place, except where otherwise noted. [b] 75% consumption of **2.2r**; GC analysis revealed a very complex mixture and a thick film formed on the test tube walls. [c] The addition of the acid caused a precipitation of the photocatalyst and the mixture was not irradiated, accordingly. [d] 60% consumption of **2.2r**.*

Given the well-known tendency of vinylaromatics to undergo polymerization, I started with a blank experiment, irradiating a MeCN solution of **3.1g** (0.5 M) and **2.2r** (0.1 M) with 10×15 W phosphor-coated lamps (λ_{IRR} centered at 310 nm). As expected, a massive precipitation of a spongy solid was observed and, despite olefin **2.2r** was almost completely consumed, only traces of the product were observed (*entry 1*). On the other hand, I was pleased to observe that the use of 1 mol% of TBADT as a photocatalyst allowed to address the reactivity of interest (*entry 2*). A rapid screening of the photocatalyst loading (*entry 3 and 4*) demonstrated that 2 mol% was the optimal concentration. Solvent screening did not result in improved yields (*entry 5 and* 6) and neither did the addition of additives capable of decreasing the LUMO energy of vinylpyridine **2.2r**, namely Brönsted acids (*entry 7-9*).

With the optimized conditions in hand, I started investigating the scope of the present approach by testing several other hydrogen donors (ethers **3.1a**, **3.1b**, acetal **3.1c**, amides **3.1d**,**3.1e**, nitrile **3.1f**, silane **3.1h** and aldehydes **3.1i-3.1m**, Chart 3.1) in the reaction with vinylpyridines **2.2r**, **3.2a-3.2f**, adopting the optimized conditions by using the minimum excess of **3.1**.

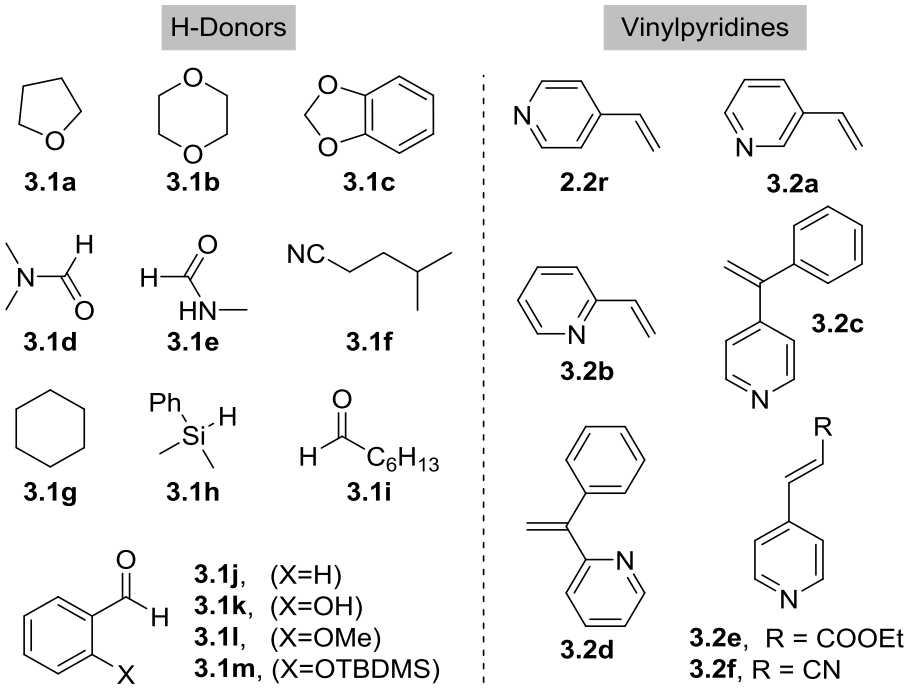

*Chart 3.1 Hydrogen donors (**3.1a-3.1m**) and vinylpyridines (**2.2r**, **3.2a-3.2f**) used in this work.*

4-Vinylpyridine (**2.2r**) was first tested and in most cases the expected products were formed in good to excellent yields (Table 3.2). As for ethers, tetrahydrofuran (**3.1a**) and 1,4-dioxane (**3.1b**) gave the Giese adducts **3.3** and **3.4** in 68 and 62% yields, respectively. A similar yield (64%; compound **3.5**) was achieved when shifting to 1,3-benzodioxole (**3.1c**) as hydrogen donor. Elective substrates for this reaction appeared to be aliphatic amides, since both *N*,*N*-dimethylformamide (**3.1d**) and *N*-methylformamide (**3.1e**) gave excellent yields of **3.6** and **3.7** (94 and 87%, respectively). The reactivity of **3.1d** was also investigated under different conditions, by changing the light source.

*Table 3.2 TBADT photocatalyzed synthesis of alkylpyridines **3.3-3.20**.*[a]

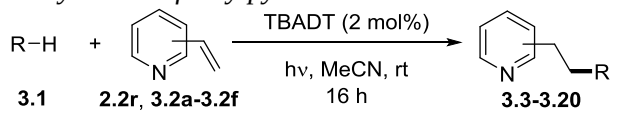

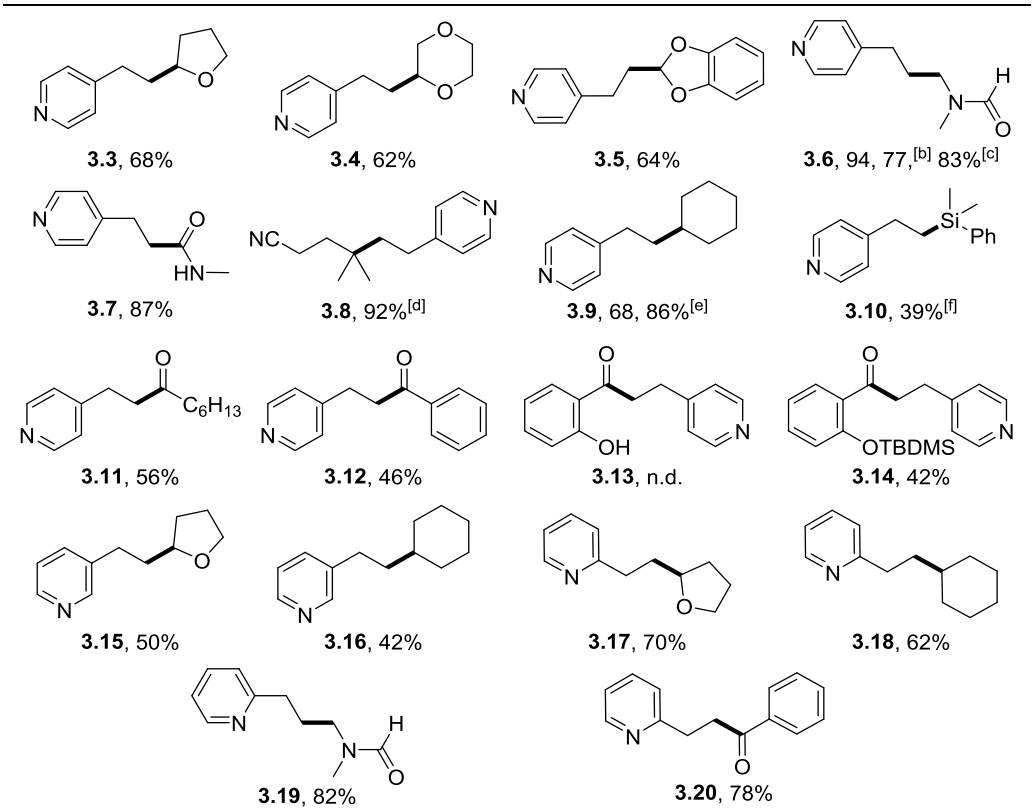

[a] *Conditions: A MeCN solution (15 mL) of **3.1a-3.1m** (1.5-7.5 mmol, 0.1-0.5 M, 1-5 equiv.) and **2.2r**, **3.2a**, **3.2b** (1.5 mmol, 0.1 M, 1 equiv.), in the presence of TBADT (2×10^{-3} M, 2 mol%) irradiated with 10×15 W phosphor-coated lamps (λ_{exc} centered at 310 nm) for 16 h. Isolated yields reported.* [b] *Irradiation carried out by placing the solution (50 mL) in a solar simulator (500 $W\cdot m^{-2}$).* [c] *Irradiation carried out by placing the solution (50 mL) in a Pyrex vessel exposed on a window ledge for 8 h.* [d] *1.6 M **3.1f**.* [e] *Reaction carried out under flow conditions (see text, Experimental section and Figure 3.2).* [f] *TBADT 4 mol%.*

As an example, formamide **3.6** was obtained in a very good yield (77%) when the reaction was performed in a solar simulator and in 83% yield when the solution was irradiated with direct sunlight in a Pyrex vessel on a window ledge (Table 3.2).

Isocapronitrile (**3.1f**) reacted with **2.2r** to afford **3.8** as the only product in 92% yield, with a complete regioselectivity towards C-H cleavage at the methine site. Noteworthy, in the preparation of alkylpyridine **3.9**, a higher yield (86% vs 68%) was obtained when carrying out the reaction under flow conditions[57,58] (flow rate = 0.2 mL/min). The flow photoreactor (total volume: 12 mL) employed here is based on a PTFE tubing (internal diameter: 1.3 mm) wrapped around an immersion well apparatus (125 W Hg vapors lamp as the light source).[55]

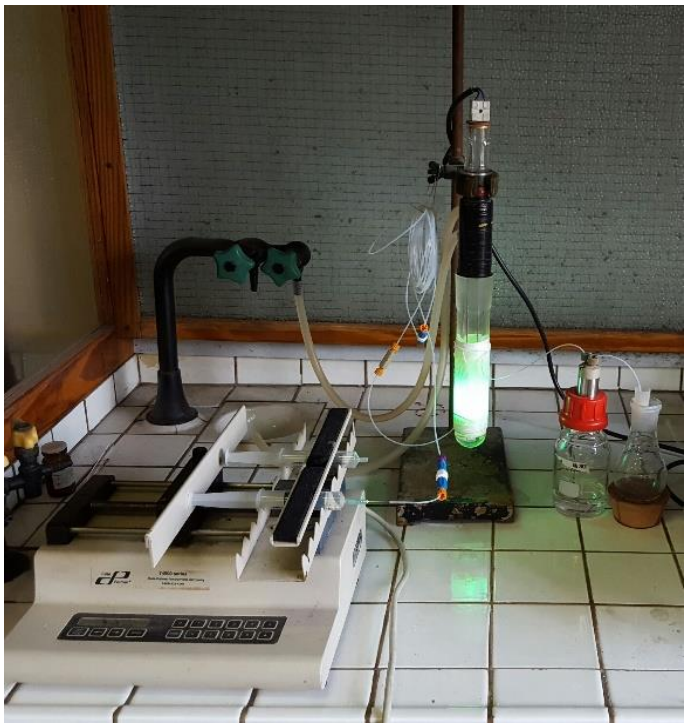

Figure 3.2 Picture of the flow reactor used in this work, equipped with a syringe pump.

4-Vinylpyridine was also capable of trapping silyl radicals, even though a higher amount of TBADT was required (4 mol%): the Si-H bond in dimethylphenylsilane (**3.1h**) was homolytically broken and trapping of the thus-formed radical afforded silane **3.10** in a modest yield (39%). Activation of C(sp^2)-H bonds in aldehydes (whether aliphatic or aromatic) allowed the preparation of unsymmetrical ketones. In particular, heptanal (**3.1i**) gave ketone **3.11** in 56% yield, whereas aromatic aldehydes gave contrasting results. While unsubstituted benzaldehyde (**3.1j**) reacted quite

well with **3.2a**, giving **3.12** in 46% yield, the reaction of salicylaldehyde (**3.1k**) to give **3.13** failed, probably due to the presence of the phenolic group.[56] Protection of the -OH group as TBDMS ether restored the usual reactivity (product **3.14** formed in 42% yield, Table 3.2, and **3.13** from it by basic treatment, see Experimental Section).

The reaction was also extended to 3-vinyl (**3.2a**) and 2-vinylpyridine (**3.2b**, Chart 3.1). Alkylated pyridines **3.15** and **3.16** were formed in 50 and 42% yield, respectively, in the photocatalyzed addition of **3.1a** and **3.1g** onto **3.2a**. By contrast, 2-vinylpyridine gave results comparable with those of **2.2r** (products **3.17**-**3.20** obtained in up to 82% yield, Table 3.2). Attempted alkylation of 2-vinylpyrazine failed due to polymerization.

With the aim to prepare compounds of potential industrial interest, **3.2b** was reacted with protected salicylaldehydes **3.1l** and **3.1m** to give ketones **3.21** and **3.22** (Scheme 3.4). In the former case, compound **3.21** was formed in the same yield under flow conditions in only 5 h. In the latter case, treatment of crude **3.22** under basic conditions (LiOH) formed phenol **3.23**. Notably, compounds **3.21** and **3.23** belong to a class of compounds mimicking the umami flavor.[27,28]

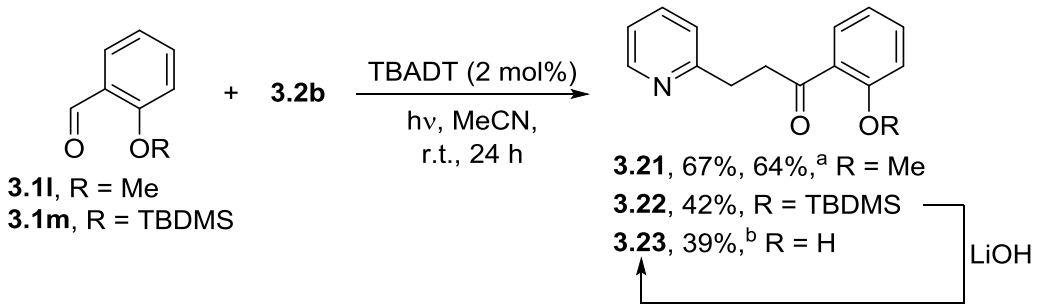

*Scheme 3.4 Photocatalyzed synthesis of derivatives **3.21** and **3.23** having umami flavor. [a] Flow conditions (time: 5 h, see Figure 3.2 and Experimental Section); [b] Yield over two steps.*

Photocatalytic addition of cyclohexane onto **3.2c** led to compound **3.24** in a good yield (71%). The versatility of the present approach made possible the smooth preparation of **3.25** (precursor of the antihistamine drug pheniramine, see Figure 3.1) in a single step and in 68% yield starting from DMF and **3.2d** (Scheme 3.5).

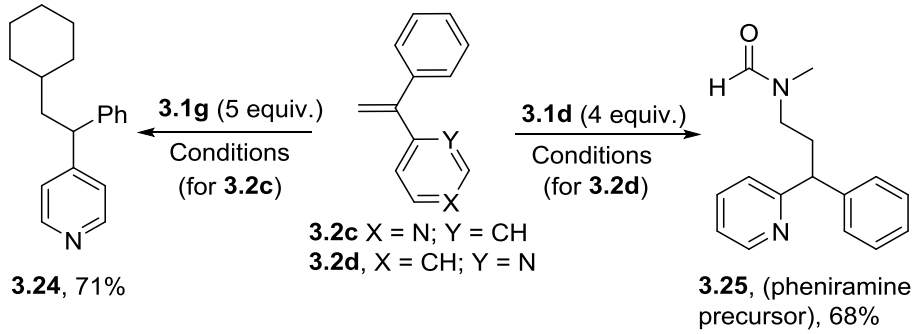

Scheme 3.5 Radical addition onto (1-phenylvinyl)pyridines and synthesis of valuable drugs intermediates.

Since the scope of the reaction evidently showed the preference for the radical attack onto the β position of vinylpyridines, I concluded that the pyridine ring actually behaved as an ordinary electron-withdrawing group (EWG) in this reaction. To qualitatively assess this behavior, vinylpyridines bearing an additional EWG such as **3.2e** and **3.2f** (see Chart 3.1) were subjected to the photocatalyzed reaction with **3.1g** (Scheme 3.6).

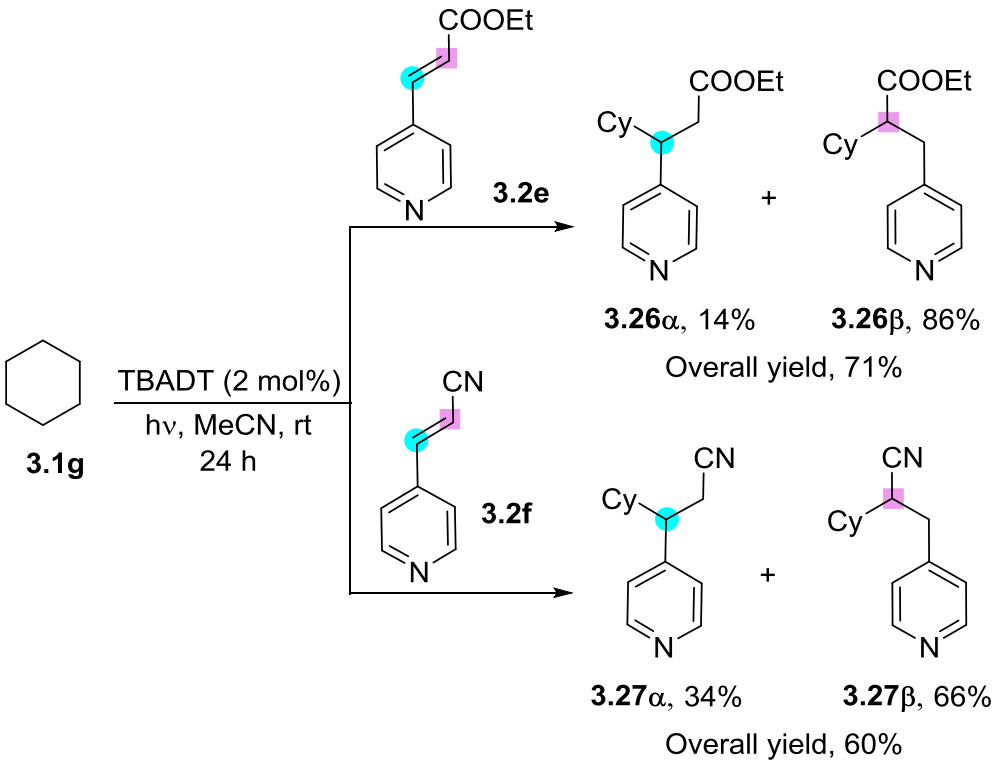

Scheme 3.6 Regioselectivity in the addition of radicals onto substituted vinylpyridines.

Compound **3.2e** gave ethyl esters **3.26** as a mixture of isomers (α/β ratio of 14:86) in a 71% overall yield, whereas olefin **3.2f** afforded nitriles **3.27** (α/β ratio of 34:66) in a 60% yield. The

regioselectivity observed in compound **3.2e** is similar to that found in the cyclohexyl radical addition onto ethyl cinnamate.[59–61]

From these experiments, it is possible to observe a trend in terms of regioselectivity: the pyridine ring has a more powerful β-directing effect than the cyano group, while the ester group is the weakest in the series.

In light of what presented so far, it is proposed that the formation of carbon-centered radicals is promoted by excited TBADT via a hydrogen atom transfer reaction (Scheme 3.7).[1,8,12] Vinylpyridines behave as radical traps and regioselective addition at the β position smoothly takes place. The efficient back hydrogen donation from $[HW_{10}O_{32}]^{4-}$ to the adduct radical hampered the otherwise fast polymerization of vinylpyridines.[24,62]

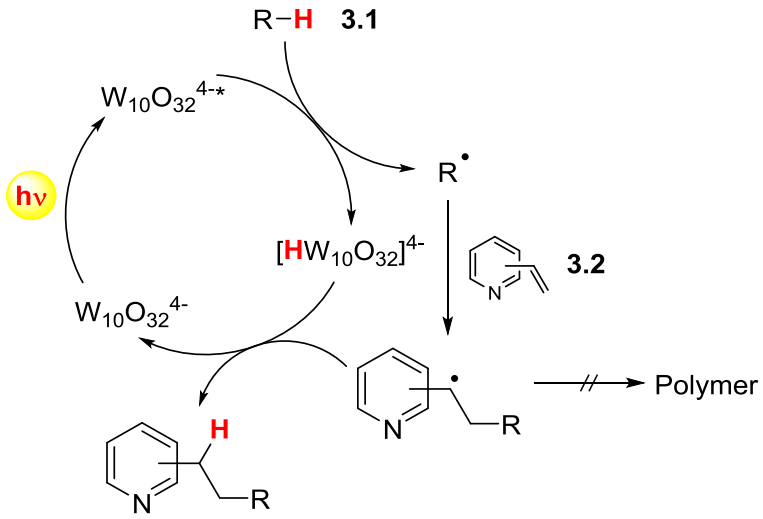

Scheme 3.7 Proposed reaction mechanism.

Moreover, the high absorptivity of TBADT at the wavelength used prevented light absorption of the starting vinylpyridines (see Figure S.3.2 in Experimental Section) and of the products. This was beneficial to the overall process, since it avoided again a photopolymerization of **3.2**[24,62] and at the same time made negligible intramolecular hydrogen abstraction side reactions from the resulting 2-alkylpyridines.[63]

Conclusions

In conclusion, I have demonstrated that vinylpyridines are interesting building blocks for the preparation of valuable alkylpyridines via a TBADT-photocatalyzed HAT process. These compounds have both biological (**3.25**) and commercial relevance (compounds **3.21** and **3.23** endowed with the umami flavor). The process is very simple and can be also carried out both under sunlight irradiation and under flow conditions.

References

(1) Capaldo, L.; Ravelli, D. *Eur. J. Org. Chem.* **2017**, *2017* (15), 2056–2071.

(2) *Hydrogen-Transfer Reactions*; Hynes, J. T., Klinman, J. P., Limbach, H.-H., Schowen, R. L., Eds.; Wiley-VCH Verlag GmbH & Co. KGaA: Weinheim, Germany, 2006.

(3) *Encyclopedia of Radicals in Chemistry, Biology and Materials*; Chatgilialoglu, C., Studer, A., Eds.; John Wiley & Sons, Ltd: Chichester, UK, 2012.

(4) Hammes-Schiffer, S.; Stuchebrukhov, A. A. *Chem. Rev.* **2010**, *110* (12), 6939–6960.

(5) Ortiz de Montellano, P. R. *Chem. Rev.* **2010**, *110* (2), 932–948.

(6) *Cytochrome P450*; Ortiz de Montellano, P. R., Ed.; Springer US: Boston, MA, 2005.

(7) Ingold, K. U.; Pratt, D. A. *Chem. Rev.* **2014**, *114* (18), 9022–9046.

(8) Protti, S.; Fagnoni, M.; Ravelli, D. *ChemCatChem* **2015**, *7* (10), 1516–1523.

(9) Ravelli, D.; Fagnoni, M.; Albini, A. *Chem. Soc. Rev.* **2013**, *42* (1), 97–113.

(10) Hoffmann, N. *Synthesis* **2016**, *48* (12), 1782–1802.

(11) Oelgemöller, M.; Hoffmann, N. *Pure Appl. Chem.* **2015**, *87* (6).

(12) Ravelli, D.; Protti, S.; Fagnoni, M. *Acc. Chem. Res.* **2016**, *49* (10), 2232–2242.

(13) Tzirakis, M. D.; Lykakis, I. N.; Orfanopoulos, M. *Chem. Soc. Rev.* **2009**, *38* (9), 2609.

(14) Zhang, X.; MacMillan, D. W. C. *J. Am. Chem. Soc.* **2017**, *139* (33), 11353–11356.

(15) Tyson, E. L.; Niemeyer, Z. L.; Yoon, T. P. *J. Org. Chem.* **2014**, *79* (3), 1427–1436.

(16) Jin, J.; MacMillan, D. W. C. *Nature* **2015**, *525* (7567), 87–90.

(17) Cuthbertson, J. D.; MacMillan, D. W. C. *Nature* **2015**, *519* (7541), 74–77.

(18) Keylor, M. H.; Park, J. E.; Wallentin, C.-J.; Stephenson, C. R. J. *Tetrahedron* **2014**, *70* (27–28), 4264–4269.

(19) Jouffroy, M.; Kelly, C. B.; Molander, G. A. *Org. Lett.* **2016**, *18* (4), 876–879.

(20) Devari, S.; Rizvi, M. A.; Shah, B. A. *Tetrahedron Lett.* **2016**, *57* (30), 3294–3297.

(21) Choi, G. J.; Zhu, Q.; Miller, D. C.; Gu, C. J.; Knowles, R. R. *Nature* **2016**, *539* (7628), 268–

271.

(22) Quattrini, M. C.; Fujii, S.; Yamada, K.; Fukuyama, T.; Ravelli, D.; Fagnoni, M.; Ryu, I. *Chem. Commun.* **2017**, *53* (15), 2335–2338.

(23) Capaldo, L.; Fagnoni, M.; Ravelli, D. *Chem. Eur. J.* **2017**, *23* (27), 6527–6530.

(24) Lewis, G. T.; Nguyen, V.; Cohen, Y. *J. Polym. Sci. Part A Polym. Chem.* **2007**, *45* (24), 5748–5758.

(25) Krüger, K.; Tauer, K.; Yagci, Y.; Moszner, N. *Macromolecules* **2011**, *44* (24), 9539–9549.

(26) Pinder, A. R. *Nat. Prod. Rep.* **1992**, *9* (5), 491.

(27) Bhowmik, T.; Wang, Y.; Krawec, P. V. Taste Enhancement. WO2012035032 (A3), 2012.

(28) Wang, Y.; Daniher, A.; Klerk, A. De; Winkel, C. Pyridine derivatives with umami flavour. US9173424 (B2), 2015.

(29) Ghatee, M. H.; Fotouhabadi, Z.; Zolghadr, A. R.; Borousan, F.; Ghanavati, F. *Ind. Eng. Chem. Res.* **2013**, *52* (37), 13384–13392.

(30) Quagliotto, P.; Viscardi, G.; Barolo, C.; Barni, E.; Bellinvia, S.; Fisicaro, E.; Compari, C. *J. Org. Chem.* **2003**, *68* (20), 7651–7660.

(31) Jónsson, S.; Odille, F. G. J.; Norrby, P.-O.; Wärnmark, K. *Org. Biomol. Chem.* **2006**, *4* (10), 1927–1948.

(32) Tang, S.; Gao, X.; Lei, A. *Adv. Synth. Catal.* **2016**, *358* (18), 2878–2882.

(33) Majima, S.; Shimizu, Y.; Kanai, M. *Tetrahedron Lett.* **2012**, *53* (33), 4381–4384.

(34) Maekawa, H.; Nishiyama, Y. *Tetrahedron* **2015**, *71* (38), 6694–6700.

(35) Gill, A. L.; Frederickson, M.; Cleasby, A.; Woodhead, S. J.; Carr, M. G.; Woodhead, A. J.; Walker, M. T.; Congreve, M. S.; Devine, L. A.; Tisi, D.; O'Reilly, M.; Seavers, L. C. A.; Davis, D. J.; Curry, J.; Anthony, R.; Padova, A.; Murray, C. W.; Carr, R. A. E.; Jhoti, H. *J. Med. Chem.* **2005**, *48* (2), 414–426.

(36) Schedler, M.; Wang, D.-S.; Glorius, F. *Angew. Chem. Int. Ed.* **2013**, *52* (9), 2585–2589.

(37) Lautens, M.; Roy, A.; Fukuoka, K.; Fagnou, K.; Martín-Matute, B. *J. Am. Chem. Soc.* **2001**,

123 (22), 5358–5359.

(38) Kobayashi, T.; Yorimitsu, H.; Oshima, K. *Chem. Asian J.* **2009**, *4* (7), 1078–1083.

(39) Ogiwara, Y.; Kochi, T.; Kakiuchi, F. *Org. Lett.* **2011**, *13* (12), 3254–3257.

(40) Wang, S.; Li, X.; Liu, H.; Xu, L.; Zhuang, J.; Li, J.; Li, H.; Wang, W. *J. Am. Chem. Soc.* **2015**, *137* (6), 2303–2310.

(41) Russell, G. A.; Rajaratnam, R.; Wang, L.; Shi, B. Z.; Kim, B. H.; Yao, C. F. *J. Am. Chem. Soc.* **1993**, *115* (23), 10596–10604.

(42) Mineyama, K.; Maekawa, H.; Kohsaka, A.; Yamamoto, Y.; Nishiguchi, I. *Tetrahedron* **2009**, *65* (36), 7706–7711.

(43) Ravelli, D.; Protti, S.; Fagnoni, M. *Chem. Rev.* **2016**, *116* (17), 9850–9913.

(44) Ghosh, I.; Marzo, L.; Das, A.; Shaikh, R.; König, B. *Acc. Chem. Res.* **2016**, *49* (8), 1566–1577.

(45) Wang, S.; Jia, W.-L.; Wang, L.; Liu, Q.; Wu, L.-Z. *Chem. Eur. J.* **2016**, *22* (39), 13794–13798.

(46) Miyazawa, K.; Yasu, Y.; Koike, T.; Akita, M. *Chem. Commun.* **2013**, *49* (65), 7249.

(47) Schwarz, J.; König, B. *Green Chem.* **2016**, *18* (17), 4743–4749.

(48) Miyazawa, K.; Koike, T.; Akita, M. *Adv. Synth. Catal.* **2014**, *356* (13), 2749–2755.

(49) Choi, G. J.; Knowles, R. R. *J. Am. Chem. Soc.* **2015**, *137* (29), 9226–9229.

(50) Capaldo, L.; Buzzetti, L.; Merli, D.; Fagnoni, M.; Ravelli, D. *J. Org. Chem.* **2016**, *81* (16), 7102–7109.

(51) Murphy, J. J.; Bastida, D.; Paria, S.; Fagnoni, M.; Melchiorre, P. *Nature* **2016**, *532* (7598), 218–222.

(52) Qrareya, H.; Dondi, D.; Ravelli, D.; Fagnoni, M. *ChemCatChem* **2015**, *7* (20), 3350–3357.

(53) Symeonidis, T. S.; Tamiolakis, I.; Armatas, G. S.; Lykakis, I. N. *Photochem. Photobiol. Sci.* **2015**, *14* (3), 563–568.

(54) Yamada, K.; Okada, M.; Fukuyama, T.; Ravelli, D.; Fagnoni, M.; Ryu, I. *Org. Lett.* **2015**, *17*

(5), 1292–1295.

(55) Fagnoni, M.; Bonassi, F.; Palmieri, A.; Protti, S.; Ravelli, D.; Ballini, R. *Adv. Synth. Catal.* **2014**, *356* (4), 753–758.

(56) Ravelli, D.; Albini, A.; Fagnoni, M. *Chem. Eur. J.* **2011**, *17* (2), 572–579.

(57) Cambié, D.; Bottecchia, C.; Straathof, N. J. W.; Hessel, V.; Noël, T. *Chem. Rev.* **2016**, *116* (17), 10276–10341.

(58) Cambié, D.; Zhao, F.; Hessel, V.; Debije, M. G.; Noël, T. *Angew. Chem. Int. Ed.* **2017**, *56* (4), 1050–1054.

(59) Metzger, J. O. *Angew. Chem. Int. Ed. Eng.* **1986**, *25* (1), 80–81.

(60) Metzger, J. O.; Klenke, K.; Hartmanns, J.; Eisermann, D. *Chem. Ber.* **1986**, *119* (2), 508–513.

(61) Giese, B.; Lachhein, S. *Chem. Ber.* **1985**, *118* (4), 1616–1620.

(62) Chalari, I.; Pispas, S.; Hadjichristidis, N. *J. Polym. Sci. Part A Polym. Chem.* **2001**, *39* (17), 2889–2895.

(63) Mukherjee, A.; Duggan, S. A. M.; Agosta, W. C. *J. Org. Chem.* **1994**, *59* (1), 178–181.

CHAPTER 4

PROMISING PHOTOCATALYSTS FOR VISIBLE LIGHT HAT

As mentioned in the introduction of this work, photoredox catalysis has been extensively exploited due to its intrinsic advantages, one of which being the fact that most photocatalysts used in this field can be excited with low-energy visible light irradiation. On the other side, to match the redox features of the substrate with those of the photocatalyst, the presence of an electroactive moiety on the substrate is often crucial (see also Chapter 2).

Photocatalyzed HAT offers the unique possibility to directly cleave a C-H bond in the substrate and bypass tedious synthetic steps needed to introduce activating moieties (see Chapter 3). However, there has been a frustrated growth of this research field, mainly due to i) the scarce number of available photocatalysts (PC_{HAT}) known to perform this chemistry, being restricted to the families of aromatic ketones and polyoxometalates (mainly the decatungstate anion $[W_{10}O_{32}]^{4-}$)[1–3] and ii) the scarcity of PC_{HAT} operating under visible light.

Very recently, some remarkable efforts have been made in this direction, disclosing new synthetic protocols based on a visible-light photocatalyzed HAT step. For example, in one instance, the use of 5,7,12,14-pentacenetetrone (PT, see Figure 4.1) in the role of the photocatalyst in the radical allylation under visible light was reported.[4] In this study, the authors noted that photoirradiation of PT at 365 nm and 425 nm gave comparable results and, for example, cyclooctane could be functionalized in the presence of 1,2-bis(phenylsulfonyl)-2-propene under LED lamps in 58% and 55% yield, respectively. The activation step was a photocatalyzed HAT and the authors reported a KIE (Kinetic Isotope Effect) of 3.6, indicating that the C(sp^3)-H was involved in the rate-determining step of the process. Additionally, trapping with TEMPO afforded the cyclooctane-TEMPO adduct, proving the generation of the cyclooctyl radical during the course of the reaction.

At the time of writing, an impressive study on the use of Eosin Y as a photocatalyst operating via *d*-HAT under white and blue light irradiation was published.[5] In this paper, the authors developed an elegant approach for the visible-light alkylation of C-H bonds (see Figure 4.1), showing a broad substrate scope obtained with operational simplicity that allowed them to run the reaction in a large scale and even using continuous-flow technology. Based on the structural similarity with quinones,

the authors speculated that, upon absorption of a visible-light photon, the excited state of Eosin Y might undergo HAT with a C-H bond to form a relatively stable radical intermediate due to both captodative and steric effects, which is unlikely to participate in a side coupling reaction, thus enabling a more effective back-HAT.[5]

As for the conversion of C-H to C-F bonds, fluorenone was used to accomplish a metal-free benzylic C-H activation under the light of a bright white bulb.[6,7] The authors reported the monofluorination (shown in Figure 4.1) and difluorination of alkylaromatics in the benzylic position with a good tolerance of functional groups and in good yields. Both reactions occurred under visible light and via an initial HAT.

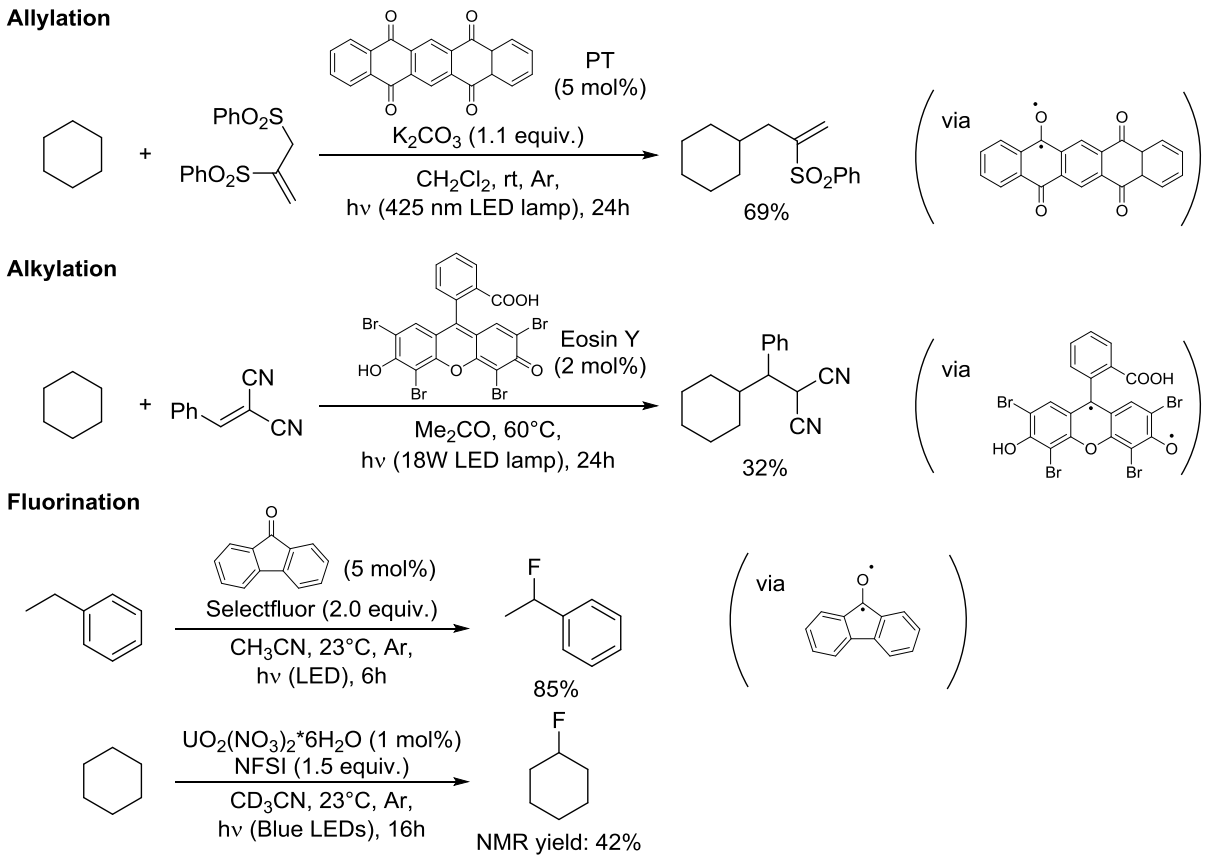

Figure 4.1 Example of synthetic protocols via visible-light HAT.

More recently, the fluorination of cycloalkanes and oxygenated compounds (such as ketones, acetals, ethers and esters) by means of the uranyl cation, in the form of its nitrate salt $UO_2(NO_3)_2*6H_2O$, was performed under blue light irradiation (Figure 4.1).[8] Even if products were

obtained in low yields, this is a proof of concept for the viability of C-H activation via visible-light photocatalyzed HAT operated by the uranyl cation. This chapter reports some unpublished preliminary data on the use of two visible-light photocatalysts for C-H to C-C bond conversion via direct HAT.

CHAPTER 4

VISIBLE-LIGHT PHOTOCATALYZED HAT FOR C-C BOND FORMATION:

THE CASE OF URANYL CATION.

Introduction

Prompted by the interest in photocatalysis via HAT by polyoxometalates (see Chapter 3), where an M=O (M: metal) functionality in the excited state is responsible for the relevant H-atom abstraction, I started wondering whether the uranyl cation could be implemented in a synthetic protocol to forge C-C bonds from unactivated C-H bonds.

Although the presence of an uranium atom might trigger an instinctive concern as demonstrated by the existence of a plethora of analytical methods to detect uranium compounds in traces and ultratraces,[9–15] it is a common position that the main risks deriving from its use in form of salts are associated with chemical toxicity, instead of toxicity deriving from radioactivity.[16–20] Thus, a judicious use of PPE (Personal Protection Equipment) makes most common uranium compounds, such as uranyl nitrate or uranyl acetate, no more noxious than any other heavy metal complex.

Since the discovery of its photochemical activity,[21] the uranyl cation has received a great deal of attention for its photophysics[22–28] and photochemistry.[23,29–38] This linear triatomic ion, where uranium is in the oxidation state +6, is the most stable derivative containing U(VI). Contrary to what reported for tetrabutylammonium decatungstate,[38] the uranyl cation is stable over a considerable pH range (2-7) and coordination by anions (such as citrate) can extend this range even further up to pH = 10.[22]

As for photophysics, absorption and fluorescence bands of most dissolved uranyl salts in the visible and near UV range belong to this ion and are not considerably affected by changing counterion. There is no serious doubt in attributing bands in the UO_2^{2+} absorption spectrum to LMCT transitions.[30,39]

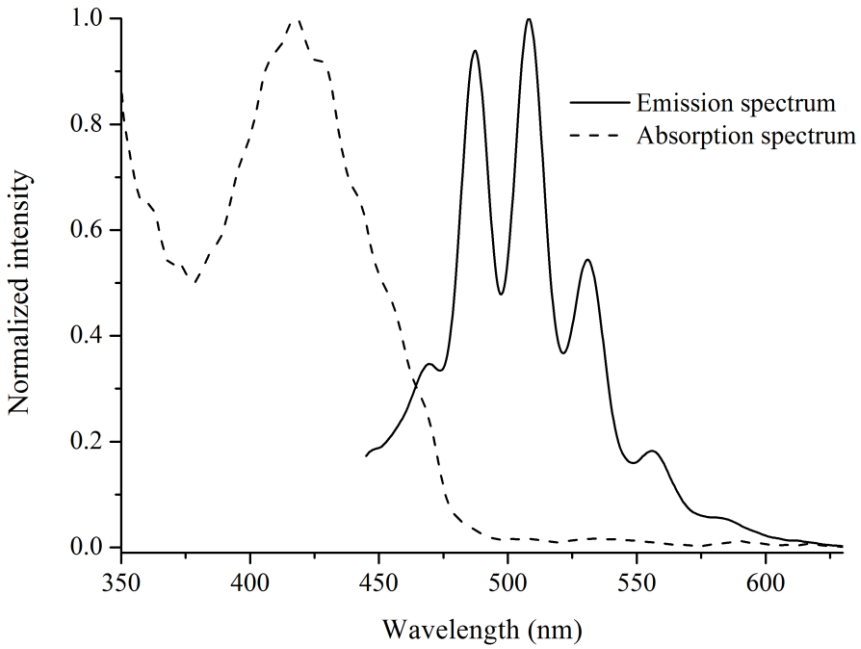

Figure 4.2 Normalized absorption and emission spectra of uranyl nitrate in acetonitrile solution.

It has been proposed that the weak bands in the visible range of the absorption spectrum are due to a Laporte-forbidden transition, due to a charge transfer from the oxygen atoms orbital to an empty 5f-orbital of the uranium atom.[26] Others suggest that the charge transfer involves the U=O π-orbital and an empty orbital on the uranium center.[40] Such an excited state is expected to have a certain free-radical character, as corroborated by reactivity via HAT observed experimentally.[23–25,27,36] Additionally, this state shows incredible chemical properties, such as an extraordinarily high oxidation potential of $E(^*UO_2^{6+}/UO_2^{5+})$ = +2.36 V vs SCE and an extremely long lifetime (ca. 2 μs).[27] This translates into a really peculiar photochemical reactivity.

In the frame of our interest towards photocatalytic HAT processes for the C-H to C-C bond conversion, I decided to test the reactivity of the uranyl cation as a visible light photocatalyst for the generation of highly reactive intermediates. The so-formed radicals were then trapped with electrophilic olefins or electron-poor styrenes to afford Giese addition products in a redox-neutral overall process.

Result and discussion

I started the investigation by studying the model reaction between cyclohexane (**3.1g**) and benzylidenemalononitrile (**2.2c**).

Table 4.1 Optimization of reaction conditions.[a]

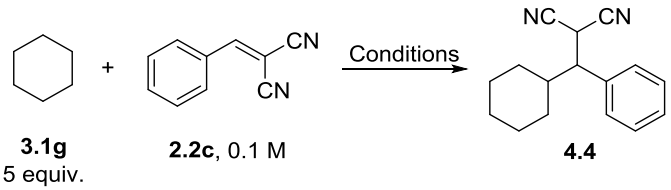

Entry	Photocatalyst	Light Source	Solvent	Time	Consumption of 2.2c (%)	Yield of 4.4 (%)[b]
1	$UO_2(OAc)_2$*$4H_2O$ (4 mol%)	410 nm	CH_3CN	24 h	< 5	n.d.[c]
2	$UO_2(NO_3)_2$*$6H_2O$ (4 mol%)	410 nm	CH_3CN	24 h	40	36
3	$UO_2(NO_3)_2$*$6H_2O$ (4 mol%)	410 nm	CH_3CN/H_2O 9:1	24 h	46	37
4	$UO_2(NO_3)_2$*$6H_2O$ (4 mol%)	410 nm	$(CH_3)_2CO$	24 h	72	70
5	$UO_2(NO_3)_2$*$6H_2O$ (6 mol%)	410 nm	$(CH_3)_2CO$	24 h	93	93
6	$UO_2(NO_3)_2$*$6H_2O$ (8 mol%)	410 nm	$(CH_3)_2CO$	24 h	100	>95
7	$UO_2(NO_3)_2$*$6H_2O$ (8 mol%)	310 nm	$(CH_3)_2CO$	24 h	29	7[d]
8	$UO_2(NO_3)_2$*$6H_2O$ (8 mol%)	366 nm	$(CH_3)_2CO$	24 h	17	3[d]
9	$UO_2(NO_3)_2$*$6H_2O$ (8 mol%)	Kessil 456 nm	$(CH_3)_2CO$	24 h	100	>95
10	$UO_2(NO_3)_2$*$6H_2O$ (8 mol%)	505 nm	$(CH_3)_2CO$	24 h	26	15
11	**$UO_2(NO_3)_2$*$6H_2O$ (8 mol%)**	**Kessil 456 nm**	**$(CH_3)_2CO$**	**24 h**	**100**	**>95**[e]
12	-	Kessil 456 nm	$(CH_3)_2CO$	24 h	< 5	traces
13	$UO_2(NO_3)_2$*$6H_2O$ (8 mol%)	-	$(CH_3)_2CO$	24 h	26	n.d.

*[a] Reaction conditions: **3.1g** (5 equiv.), **2.2c** (1 equiv.), photocatalyst (n mol%) in 1 mL of the chosen solvent (0.1 M). Solutions were bubbled for 1 min with N_2 prior to irradiation, unless otherwise noted. [b] GC yield using n-dodecane as external standard. [c] Heterogeneous mixture: suspension irradiated under stirring. [d] Reaction carried out in quartz tubes. [e] Solution irradiated under air-equilibrated conditions.*

My choice was based on the assumption that **3.1g** can only be activated through hydrogen atom transfer (calcd $E_{1/2}(C_6H_{12}^{\bullet+}/ C_6H_{12}) > +3$ V vs SCE),[41,42] ruling out a possible (competitive) single-electron transfer with the substrate. On the other side, **2.2c** was chosen because of its light-absorbing nature in the near UV range, making a visible-light irradiation desirable, if not mandatory, due to competitive absorption. Furthermore, recent works have demonstrated the efficiency of olefin **2.2c** in trapping radicals for the formation of C-C bonds.[5,43]

The irradiation of a suspension of uranyl acetate (4 mol%) in CH_3CN in the presence of **2.2c** and cyclohexane (5 equiv.) did not afford the desired product **4.4**, even after 24 h of irradiation with 1 W 410 nm LEDs (Table 4.1, *entry 1*). I reasoned that the partial insolubility of the salt might play a detrimental role; accordingly, I decided to use uranyl nitrate hexahydrate as the source of uranyl cation. Nitrate ion is much less coordinating with respect to acetate, which results in improved solubility of the uranyl salt, even in organic solvents. This change allowed me to obtain the desired product in a 36% yield (*entry 2*). I then started a screening of the solvent (see Experimental Section): the addition of water did not improve the reactivity (entry 3), while the use of acetone as the reaction solvent turned out to be extremely advantageous (70%, *entry 4*).[8] I noticed that, after 24 h of irradiation, a brown precipitate was formed on the bottom of the reaction vessel, which was tentatively identified as UO_2, based on literature evidence.[32] As a matter of fact, two U(V) are known to react in a disproportionation reaction, affording U(VI) and U(IV), the latter being insoluble.[26] I interpreted this as a symptom of decomposition of the photocatalyst and decided to increase its amount (*entries 5* and *6*), accordingly. An excellent yield was then obtained with 8 mol% of uranyl nitrate hexahydrate (> 95%). Next, I demonstrated the activity of the uranyl cation as a visible light photocatalyst by testing the model reaction under different irradiation conditions (*entries 7-9*). Pleasingly, I found that the reaction worked very well (>95%) by using a 410 nm LED (1 W) and a Kessil Lamp 456 nm (36 W; 50% intensity), while only modest yields were obtained under UV irradiation. Green light irradiation (*entry 10*) was tested too, but the reaction proceeded slowly (only 15% yield at 26% consumption of the olefin, 58% based on olefin consumption), as I

expected by studying the absorption spectrum of the uranyl cation (see Experimental Section). Remarkably, the excited state of the photocatalyst was not affected by the presence of oxygen, as the reaction afforded **4.4** in excellent yields also under air-equilibrated conditions (*entry 11*). Finally, blank experiments demonstrated that both the light and the photocatalyst were necessary for the reaction to occur (*entries 12, 13*).

With the optimized conditions in hand (see Table 4.1, *entry 11*), I started investigating the scope of the reaction in terms of hydrogen atom donors by using the electron-poor styrene **2.2c** in the role of the electrophilic trap (Table 4.2).

*Table 4.2 H-donor scope for the radical addition onto **2.2c**.*[a,b]

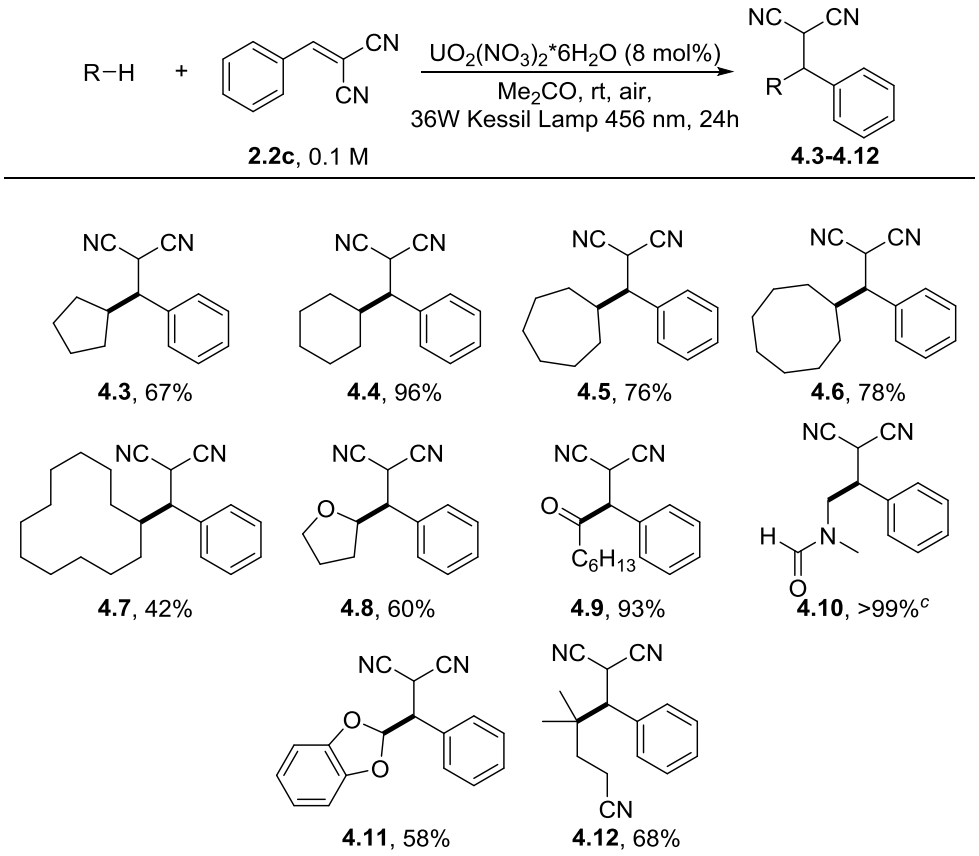

[a] *Reaction conditions: H-donor (1-5 equiv., see Experimental Section), **2.2c** (1 equiv.), photocatalyst (8 mol%) in 10 mL of acetone (0.1 M).* [b] *Isolated yield.* [c] *mixture of two constitutional isomers in a 2:1 ratio (only the major is reported in this table), see text.*

Cycloalkanes (C5 to C8 and C12) reacted well under optimized conditions, affording the corresponding Giese adducts **4.3**-**4.7** in yields ranging from 42% to 96%, while tetrahydrofuran (**3.1a**) afforded **4.8** in decent yields (60%). Freshly distilled heptanal (**3.1i**) reacted at the formyl C-

H position to afford asymmetric ketone **4.9** in excellent yields (93%). Interestingly, *N*,*N*-dimethylformamide (**3.1d**) turned out to be a singular case: although the overall yield was quantitative, the reaction showed the formation of two isomers. In fact, **3.1d** has two non-equivalent bonds prone to undergo activation: the formyl C-H bond and the α-to-N C-H bond, whose homolytic cleavages yield a carbamoyl radical or an α-amidoalkyl radical, respectively. Contrary to what observed for TBADT,[44] where selectivity was complete towards the α-to-N C-H bond, in the presence of the uranyl cation, 30% of the product deriving from the attack of the carbamoyl radical was observed. As for 1,3-benzodioxole **3.1c** and isocapronitrile **3.1f**, the corresponding Giese adducts were obtained in 58% and 68% yield, respectively.

To ascertain the activation mechanism I studied the KIE (Kinetic Isotope Effect) related to the key HAT step. Two Stern-Volmer experiments were carried out following the fluorescence intensity of a solution of $UO_2(NO_3)_2$*$6H_2O$ in acetone ($8 \cdot 10^{-3}$ M) upon addition of protiated and deuterated cyclohexane in increasing amounts (Figure 4.3).

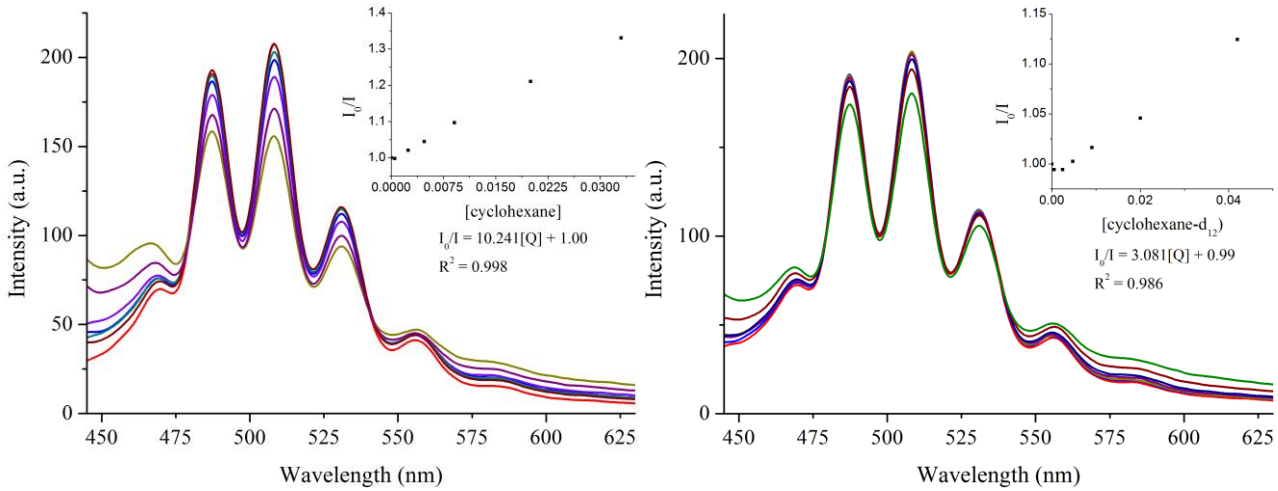

Figure 4.3 Stern-Volmer experiments: quenching of uranyl cation fluorescence with C_6H_{12} (left) and C_6D_{12} (right). Insets: Stern-Volmer plot obtained monitoring fluorescence at 508 nm.

The KIE was determined as the ratio of the product $k_0\tau$ obtained in the experiment with protiated **3.1g** divided by that obtained in the experiment with deuterated **3.1g**:

$$KIE = \frac{(k_0\tau)_{C_6H_{12}}}{(k_0\tau)_{C_6D_{12}}} = \frac{10.2}{3.1} = 3.3$$

This result strongly suggests that HAT is the activation pathway operating in this case.

I then turned my attention to the investigation of the olefin scope and cyclohexane was selected as the model H-donor (see Table 4.3). I then modified the aromatic ring of compound **2.2c**, moving a chlorine substituent in *para*- (**4.13**), *meta*- (**4.14**) and *ortho*- (**4.15**) positions. The reaction worked well, with a gradual increase in isolated yields from 63% to 82%.

*Table 4.3 Electrophilic traps scope for the radical addition of **3.1g**.*[a,b]

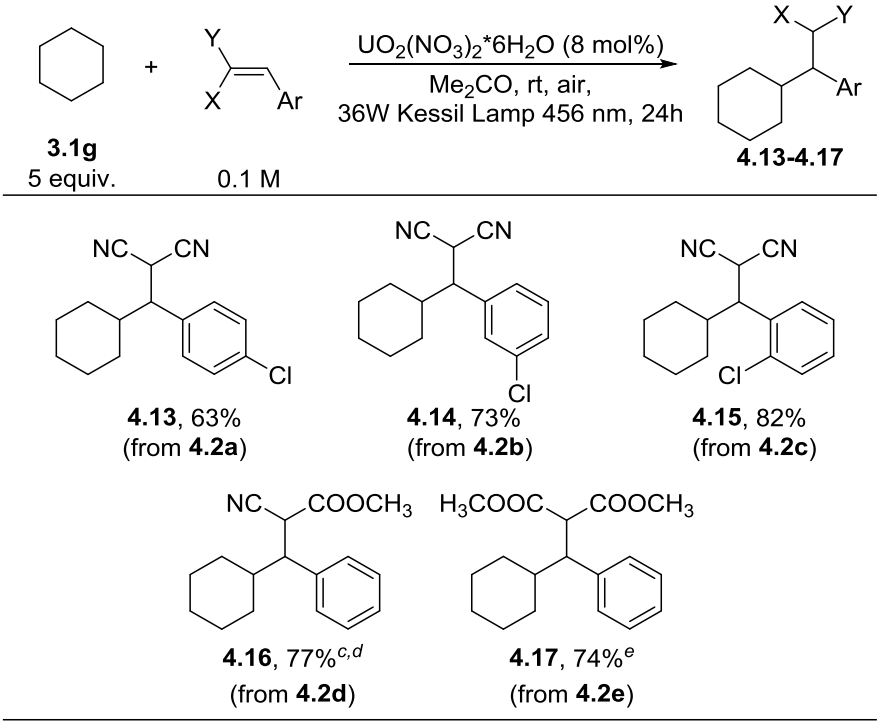

[a] *Reaction conditions: **3.1g** (5 equiv.), electrophilic trap (1 equiv.), photocatalyst (8 mol%) in 10 mL of solvent (0.1 M).* [b] *Isolated yield.* [c] *A diastereomeric mixture was obtained in a 1:1 ratio.* [d] *Irradiation for 30 h.* [e] *Irradiation for 65 h.*

I next focused on the di-substituted carbon of the electrophilic trap (see for example traps **4.2d** and **4.2e**). I rapidly recognized the importance of the nature of the two electron-withdrawing groups. As a matter of fact, when ethyl 2-cyano-3-phenylacrylate **4.2d** and dimethyl 2-benzylidenemalonate **4.2e** were used as the olefinic counterpart, the corresponding adducts were obtained in good yields (77% and 74%, respectively), but longer irradiation times were required (30 and 65 hours, respectively).

Finally, I started a screening of additional traps but, for a reason of time, I can only provide a qualitative assessment of the observed reactivity profile based on the evaluation of GC and GC-MS

chromatograms. I analyzed the crude reaction mixtures of **3.1g** with dimethyl fumarate (**2.2d**), dimethyl maleate (**2.2e**), 2-(4-cyanobenzylidene)malononitrile (**4.2f**), 2-(4-methylbenzylidene)malononitrile (**4.2g**), and 2-(4-methoxybenzylidene)malononitrile (**4.2h**) under optimized conditions (Chart 4.1).

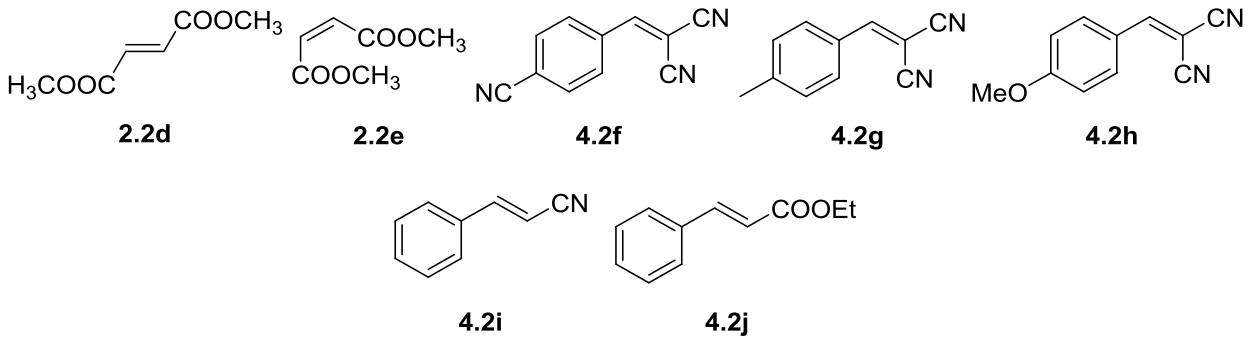

Chart 4.1 Additional traps used in this work.

While the reaction with **2.2d** or **2.2e** gave the corresponding product (attribution based on the comparison with an authentic sample), several peaks attributable to oligo- and polymerization by-products were observed at high-retention times. In contrast, **4.2f** and **4.2g** worked well and showed a clean reaction crude after irradiation and complete conversion of the olefinic trap. As for trap **4.2h**, incomplete conversion was obtained after 24 hours. Finally, when cinnamonitrile **4.2i** and ethyl cinnamate **4.2j** were used, no product was detected; instead, only cis-trans isomerization was observed. Any direct photon absorption by cinnamonitrile and ethyl cinnamate can be safely excluded.

All the results on the different employed olefins reported so far give insights into the mechanism operating in this reaction.

First, the slowdown of the reaction rate when passing from cyano-cyano **2.2c** (24 hours) to cyano-ester **4.2d** (30 hours) and then ester-ester traps **4.2e** (65 hours) mirrors the decrease in the electron-withdrawing character of the substituents of the double bond. Likewise, this trend is qualitatively appreciated in the reaction of **3.1g** with **4.2f**-**4.2h**. Taken all together, these data stress the importance of the electrophilicity of the C=C double bond of the trap.[45]

Second, the analysis of the outcome of reactions with **4.2i** and **4.2j** suggests that a competitive mechanism is ruling out the HAT. Fluorescence quenching experiments were carried out and, indeed, fluorescence was quenched upon addition of both cinnamonitrile and ethyl cinnamate (see Figure 4.4).

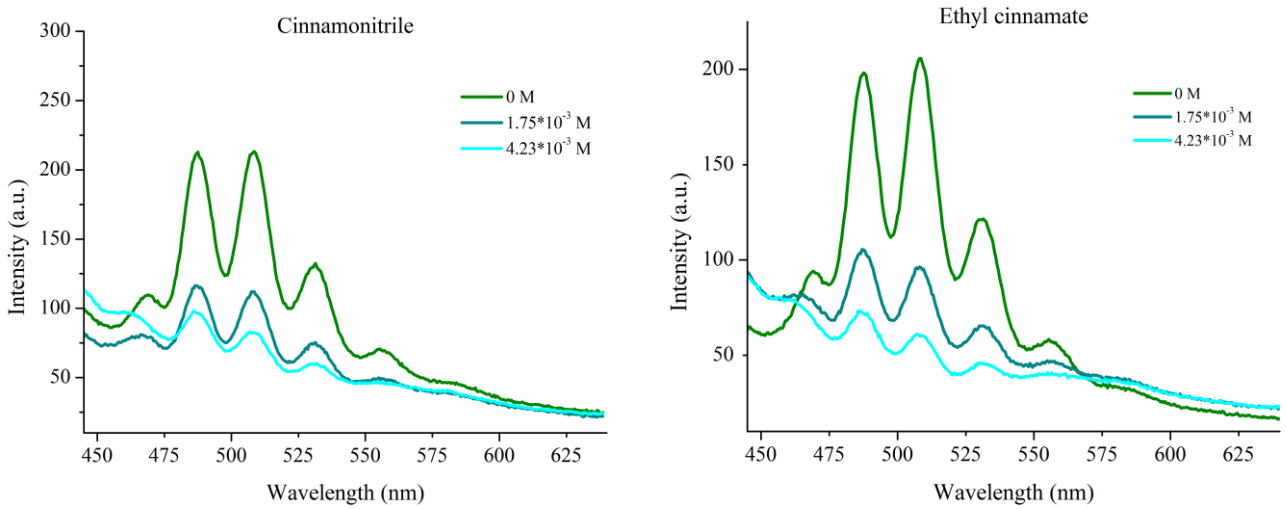

*Figure 4.4 Fluorescence quenching experiment of $UO_2(NO_3)_2$*$6H_2O$ (conc: $8\cdot10^{-3}$M) in acetone. λ_{exc}=410 nm. The quencher (i.e. cinnamonitrile or ethyl cinnamate) was added progressively in a concentration ranging from 0 to $4.23\cdot10^{-3}$ M.*

These quenching experiments, together with the isomerization observed, hint that Energy Transfer is occurring. Accordingly, I tried to check the feasibility of a Dexter-type Energy Transfer from the excited state of the uranyl cation to the olefin.

In Figure 4.2, the emission spectrum of the uranyl nitrate hexahydrate is reported and one can calculate the triplet energy of the uranyl cation from the band at 468 nm (eq. 4.1):

$$E < \underbrace{6.02\cdot10^{23}/mol}_{n}\cdot\underbrace{6.63\cdot10^{-34}Js}_{h}\cdot\frac{\overbrace{3.00\cdot10^{8}ms^{-1}}^{c}}{\underbrace{4.68\cdot10^{-7}m}_{\lambda}} < 256\ kJ/mol \qquad \text{(eq. 4.1)}$$

Remarkably, triplet energy of **2.2c**, **4.2i** and **4.2j** were calculated (computational study by Dr. Davide Ravelli) to be 190, 196 and 204 kJ mol^{-1} (level of theory: DFT-UωB97XD-def2TZVP in gas phase), respectively (see Appendix II). We think that, although energy transfer from the excited state of the uranyl cation to the three traps is thermodynamically feasible, in the case of **2.2c** it is not detrimental in the formation of compound **4.4**.

Summing up, I propose that **3.1g** is activated via a visible-light HAT step by the uranyl cation; the so-formed radical is readily trapped by the electrophilic trap to afford intermediate **I**$^{\bullet}$ (Figure 4.5). This radical adduct is accountable for the monoelectronic oxidation of the $[UO_2]^{+}$-H^{+} species to afford UO_2^{2+}-H^{+} and **I**$^{-}$, thus closing the photocatalytic cycle. A proton transfer from UO_2^{2+}-H^{+} to **I**$^{-}$ affords the Giese adduct.

In fact, I suspect that the closure of the photocatalytic cycle is a stepwise electron transfer-proton transfer (ET-PT) instead of a classical back-HAT.

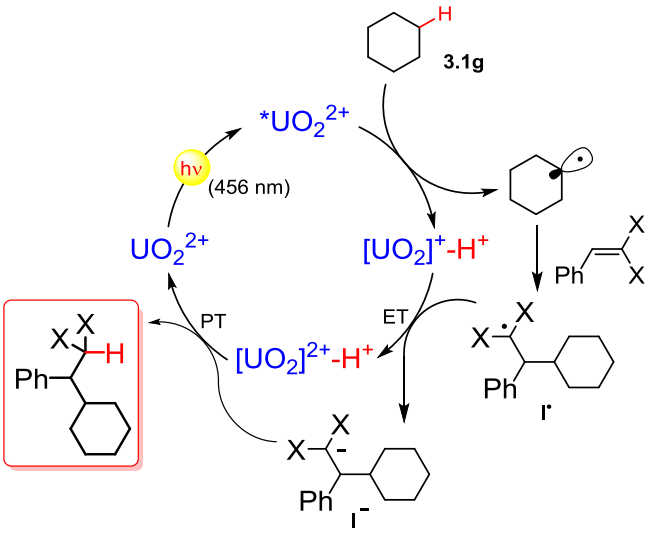

Figure 4.5 Proposed mechanism.

I base my hypothesis on the following observations:

- the Giese reaction between **3.1g** and **2.2e** is known to work well in the case of TBADT (yield: 68%);[46] on the contrary, slow conversion and polymerization are observed when the uranyl cation is used. This suggests that the problem is not in the radical addition step and that the uranyl cation might be responsible for the *impasse*;
- the excellent results obtained in the trapping of **3.1g** (see Table 4.3) indicate that the weak step is unlikely to be the initial HAT. Accordingly, I deem that the critic step depends on the trap and probably is the closure of the photocatalytic cycle;
- reactions with strongly electrophilic traps (see reactions with **2.2c**, **4.2f** and **4.2g**) that generate easily reducible **I**$^{\bullet}$ worked the best. Just as a yardstick, I measured the redox

potentials of deprotonated **4.17**, E($\mathbf{I}^{\bullet}/\mathbf{I}^{-}$) = + 0.78 V (see Chart 4.2) and of the uranyl cation E(UO_2^{2+}/UO_2^{+}) = + 0.32 V vs SCE, in acetone.

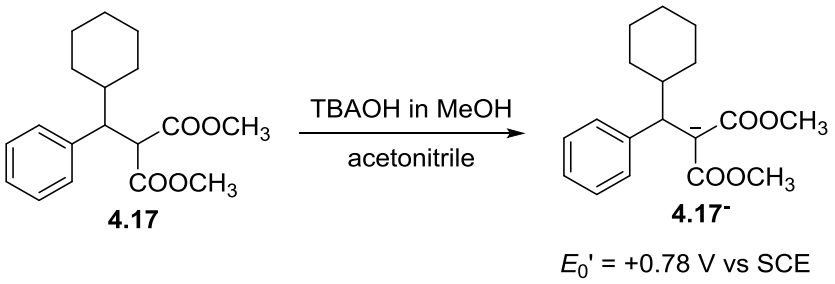

Chart 4.2

Thus the closure of the photocatalytic cycle is thermodynamically favored. In case $\mathbf{I}^{\bullet}$ is a weaker oxidant, its reduction by UO_2^{+}-H^{+} might be thermodynamically uphill.

Conclusion and Perspectives

Even though preliminary, data regarding the use of uranyl cation as a visible-light photocatalyst for the C-H to C-C conversion are sound. Cycloalkanes, an aliphatic aldehyde, an amide, an ether, a nitrile and an acetal have been activated via a HAT under 456 nm irradiation and the formed radicals were intercepted by electrophilic traps in a Giese reaction. The scope is currently being expanded with particular attention devoted to mechanistic aspects: I deem that H-shuttle molecules, such as 2-phenylmalononitrile or 9-phenylfluorene,[47] may be precious in helping the closure of the photocatalytic cycle.

VISIBLE-LIGHT PHOTOCATALYZED HAT FOR C-C BOND FORMATION:

THE CASE OF ANTIMONY-OXO PORPHYRINS.

Introduction

On my way towards the development of new visible-light photocatalysts for HAT, I came across the class of metallo porphyrins. A plethora of papers have been published on their use as catalysts for the functionalization of organic compounds, including hydroxylation[48,49] and halogenation of hydrocarbons.[50] Both these reactions involve a thermal HAT step for the activation of the chosen substrate.

As far as hydroxylation of hydrocarbons is concerned, the reaction typically starts with the *in-situ* generation of a metallo-oxo porphyrin via reaction with a terminal oxidant, such as hypochlorite anion,[51] *m*CPBA,[52] ozone,[53] iodosyl benzene[54,55] or dimethyldioxirane.[56] Once the metal-oxo function is installed, the M^{n+}=O function is capable of homolytically cleave a C-H bond in the substrate to yield a metallo-hydroxo compound ($M^{(n-1)+}$-OH) and a C-centered radical. This latter radical recombines with the hydroxy group axial to the metallo porphyrin to afford the oxygenated compound. This mechanism, typical for Citochrome P450, is known as *oxygen rebound mechanism* and electronic factors were proved to be crucial: the more electron-deficient the porphyrin ring, the better the yield (Figure 4.6).[57]

As for halogenation reactions, once the metallo-oxo porphyrin has been generated and the thermal HAT has occurred, the generated $M^{(n-1)+}$-OH exchanges the hydroxyl ligand with a fluoride or a hypohalide anion (typically, ClO^- or BrO^-). The resulting species is an exceptional halogen atom donor and can quench the C-centered radical (Figure 4.6).[50]

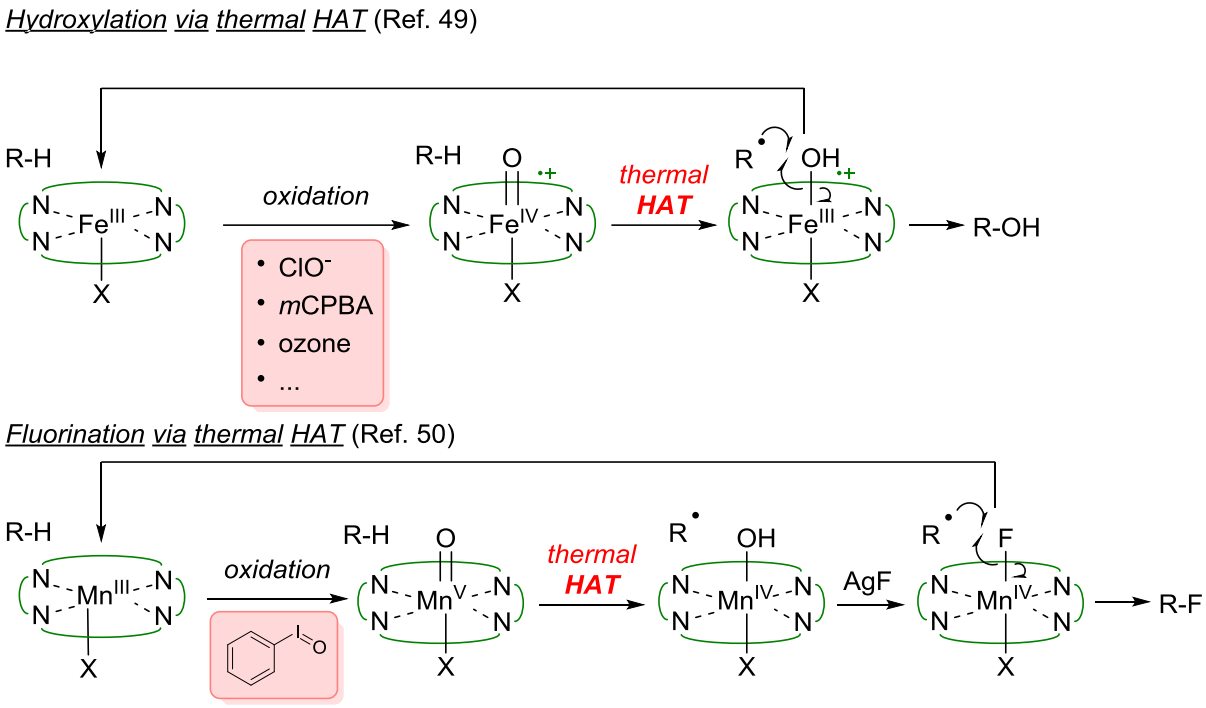

Figure 4.6 Metallo-oxo porphyrins for thermal C-H bond activation via HAT for hydroxylation and fluorination reactions.

These two reactions, *viz.* hydroxylation and halogenation, mainly rely on the use of iron-oxo and manganese-oxo porphyrins.[49,50] Even though these compounds show great tunability and versatility, they are based on a thermal HAT.

It would be highly desirable to have such features in a photocatalyst: the ease of functionalization of porphyrins, combined with the great tunability of their redox behavior according to the attached substituents, would pave the way to all kinds of opportunities in synthetic photocatalysis. Accordingly, I started wondering about the existence of metallo-oxo porphyrins capable of performing a HAT triggered by visible light; in other words, I started looking for metallo-oxo porphyrins showing the behavior previously mentioned, but uniquely in the excited state. Unfortunately, to the best of my knowledge, no such phenomenon has been unequivocally reported in the literature, even if some papers hinted this possibility. Antimony dihydroxo complexes $[Sb(tpp)(OH)_2]^+X^-$ (tpp: tetraphenylporphyrin) are rather stable coordination compounds that can be stored for several years in the dark without decomposition; upon deprotonation, however, an antimony-oxo complex SbO(tpp)OH, containing the desired M=O (actually, Sb is a semi-metal)

function, can be generated. This compound was used in the generation of acetaldehyde starting from ethanol under visible light irradiation via hydrogen abstraction.[58] In fact, while no significant thermal reaction of the catalyst with the alcohol was observed under neutral aerated solution, addition of a base (OH^-) and irradiation with light centered at 546 nm were found to be sufficient to activate the compound for immediate conversion. Later, in 2012, it was reported that the same compound was responsible for a controlled multistep photocatalytic oxidation of benzyl alcohols and aldehydes to carboxylic acids using air and sunlight.[59] In the introduction, it was reported that "an excited state species with oxyl-radical reactivity is involved in the rate-determining hydrogen abstraction step".[59]

Accordingly, I decided to test this class of compounds for the photocatalyzed C-H to C-C bond conversion under visible light. We contacted Prof. Günther Knör, at JKU in Linz (Austria), to start a collaboration for this project. The present thesis only reports a proof of concept of the synthetic aspect, which was carried out in our laboratory in Pavia, while a detailed spectroscopic investigation is currently ongoing in Austria.

Results and discussion

I received and tested the reactivity of the tetraaryl-substituted porphyrin complex **I** (Ar = 4-$MeOC_6H_4$, Figure 4.7).

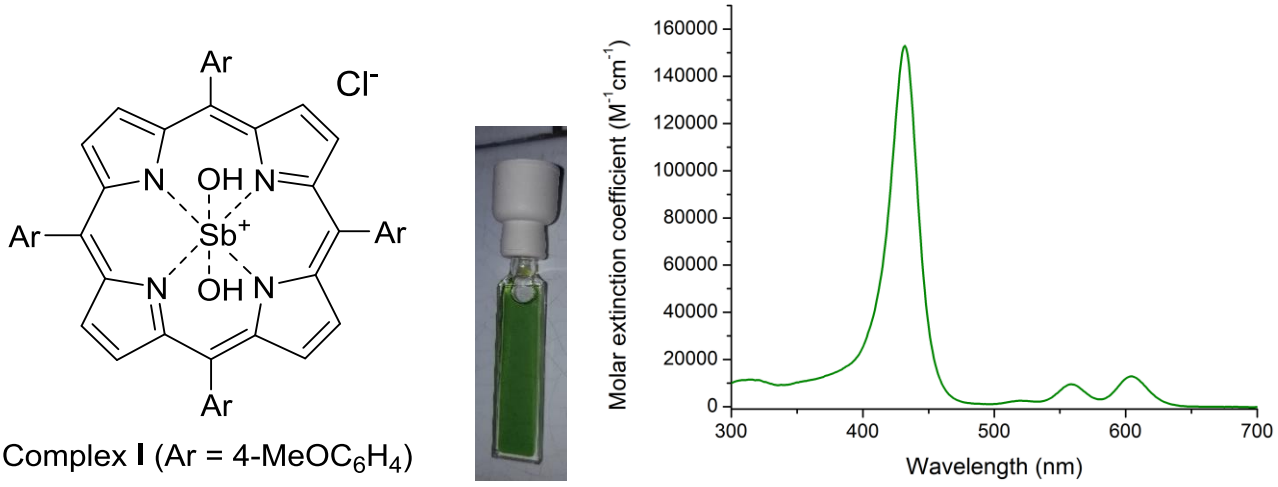

*Figure 4.7 Structure of the porphyrin complex **I** (left), picture of a solution containing $5 \cdot 10^{-4}$ M **I** (middle) and UV-Vis spectrum of **I** $5 \cdot 10^{-6}$ M in MeCN/H_2O 95:5.*

I initially studied the addition of THF (**3.1a**) onto dimethyl maleate (**2.2e**) in the presence of **I** (see Figure 4.7), as detailed in Table 4.4, promoted by simulated sunlight to cover a broad spectrum of wavelengths. Thus, when a MeCN solution of **2.2e** (0.05 M), **3.1a** (0.5 M, 10 equiv.) and complex **I** (1 mol%) in a 1 mm optical path cuvette was irradiated for 48 h, no consumption of the olefin was observed and the desired succinate **4.18** was not detected (*entry 1*). However, shifting to MeCN-H_2O 95:5 along with the addition of 1 mol% NaOH caused the formation of **4.18** (60% yield, based on 67% consumption of **2.2e**, *entry 2*).[58,59] Any variation of catalyst loading in the 0.2 to 2 mol% range confirmed that 1 mol% was the optimal choice (*entries 3-5*). Increasing the amount of water (up to 50%) had a detrimental effect (*entry 6*), while the presence of oxygen inhibited the process (*entry 7*). Blank experiments demonstrated that both light and the catalyst were required for the desired process to occur (Table 4.4, *entries 8-9*). The use of isomeric dimethyl fumarate (**2.2d**) allowed the preparation of **4.18** in 77% yield after only 24 h irradiation (*entry 10*). Indeed, the latter reaction gave the opportunity to evaluate the effect of the light source by choosing different wavelengths, according to the absorption bands in the UV-Vis spectrum of **I** (see Figure 4.7, right part).

Thus, irradiation of **I** with 10×15 W phosphor-coated lamps (λ_{em} centered at 366nm) under the optimized conditions in *entry 10* did not lead to any appreciable consumption of **2.2d** (*entry 11*). The situation changed dramatically, however, when employing monochromatic visible-light LEDs (1 W) with emission at 410 and 450 nm, respectively, since I consistently observed the formation of product **4.18** in 70% yield, albeit in the former case a higher conversion of **2.2d** (80 *vs* 53%) was observed (compare *entries 12* and *13*). Furthermore, I also adopted a sodium vapors lamp (emission centered at 589 nm), but again the olefin remained untouched (*entry 14*). The photocatalyzed addition of THF to a bulky electron-poor olefin (cyclohexylidene malononitrile, **4.2k**) was likewise successful and dinitrile **4.19** was obtained in a good yield (77 %, *entry 15*), despite a low conversion of the olefin (39%).

*Table 4.4 Photocatalyzed addition of THF (**3.1a**) onto electron-poor olefins **2.2d**, **2.2e** and **4.2k** in the presence of porphyrin complex **I**.*[a]

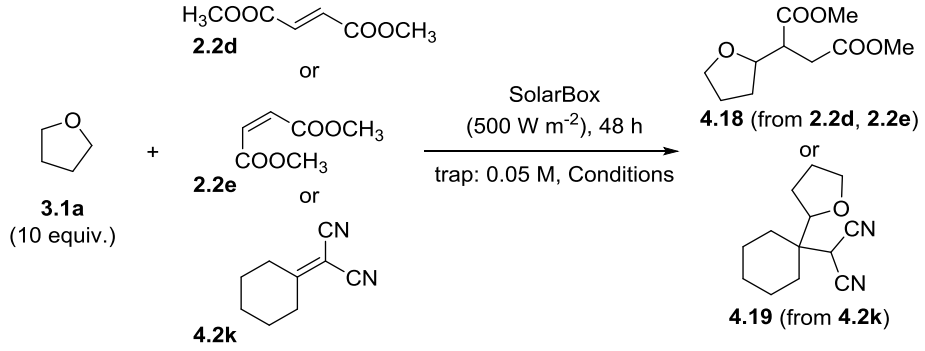

Entry	NaOH (mol%)	Complex I (mol %)	Olefin	Light Source	Solvent	Olefin Consumption	Products Yield[b]
1	-	1.0	**2.2e**	SolarBox[c]	MeCN	0%	n.d.
2	**1.0**	**1.0**	**2.2e**	**SolarBox[c]**	**MeCN/H_2O 95:5**	**67%**	**4.18, 60%**
3	0.2	0.2	**2.2e**	SolarBox[c]	MeCN/H_2O 95:5	19%	**4.18**, 11%
4	0.4	0.4	**2.2e**	SolarBox[c]	MeCN/H_2O 95:5	18%	**4.18**, 15%
5	2.0	2.0	**2.2e**	SolarBox[c]	MeCN/H_2O 95:5	32%	**4.18**, 28%
6	1.0	1.0	**2.2e**	SolarBox[c]	MeCN/H_2O 50:50	90%	**4.18**, 43%
7[d]	1.0	1.0	**2.2e**	SolarBox[c]	MeCN/H_2O 95:5	15%	**4.18**, traces
8[e]	1.0	1.0	**2.2e**	SolarBox[c]	MeCN/H_2O 95:5	0%	n.d.
9	1.0	-	**2.2e**	SolarBox[c]	MeCN/H_2O 95:5	0%	n.d.
10[f]	**1.0**	**1.0**	**2.2d**	**SolarBox[c]**	**MeCN/H_2O 95:5**	**100%**	**4.18, 77%**
11	1.0	1.0	**2.2d**	366 nm[g]	MeCN/H_2O 95:5	0 %	n.d.
12	1.0	1.0	**2.2d**	410 nm[h]	MeCN/H_2O 95:5	80%	**4.18**, 70%
13	1.0	1.0	**2.2d**	450 nm[i]	MeCN/H_2O 95:5	53 %	**4.18**, 70%
14	1.0	1.0	**2.2d**	589 nm[j]	MeCN/H_2O 95:5	0 %	n.d.
15	**1.0**	**1.0**	**4.2k**	**SolarBox[c]**	**MeCN/H_2O 95:5**	**39 %**	**4.19, 77%**

*[a] Conditions: Reaction performed in a 1 mm cuvette on a 300 μL nitrogen-purged solution containing **3.1a** (0.5 M), **2.2d**, **2.2e** or **4.2k** (0.05 M) and complex **I** ($1\cdot10^{-4}$ to $1\cdot10^{-3}$ M, 0.2-2.0 mol%) in the chosen reaction medium. [b] Gas Chromatography (GC) yields referred to the consumption of the limiting reagent (**2.2d**, **2.2e** or **4.2k**), using n-dodecane as external standard. [c] SolarBox: (1500 W Xe lamp; 500 W m^{-2}). [d] Under air-equilibrated conditions. [e] In the absence of light. [f] 24 h irradiation. [g] Ten 15 W phosphor-coated lamps with emission centered at 366 nm [h] 1W LEDs with emission at 410 nm. [i] 1W LED with emission at 450 nm. [j] 250 W sodium lamp (emission at 589 nm).*

In order to confirm the radical nature of the process I repeated the reaction between **3.1a** and **2.2d** under the optimized conditions of Table 4.4, *entry 10*, in the presence of a radical scavenger. As a result, the presence of 1 equiv. of TEMPO completely inhibited the reaction (negligible consumption of **2.2d**, see Experimental section for details).

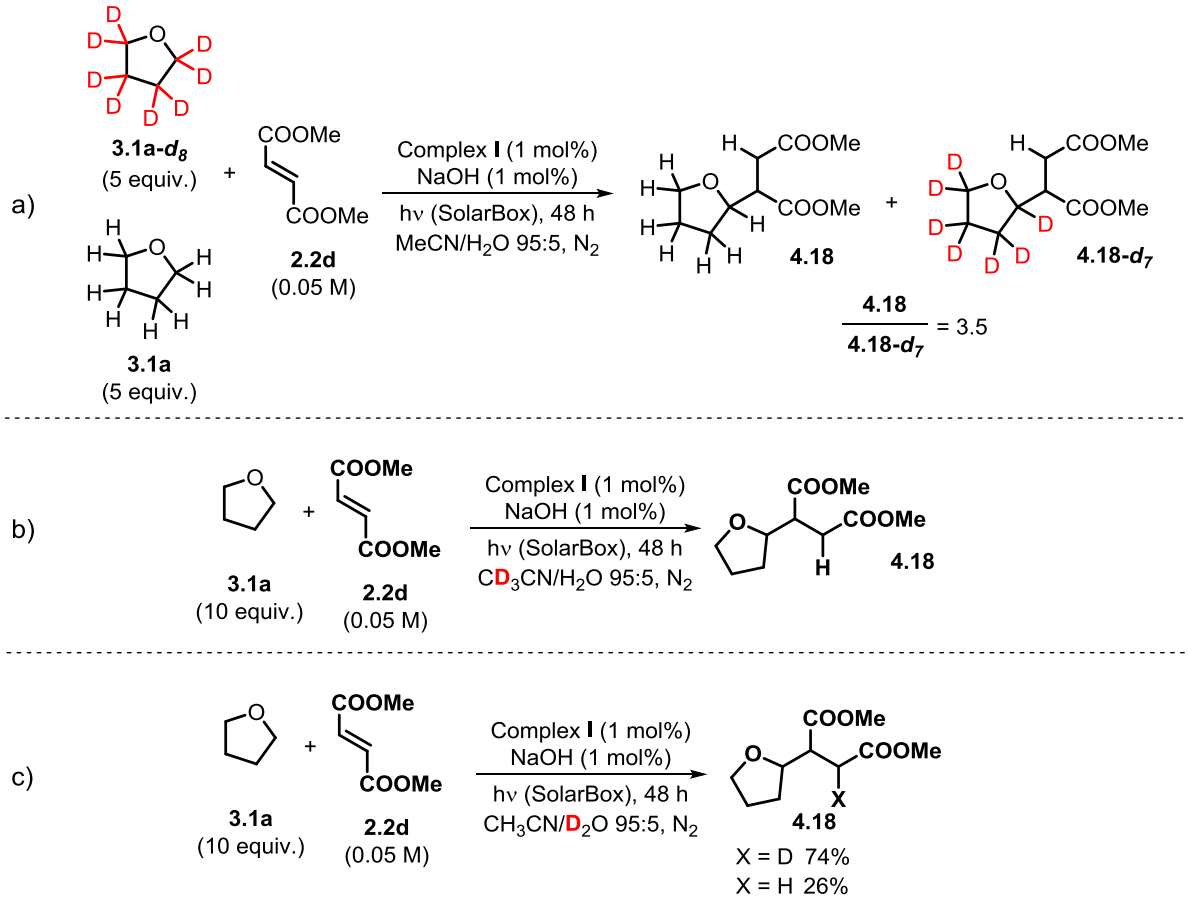

*Scheme 4.1 Isotopic substitution studies in the reaction between **3.1a** and **2.2d**: a) cross-over experiment; b) use of deuterated acetonitrile; c) use of deuterated water.*

Furthermore, when the reaction between THF and **2.2d** was performed in the presence of an equimolar mixture of **3.1a** and perdeuterated **3.1a**-d_8 (5 equiv. each), a preferential activation of the former compound occurred, with formation of **4.18** and **4.18**-d_7 in a 3.5:1 ratio (see Scheme 4.1a) according to GC-MS analysis (see Experimental Section for details). This experiment suggests that the HAT process is involved in the rate-determining step.

Next, I tried to rule out a possible role of the organic solvent in a radical chain-type mechanism: as a matter of fact, in Scheme 4.1b, the experiment shows that the D-atom in the organic solvent

CD_3CN is not retained in the product. This implies that acetonitrile is not taking part to the radical reaction.

Finally, in Scheme 4.1c, the experiment shows that, when deuterated water is used, deuterium is largely retained in the product.

Based on these observations, I propose the mechanism reported in Scheme 4.2. The dihydroxo antimony porphyrin is not active for the photoreaction but, upon addition of a stoichiometric amount of a base (aqueous NaOH), the antimony-oxo functionality is generated *in-situ*.

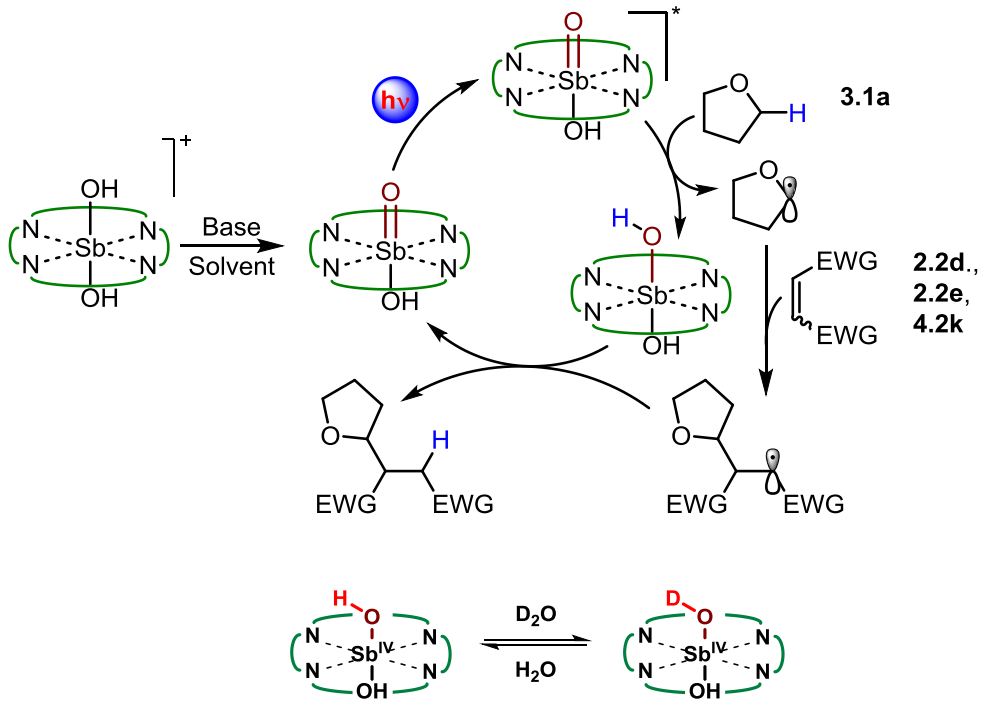

Scheme 4.2 Mechanism proposed.

After visible light absorption, the excited state is generated and **3.1a** is activated via a visible-light induced HAT. The resulting radical is then trapped by **2.2d**, **2.2e** and **4.2k** to afford the Giese radical adduct. The last step consists in the closure of the photocatalytic cycle, restoring the active form of the photocatalyst; however, based on Scheme 4.1c, I suggest that a proton-scrambling between the reduced photocatalyst and water is operating.

Conclusion and Future Perspectives

These data show that Complex **I** is a promising photocatalyst for visible light HAT. As a matter of fact, tetrahydrofuran was chosen as a benchmark and it was successfully activated via the homolytic cleavage of a C-H bond to generate an α-alkoxyalkyl radical that was readily intercepted by electrophilic olefins. To the best of my knowledge, this is the first time that a metallo-oxo porphyrin is used for a photocatalytic C-H to C-C bond conversion. Trapping experiments with a radical scavenger and deuteration experiments show the radical nature of the process and the KIE value is typical for rate-determining HAT steps. Finally, I speculate that the resting state of the photocatalyst is the reduced state, since a proton-scrambling equilibrium was highlighted by experiment reported in Scheme 4.1c. To fully elucidate the behavior of the excited state of the photocatalyst, Prof. Günther Knör is currently carrying out a deep and meticulous spectroscopic investigation.

References

(1) Protti, S.; Fagnoni, M.; Ravelli, D. *ChemCatChem* **2015**, *7* (10), 1516–1523.

(2) Ravelli, D.; Protti, S.; Fagnoni, M. *Acc. Chem. Res.* **2016**, *49* (10), 2232–2242.

(3) Capaldo, L.; Ravelli, D. *Eur. J. Org. Chem.* **2017**, *2017* (15), 2056–2071.

(4) Kamijo, S.; Kamijo, K.; Maruoka, K.; Murafuji, T. *Org. Lett.* **2016**, *18* (24), 6516–6519.

(5) Fan, X.-Z.; Rong, J.-W.; Wu, H.-L.; Zhou, Q.; Deng, H.-P.; Tan, J. Da; Xue, C.-W.; Wu, L.-Z.; Tao, H.-R.; Wu, J. *Angew. Chem. Int. Ed.* **2018**, *57* (28), 8514–8518.

(6) Xia, J.-B.; Zhu, C.; Chen, C. *Chem. Commun.* **2014**, *50* (79), 11701–11704.

(7) Xia, J.-B.; Zhu, C.; Chen, C. *J. Am. Chem. Soc.* **2013**, *135* (46), 17494–17500.

(8) West, J. G.; Bedell, T. A.; Sorensen, E. J. *Angew. Chem. Int. Ed.* **2016**, *55* (31), 8923–8927.

(9) Lu, G.; Forbes, T. Z.; Haes, A. J. *Analyst* **2016**, *141* (17), 5137–5143.

(10) Dhara, S.; Misra, N. L.; Aggarwal, S. K. *Spectrochim. Acta - Part B At. Spectrosc.* **2008**, *63* (12), 1395–1398.

(11) Brina, R.; Miller, A. G. *Anal. Chem.* **1992**, *64* (13), 1413–1418.

(12) Dhara, S.; Khooha, A.; Singh, A. K.; Tiwari, M. K.; Misra, N. L. *Spectrochim. Acta - Part B At. Spectrosc.* **2018**, *144*, 87–91.

(13) Abbasi, S. A. *Int. J. Environ. Anal. Chem.* **1989**, *36* (3), 163–172.

(14) Ye, J.; Bogale, R. F.; Shi, Y.; Chen, Y.; Liu, X.; Zhang, S.; Yang, Y.; Zhao, J.; Ning, G. *Chem. Eur. J.* **2017**, *23* (32), 7657–7662.

(15) Peled, Y.; Krent, E.; Tal, N.; Tobias, H.; Mandler, D. *Anal. Chem.* **2015**, *87* (1), 768–776.

(16) Arfsten, D. P.; Still, K. R.; Ritchie, G. D. *Toxicol. Ind. Health* **2001**, *17* (10), 180–191.

(17) Domingo, J. L. *Reprod. Toxicol.* **2001**, *15* (6), 603–609.

(18) Hartmann, H. M.; Monette, F. A.; Avci, H. I. *Hum. Ecol. Risk Assess.* **2000**, *6* (5), 851–874.

(19) Hamilton, E. I. *Sci. Total Environ.* **2001**, *281* (1–3), 5–21.

(20) Hindin, R.; Brugge, D.; Panikkar, B. *Environ. Heal. A Glob. Access Sci. Source* **2005**, *4*, 4–

17.

(21) Bucholz, A. *Ann. Chim.* **1805**, *56*, 142–149.

(22) McGlynn, S. P. *J. Am. Chem. Soc.* **1965**, *87* (11), 2527.

(23) Matsushima, R. *J. Am. Chem. Soc.* **1972**, *94* (17), 6010–6016.

(24) Azenha, M. E. D. G.; Burrows, H. D.; Formosinho, S. J.; Miguel, M. de G. M. *J. Chem. Soc. Faraday Trans. 1 Phys. Chem. Condens. Phases* **1989**, *85* (8), 2625.

(25) Hill, R. J.; Kemp, T. J.; Allen, D. M.; Cox, A. *J. Chem. Soc. Faraday Trans. 1 Phys. Chem. Condens. Phases* **1974**, *70* (1), 847–857.

(26) Jørgensen, C. K.; Reisfeld, R. *Top. Inorg. Phys. Chem.* **1982**, *50*, 121–171.

(27) Formosinho, S. J.; Burrows, H. D.; da Graça Miguel, M.; Azenha, M. E. D. G.; Saraiva, I. M.; Ribeiro, A. C. D. N.; Khudyakov, I. V.; Gasanov, R. G.; Bolte, M.; Sarakha, M. *Photochem. Photobiol. Sci.* **2003**, *2* (5), 569–575.

(28) Ghosh, R.; Mondal, J. A.; Ghosh, H. N.; Palit, D. K. *J. Phys. Chem. A* **2010**, *114* (16), 5263–5270.

(29) Matushima, R.; Mori, K.; Suzuki, M. *Bull. Chem. Soc. Jpn.* **1976**, *49*, 38–41.

(30) Berto, S.; Crea, F.; Daniele, P. G.; de Stefano, C.; Prenesti, E.; Sammartano, S. *Ann. Chim.* **2006**, *96* (7–8), 399–420.

(31) Sandhu, S. S.; Kohli, K. B.; Brar, A. S. *Inorg. Chem.* **1984**, *23* (22), 3609–3612.

(32) Burrows, H. D.; Kemp, T. J. *Chem. Soc. Rev.* **1974**, *3* (2), 139–165.

(33) Hoffman, M. Z.; Bolletta, F.; Moggi, L.; Hug, G. L. *J. Phys. Chem. Ref. Data* **1989**, *18* (1), 219–543.

(34) Bhatt, B. R.; Shrimali, P. S.; Amete, S. C.; Chowdhry, H. C. *Z. Phys. Chem.* **1986**, *267*, 817–820.

(35) Mao, Y.; Bakac, A. *Inorg. Chem.* **1996**, *35* (13), 3925–3930.

(36) Sakuraba, S.; Matsushima, R. *Bull. Chem. Soc. Jpn.* **1970**, *43* (8), 2359–2363.

(37) Sakuraba, S.; Matsushima, R. *Bull. Chem. Soc. Jpn.* **1971**, *44* (11), 2915–2918.

(38) Capaldo, L.; Buzzetti, L.; Merli, D.; Fagnoni, M.; Ravelli, D. *J. Org. Chem.* **2016**, *81* (16), 7102–7109.

(39) Umreiko, D. S. *J. Appl. Spectrosc.* **1965**, *2* (5), 302–304.

(40) McGlynn, S. P.; Smith, J. K. *J. Mol. Spectrosc.* **1961**, *6*, 164–187.

(41) Alfassi, Z. B.; Huie, R. E.; Mittal, J. P.; Neta, P.; Shoute, L. C. T. *J. Phys. Chem.* **1993**, *97* (36), 9120–9123.

(42) Miller, L. L.; Nordblom, G. D.; Mayeda, E. A. *J. Org. Chem.* **1972**, *37* (6), 916–918.

(43) Xin, J.-R.; He, Y.-H.; Guan, Z. *Org. Chem. Front.* **2018**, *5* (10), 1684–1688.

(44) Capaldo, L.; Fagnoni, M.; Ravelli, D. *Chem. - A Eur. J.* **2017**, *23* (27), 6527–6530.

(45) Allgäuer, D. S.; Mayr, H. *Eur. J. Org. Chem.* **2014**, *2014* (14), 2956–2963.

(46) Protti, S.; Ravelli, D.; Fagnoni, M.; Albini, A. *Chem. Commun.* **2009**, No. 47, 7351.

(47) Hamilton, D. S.; Nicewicz, D. A. *J. Am. Chem. Soc.* **2012**, *134* (45), 18577–18580.

(48) Song, W. J.; Ryu, Y. O.; Song, R.; Nam, W. *J. Biol. Inorg. Chem.* **2005**, *10* (3), 294–304.

(49) Nam, W. *Acc. Chem. Res.* **2007**, *40* (7), 522–531.

(50) Liu, W.; Groves, J. T. *Acc. Chem. Res.* **2015**, *48* (6), 1727–1735.

(51) Liu, W.; Groves, J. T. *J. Am. Chem. Soc.* **2010**, *132* (37), 12847–12849.

(52) Groves, J. T.; Haushalter, R. C.; Nakamura, M.; Nemo, T. E.; Evans, B. J. *J. Am. Chem. Soc.* **1981**, *103* (10), 2884–2886.

(53) Gross, Z.; Nimri, S. *Inorg. Chem.* **1994**, *33* (9), 1731–1732.

(54) Huang, X.; Liu, W.; Ren, H.; Neelamegam, R.; Hooker, J. M.; Groves, J. T. *J. Am. Chem. Soc.* **2014**, *136* (19), 6842–6845.

(55) Nam, W.; Lim, M. H.; Oh, S.-Y. *Inorg. Chem.* **2000**, *39* (24), 5572–5575.

(56) Wołowiec, S.; Latos-Grażyński, L. *Inorg. Chem.* **1998**, *37* (12), 2984–2988.

(57) Goh, Y. M.; Nam, W. *Inorg. Chem.* **1999**, *38* (5), 914–920.

(58) Knör, G. *ChemBioChem* **2001**, *2* (7–8), 593–596.

(59) Hajimohammadi, M.; Schwarzinger, C.; Knör, G. *RSC Adv.* **2012**, *2* (8), 3257.

CHAPTER 5

PHOTOCATALYSIS VIA ENERGY TRANSFER

Introduction

As pointed out in Chapter 1, three mechanisms can be exploited to activate organic molecules in photocatalysis: Single-Electron Transfer (SET, see Chapter 2), Hydrogen Atom Transfer (HAT, see Chapters 3 and 4) and Energy Transfer (ET).

I was intrigued by this last activation path based on the following observations:

- Organic molecules own incredible reactivities in their (triplet) excited state and this reactivity has been relatively less explored than photogenerated organoradical chemistry in recent years;
- Direct excitation of organic molecules mostly occurs under highly energetic UV light and is often responsible for their photodecomposition or polymerization;
- Even if an organic molecule is excited, it usually ends up in a singlet state (S_1), but this state is usually too short-lived to be involved in chemical reactions; on the other hand, Inter-System Crossing (ISC) to a more long-lived T_1 is often inefficient, thus triplet reactivity can be hard to trigger, notwithstanding more intriguing;

A possible way out is represented by energy transfer from transition metal complexes (TMCs), compounds with extremely efficient ISC, due to the presence of a heavy metal center, which enables spin-orbit effects. In these reactions, Ru- or, more frequently, Ir-based complexes are responsible for visible light absorption to yield a singlet excited state (S_1): thanks to the presence of a heavy metal, the obtained S_1 is rapidly and efficiently interconverted to the triplet excited state (T_1).[1] The latter owns an amazingly long lifetime, typically spanning from hundreds of nanoseconds to microseconds; this time is more than enough to engage in chemical reactions with organic substrates. As for ET, the energies of the triplet state T_1 of the photocatalyst and of the substrate are the key thermodynamic factors, just as much as the bond dissociation energy (BDEs) is for HAT and redox potentials are for SET. Hence, if the T_1 of the photocatalyst is more energetic than that of the substrate, ET can occur, usually according to a double-electron exchange (Dexter mechanism,

see Chapter 1). This process leads to the generation of the T_1 state of the substrate, responsible for the follow-up reactivity.

A typical example where ET has been used to disclose a new synthetic approach consists in the synthesis of cyclobutanes via photocatalyzed [2+2] cycloadditions. Recently, the Yoon Group has initiated a program focusing on the use of visible-light triplet sensitization as an enabling technique in organic synthesis.[2–8] Remarkably, they have utilized this strategy for the intramolecular [2+2] cycloaddition of styrene[3] and 1,3-diene[5] substrates to generate a diverse set of fused bicyclic and tricyclic cyclobutanes. As part of my Ph.D. project, I decided to spend a visiting period (January - June 2018) at the University of Wisconsin-Madison, in Prof. Tehshik P. Yoon's research group, to study the synthetic potential of Energy Transfer.

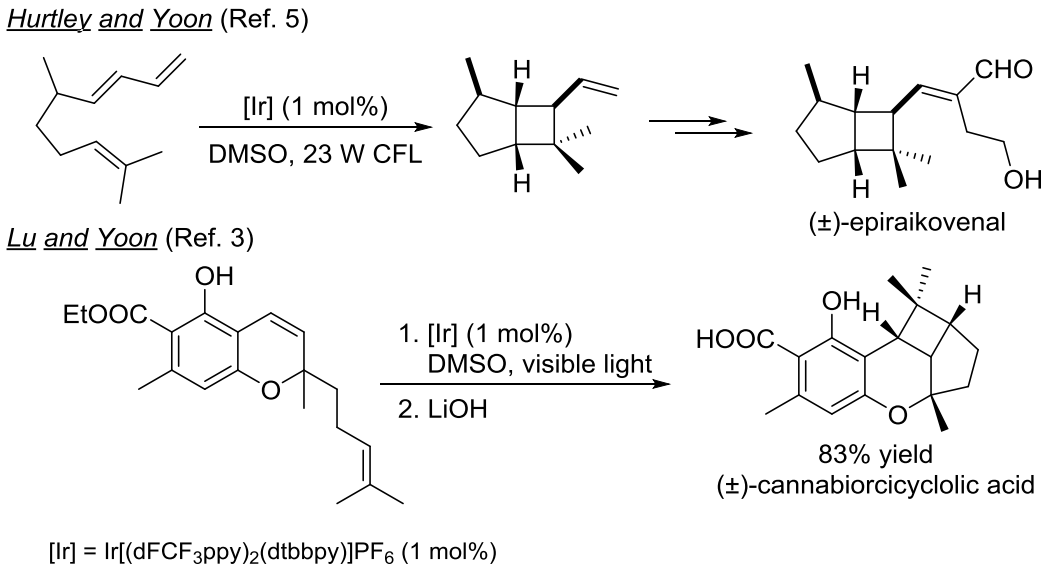

Chart 5.1 Chosen examples of synthetic application of photocatalyzed [2+2] cycloaddition by the Yoon Group.

We reasoned that, given the importance of cyclobutanes in natural products with biological activities,[9,10] the possibility of late-stage diversification of this core would be extremely desirable. Accordingly, we started looking for a compatible and versatile synthetic handle to be introduced in the substrate that could undergo photocatalyzed [2+2] cycloadditions and we came across the class of vinyl boronate esters. In particular, I contributed to explore the scope of intramolecular photocycloadditions between styrenes and vinyl boronate esters (see Figure 5.1), with the

hypothesis that the resulting boronate-functionalized cyclobutanes could serve as branching points for the rapid diversification of these novel scaffolds in medicinal chemistry campaigns.

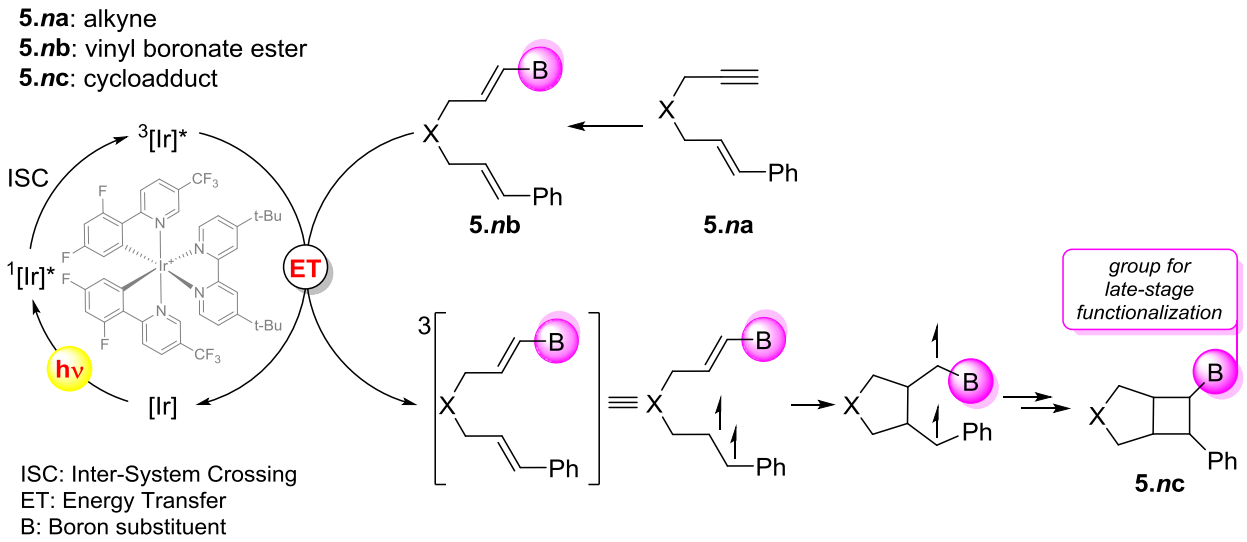

Figure 5.1 Proposed mechanistic pathway for photocatalyzed [2+2] cycloadditions with vinyl boronate esters.

This project was initiated by a former Ph.D. student, Dr. Spencer O. Scholz, whose preliminary work will be integrated herein for reasons of clarity.

Results and discussion

With the speculation that a boron-based substituent would have offered a wide array of reactions for late-stage functionalization of cyclobutanes, compound **5.1b** (Table 5.1) was synthesized from terminal alkyne **5.1a** (see Appendix I)[11] and used as the model substrate to test the feasibility of the sensitized [2+2] photocycloaddition. Gratifyingly, Dr. Scholz found that a high yield of the cycloadduct **5.1c** (see Table 5.1) was obtained using reaction conditions similar to those reported in the literature.[3] In particular, the use of Ir[(dFCF$_3$ppy)$_2$dtbbpy]PF$_6$ (1 mol%) in the role of triplet sensitizer in acetonitrile, under visible light irradiation, allowed to obtain the desired product in 97% isolated yield.

With the optimized conditions for cycloaddition in hand, we then moved to the optimization of the boron substituent (Table 5.1). A practical way to do this was to hydrolyze **5.1b** by using a mixture

of $NaIO_4/NH_4OAc$ to get the corresponding boronic acid **5.2b**,[12] which was finally manipulated to synthesize compounds **5.3b-5.5b** (see Dr. Scholz's thesis and Appendix I). However, these compounds gave lower yields in the photocycloaddition reaction compared with **5.1b** (Table 5.1); accordingly, the pinacolate ester was elected as the ideal boron substituent for the present reaction.

Table 5.1 Optimization of the boron substituent.

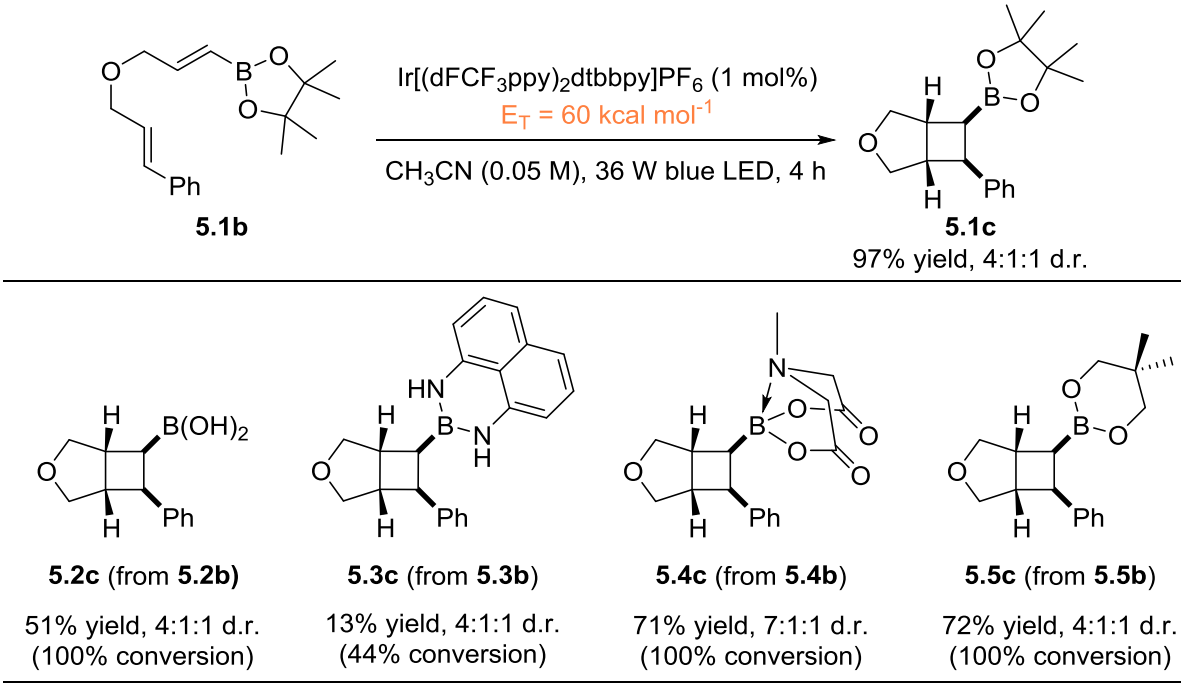

With the optimized conditions and the best boron substituent in hand, we focused our efforts on the scope of the reaction. For reasons of clarity, I report two tables: the first one gathers vinyl boronate esters synthesized in this work (**5.*n*b**, see Table 5.2), the second one contains cycloadducts (**5.*n*c**, see Table 5.3).

A reliable and versatile procedure for the synthesis of vinyl pinacolate boronate esters was needed; accordingly, after a deep research in the literature, I chose the hydroboration of alkynes **5.*n*a** in the presence of the Schwartz's reagent as the election method for the synthesis of compounds **5.*n*b** (see Table 5.2, see also Experimental Section for details).[11]

Table 5.2 Synthesis of vinyl pinacolate boronate esters.

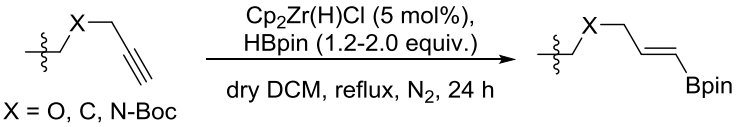

X = O, C, N-Boc

5.1a, 5.6a-5.20a **5.1b, 5.6b-5.20b**

product	yield	product	yield
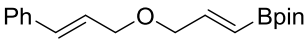	‡81%, **5.1b**	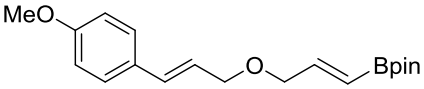	70%, **5.13b**
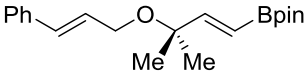	‡79%, **5.6b**	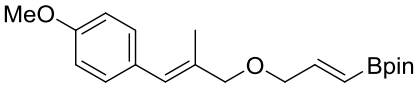	100%, **5.14b**
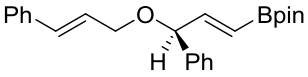	‡48%, **5.7b**	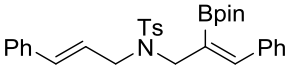	‡95%, **5.15b***
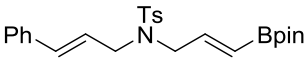	‡74%, **5.8b**	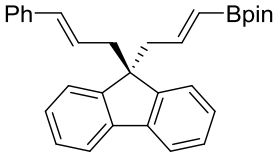	56%, **5.16b**
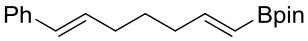	‡53%, **5.9b**	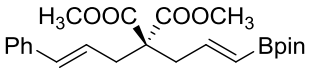	76%, **5.17b**
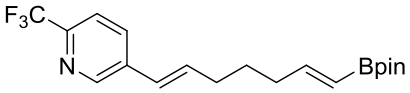	‡68%, **5.10b**	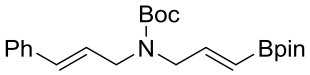	67%, **5.18b**
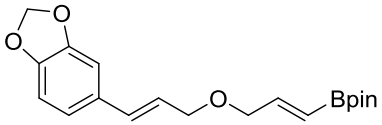	‡81%, **5.11b**	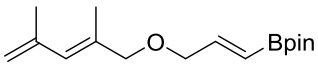	46%, **5.19b**
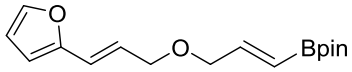	77%, **5.12b**	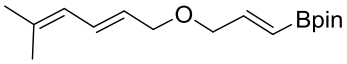	47%, **5.20b**

‡ synthesized by Dr. Spencer O. Scholz

* synthesized using a different procedure (Ref. 13)

Despite the presence of conjugated C=C double bonds, the reaction was chemoselective towards the most electron-rich alkyne function; however, if more than 2.0 equivalents of HBpin were used, overreaction by-products were observed, especially in the case of **5.19b** and **5.20b**. Besides, the latters were synthesized with lower yields (46% and 47%, respectively). The scope of the present reaction was planned also to appreciate the effect of hindered substituents on the photocycloadditions and I synthesized vinyl boronate esters **5.14b**-**5.17b**, accordingly. Again, in

this perspective, we synthesized compound **5.15b** with a different procedure,[13] where the alkyne was hydroborated with Markovnikov regioselectivity.

Table 5.3 Synthesis of cyclobutanes via photocatalyzed [2+2] cycloaddition.

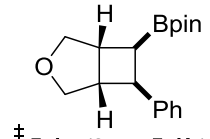 ‡**5.1c** (from **5.1b**) 87% yield, 4:1:1 d.r.	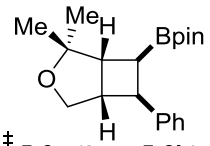 ‡**5.6c** (from **5.6b**) 93% yield, 4:1 d.r.	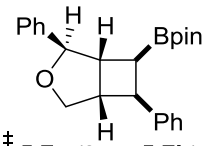 ‡**5.7c** (from **5.7b**) 84% yield, 5:1 d.r.	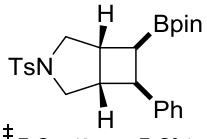 ‡**5.8c** (from **5.8b**) 84% yield, 4:1:1 d.r.
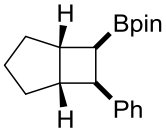 ‡**5.9c** (from **5.9b**) 89% yield[a], 4:1 d.r.	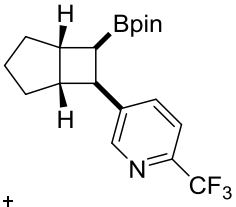 ‡**5.10c** (from **5.10b**) 65% yield[b], 6:1:1 d.r.	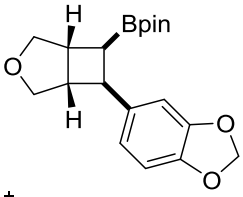 ‡**5.11c** (from **5.11b**) 63% yield, 4:1:1 d.r.	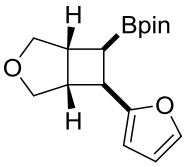 **5.12c** (from **5.12b**) 89% yield, 4:1:1 d.r.
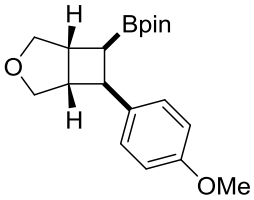 **5.13c** (from **5.13b**) 80% yield, 4:1:1 d.r.	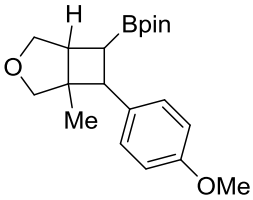 **5.14c** (from **5.14b**) 81% yield, 3:1.3:1 d.r.	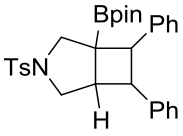 **5.15c** (from **5.15b**) 92% yield, 2:1.4:1 d.r.	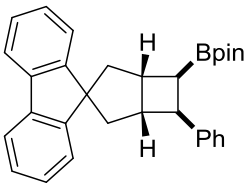 **5.16c** (from **5.16b**) 97% yield, 4:2:1 d.r.
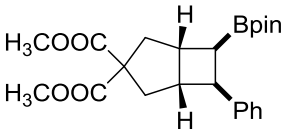 **5.17c** (from **5.17b**) 80% yield, 4:1.4:1 d.r.	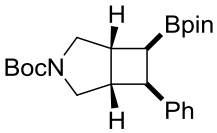 **5.18c** (from **5.18b**) 92% yield[d], 8:1 d.r.	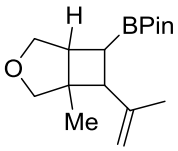 **5.19c** (from **5.19b**) 76% yield, 4:2:1 d.r.	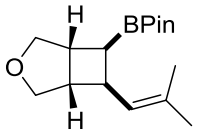 **5.20c** (from **5.20b**) 41% yield[c], 4:1 d.r.

All reactions were conducted at 0.3 mmol of substrate in degassed CH_3CN using a 36 W blue LED under N_2. Isolated yields are reported. [a] 95% conversion. [b] 90% conversion. [c] polymers were observed by ^1H NMR of the crude mixture. [d] 15 hours of irradiation

‡ Synthesized by Dr. Scholz

With these vinyl boronate esters in hand, I proceeded to the evaluation of the [2+2] photocycloaddition reaction under visible light. I used $Ir[(dFCF_3ppy)_2dtbbpy]PF_6$ (1 mol%) as the photocatalyst because of its high-energy triplet excited state (60 kcal mol^{-1}), acetonitrile as the

solvent and substrate 0.05 M to obtain, after 4 hours of irradiation with a 36 W blue LED, excellent yields of the corresponding cycloadducts **5.1c**,**5.6-5.20c** (Table 5.3).

Taken together, these results suggested the robustness of the present synthetic approach: indeed, tetrahydrofuran (**5.1c**), cyclopentane (**5.8c**) or (protected) pyrrolidine (**5.9c**) tethers could be used, even in the presence of sterically demanding groups (**5.6c**-**5.7c**). Electronically non-innocent substituents on the styrene moiety did not impede the reaction, as demonstrated by the results obtained with compounds **5.10c** and **5.11c**.

The reaction worked well in the presence of heterocycles (**5.12c**) and electron-rich aromatics (**5.13c**), showing once again versatility and robustness. As expected, when the substituents were on the bridgehead (**5.14c** and **5.15c**) the diastereomeric ratio decreased, while substitution on the remaining positions of the fused bicyclic compounds did not compromise diastereomeric ratio (**5.16c**-**5.18c**). Next, I expanded the scope of the present reaction to 1,3-diene substrates **5.19b** and **5.20b**, to obtain **5.19c** and **5.20c** in 76% and 41% yield, respectively (Table 5.3).[2] In the last case, polymerization was observed after irradiation by ^{1}H NMR, which explains the poor mass balance. Interestingly, I noted that alkyne **5.20a** was not shelf-stable and, after 7 days, spontaneously underwent a Diels-Alder reaction.

As for the mechanistic aspects, as already mentioned the present reaction works via a visible light triplet sensitization (see Figure 5.1) where the highly energetic triplet state of the Ir-based photocatalyst can engage in Energy Transfer via Dexter mechanism with vinyl boronates **5.*n*b** promoting the formation of the triplet excited state of the substrate and, finally, the stepwise cyclization (see Figure 5.1).

However, it is worth noting that the triplet energy of the styrene moiety and that of the vinyl boronate ester are both around 60 kcal mol^{-1} (datum was obtained from calculations by Dr. Scholz at the B3LYP/6-31G(d) level of theory): this means that both may quench the excited state of the photocatalyst. However, as reported by Dr. Scholz, compound **5.21b** did <u>not</u> undergo the

photocycloaddition, suggesting that energy transfer to the styrene moiety is responsible for the observed reactivity (Chart 5.2).

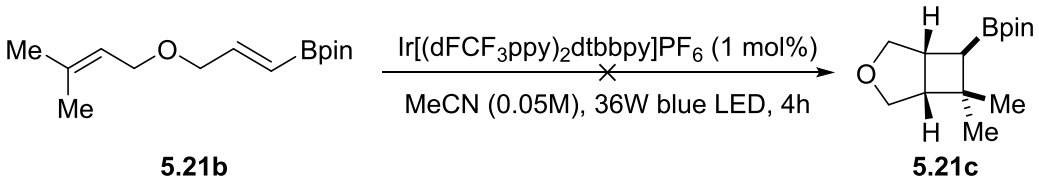

5.21b **5.21c**

Chart 5.2

Conclusions and Future Perspectives

In conclusion, we have developed a robust, operationally simple approach that well tolerates a wide range of functional groups and substituents. The present reaction paves the way toward a library of densely functionalized cyclobutanes featuring a synthetic handle for late-stage diversification and consists in the use of an Ir-based complex as a triplet sensitizer in a photocatalytic intramolecular [2+2] cycloaddition between styrenes and vinyl boronate esters. Additionally, 1,3-dienes were well tolerated and this allowed to have C=C double bonds in the final products (see **5.19c**, **5.20c**): this function is orthogonal to the boronate ester one, stressing the synthetic value of this transformation.

Finally, the boron substituent is extremely advantageous from a synthetic standpoint, mainly because of its versatility: it can be readily oxidized,[14] hydrolyzed,[12] or transformed into the corresponding trifluoroborate ion.[15]

As an example, just before finishing my visiting period, I undertook the synthesis of trifluoroborate ions. Trifluoroborate salts have several advantages over boronic acids or boronate esters: for example, the latters are susceptible to protodeborylation in Suzuki reactions. In general, potassium organotrifluoroborate compounds are less susceptible to deleterious reactivity due to the lack of an empty p-orbital on the boron center.[15]

Actually, preliminary attempts showed that conversion of **5.18c** to organotrifluoroborate **5.18d** was effective (see Chart 5.3), and a deeper analysis of this transformation and the study of **5.18d** in a follow-up C(sp^3)-C(sp^2) bond formation via cross-coupling[16] is currently ongoing in the Yoon Group.

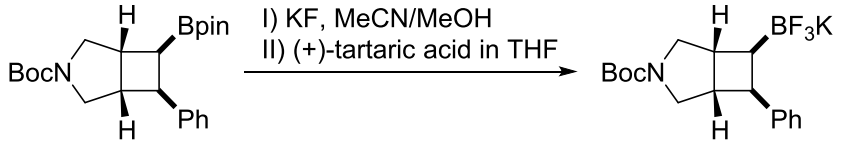

0.6 mmol, **5.18c** 60% yield, **5.18d**

Chart 5.3 Proof-of-concept for the synthesis of organotrifluoroborates from pinacolate boronate esters.[15]

References

(1) Prier, C. K.; Rankic, D. A.; MacMillan, D. W. C. *Chem. Rev.* **2013**, *113* (7), 5322–5363.

(2) Farney, E. P.; Yoon, T. P. *Angew. Chem. Int. Ed.* **2014**, *53* (3), 793–797.

(3) Lu, Z.; Yoon, T. P. *Angew. Chem. Int. Ed.* **2012**, *51* (41), 10329–10332.

(4) Scholz, S. O.; Farney, E. P.; Kim, S.; Bates, D. M.; Yoon, T. P. *Angew. Chem. Int. Ed.* **2016**, *55* (6), 2239–2242.

(5) Hurtley, A. E. E.; Lu, Z.; Yoon, T. P. P. *Angew. Chem. Int. Ed.* **2014**, *53* (34), 8991–8994.

(6) Blum, T. R.; Miller, Z. D.; Bates, D. M.; Guzei, I. A.; Yoon, T. P. *Science* **2016**, *354* (6318), 1391–1395.

(7) Skubi, K. L.; Kidd, J. B.; Jung, H.; Guzei, I. A.; Baik, M.-H.; Yoon, T. P. *J. Am. Chem. Soc.* **2017**, *139* (47), 17186–17192.

(8) Miller, Z. D.; Lee, B. J.; Yoon, T. P. *Angew. Chem. Int. Ed.* **2017**, *56* (39), 11891–11895.

(9) Hansen, T. V.; Stenstrom, Y. In *Organic Synthesis: Theory and Application*; Hudlicky, T., Ed.; Oxford, U.K: Elsevier, U.K: Elsevier, 2001; pp 1–38.

(10) Dembitsky, V. M. *J. Nat. Med.* **2007**, *62* (1), 1–33.

(11) Pereira, S.; Srebnik, M. *Organometallics* **1995**, *14* (7), 3127–3128.

(12) Coutts, S. J.; Adams, J.; Krolikowski, D.; Snow, R. J. *Tetrahedron Lett.* **1994**, *35* (29), 5109–5112.

(13) Moure, A. L.; Mauleón, P.; Arrayás, R. G.; Carretero, J. C. *Org. Lett.* **2013**, *15* (8), 2054–2057.

(14) Ito, H.; Toyoda, T.; Sawamura, M. *J. Am. Chem. Soc.* **2010**, *132* (17), 5990–5992.

(15) Molander, G. A.; Canturk, B. *Angew. Chem. Int. Ed.* **2009**, *48* (49), 9240–9261.

(16) Dreher, S. D.; Dormer, P. G.; Sandrock, D. L.; Molander, G. A. *J. Am. Chem. Soc.* **2008**, *130* (29), 9257–9259.

CHAPTER 6

EXPERIMENTAL SECTION

EXPERIMENTAL SECTION RELATIVE TO

CHAPTER 2

SMOOTH PHOTOCATALYZED BENZYLATION OF ELECTROPHILIC OLEFINS VIA DECARBOXYLATION OF ARYLACETIC ACIDS.[1]

Electrochemical Study

The electrochemical measurements were carried out by a BASi computer-controlled electrochemical analyzer. Electrochemical measurements (cyclic voltammetry) were performed in a three-electrode cell (volume 10 mL; acetonitrile as solvent, $nBu_4N^+ClO_4^-$ 0.1 M as the supporting electrolyte, 2 mM concentration of the tested compound)[1] at glassy carbon (diameter 2 mm, BASi) as the working electrode, Pt wire as the auxiliary electrode, and Ag/AgCl (3 M NaCl) as the reference electrode. Scan speed was 100 mV/s^{-1}.

The potential range investigated was 0/+2.0 V vs Ag/AgCl (3 M NaCl) for oxidation and 0/-2.0V vs Ag/AgCl (3 M NaCl) for reduction processes, respectively. The potentials measured were then referred to SCE by applying the equation:

$$E\ (vs\ SCE) = E\ (vs\ Ag/AgCl;\ 3\ M\ NaCl) - 35\ mV$$

In the case of arylacetic acids **2.1**, no redox signal was registered unless a base was added (1 equiv. of a 1.0 N $nBu_4N^+OH^-$ in MeOH was used) to liberate the corresponding carboxylate anion **2.1**$^-$. The analysis on **2.2c** was performed without adding any base.

In the case of derivatives **2.1**$^-$, typically irreversible or quasi reversible redox behaviors were observed. In all cases, the cathodic peaks observed were < 0.5 times the anodic peaks in term of intensity, meaning that a chemical irreversible process (C) followed the electron transfer (E), leading to an EC mechanism.[2] For this reason, the data reported in Table 2.1 refer to $E_{1/2}$ values of the oxidation process, better appreciated by plotting the cyclic voltammogram in the semi-

differential mode. In all cases, a transfer of two electrons in the anodic process was observed, in accordance with previous reports.[1,2]

By contrast, for **2.2c** a reversible redox behavior was observed. For this reason, the $E_{1/2}$ value can be approximated with the formal redox potential (E_0'; see Table 2.2), in accordance with a previous work by our group.[3]

Experimental Data

General Procedure for the TBADT-photocatalyzed Decarboxylative Benzylation of Electron-poor Olefins: An acetonitrile/water 2:1 solution (15 mL) of the acid **2.1** (0.75 mmol, 0.05 M, 1 equiv.) and the olefin **2.2** (1 equiv.), in the presence of TBADT (2×10^{-3} M, 4 mol%), $NaHCO_3$ (1 equiv.), $NaClO_4$ (1 equiv.) and biphenyl (1 equiv.), was poured in a quartz tube and purged for 3 minutes with nitrogen, septum capped and irradiated for 24 h in a multi-lamp apparatus fitted with 10×15 W phosphor-coated lamps (emission centered at 310 nm). The solvent was removed under reduced pressure from the photolyzed solution and the product isolated by purification of the residue by column chromatography (hexane/ethyl acetate as eluants).

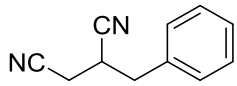

2-Benzylsuccinonitrile (2.3). From 2-phenylacetic acid **2.1a** (0.75 mmol, 1 equiv., 102 mg) and fumaronitrile **2.2a** (0.75 mmol, 1 equiv., 58 mg). Colorless oil (102 mg, 80% yield). Purification: silica gel chromatography (hexane/ethyl acetate 8:2). Spectroscopic data of **2.3** were in accordance with the literature.[4] Anal. Calcd. for $C_{11}H_{10}N_2$: C, 77.62; H, 5.92; N, 16.46. Found: C: 77.7; H 5.8; N, 16.2.

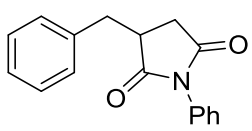

3-Benzyl-1-phenylpyrrolidine-2,5-dione (2.4). From 2-phenylacetic acid **2.1a** (0.75 mmol, 1 equiv., 102 mg) and *N*-phenyl maleimide **2.2b** (0.75 mmol, 1 equiv., 130 mg). White solid (143 mg, 72% yield). Purification: silica gel chromatography (hexane/ethyl acetate 8:2). M.p. 123-125 °C (Lit.[3] 128-130 °C). Spectroscopic data of **2.4** were in

accordance with the literature.[3] Anal. Calcd. for $C_{17}H_{15}NO_2$: C, 76.96; H, 5.70; N, 5.28. Found: C, 76.8; H, 5.9; N, 5.2.

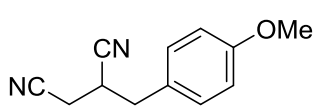

2-(4-Methoxybenzyl)succinonitrile (2.5). From 2-(4-methoxy)phenylacetic acid **2.1b** (0.75 mmol, 1 equiv., 124 mg) and fumaronitrile **2.2a** (0.75 mmol, 1 equiv., 58 mg). Colorless oil (122 mg; 81% yield). Purification: silica gel chromatography (hexane/ethyl acetate 8:2). Spectroscopic data of **2.5** were in accordance with the literature.[3] Anal. Calcd. for $C_{12}H_{12}N_2O$: C, 71.98; H, 6.04; N, 13.99. Found: C, 72.0; H, 6.2; N, 13.9.

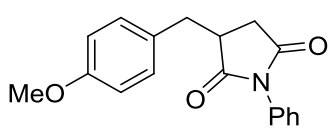

3-(4-Methoxybenzyl)-1-phenylpyrrolidine-2,5-dione (2.6). From 2-(4-methoxy)phenylacetic acid **2.1b** (0.75 mmol, 1 equiv., 124 mg) and *N*-phenyl maleimide **2.2b** (0.75 mmol, 1 equiv., 130 mg). Off-white solid (133 mg, 60% yield). Purification: silica gel chromatography (hexane/ethyl acetate 8:2). M.p. 128-130 °C. ^{1}H NMR ($CDCl_3$, 300 MHz) δ 7.49-7.35 (m, 3H), 7.19-7.12 (m, 4H), 6.86 (d, J = 8.7 Hz, 2H), 3.80 (s, 3H) 3.33-3.24 (m, 1H), 3.19-3.03 (m, 2H), 2.88 (dd, J = 18, 9 Hz, 1H), 2.64 (dd, J = 18, 5 Hz, 1H). ^{13}C NMR ($CDCl_3$, 75 MHz) δ 178.5, 175.5, 159.0, 132.0, 130.4, 129.3, 128.8, 128.7, 126.6, 114.4, 55.4, 41.6, 35.8, 33.4. Anal. Calcd. for $C_{18}H_{17}NO_3$: C, 73.20; H, 5.80; N, 4.74. Found: C, 73.2; H, 5.9; N, 4.6.

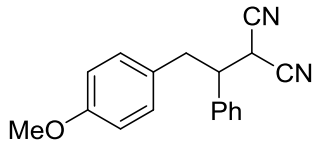

2-(2-(4-Methoxyphenyl)-1-phenylethyl)malononitrile (2.7). From 2-(4-methoxy)phenylacetic acid **2.1b** (0.75 mmol, 1 equiv., 124 mg) and 2-benzylidenemalononitrile **2.2c** (0.75 mmol, 1 equiv., 116 mg). Colorless oil (205 mg; 99% yield). Purification: silica gel chromatography (hexane/ethyl acetate 8:2). ^{1}H NMR ($CDCl_3$, 300 MHz) δ 7.48-7.33 (m, 5H), 7.09 (d, J = 8.6 Hz, 2H), 6.86 (d, J = 8.5 Hz, 2H), 3.86 (d, J = 5.1 Hz, 1H), 3.79 (s, 3H), 3.44-3.38 (m, 1H), 3.21 (d, J = 8 Hz, 2H). ^{13}C NMR ($CDCl_3$, 75 MHz) δ 159.1, 136.6, 130.1, 129.3, 129.2, 128.6, 128.2, 114.7, 112.3, 111.6, 55.4, 48.7, 37.8, 28.5. Anal. Calcd. for $C_{18}H_{16}N_2O$: C, 78.24; H, 5.84; N, 10.14. Found: C, 78.2; H, 5.9; N, 10.0.

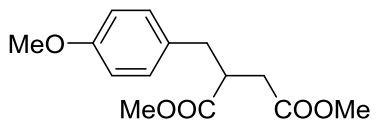

Dimethyl 2-(4-methoxybenzyl)succinate (2.8). From 2-(4-methoxy)phenylacetic acid **2.1b** (0.75 mmol, 1 equiv., 124 mg) and dimethyl fumarate **2.2d** (0.75 mmol, 1 equiv., 108 mg). Colorless oil (80 mg; 40% yield). Purification: silica gel chromatography (hexane/ethyl acetate 8:2). Spectroscopic data of **2.8** were in accordance with the literature.[4] Anal. Calcd. for $C_{14}H_{18}O_5$: C, 63.15; H, 6.81. Found: C, 63.2; H, 6.7.

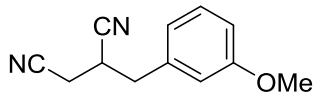

2-(3-Methoxybenzyl)succinonitrile (2.9). From 2-(3-methoxy)phenylacetic acid **2.1c** (0.75 mmol, 1 equiv., 124 mg) and fumaronitrile **2.2a** (0.75 mmol, 1 equiv., 58 mg). Colorless oil (81 mg; 54% yield). Purification: silica gel chromatography (hexane/ethyl acetate 8:2). Spectroscopic data of **2.9** were in accordance with the literature.[3] Anal. Calcd. for $C_{12}H_{12}N_2O$: C, 71.98; H, 6.04; N, 13.99. Found: C, 71.8; H, 6.1; N, 13.9.

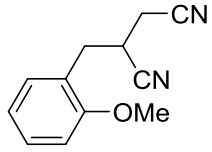

2-(2-Methoxybenzyl)succinonitrile (2.10). From 2-(2-methoxy)phenylacetic acid **2.1d** (0.75 mmol, 1 equiv., 124 mg) and fumaronitrile **2.2a** (0.75 mmol, 1 equiv., 58 mg). Colorless oil (105 mg; 70% yield). Purification: silica gel chromatography (hexane/ethyl acetate 8:2). ^{1}H NMR ($CDCl_3$, 300 MHz) δ 7.31 (td, J = 8, 2 Hz, 1H), 7.21 (dd, J = 7, 1 Hz, 1H), 6.95 (td, J = 7, 1 Hz, 1H), 6.90 (d, J = 8.3 Hz, 1H), 3.85 (s, 3H), 3.41-3.23 (m, 1H), 3.16-3.00 (m, 2H), 2.71-2.54 (m, 2H). ^{13}C NMR ($CDCl_3$, 75 MHz) δ 157.4, 131.3, 129.6, 123.1, 121.0, 119.1, 115.9, 110.7, 55.4, 32.9, 28.3, 20.4. Anal. Calcd. for $C_{12}H_{12}N_2O$: C, 71.98; H, 6.04; N, 13.99. Found: C, 71.9; H, 6.2; N, 13.8.

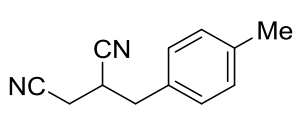

2-(4-Methylbenzyl)succinonitrile (2.11). From 2-(4-methyl)phenylacetic acid **2.1e** (0.75 mmol, 1 equiv., 112 mg) and fumaronitrile **2.2a** (0.75 mmol, 1 equiv., 58 mg). Colorless oil (72 mg; 52% yield). Purification: silica gel chromatography (hexane/ethyl acetate 9:1). Spectroscopic data of **2.11** were in accordance with the literature.[5] Anal. Calcd. for $C_{12}H_{12}N_2$: C, 78.23; H, 6.57; N, 15.21. Found: C, 78.2; H, 6.7; N, 15.1.

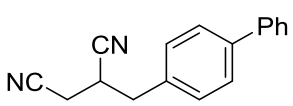

2-([1,1'-Biphenyl]-4-ylmethyl)succinonitrile (2.12). From 2-([1,1'-biphenyl]-4-yl)acetic acid **2.1f** (0.75 mmol, 1 equiv., 159 mg) and fumaronitrile **2.2a** (0.75 mmol, 1 equiv., 58 mg). White solid (116 mg, 63% yield). Purification: silica gel chromatography (hexane/ethyl acetate 8:2). M.p.: 117-119 °C. ^{1}H NMR ($CDCl_3$, 300 MHz) δ 7.62-7.57 (m, 4H), 7.48-7.43 (m, 2H), 7.40-7.33 (m, 3H), 3.26-3.08 (m, 3H), 2.70 (d, J = 6 Hz, 2H). ^{13}C NMR ($CDCl_3$, 75 MHz) δ 141.3, 140.4, 133.4, 129.7, 129.0, 128.1, 127.8, 127.2, 118.6, 115.6, 36.8, 30.2, 20.3. Anal. Calcd. for $C_{17}H_{14}N_2$: C, 82.90; H, 5.73; N, 11.37. Found: C, 82.8; H, 5.9; N, 11.3.

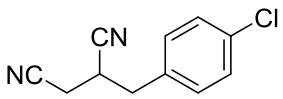

2-(4-Chlorobenzyl)succinonitrile (2.13). From 2-(4-chloro)phenylacetic acid **2.1g** (0.75 mmol, 1 equiv., 128 mg) and fumaronitrile **2.2a** (0.75 mmol, 1 equiv., 58 mg). White solid (68 mg, 44% yield). Purification: silica gel chromatography (hexane/ethyl acetate 8:2). M.p.: 79-82 °C (Lit.[6] 80-82 °C). The spectroscopic data of **2.13** were in accordance with the literature.[3] Anal. Calcd. for $C_{11}H_9ClN_2$: C, 64.56; H, 4.43; N, 13.69. Found: C, 64.4; H, 4.5; N, 13.6.

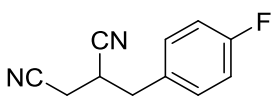

2-(4-Fluorobenzyl)succinonitrile (2.14). From 2-(4-fluoro)phenylacetic acid **2.1h** (0.75 mmol, 1 equiv., 115 mg) and fumaronitrile **2.2a** (0.75 mmol, 1 equiv., 58 mg). Colorless oil, that solidified upon standing (79 mg, 56% yield). Purification: silica gel chromatography (hexane/ethyl acetate 8:2). M.p.: 82-85 °C (Lit.[6] 84-86 °C). Spectroscopic data of **2.14** were in accordance with the literature.[6] Anal. Calcd. for $C_{11}H_9FN_2$: C, 70.20; H, 4.82; N, 14.88. Found: C, 70.1; H, 4.9; N, 14.8.

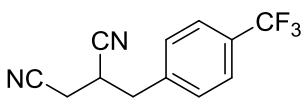

2-(4-(Trifluoromethyl)benzyl)succinonitrile (2.15). From 2-(4-(trifluoromethyl)phenyl)acetic acid **2.1j** (0.75 mmol, 1 equiv., 153 mg) and fumaronitrile **2.2a** (0.75 mmol, 1 equiv., 58 mg). Colorless oil (79 mg, 44% yield). Purification: silica gel chromatography (hexane/ethyl acetate 8:2). ^{1}H NMR (300 MHz, $CDCl_3$) δ 7.65 (d, J = 8.1 Hz, 2H), 7.42 (d, J = 8.0 Hz, 2H), 3.28-3.08 (m, 3H), 2.70 (d, J = 5.9 Hz, 2H). ^{13}C NMR (75 MHz, $CDCl_3$) δ 138.6 (s), 130.5 (q, J = 33 Hz), 129.7 (s), 126.2 (q, J = 4 Hz), 123.7 (q, J = 272 Hz), 118.5

(s), 115.5 (s), 36.8 (s), 30.0 (s), 20.4 (s). Anal. Calcd. for $C_{12}H_9F_3N_2$: C, 60.51; H, 3.81; N, 11.76. Found: C, 60.4; H, 3.9; N, 11.8.

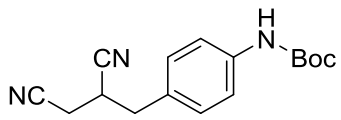

tert-Butyl (4-(2,3-dicyanopropyl)phenyl)carbamate (2.16). From 2-(4-((tert-butoxycarbonyl)amino)phenyl)acetic acid **2.1i** (0.75 mmol, 1 equiv., 188 mg) and fumaronitrile **2.2a** (0.75 mmol, 1 equiv., 58 mg). White solid (169 mg, 79% yield). Purification: silica gel chromatography (hexane/ethyl acetate 8:2). M.p.: 146-148 °C. ^{1}H NMR (300 MHz, $CDCl_3$) δ 7.38 (d, J = 8.5 Hz, 2H), 7.20 (d, J = 8.5 Hz, 2H), 6.49 (s, 1H), 3.24-2.88 (m, 3H), 2.63 (d, J = 5.9 Hz, 2H), 1.52 (s, 9H). ^{13}C NMR (75 MHz, $CDCl_3$) δ 152.8, 138.5, 129.9, 128.8, 119.2, 119.1, 118.6, 115.6, 36.5, 30.3, 28.5, 20.1. Anal. Calcd. for $C_{16}H_{19}N_3O_2$: C, 67.35; H, 6.71; N, 14.73. Found: C, 67.2; H, 6.9; N, 14.6.

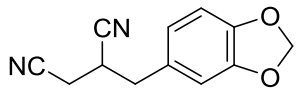

2-(1,3-Benzodioxol-5-ylmethyl)succinonitrile (2.17). From 2-(benzo[d][1,3]dioxol-5-yl)acetic acid **2.1k** (0.75 mmol, 1 equiv., 135 mg) and fumaronitrile **2.2a** (0.75 mmol, 1 equiv., 58 mg). Colorless oil (114 mg; 71% yield). Purification: silica gel chromatography (hexane/ethyl acetate 8:2). ^{1}H NMR ($CDCl_3$, 300 MHz) δ 6.79 (d, J = 8.0 Hz, 1H), 6.76-6.69 (m, 2H), 5.97 (s, 2H), 3.18-2.91 (m, 3H), 2.65 (d, J = 6.3 Hz, 2H). ^{13}C NMR ($CDCl_3$, 75 MHz) δ 148.3, 147.6, 128.0, 122.6, 118.7, 115.7, 109.3, 108.9, 101.4, 36.8, 30.3, 20.1. Anal. Calcd. for $C_{12}H_{10}N_2O_2$: C, 67.28; H, 4.71; N, 13.08. Found: C, 67.2; H, 4.9; N, 13.0.

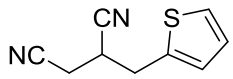

2-(Thiophen-2-ylmethyl)succinonitrile (2.18). From 2-(thiophen-2-yl)acetic acid **2.1l** (0.75 mmol, 1 equiv., 107 mg) and fumaronitrile **2.2a** (0.75 mmol, 1 equiv., 58 mg). Slightly yellow oil (69 mg; 52% yield). Purification: silica gel chromatography (hexane/ethyl acetate 8:2). ^{1}H NMR ($CDCl_3$, 300 MHz) δ 7.29 (dd, J = 5, 2 Hz, 1H), 7.12-6.97 (m, 2H), 3.43-3.13 (m, 3H), 2.75-2.67 (m, 2H). ^{13}C NMR ($CDCl_3$, 75 MHz) δ 135.9, 127.8, 127.6, 125.9, 118.4, 115.5, 31.3, 30.4, 20.0. Anal. Calcd. for $C_9H_8N_2S$: C, 61.34; H, 4.58; N, 15.90. Found: C, 61.4; H, 4.7; N, 15.8.

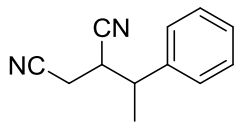

2-(1-Phenylethyl)succinonitrile (2.19). From 2-phenylpropanoic acid **2.1m** (0.75 mmol, 1 equiv., 113 mg) and fumaronitrile **2.2a** (0.75 mmol, 1 equiv., 58 mg). Colorless oil (111 mg; 80% yield; 1:1 mixture of diastereoisomers). Purification: silica gel chromatography (hexane/ethyl acetate 9:1). Spectroscopic data of **2.19** were in accordance with the literature.[3] Anal. Calcd. for $C_{12}H_{12}N_2$: C, 78.23; H, 6.57; N, 15.21. Found: C, 78.1; H, 6.6; N, 15.2

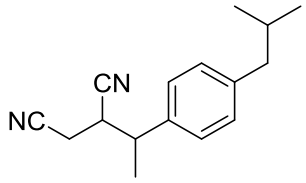

2-(1-(4-Isobutylphenyl)ethyl)succinonitrile (2.20). From 2-(4-isobutylphenyl)propanoic acid **2.1n** (0.75 mmol, 1 equiv., 155 mg) and fumaronitrile **2.2a** (0.75 mmol, 1 equiv., 58 mg). Colorless oil (103 mg; 57% yield; 1:1 mixture of diastereoisomers). Purification: silica gel chromatography (hexane/ethyl acetate 9:1). ^{1}H NMR (300 MHz, $CDCl_3$) δ 7.28-7.12 (m, 8H), 3.22-2.95 (m, 4H), 2.65-2.37 (m, 8H), 1.93-1.82 (m, 2H), 1.57 (d, J = 7 Hz, 3H), 1.56 (d, J = 7 Hz, 3H), 0.93 (d, J = 7 Hz, 6H), 0.92 (d, J = 7 Hz, 6H). ^{13}C NMR (75 MHz, $CDCl_3$) δ 142.1, 142.0, 137.5, 136.0, 130.2, 129.9, 127.6, 126.8, 118.5, 117.9, 116.0, 115.7, 45.1, 45.1, 41.1, 39.7, 36.1, 35.8, 30.3, 22.5, 22.5, 20.1, 19.7, 19.5, 19.2. Anal. Calcd. for $C_{16}H_{20}N_2$: C, 79.96; H, 8.39; N, 11.66. Found: C, 79.9; H, 8.5; N, 11.5.

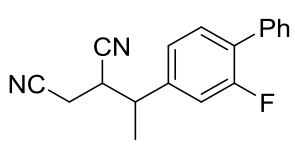

2-(1-(2-Fluoro-[1,1'-biphenyl]-4-yl)ethyl)succinonitrile (2.21). From 2-(4-isobutylphenyl)propanoic acid **2.1o** (0.75 mmol, 1 equiv., 183 mg) and fumaronitrile **2.2a** (0.75 mmol, 1 equiv., 58 mg). White thick paste (184 mg; 88% yield; 1:1 mixture of diastereoisomers). Purification: silica gel chromatography (hexane/ethyl acetate 8:2). ^{1}H NMR (300 MHz, $CDCl_3$) δ 7.56-6.99 (m, 16H), 3.35-3.10 (m, 2H), 3.09-2.92 (m, 2H), 2.73-2.63 (m, 2H), 2.55-2.44 (m, 2H), 1.59 (d, J = 7 Hz, 3H), 1.58 (d, J = 7 Hz, 3H). ^{13}C NMR (75 MHz, $CDCl_3$) δ 159.9 (d, J = 248 Hz), 159.8 (d, J = 248 Hz), 141.4 (d, J = 7 Hz), 140.0 (d, J = 7 Hz), 135.1 (d, J = 8 Hz), 135.1 (d, J = 8 Hz), 131.9 (d, J = 4 Hz), 131.6 (d, J = 4 Hz), 129.3 (d, J = 14 Hz), 129.2 (d, J = 14 Hz), 129.1, 129.0, 128.7, 128.7, 128.6, 128.2, 128.1, 127.5, 124.0 (d, J = 3 Hz), 123.3 (d, J = 3 Hz), 118.0, 117.6, 115.7, 115.6 (d, J = 23 Hz), 115.4, 114.8 (d, J = 23 Hz), 40.8, 39.7, 35.9, 35.6, 20.2, 19.6, 19.3. Anal. Calcd. for $C_{18}H_{15}FN_2$: C, 77.68; H, 5.43; N, 10.07. Found: C, 77.6; H, 5.5; N, 10.0.

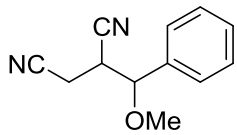

2-(Methoxy(phenyl)methyl)succinonitrile (2.23). From 2-methoxy-2-phenylacetic acid **2.1q** (0.75 mmol, 1 equiv., 125 mg) and fumaronitrile **2.2a** (0.75 mmol, 1 equiv., 58 mg). Colorless oil (117 mg; 78% yield; 1:1 mixture of diastereoisomers). Purification: silica gel chromatography (hexane/ethyl acetate 8:2). ^{1}H NMR (300 MHz, $CDCl_3$) δ 7.53-7.34 (m, 10H), 4.49-4.43 (m, 2H), 3.35 (s, 3H), 3.31 (s, 3H), 3.26-3.11 (m, 2H), 2.97-2.60 (m, 4H). ^{13}C NMR (75 MHz, $CDCl_3$) δ 135.8, 135.8, 129.7, 129.6, 129.2, 129.2, 127.1, 126.9, 117.0, 116.9, 115.9, 115.8, 81.0, 80.8, 57.5, 57.4, 36.7, 36.3, 18.4, 17.8. Anal. Calcd. for $C_{12}H_{12}N_2O$: C, 71.98; H, 6.04; N, 13.99. Found: C, 71.8; H, 6.1; N, 13.9.

ACYL RADICALS FROM ACYLSILANES: PHOTOREDOX-CATALYZED SYNTHESIS OF UNSYMMETRICAL KETONES.[58]

Electrochemical data

The electrochemical measurements were carried out by a BASi computer-controlled electrochemical analyzer. Electrochemical measurements (cyclic voltammetry) were performed in a three-electrode cell (volume 5 mL; acetonitrile/water 5:1 as solvent, nBu$_4$N$^+$PF$_6^-$ 0.05 M as the supporting electrolyte, 2 mM concentration of the tested compound) at glassy carbon (diameter 2 mm, BASi) as the working electrode, Pt wire as the auxiliary electrode, and Ag/AgCl (3 M NaCl) as the reference electrode. Scan speed was 100 mV/s.

The potential range investigated was 0/+1.80 V vs Ag/AgCl (3 M NaCl). The potentials measured were then referred to SCE by applying the equation:

$$E \text{ (vs SCE)} = E \text{ (vs Ag/AgCl; 3 M NaCl)} - 35 \text{ mV}$$

All examined compounds showed a quasi-reversible or reversible behavior.

*Table S.2.1 Oxidation potentials (V vs SCE) of compounds **2.24a-d**.*

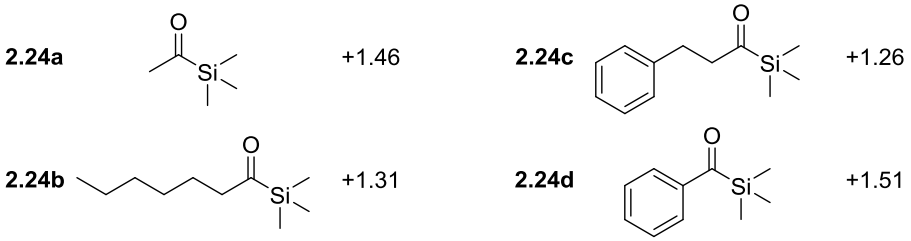

Optimization of conditions

Table S.2.2 Extended table for the optimization of reaction conditions (see Table 2.6).

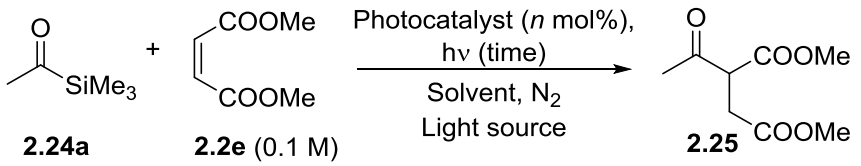

Entry	*Photocatalyst*	***2.24a*** *(M)*	*Solvent*	*Irradiation Time (h)*	*Light Source*	***2.2e*** *Consumption (%)*	***2.25*** *Yield (%)*[b]

1	TBADT (2 mol%)	0.1	MeCN	8	310 nm	30	62[c]
2	TBADT (2 mol%)	0.1	MeCN-H_2O 5/1	8	310 nm	72	71
3	TBADT (2 mol%)	0.1	0.5 M $LiClO_4$ MeCN-H_2O 5/1	8	310 nm	100	57[d]
4	**TBADT (2 mol%)**	**0.12**	**MeCN-H_2O 5/1**	**8**	**310 nm**	**100**	**72**
5	TBADT (2 mol%)	0.12	MeCN-H_2O 2/1	8	310 nm	100	47
6	TBADT (2 mol%)	0.12	MeCN-TFE 5/1	8	310 nm	32	5
7	TBADT (2 mol%)	0.12	MeCOMe-H_2O 5/1	8	310 nm	100	52
8	TBADT (1 mol%)	0.12	MeCN-H_2O 5/1	8	310 nm	70	55[d]
9	TBADT (2 mol%)	0.12	MeCN-H_2O 5/1	8	366 nm	65	52
10	TBADT (2 mol%)	0.12	MeCN-H_2O 5/1	8	SolarBox[e]	100	63
11	-	0.12	MeCN-H_2O 5/1	8	310 nm	100	4
12	TBADT (2 mol%)	0.12	MeCN-H_2O 5/1	8	-	< 5	n.d.
13	Acr^+-Mes (5 mol%)	0.12	$CHCl_3$	48	410 nm	< 5	Traces
14	Acr^+-Mes (5 mol%)	0.12	CH_2Cl_2-MeOH 9/1	48	410 nm	13	4
15[f]	Acr^+-Mes (5 mol%)	0.12	CH_2Cl_2-MeOH 9/1	48	410 nm	14	6
16[g]	Acr^+-Mes (5 mol%)	0.12	CH_2Cl_2-MeOH 9/1	48	410 nm	30	21
17	Acr^+-Mes (5 mol%)	0.12	CH_2Cl_2-MeOH 1/1	48	410 nm	23	20
18	Acr^+-Mes (5 mol%)	0.12	MeOH	48	410 nm	52	41
19	Acr^+-Mes (5 mol%)	0.15	MeOH	48	410 nm	68	65
20	Acr^+-Mes (10 mol%)	0.15	MeOH	48	410 nm	85	75
21[h]	**Acr^+-Mes (10 mol%)**	**0.15**	**MeOH**	**48**	**410 nm**	**100**	**81**

22	TPT (2 mol%)	0.12	MeCN	24	410 nm	< 5	n.d.
23	TPT (2 mol%)	0.12	MeCN-H_2O 5/1	24	410 nm	< 5	n.d.[c]
24[i]	$Ru(bpz)_3^{2+}$ (5 mol%)	0.12	MeCN-H_2O 5/1	24	450 nm	< 5	n.d.
25	DCA (0.75 mol%)	0.12	MeCN	24	410 nm	19	n.d.
26	DCA (5 mol%)	0.12	$CHCl_3$	24	410 nm	39	9

*[a] Reaction conditions: **2.24a** (0.1-0.15 M), **2.2e** (0.1 M), photocatalyst (n mol%) in 1 mL of the chosen solvent under deaerated conditions. TBADT = $(nBu_4N)_4[W_{10}O_{32}]$; Acr^+-Mes = 9-mesityl-10-methylacridinium; TPT = 2,4,6-triphenylpyrylium tetrafluoroborate; DCA: 9,10-dicyanoanthracene. [b] Gas Chromatography (GC) yields referred to the consumption of the limiting reagent (**2.2e**), using n-dodecane as internal standard. [c] A complex mixture was formed. [d] Some filming on the tube walls has been observed. [e] Irradiation carried out with a solar simulator equipped with a 1.5 kW Xe lamp (500 $W \cdot m^{-2}$). [f] Reaction performed in the presence of 0.1 M Hantzsch ester. [g] Reaction performed in the presence of 0.02 M thiophenol. [h] Air-equilibrated solution. [i] Three cycles of freeze-pump-thaw were performed prior to irradiation.*

Experimental data

Acetylsilane **2.24a** was commercially available and used as received, while acylsilanes **2.24b**,[7] **2.24c**[7] and **2.24d**[8] were prepared according to procedures adapted from the literature (see below). The photocatalyst TBADT has been prepared according to a published procedure,[9] while Acr^+-Mes tetrafluoroborate, TPT, $Ru(bpz)_3[PF_6]_2$ and DCA were commercially available. All solvents were of HPLC purity grade and employed for photochemical reactions as received. NMR spectra were recorded on a 300 (for ^1H) or 75 (for ^{13}C) MHz spectrometer; the attributions were made on the basis of ^1H and ^{13}C NMR. Data for ^1H NMR are reported as follows: chemical shift referred to TMS (δ ppm), multiplicity (s = singlet, bs = broad singlet, d = doublet, t = triplet, q = quadruplet, quint = quintuplet, sext = sextuplet, m = multiplet), coupling constant (Hz) and integration. Data for ^{13}C NMR are reported in terms of chemical shift.

Reactions were monitored by gas chromatographic (GC) analyses (HP-5 capillary column), using *n*-dodecane as external standard. Chromatographic purification of products was accomplished using flash chromatography on 60 Å, 230-400 mesh silica gel. Thin-layer chromatography (TLC) was

performed on silica gel 60 F-254 plates. Visualization of the developed plates was performed by fluorescence quenching or by $KMnO_4$ staining. UV-Vis spectra were recorded with a double beam spectrophotometer equipped with Deuterium lamp (190-350 nm) and Halogen lamp (330-900 nm) and a Photomultiplier R928.

*Synthesis of acylsilanes **2.24b-d**.*

1-(trimethylsilyl)heptan-1-one (2.24b) and 3-phenyl-1-(trimethylsilyl)propan-1-one (2.24c).

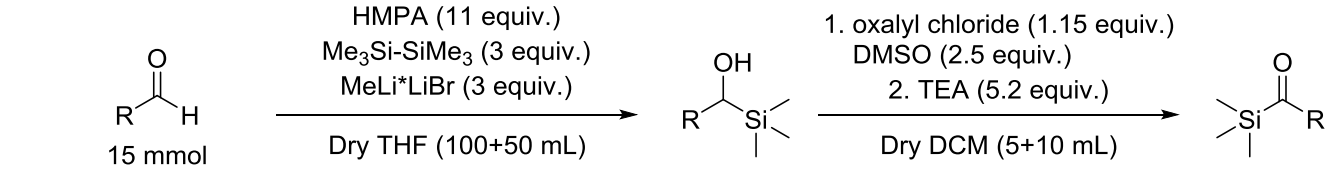

2.24b $R^1 = C_6H_{13}$
2.24c $R^2 = Ph\text{-}CH_2CH_2$

R^1 = 95%
R^2 = 75%

R^1 = 67%
R^2 = 61%

A brief description of the synthetic procedures is reported here. The first step is the silylation of the aldehyde.[10]

To a mixture of hexamethylphosphoramide (HMPA) and hexamethyldisilane kept under nitrogen at 0 °C placed in a 3-necks round-bottom flask equipped with a pressure-equalizing dropping funnel MeLi*LiBr was added. The resulting brick red solution was stirred for 5 min and tetrahydrofuran was added. The solution was cooled down at -78 °C and the aldehyde was added dropwise. The mixture was stirred overnight and quenched with water and washed with acidic water. After neutralization, the organic phases were collected, dried over Na_2SO_4 and the solvent was removed under reduced pressure. The raw product was used without any further purification.

The second step consists in the Swern oxidation of the silyl alcohol intermediate.[11]

Anhydrous dimethylsulfoxide (DMSO) in dichloromethane was added dropwise by means of a pressure-equalizing dropping funnel to a solution of oxalyl chloride in dichloromethane kept under nitrogen at -78 °C placed in a 3-necks round-bottom flask equipped with two pressure-equalizing dropping funnels. Then, the alcohol was dissolved in dichloromethane and added dropwise through a second pressure-equalizing dropping funnel. Finally, triethylamine (TEA) was added by means of

a syringe. After 3 h, the mixture was extracted with petroleum ether: the organic phases were collected, dried, the solvent removed under reduced pressure and the residue was distilled under reduced pressure to afford the desired product. The spectroscopic data of **2.24b** and **2.24c** were in accordance with the literature. [7,8]

phenyl(trimethylsilyl)methanone (2.24d)

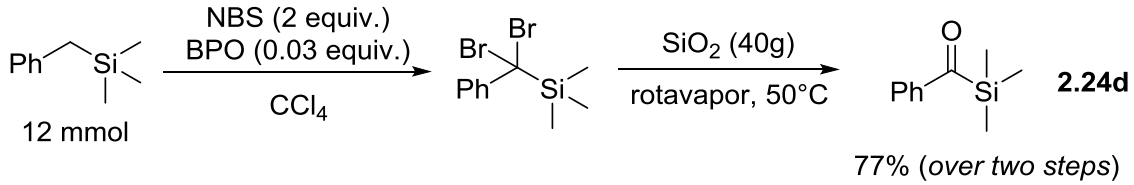

The first step consists in the dibromination of the benzylsilane. In a 3-neck round-bottom flask, a mixture of benzyltrimethylsilane, *N*-bromosuccinimide (NBS) and benzoyl peroxide (BPO) in CCl_4 was heated to reflux overnight; the formation of a white solid was observed. The mixture was cooled at room temperature and filtered to remove the precipitate, the solvent was removed in vacuo and the raw product was used without any further purification. The second step consists in the oxidation of the resulting α,α-dibromobenzylsilane. The crude product was dissolved in dichloromethane in the presence of SiO_2 (60 Å, 230-400 mesh) and the resulting suspension was heated (50 °C) under reduced pressure by means of a rotary evaporator. The solvent was removed within a few minutes, but heating was continued, while the colour of SiO_2 slowly turned to a bright yellow. After 5 h, SiO_2 was rinsed several times with diethyl ether to give a solution of pure **2.24d**.[12] The spectroscopic data of **2.24d** were in accordance with the literature.[8]

General procedure for the photoredox catalyzed acylation of electron-poor olefins.

***Method A*:** The olefin **2.2** (0.1 M) and TBADT (2 mol%) were dissolved in 15 mL of a MeCN/H_2O 5:1 mixture in a quartz tube. The resulting solution was N_2-flushed for five minutes and then acylsilane **2.24** (0.12 M) was added. In case of particularly volatile compounds (*e.g.* acetyltrimethylsilane or methyl vinyl ketone), these were added at the end of the N_2-flushing. The quartz tube was capped with a septum and the reaction mixture was irradiated in a multi-lamp

apparatus fitted with 10×15 W phosphor-coated lamps (emission centered at 310 nm) for 8 h. The solvent was then removed under reduced pressure and the residue was purified through flash chromatography to give the purified product.

***Method B*:** The acylsilane **2.24** (0.15 M) and the olefin **2.2** (0.1 M) were dissolved in 10 mL of MeOH in a vial; 9-mesityl-10-methylacridinium tetrafluoroborate (Acr^+-Mes, 10 mol%) was then added. The resulting air-equilibrated solution was divided into 10 vials and irradiated with 10×1 W LEDs (410 nm) for 48 h. The resulting mixtures were reunited, the solvent evaporated under reduced pressure and the residue purified through flash chromatography to give the purified product.

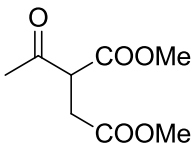

dimethyl 2-acetylsuccinate (2.25). **Method A**: From 258 μL (1.8 mmol, 0.12 M) of acetyltrimethylsilane (**2.24a**) and 188 μL (1.5 mmol, 0.1 M) of dimethyl maleate (**2.2e**). Purification of the residue by column chromatography (cyclohexane/ethyl acetate 9:1 as the eluant) afforded 195 mg of dimethyl 2-acetylsuccinate (**2.25**, 69% yield) as a colorless oil.

Flow conditions (see image of the apparatus on the left): reactor volume: 12 mL; flow rate: 0.05 mL min^{-1}, PTFE tube wrapped around a medium pressure Hg-lamp (**2.25** yield: 72%).

Sunlight irradiation: 2 days, 8 h per day, in a reaction vessel (see the image on the right) on the window ledge (**2.25** yield: 73%).

Method B: From 215 μL (1.5 mmol, 0.15 M) of **2.24a** and 125 μL (1.0 mmol, 0.1 M) of **2.2e**. Purification of the residue by column chromatography (cyclohexane/ethyl acetate 9:1 as the eluant) afforded 153 mg of dimethyl 2-acetylsuccinate (**2.25**, 81% yield) as a colorless oil.

Sunlight irradiation: 5 days, 8 h per day, in a reaction vessel on the window ledge (Yield: 71%).

The spectroscopic data of **2.25** were in accordance with the literature. [11] Anal. Calcd. for $C_8H_{12}O_5$: C, 51.06; H, 6.43. Found: C, 51.1; H, 6.4.

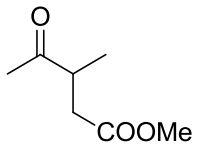

methyl 3-methyl-4-oxopentanoate (2.26). **Method A**: From 258 μL (1.8 mmol, 0.12 M) of acetyltrimethylsilane (**2.24a**) and 159 μL (1.5 mmol, 0.1 M) of methyl crotonate (**2.2f**). Purification of the residue by column chromatography (cyclohexane/ethyl acetate 8:2 as the eluant) afforded 130 mg of methyl 3-methyl-4-oxopentanoate (**2.26**, 60% yield) as a colorless oil. The spectroscopic data of **2.26** were in accordance with the literature. [12] Anal. Calcd. for $C_7H_{12}O_3$: C, 58.32; H, 8.39. Found: C, 58.3; H, 8.4.

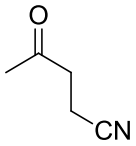

methyl 4-oxopentanenitrile (2.27). **Method A**: From 322 μL (2.25 mmol, 0.15 M) of acetyltrimethylsilane (**2.24a**) and 98 μL (1.5 mmol, 0.1 M) of acrylonitrile (**2.2g**). Purification of the residue by column chromatography (cyclohexane/ethyl acetate 8:2 as the eluant) afforded 68 mg of methyl 4-oxopentanenitrile (**2.27**, 47% yield) as a colorless oil. The spectroscopic data of **2.27** were in accordance with the literature. [13] Anal. Calcd. for C_5H_7NO: C, 61.84; H, 7.27; N, 14.42. Found: C, 61.8; H, 7.3; N, 14.4.

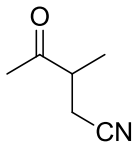

3-methyl-4-oxopentanenitrile (2.28). **Method A**: From 258 μL (1.8 mmol, 0.12 M) of acetyltrimethylsilane (**2.24a**) and 122 μL (1.5 mmol, 0.1 M) of crotonitrile (**2.2h**). Purification of the residue by column chromatography (cyclohexane/ethyl acetate 8:2 as the eluant) afforded 93 mg of 3-methyl-4-oxopentanenitrile (**2.28**, 56% yield) as a colorless oil. ^{1}H NMR ($CDCl_3$, 300 MHz) δ: 2.85 (sext, J = 7 Hz, 1H), 2.58 (dd, J_1 = 17 Hz, J_2 = 6 Hz, 1H), 2.40 (dd, J_1 = 17 Hz, J_2 = 8 Hz, 1H), 2.20 (s, 3H), 1.31 (d, J = 7 Hz, 3H). ^{13}C NMR ($CDCl_3$, 75 MHz) δ: 207.8, 118.5, 43.4, 27.9, 19.6, 16.4. Anal. Calcd. for C_6H_9NO: C, 64.84; H, 8.16; N, 12.60. Found: C, 64.8; H, 8.2; N, 12.6.

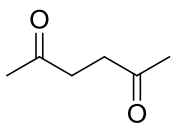

hexane-2,5-dione (2.29). **Method A**: From 258 μL (1.8 mmol, 0.12 M) of acetyltrimethylsilane (**2.24a**) and 125 μL (1.5 mmol, 0.1 M) of methyl vinyl ketone (**2.2i**). Purification of the residue by column chromatography (cyclohexane/ethyl acetate 8:2 as the eluant) afforded 92 mg of hexane-2,5-dione (**2.29**, 55% yield) as a colorless oil.

Method B: From 215 μL (1.5 mmol, 0.15 M) of **2.24a** and 83 μL (1.0 mmol, 0.1 M) of **2.2i**. Purification of the residue by column chromatography (cyclohexane/ethyl acetate 8:2 as the eluant) afforded 79 mg of hexane-2,5-dione (**2.29**, 71% yield) as a colorless oil. The spectroscopic data of **2.29** were in accordance with the literature.[14,15] Anal. Calcd. for $C_6H_{10}O_2$: C, 63.14; H, 8.83. Found: C, 63.1; H, 8.8.

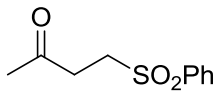

4-(phenylsulfonyl)butan-2-one (2.30). **Method A**: From 258 μL (1.8 mmol, 0.12 M) of acetyltrimethylsilane (**2.24a**) and 251 mg (1.5 mmol, 0.1 M) of phenyl vinyl sulfone (**2.2j**). Purification of the residue by column chromatography (cyclohexane/ethyl acetate 8:2 as the eluant) afforded 194 mg of 4-(phenylsulfonyl)butan-2-one (**2.30**, 61% yield) as a colorless oil.

Method B: From 215 μL (1.5 mmol, 0.15 M) of **2.24a** and 167 mg (1.0 mmol, 0.1 M) of **2.2j**. Purification of the residue by column chromatography (cyclohexane/ethyl acetate 8:2 as the eluant) afforded 151 mg of 4-(phenylsulfonyl)butan-2-one (**2.30**, 75% yield) as a colorless oil. The spectroscopic data of **2.30** were in accordance with the literature.[16] Anal. Calcd. for $C_{10}H_{12}O_3S$: C, 56.58; H, 5.70. Found: C, 56.6; H, 5.7.

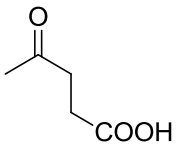

4-oxopentanoic acid (2.31). **Method A**: From 258 μL (1.8 mmol, 0.12 M) of acetyltrimethylsilane (**2.24a**) and 147 mg (1.5 mmol, 0.1 M) of maleic anhydride (**2.2k**). Purification of the residue by column chromatography (cyclohexane/ethyl acetate 8:2 as the eluant) afforded 110 mg of 4-oxopentanoic acid (**2.31**, 63% yield) as a colorless oil. The spectroscopic data of **2.31** were in accordance with the literature.[17] Anal. Calcd. for $C_5H_8O_3$: C, 51.72; H, 6.94. Found: C, 51.7; H, 7.0.

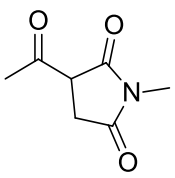

3-acetyl-1-methylpyrrolidine-2,5-dione (2.32). **Method A**: From 258 μL (1.8 mmol, 0.12 M) of acetyltrimethylsilane (**2.24a**) and 167 mg (1.5 mmol, 0.1 M) of *N*-methylmaleimide (**2.2l**). Purification of the residue by column chromatography (cyclohexane/ethyl acetate 9:1 as the eluant) afforded 184 mg of 3-acetyl-1-methylpyrrolidine-2,5-dione (**2.32**, 79% yield) as a colorless oil. ^{1}H NMR ($CDCl_3$, 300 MHz) δ: 3.95 (dd, J_1 = 9 Hz, J_2 = 4

Hz, 1H), 3.31 (dd, J_1 = 18 Hz, J_2 = 4 Hz, 1H), 2.96 (s, 3H), 2.65 (dd, J_1 = 18 Hz, J_2 = 9 Hz, 1H), 2.50 (s, 3H). ^{13}C NMR ($CDCl_3$, 75 MHz) δ: 199.3, 175.6, 172.6, 53.9, 30.3, 29.7, 25.3. Anal. Calcd. for $C_7H_9NO_3$: C, 54.19; H, 5.85; N, 9.03. Found: C, 54.2; H, 5.9; N, 9.0.

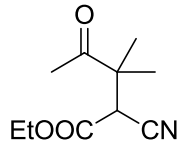

ethyl 2-cyano-3,3-dimethyl-4-oxopentanoate (2.33). **Method A**: From 258 μL (1.8 mmol, 0.12 M) of acetyltrimethylsilane (**2.24a**) and 230 μL (1.5 mmol, 0.1 M) of ethyl 2-cyano-3-methylbut-2-enoate (**2.2m**). Purification of the residue by column chromatography (cyclohexane/ethyl acetate 9:1 as the eluant) afforded 186 mg of ethyl 2-cyano-3,3-dimethyl-4-oxopentanoate (**2.33**, 63% yield) as a colorless oil. ^{1}H NMR ($CDCl_3$, 300 MHz) δ: 4.17 (q, J = 7 Hz, 2H), 4.10 (s, 1H), 2.20 (s, 3H), 1.40 (s, 3H), 1.28 (s, 3H), 1.25 (t, J = 7 Hz, 3H). ^{13}C NMR ($CDCl_3$, 75 MHz) δ: 209.3, 164.8, 115.4, 62.9, 48.8, 45.1, 25.3, 24.7, 20.8, 13.9. Anal. Calcd. for $C_{10}H_{15}NO_3$: C, 60.90; H, 7.67; N, 7.10. Found: C, 60.9; H, 7.7; N, 7.1.

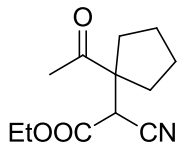

ethyl 2-(1-acetylcyclopentyl)-2-cyanoacetate (2.34). **Method A**: From 258 μL (1.8 mmol, 0.12 M) of acetyltrimethylsilane (**2.24a**) and 268 μL (1.5 mmol, 0.1 M) of ethyl 2-cyano-2-cyclopentylideneacetate (**2.2n**). Purification of the residue by column chromatography (cyclohexane/ethyl acetate 9:1 as the eluant) afforded 214 mg of ethyl 2-(1-acetylcyclopentyl)-2-cyanoacetate (**2.34**, 64% yield) as a colorless oil. ^{1}H NMR ($CDCl_3$, 300 MHz) δ: 4.21 (q, J = 7 Hz, 2H), 4.16 (s, 1H), 2.39-2.30 (m, 1H), 2.24 (s, 3H), 1.95-1.77 (m, 7H), 1.29 (t, J = 7 Hz, 3H). ^{13}C NMR ($CDCl_3$, 75 MHz) δ: 208.0, 165.0, 116.0, 62.8, 59.3, 44.6, 35.8, 33.2, 26.7, 25.9, 25.0, 13.8. Anal. Calcd. for $C_{12}H_{17}NO_3$: C, 64.55; H, 7.67; N, 6.27. Found: C, 64.5; H, 7.7; N, 6.3.

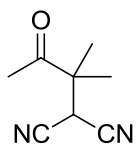

2-(2-methyl-3-oxobutan-2-yl)malononitrile (2.35). **Method A**: From 258 μL (1.8 mmol, 0.12 M) of acetyltrimethylsilane (**2.24a**) and 159 μL (1.5 mmol, 0.1 M) of 2-(propan-2-ylidene)malononitrile (**2.2o**). Purification of the residue by column chromatography (cyclohexane/ethyl acetate 9:1 as the eluant) afforded 200 mg of 2-(2-methyl-3-oxobutan-2-yl)malononitrile (**2.35**, 89% yield) as a colorless oil. ^{1}H NMR[S16] ($CDCl_3$, 300 MHz) δ:

4.13 (s, 1H), 2.26 (s, 3H), 1.49 (s, 6H). ^{13}C NMR ($CDCl_3$, 75 MHz) δ: 206.8, 111.8, 51.1, 30.8, 24.3, 22.0. Anal. Calcd. for $C_8H_{10}N_2O$: C, 63.98; H, 6.71; N, 18.65. Found: C, 64.0; H, 6.7; N, 18.6.

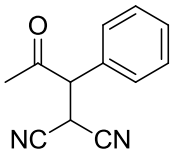

dimethyl 2-heptanoylsuccinate (2.36). **Method A**: From 258 μL (1.8 mmol, 0.12 M) of acetyltrimethylsilane (**2.24a**) and 231 mg (1.5 mmol, 0.1 M) of 2-benzylidenemalononitrile (**2.2c**). A complex mixture was obtained.

Method B: From 215 μL (1.5 mmol, 0.15 M) of **2.24a** and 154 mg (1.0 mmol, 0.1 M) of **2.2c**. Purification of the residue by column chromatography (cyclohexane/ethyl acetate 7:3 as the eluant) afforded 163 mg of 2-(2-methyl-3-oxobutan-2-yl)malononitrile (**2.36**, 55% yield) as an oil. ^{1}H NMR[18] ($(CD_3)_2CO$, 300 MHz) δ: 8.23 (m, 5H), 5.77 (d, *J* = 7 Hz, 1H), 5.99 (d, *J* = 7 Hz, 1H), 2.90 (s, 3H). ^{13}C NMR ($(CD_3)_2CO$, 75 MHz) δ: 203.0, 132.9, 130.4, 130.3, 130.0, 113.8, 113.46, 58.5, 28.2, 26.0. Anal. Calcd. for $C_{12}H_{10}N_2O$: C, 72.71; H, 5.08; N, 14.13; Found: C, 72.6; H, 5.2; N, 14.0.

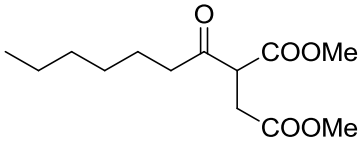

dimethyl 2-heptanoylsuccinate (2.37). **Method A**: From 335 mg (1.8 mmol, 0.12 M) of 1-(trimethylsilyl)heptan-1-one (**2.24b**) and 188 μL (1.5 mmol, 0.1 M) of dimethyl maleate (**2.2e**). Purification of the residue by column chromatography (cyclohexane/ethyl acetate 9:1 as the eluant) afforded 283 mg of dimethyl 2-heptanoylsuccinate (**2.37**, 73% yield) as an oil.

Method B: From 280 mg (1.5 mmol, 0.15 M) of **2.24b** and 125 μL (1.0 mmol, 0.1 M) of **2.2e**. Purification of the residue by column chromatography (cyclohexane/ethyl acetate 9:1 as the eluant) afforded 80 mg of dimethyl 2-heptanoylsuccinate (**2.37**, 31% yield) as an oil. The spectroscopic data of **15** were in accordance with the literature.[19] Anal. Calcd. for $C_{13}H_{22}O_5$: C, 60.45; H, 8.58. Found: C, 60.4; H, 8.6.

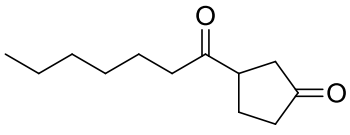

3-heptanoylcyclopentanone (2.38). **Method A**: From 335 mg (1.8 mmol, 0.12 M) of 1-(trimethylsilyl)heptan-1-one (**2.24b**) and 125 μL (1.5 mmol, 0.1 M) of 2-cyclopenten-1-one. Purification of the residue

by column chromatography (cyclohexane/ethyl acetate 9:1 as the eluant) afforded 171 mg of 3-heptanoylcyclopentanone (**2.38**, 58% yield) as an oil.

Method B: From 280 mg (1.5 mmol, 0.15 M) of **2.24b** and 83 μL (1.0 mmol, 0.1 M) of 2-cyclopenten-1-one. Purification of the residue by column chromatography (cyclohexane/ethyl acetate 9:1 as the eluant) afforded 85 mg of 3-heptanoylcyclopentanone (**2.38**, 43% yield) as an oil. ^{1}H NMR ($CDCl_3$, 300 MHz) δ: 3.27-3.17 (m, 1H), 2.58-2.39 (m, 3H), 2.37-2.11 (m, 4H), 2.02-1.87 (m, 1H), 1.56 (m, 2H) 1.31-1.26 (m, 6H), 0.84 (m, 3H). ^{13}C NMR ($CDCl_3$, 75 MHz) δ: 216.8, 210.9, 47.8, 41.8, 40.2, 37.6, 31.7, 29.0, 26.1, 23.6, 22.5, 14.1. Anal. Calcd. for $C_{12}H_{20}O_2$: C, 73.43; H, 10.27. Found: C, 73.4; H, 10.3.

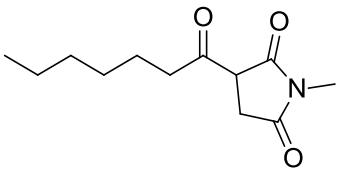

3-heptanoyl-1-methylpyrrolidine-2,5-dione (2.39). **Method A**: From 335 mg (1.8 mmol, 0.12 M) of 1-(trimethylsilyl)heptan-1-one (**2.24b**) and 167 mg (1.5 mmol, 0.1 M) of *N*-methylmaleimide (**2.2l**). Purification of the residue by column chromatography (cyclohexane/ethyl acetate 9:1 as the eluant) afforded 206 mg of 3-heptanoyl-1-methylpyrrolidine-2,5-dione (**2.39**, 61% yield) as an oil.

Method B: From 280 mg (1.5 mmol, 0.15 M) of **2.24b** and 111 mg (1.0 mmol, 0.1 M) of **2.2l**. Purification of the residue by column chromatography (cyclohexane/ethyl acetate 9:1 as the eluant) afforded 176 mg of 3-heptanoyl-1-methylpyrrolidine-2,5-dione (**2.39**, 78% yield) as an oil. ^{1}H NMR ($CDCl_3$, 300 MHz) δ: 3.92 (dd, J_1 = 9 Hz, J_2 = 4 Hz, 1H), 3.26 (dd, J_1 = 18 Hz, J_2 = 4 Hz, 1H), 3.06-2.97 (m, 1H), 2.93 (s, 3H), 2.68-2.57 (m, 2H), 1.57 (m, 2H), 1.32-1.26 (m, 6H), 0.85 (t, J = 7 Hz, 3H). ^{13}C NMR ($CDCl_3$, 75 MHz) δ: 201.9, 175.7, 172.8, 53.1, 43.2, 31.6, 30.0, 28.7, 25.3, 23.3, 22.5, 14.1. Anal. Calcd. for $C_{12}H_{19}NO_3$: C, 63.98; H, 8.50; N, 6.22. Found: C, 64.0; H, 8.5; N, 6.2.

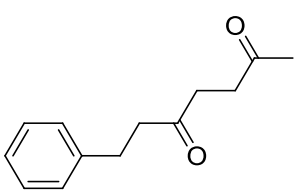

7-phenylheptane-2,5-dione (2.40). **Method A**: From 371 mg (1.8 mmol, 0.12 M) of 3-phenyl-1-(trimethylsilyl)propan-1-one (**2.24c**) and 122 μL (1.5 mmol, 0.1 M) of methyl vinyl ketone (**2.2i**). Purification of the

residue by column chromatography (cyclohexane/ethyl acetate 9:1 as the eluant) afforded 49 mg of 7-phenylheptane-2,5-dione (**2.40**, 16% yield) as an oil.

Method B: From 309 mg (1.5 mmol, 0.15 M) of **2.24c** and 81 μL (1.0 mmol, 0.1 M) of **2.2i**. Purification of the residue by column chromatography (cyclohexane/ethyl acetate 9:1 as the eluant) afforded 47 mg of 7-phenylheptane-2,5-dione (**2.40**, 23% yield) as an oil. The spectroscopic data of **2.40** were in accordance with the literature.[20] Anal. Calcd. for $C_{13}H_{16}O_2$: C, 76.44; H, 7.90. Found: C, 76.4; H, 7.9.

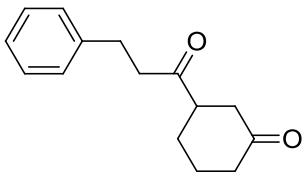

3-(3-phenylpropanoyl)cyclohexanone (2.41). **Method A**: From 371 mg (1.8 mmol, 0.12 M) of 3-phenyl-1-(trimethylsilyl)propan-1-one (**2.24c**) and 145 μL (1.5 mmol, 0.1 M) of cyclohexen-1-one. Purification of the residue by column chromatography (cyclohexane/ethyl acetate 8:2 as the eluant) afforded 35 mg of 3-(3-phenylpropanoyl)cyclohexanone (**2.41**, 10% yield) as an oil.

Method B: From 309 mg (1.5 mmol, 0.15 M) of **2.24c** and 97 μL (1.0 mmol, 0.1 M) of cyclohexen-1-one. Purification of the residue by column chromatography (cyclohexane/ethyl acetate 8:2 as the eluant) afforded 70 mg of 3-(3-phenylpropanoyl)cyclohexanone (**2.41**, 30% yield) as an oil. ^{1}H NMR ($CDCl_3$, 300 MHz) δ: 7.29-7.24 (m, 2H), 7.19-7.14 (m, 3H), 2.92-2.67 (m, 5H), 2.51-2.26 (m, 4H), 2.05-1.95 (m, 2H), 1.74-1.55 (m, 2H). ^{13}C NMR ($CDCl_3$, 75 MHz) δ: 209.9, 209.7, 140.8, 128.5, 128.2, 126.1, 50.2, 42.5, 42.3, 40.8, 29.6, 27.1, 24.7. Anal. Calcd. for $C_{15}H_{18}O_2$: C, 78.23; H, 7.88. Found: C, 78.2; H, 7.9.

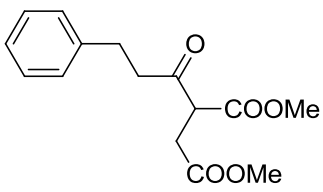

dimethyl 2-(3-phenylpropanoyl)succinate (2.42). **Method A**: From 371 mg (1.8 mmol, 0.12 M) of 3-phenyl-1-(trimethylsilyl)propan-1-one (**2.24c**) and 188 μL (1.5 mmol, 0.1 M) of dimethyl maleate (**2.2e**). Purification of the residue by column chromatography (cyclohexane/ethyl acetate 8:2 as the eluant) afforded 42 mg of dimethyl 2-(3-phenylpropanoyl)succinate (**2.42**, 10% yield) as an oil.

Method B: From 309 mg (1.5 mmol, 0.15 M) of **2.24c** and 125 μL (1.0 mmol, 0.1 M) of **2.2e**. Purification of the residue by column chromatography (cyclohexane/ethyl acetate 8:2 as the eluant)

afforded 123 mg of dimethyl 2-(3-phenylpropanoyl)succinate (**2.42**, 44% yield) as an oil. ^{1}H NMR ($CDCl_3$, 300 MHz) δ: 7.30-7.25 (m, 2H), 7.20-7.16 (m, 3H), 3.98 (dd, J_1= 8 Hz, J_2 = 6 Hz, 1H), 3.66 (s, 3H), 3.65 (s, 3H), 3.15-2.79 (m, 6H). ^{13}C NMR ($CDCl_3$, 75 MHz) δ: 203.0, 171.8, 168.7, 140.7, 128.5, 128.4, 126.2, 53.9, 52.7, 52.1, 44.4, 32.1, 29.4. Anal. Calcd. for $C_{15}H_{18}O_5$: C, 64.74; H, 6.52. Found: C, 64.7; H, 6.5.

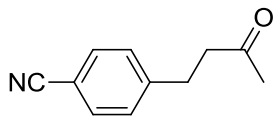

4-(3-oxobutyl)benzonitrile (2.45). Method B: From 215 μL (1.5 mmol, 0.15 M) of acetyltrimethylsilane (**2.24a**) and 129 mg (1.0 mmol, 0.1 M) of 4-vinylbenzonitrile (**2.2q**). Purification of the residue by column chromatography (cyclohexane/ethyl acetate 8:2 as the eluant) afforded 130 mg of 4-(3-oxobutyl)benzonitrile (**2.45**, 75% yield) as a colorless oil. ^{1}H NMR ($CDCl_3$, 300 MHz) δ: 7.56 (d, J = 8 Hz, 2H), 7.30 (d, J = 8 Hz, 2H), 2.95 (t, J = 7 Hz, 2H), 2.78 (t, J = 7 Hz, 2H), 2.15 (s, 3H). ^{13}C NMR ($CDCl_3$, 75 MHz) δ: 206.8, 146.8, 132.3, 129.3, 119.0, 110.1, 44.2, 30.1, 29.7. Anal. Calcd. for $C_{11}H_{11}NO$: C, 76.28; H, 6.40; N, 8.09. Found: C, 76.3; H, 6.4; N, 8.1.

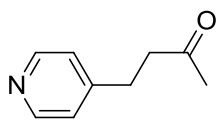

4-(pyridin-4-yl)butan-2-one (2.46). **Method B**: From 215 μL (1.5 mmol, 0.15 M) of acetyltrimethylsilane (**2.24a**) and 108 mg (1.0 mmol, 0.1 M) of 4-vinylpyridine (**2.2r**). Purification of the residue by column chromatography (cyclohexane/ethyl acetate 1:1 as the eluant) afforded 102 mg of 4-(pyridin-4-yl)butan-2-one (**2.46**, 68% yield) as a brownish oil. ^{1}H NMR ($CDCl_3$, 300 MHz) δ: 8.47 (d, J = 6 Hz, 2H), 7.11 (d, J = 6 Hz, 2H), 2.93 – 2.83 (m, 2H), 2.82 – 2.72 (m, 2H), 2.15 (s, 3H).[2113] ^{13}C NMR ($CDCl_3$, 75 MHz) δ: 206.8, 150.3, 149.8, 123.9, 43.7, 30.1, 28.9. Anal. Calcd. for $C_9H_{11}NO$: C, 72.16; H, 7.43; N, 9.39. Found: C, 72.2; H, 7.4; N, 9.4.

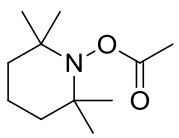

2,2,6,6-tetramethylpiperidin-1-yl acetate (2.47). 2,2,6,6-tetramethylpiperidin-1-yl acetate was synthesized as reported in the literature. See Table S.2.3 for details. ^{1}H NMR ($CDCl_3$, 300 MHz) δ: 2.09 (s, 3H), 1.75-1.39 (m, 6H), 1.15 (s, 6H), 1.06 (s, 6H).[22] ^{13}C NMR ($CDCl_3$, 75 MHz) δ: 170.9, 60.1, 39.1, 32.1, 20.6, 19.3, 17.1. Anal. Calcd. for $C_{11}H_{21}NO_2$: C, 66.29; H, 10.62; N, 7.03. Found: C, 66.3; H, 10.6; N, 7.0.

Trapping experiments

Table S.2.3 Trapping experiments.

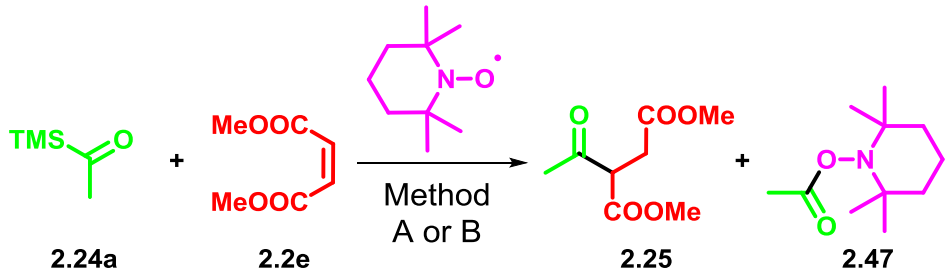

2.24a **2.2e** **2.25** **2.47**

Photocatalyst	**Method**	**2.2e**	**2.25** Yield,[a] %	**2.47** Yield,[b] %	**2.2e** Consumption, %
TBADT	A	yes	42	30	> 95
TBADT	A	no	-	30	-
Acr^+-Mes	B	yes	n.d.	46	80
Acr^+-Mes	B	no	-	19	-

[a] The yield has been calculated by considering **2.2e** as the limiting reagent.
[b] The yield has been calculated by considering TEMPO as the limiting reagent.

Trapping experiments were carried out both in the presence and the absence of olefin **2.2e**.

Method A: **2.24a** (0.12 M), [**2.2e** (0.1 M)], TBADT (2 mol%) and TEMPO (0.1 M) in 1 mL of MeCN-H_2O 5/1 irradiated at 310 nm.

Method B: **2.24a** (0.15 M), [**2.2e** (0.1 M)], Acr^+-Mes (10 mol%) and TEMPO (0.1 M) in 1 mL of MeOH irradiated at 410 nm.

Compound **2.47** was quantified by means of a calibration curve using an authentic sample synthesized as described in the literature (GC analysis; internal standard: dodecane).[22]

References

(1) Galicia, M.; Gonzalez, F. J. *J. Electrochem. Soc.* **2002**, *149*, D46–D50.

(2) Marken, F.; Neudeck, A.; Bond, A. M. *Cyclic voltammetry*; Scholz, F., Ed.; Springer: Berlin, 2002.

(3) Montanaro, S.; Ravelli, D.; Merli, D.; Fagnoni, M.; Albini, A. *Org. Lett.* **2012**, *14* (16), 4218–4221.

(4) Ueda, M.; Kondoh, E.; Ito, Y.; Shono, H.; Kakiuchi, M.; Ichii, Y.; Kimura, T.; Miyoshi, T.; Naito, T.; Miyata, O. *Org. Biomol. Chem.* **2011**, *9* (7), 2062.

(5) He, P.; Watts, P.; Marken, F.; Haswell, S. J. *Angew. Chem. Int. Ed.* **2006**, *45* (25), 4146–4149.

(6) Qrareya, H.; Dondi, D.; Ravelli, D.; Fagnoni, M. *ChemCatChem* **2015**, *7* (20), 3350–3357.

(7) Page, P. C. B.; Klair, S. S.; Rosenthal, S. *Chem. Soc. Rev.* **1990**, *19* (2), 147.

(8) Ito, K.; Tamashima, H.; Iwasawa, N.; Kusama, H. *J. Am. Chem. Soc.* **2011**, *133* (11), 3716–3719.

(9) Protti, S.; Ravelli, D.; Fagnoni, M.; Albini, A. *Chem. Commun.* **2009**, No. 47, 7351.

(10) Gong, L.; Leung-Toung, R.; Tidwell, T. T. *J. Org. Chem.* **1990**, *55*, 3634–3639.

(11) Danheiser, R. L.; Fink, D. M.; Okano, K.; Tsai, Y.-M.; Szczepanski, S. W. *J. Org. Chem.* **1985**, *50*, 5393–5396.

(12) Degl'Innocenti, A.; Walton, D. R. M.; Seconi, G.; Pirazzini, G.; Ricci, A. *Tetrahedron Lett.* **1980**, *21* (40), 3927–3928.

(13) Maas, G.; Müller, A. *J. für Prakt. Chemie* **1998**, *340*, 315–322.

(14) Cantillo, D.; Kappe, C. O. *J. Org. Chem.* **2013**, *78* (20), 10567–10571.

(15) Lin, W.; McGinness, R.; Wilson, E.; Zercher, C. *Synthesis* **2007**, *15*, 2404–2408.

(16) Gupta, K.; Tyagi, D.; Dwivedi, A. D.; Mobin, S. M.; Singh, S. K. *Green Chem.* **2015**, *17*, 4618–4627.

(17) Mizar, P.; Wirth, T. *Angew. Chemie - Int. Ed.* **2014**, *53* (23), 5993–5997.

(18) Jegelka, M.; Plietker, B. *Chem. - A Eur. J.* **2011**, *17*, 10417–10430.

(19) Chaudhari, D. A.; Fernandes, R. A. *J. Org. Chem.* **2016**, *81* (5), 2113–2121.

(20) Itoh, K.; Nakanishi, S.; Otsuji, Y. *Bull. Chem. Soc. Jpn.* **1991**, *64*, 2965–2977.

(21) Bonassi, F.; Ravelli, D.; Protti, S.; Fagnoni, M. *Adv. Synth. Catal.* **2015**, *357* (16–17), 3687–3695.

(22) Edgar Anderson, J.; T Corrie, J. E. *J. Chem. Soc. Perkin Trans. 2* **1992**, 1027–1037.

EXPERIMENTAL SECTION RELATIVE TO

CHAPTER 3

VINYLPYRIDINES AS BUILDING BLOCKS FOR THE PHOTOCATALYZED SYNTHESIS OF ALKYLPYRIDINES[23]

Experimental data

Compounds **3.1a-3.1l** and **2.2r**, **3.2a-3.2b** were commercially available and used as received, tetrahydrofuran (THF) that was distilled prior to use. The photocatalyst TBADT has been prepared according to a published procedure.[1] Acetonitrile (HPLC purity grade) employed for photochemical reactions was used as received. NMR spectra were recorded on a 300 (for ^{1}H) or 75 (for ^{13}C) MHz spectrometer; the attributions were made on the basis of ^{1}H and ^{13}C NMR, as well as DEPT, NOE and COSY experiments. Data for ^{1}H NMR are reported as follows: chemical shift referred to TMS (δ ppm), multiplicity (s = singlet, bs = broad singlet, d = doublet, t = triplet, q = quadruplet, quint = quintuplet, sext = sextuplet, sept = septuplet, m = multiplet), coupling constant (Hz) and integration. Data for ^{13}C NMR are reported in terms of chemical shift. Reactions were monitored by gas chromatographic (GC) analyses (HP-5 capillary column). Chromatographic purification of products was accomplished using flash chromatography on 60 Å, 230-400 mesh silica gel or neutral aluminum oxide. Thin-layer chromatography (TLC) was performed on silica gel 60 F-254 plates. Visualization of the developed plates was performed by fluorescence quenching or by $KMnO_4$ staining. UV-Vis spectra were recorded with a double beam spectrophotometer equipped with Deuterium lamp (190-350 nm) and Halogen lamp (330-900 nm) and a Photomultiplier R928.

*Procedures for the synthesis of H-donors **3.1m** and vinylpyridines **3.2d-3.2f**.*

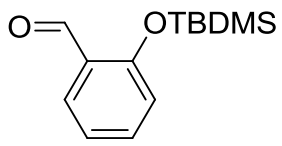

2-((tert-butyldimethylsilyl)oxy)benzaldehyde (3.1m). Prepared following a procedure previously reported in the literature,[2] starting from salicylaldehyde (**3.1k**) and *tert*-butyldimethylsilyl chloride in the presence of 1,8-diazabicyclo[5.4.0]undec-7-ene (DBU). Solvent: benzene; temperature: 25 °C; reaction time: 90 min; purification by column chromatography (Al_2O_3: cyclohexane/ethyl acetate 9:1); yield: 73%. Spectroscopic data of compound **3.1m** were in accordance with the literature.[3]

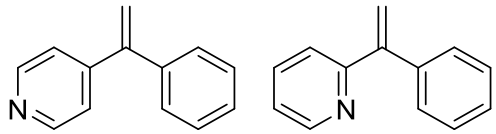

3.2d **3.2e**

4-(1-phenylvinyl)pyridine (3.2c) and 2-(1-phenylvinyl)pyridine (3.2d). Vinylpyridines **3.2c**, **3.2d** were prepared according to a procedure reported in the literature,[3] starting from 4- or 2-benzoylpyridine, respectively, and methyltriphenylphosphonium bromide.

In particular, in a N_2-filled 100 mL three-necks round bottom flask, methyltriphenylphosphonium bromide (2.14 g, 6.0 mmol, 1.1 equiv.) and potassium *tert*-butoxide (0.67 g, 6.0 mmol, 1.1 equiv.) were dissolved in dry THF (20 mL) and stirred for 20 min to obtain a yellow suspension. Afterwards, 4-benzoylpyridine or 2-benzoylpyridine (1 g, 5.5 mmol, 1.0 equiv.), dissolved in dry THF (6 mL), was added dropwise to the reaction mixture: the suspension turned gradually to white. The reaction was stirred overnight, quenched with a saturated NH_4Cl solution (20 mL) and extracted with ethyl acetate (3×15 mL). Finally, the organic phases were collected, dried over Na_2SO_4, filtered and the solvent was removed under reduced pressure. Flash chromatography (**3.2c**: cyclohexane/ethyl acetate 8:2; **3.2d**: cyclohexane/ethyl acetate 9:1) allowed to obtain the pure products as colorless liquids (**3.2c**: 0.82 g, 75%; **3.2d**: 0.51 g, 50%). Spectroscopic data of compounds **3.2c**[3] and **3.2d**[4] were in accordance with the literature.

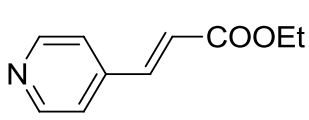

(E)-3-[4-(dimethylamino)phenyl]acrylate (3.2e). Compound **3.2e** was synthesized by modifying a procedure previously reported.[5] A solution of triethyl phosphonoacetate (984 μL, 4.96 mmol, 1.2 equiv.) in THF (20 mL) was stirred for 10 minutes and then potassium *tert*-butoxide (500 mg, 4.45 mmol, 1.1 equiv.) was added as a powder to form a white suspension that gradually turned to yellow. 4-Pyridinecarboxaldehyde (388 μL, 4.1 mmol, 1 equiv.) was added dropwise and the resulting brownish suspension was stirred for 18 h. The reaction was quenched by the addition of saturated aqueous NH_4Cl (20 mL) and the resulting mixture was extracted with ethyl acetate (3×15 mL). The combined organic phases were washed with brine, dried over Na_2SO_4, and concentrated under reduced pressure. The residue was purified

by column chromatography (SiO_2, cyclohexane/ethyl acetate 7:3 as the eluant) to give a white solid (636 mg, 88%). m.p. 62-64 °C (Lit. 64 °C).[6] The spectroscopic data of **3.2e** were in accordance with the literature.[7]

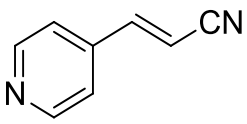

(E)-3-(pyridin-4-yl)acrylonitrile (3.2f). A solution of diethyl cyanomethylphosphonate (879 μL, 6.89 mmol, 1.2 equiv.) in THF (20 mL) was stirred for 20 minutes and then potassium *tert*-butoxide (0.8 g, 7 mmol, 1.2 equiv.) was added as a powder to form a white suspension that gradually turned to pink. 4-Pyridinecarboxaldehyde (565 μL, 6 mmol, 1 equiv.) was added dropwise and the resulting brownish suspension was stirred for 18 h. The reaction was quenched by the addition of saturated aqueous NH_4Cl (20 mL) and the resulting mixture was extracted with ethyl acetate (3×15 mL). The combined organic layers were dried over Na_2SO_4, and concentrated under reduced pressure. The residue was purified through recrystallization from *n*-hexane to yield **3.2f** as a white crystalline solid (554 mg, 71%). m.p. 70-72 °C (Lit. 71-72 °C).[8] ^{1}H NMR[8] ($CDCl_3$, 300 MHz) δ: 8.69 (dd, *J* = 5 Hz, *J* = 2 Hz, 2H), 7.35 (d, *J* = 17 Hz, 1H), 7.29 (dd, *J* = 5 Hz, *J* = 2 Hz, 2H), 6.09 (d, *J* = 17 Hz, 1H). ^{13}C NMR ($CDCl_3$, 75 MHz) δ: 151.0, 148.1, 140.5, 121.1, 117.0, 101.6. Anal. Calcd. for $C_8H_6N_2$: C, 73.83; H, 4.65; N, 21.52. Found: C, 73.8; H, 4.7; N, 21.5.

General Procedure for the TBADT-Photocatalyzed Functionalization of Vinylpyridines: An acetonitrile solution (15 mL) of the H-donor (**3.1a-3.1m**; 1.5-7.5 mmol, 0.1-0.5 M, 1-5 equiv., except for **3.1f**, see below) and the vinylpyridine (**2.2r**, **3.2a-3.2f**; 1.5 mmol, 0.1 M, 1 equiv.), in the presence of TBADT ($2\cdot10^{-3}$ M, 2 mol%) was poured in a quartz tube and then purged for 3 min with nitrogen, capped with a septum, and irradiated for 16 h in a multi-lamp apparatus fitted with 10×15 W phosphor-coated lamps (emission centered at 310 nm). The solvent was removed under reduced pressure from the photolyzed solution and the product isolated by purification of the residue by column chromatography.

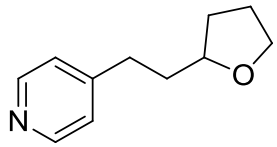

4-(2-(Tetrahydrofuran-2-yl)ethyl)pyridine (3.3). From 601 μL (7.5 mmol, 0.5 M) of THF (**3.1a**) and 161 μL (1.5 mmol, 0.1 M) of 4-vinylpyridine (**2.2r**). Purification of the residue by column chromatography (ethyl acetate as the eluant) afforded 180 mg of 4-(2-(tetrahydrofuran-2-yl)ethyl)pyridine (**3.3**, 68% yield) as an oil. ^{1}H NMR ($CDCl_3$, 300 MHz) δ: 8.42 (d, *J* = 5 Hz, 2H), 7.08 (d, *J* = 5 Hz, 2H), 3.84-3.61 (m, 3H), 2.74-2.52 (m, 2H), 1.95-1.67 (m, 5H), 1.46-1.34 (m, 1H). ^{13}C NMR ($CDCl_3$, 75 MHz) δ: 151.0, 149.4, 123.7, 78.0, 67.5, 36.0, 31.8, 31.2, 25.6. Anal. Calcd. for $C_{11}H_{15}NO$: C, 74.54; H, 8.53; N, 7.90. Found: C, 74.5; H, 8.6; N, 7.8.

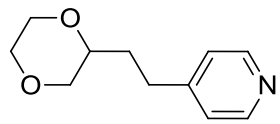

4-(2-(1,4-Dioxan-2-yl)ethyl)pyridine (3.4). From 639 μL (7.5 mmol, 0.5 M) of 1,4-dioxane (**3.1b**) and 161 μL (1.5 mmol, 0.1 M) of 4-vinylpyridine (**2.2r**). Purification of the residue by column chromatography (ethyl acetate as the eluant) afforded 179 mg of 4-(2-(1,4-dioxan-2-yl)ethyl)pyridine (**3.4**, 62% yield) as an oil. ^{1}H NMR ($CDCl_3$, 300 MHz) δ: 8.49 (d, *J* = 6 Hz, 2H), 7.11 (d, *J* = 6 Hz, 2H), 3.86-3.43 (m, 6H), 3.34-3.27 (m, 1H), 2.95-2.55 (m, 2H), 1.93-1.45 (m, 2H). ^{13}C NMR ($CDCl_3$, 75 MHz) δ: 150.5, 149.7, 123.7, 74.1, 71.0, 66.7, 66.4, 31.9, 30.4. Anal. Calcd. for $C_{11}H_{15}NO_2$: C, 68.37; H, 7.82; N, 7.25. Found: C, 68.4; H, 7.8; N, 7.3.

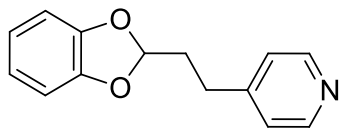

4-(2-(1,3-Benzodioxol-2-yl)ethyl)pyridine (3.5). From 861 μL (7.5 mmol, 0.5 M) of 1,3-benzodioxole (**3.1c**) and 161 μL (1.5 mmol, 0.1 M) of 4-vinylpyridine (**2.2r**). Purification of the residue by column chromatography (cyclohexane/ethyl acetate 7:3 as the eluant) afforded 220 mg of 4-(2-(1,3-benzodioxol-2-yl)ethyl)pyridine (**3.5**, 64% yield) as an oil. ^{1}H NMR ($CDCl_3$, 300 MHz) δ: 8.53 (d, *J* = 6 Hz, 2H), 7.18 (d, *J* = 6 Hz, 2H), 6.94-6.70 (m, 4H), 6.17 (t, *J* = 5 Hz, 1H), 2.90-2.85 (m, 2H), 2.34-2.27 (m, 2H). ^{13}C NMR ($CDCl_3$, 75 MHz) δ: 150.0, 149.8, 147.6, 123.9, 121.7, 110.4, 108.6, 35.0, 28.4. Anal. Calcd. for $C_{14}H_{13}NO_2$: C, 73.99; H, 5.77; N, 6.16. Found: C, 74.0; H, 5.8; N, 6.1.

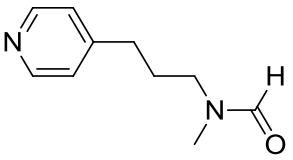

***N*-Methyl-*N*-(3-(pyridin-4-yl)propyl)formamide (3.6).** From 464 μL (6.0 mmol, 0.4 M) of *N*,*N*-dimethylformamide (**3.1d**) and 161 μL (1.5 mmol, 0.1 M) of 4-vinylpyridine (**2.2r**). Purification of the residue by column chromatography (acetone as the eluant) afforded 255 mg of *N*-methyl-*N*-(3-(pyridin-4-yl)propyl)formamide (**3.6**, 94% yield) as an oil. The same reaction mixture (50 mL) placed in a Pyrex vessel (see Figure S.3.1)[1,9] was irradiated both in a solar simulator (SolarBox) for 24 h to give **3.6** in 77% yield and exposed on a window ledge for 8 h to give **3.6** in 83% yield. ^{1}H NMR (CD_3OD, 300 MHz, mixture of two conformers) δ: 8.46-8.38 (m, 4H), 8.03 (s, 1H, minor), 8.02 (s, 1H, major), 7.34 (m, 4H), 3.43-3.37 (m, 4H), 3.01 (s, 3H, minor), 2.87 (s, 3H, major), 2.71-2.64 (m, 4H), 2.02-2.09 (m, 4H). ^{13}C NMR (CD_3OD, 75 MHz) δ: 165.1, 153.7, 153.4, 150.0, 149.9, 125.6, 50.2, 44.8, 35.0, 33.2, 32.8, 29.7, 29.4, 28.2. Anal. Calcd. for $C_{10}H_{14}N_2O$: C, 67.39; H, 7.92; N, 15.72. Found: C, 67.4; H, 8.0; N, 15.7.

Figure S.3.1 Pyrex reaction vessel used in this work

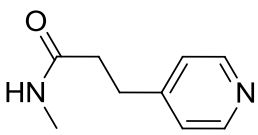

***N*-Methyl-3-(pyridin-4-yl)propanamide (3.7).** From 354 μL (6.0 mmol, 0.4 M) of *N*-methylformamide (**3.1e**) and 161 μL (1.5 mmol, 0.1 M) of 4-vinylpyridine (**2.2r**). Purification of the residue by column chromatography (ethyl acetate/methanol 9:1 as the eluant) afforded 214 mg of *N*-methyl-3-(pyridin-4-yl)propanamide (**3.7**, 87% yield) as a white solid. mp 50-52 °C. ^{1}H NMR ($CDCl_3$, 300 MHz) δ: 8.49 (d, *J* = 5 Hz, 2H), 7.13 (d, *J* = 6 Hz,

2H), 5.47 (bs, 1H), 2.97 (t, *J* = 8 Hz, 2H), 2.85-2.73 (m, 3H), 2.47 (t, *J* = 8 Hz, 2H). ^{13}C NMR ($CDCl_3$, 75 MHz) δ: 171.9, 150.0, 123.9, 37.0, 30.9, 26.5. Anal. Calcd. for $C_9H_{12}N_2O$: C, 65.83; H, 7.37; N, 17.06. Found: C, 65.8; H, 7.4; N, 17.0.

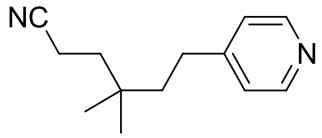

4,4-Dimethyl-6-(pyridin-4-yl)hexanenitrile (3.8). From 2.914 mL (4.6 mmol, 1.6 M) of isocapronitrile (**3.1f**) and 161 μL (1.5 mmol, 0.1 M) of 4-vinylpyridine (**2.2r**). Purification of the residue by column chromatography (cyclohexane/ethyl acetate 1:1 as the eluant) afforded 280 mg of 4,4-dimethyl-6-(pyridin-4-yl)hexanenitrile (**3.8**, 92% yield) as an oil. ^{1}H NMR ($CDCl_3$, 300 MHz) δ: 8.49 (d, *J* = 6 Hz, 2H), 7.11 (d, *J* = 6 Hz, 2H), 2.61-2.52 (m, 2H), 2.36-2.29 (m, 2H), 1.74-1.68 (m, 2H), 1.57-1.48 (m, 2H), 0.99 (s, 6H). ^{13}C NMR ($CDCl_3$, 75 MHz) δ: 151.5, 149.9, 123.8, 120.4, 42.6, 37.2, 33.1, 30.0, 26.3, 12.5. Anal. Calcd. for $C_{13}H_{18}N_2$: C, 77.18; H, 8.97; N, 13.85. Found: C, 77.2; H, 9.0; N, 13.8.

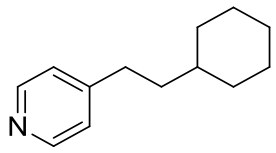

4-(2-Cyclohexylethyl)pyridine (3.9). From 808 μL (7.5 mmol, 0.5 M) of cyclohexane (**3.1g**) and 161 μL (1.5 mmol, 0.1 M) of 4-vinylpyridine (**2.2r**). Purification of the residue by column chromatography (cyclohexane/ethyl acetate 8:2 as the eluant) afforded 194 mg of 4-(2-cyclohexylethyl)pyridine (**3.9**, 68% yield) as an oil. The same reaction was carried out under flow conditions[10] (125 W medium pressure Hg vapors lamp; V_{tot}: 12 mL; Flow rate: 0.2 mL min^{-1}; see Figure 3.2) to give **3.9** in 86% yield. ^{1}H NMR ($CDCl_3$, 300 MHz) δ: 8.47 (d, *J* = 5 Hz, 2H), 7.10 (d, *J* = 5 Hz, 2H), 2.66-2.55 (m, 2H), 1.76-1.65 (m, 5H), 1.54-1.47 (m, 2H), 1.35-1.07 (m, 4H), 1.03-0.82 (m, 2H). ^{13}C NMR ($CDCl_3$, 75 MHz) δ: 152.3, 149.8, 124.0, 38.2, 37.4, 33.4, 32.7, 26.7, 26.4. Anal. Calcd. for $C_{13}H_{19}N$: C, 82.48; H, 10.12; N, 7.40. Found: C, 82.5; H, 10.1; N, 7.4.

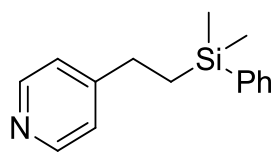

4-(2-(Dimethyl(phenyl)silyl)ethyl)pyridine (3.10). From 460 μL (3.0 mmol, 0.2 M) of dimethylphenylsilane (**3.1h**) and 161 μL (1.5 mmol, 0.1 M) of 4-vinylpyridine (**2.2r**) in the presence of $4\cdot10^{-3}$ M TBADT (4 mol%). Purification of the residue by column chromatography (Al_2O_3, cyclohexane/ethyl acetate 7:3 as the

eluant) afforded 140 mg of 4-(2-(dimethyl(phenyl)silyl)ethyl)pyridine (**3.10**, 39% yield) as an oil. ^{1}H NMR ($CDCl_3$, 300 MHz) δ: 8.45 (d, *J* = 5 Hz, 2H), 7.58-7.47 (m, 2H), 7.44-7.34 (m, 3H), 7.09 (d, *J* = 5 Hz, 2H), 2.81-2.45 (m, 2H), 1.20-0.95 (m, 2H), 0.32 (s, 6H). ^{13}C NMR ($CDCl_3$, 75 MHz) δ: 153.9, 149.8, 138.5, 133.7, 129.3, 128.0, 123.4, 29.5, 16.7, 1.6, -3.1. Anal. Calcd. for $C_{15}H_{19}NSi$: C, 74.63; H, 7.93; N, 5.80. Found: C, 74.6; H, 8.0; N, 5.8.

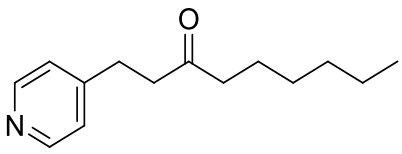

1-(Pyridin-4-yl)nonan-3-one (3.11). From 201 μL (1.5 mmol, 0.1 M) of heptanal (**3.1i**) and 161 μL (1.5 mmol, 0.1 M) of 4-vinylpyridine (**2.2r**). Purification of the residue by column chromatography (cyclohexane/ethyl acetate 7:3 as the eluant) afforded 183 mg of 1-(pyridin-4-yl)nonan-3-one (**3.11**, 56% yield) as an oil. ^{1}H NMR ($CDCl_3$, 300 MHz) δ: 8.48 (d, *J* = 5 Hz, 2H), 7.11 (d, *J* = 5 Hz, 2H), 2.89 (t, *J* = 7 Hz, 2H), 2.74 (t, *J* = 7 Hz, 2H), 2.39 (t, *J* = 7 Hz, 2H), 1.61-1.49 (m, 2H), 1.33-1.20 (m, 6H), 0.86 (t, *J* = 7 Hz, 3H). ^{13}C NMR ($CDCl_3$, 75 MHz) δ: 209.4, 150.4, 149.9, 123.9, 43.2, 42.8, 31.7, 29.0, 23.9, 22.6, 14.1. Anal. Calcd. for $C_{14}H_{21}NO$: C, 76.67; H, 9.65; N, 6.39. Found: C, C, 76.6; H, 9.7; N, 6.3.

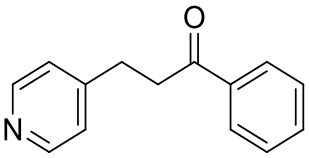

1-Phenyl-3-(pyridin-4-yl)propan-1-one (3.12). From 153 μL (1.5 mmol, 0.1 M) of benzaldehyde (**3.1j**) and 161 μL (1.5 mmol, 0.1 M) of 4-vinylpyridine (**2.2r**). Purification of the residue by column chromatography (cyclohexane/ethyl acetate 6:4 as the eluant) afforded 155 mg of 1-phenyl-3-(pyridin-4-yl)propan-1-one (**3.12**, 46% yield) as a yellowish solid. mp 81-82 °C. ^{1}H NMR ($CDCl_3$, 300 MHz) δ: 8.51 (d, *J* = 6 Hz, 2H), 7.96 (d, *J* = 7 Hz, 2H), 7.58 (t, *J* = 7 Hz, 1H), 7.47 (t, *J* = 7 Hz, 2H), 7.22 (d, *J* = 6 Hz, 2H), 3.34 (t, *J* = 7 Hz, 2H), 3.09 (t, *J* = 7 Hz, 2H). ^{13}C NMR ($CDCl_3$, 75 MHz) δ: 198.3, 151.1, 149.5, 136.7, 133.5, 128.9, 128.1, 124.2, 38.9, 29.4. Anal. Calcd. for $C_{14}H_{13}NO$: C, 79.59; H, 6.20; N, 6.63. Found: C, 79.6; H, 6.2; N, 6.6.

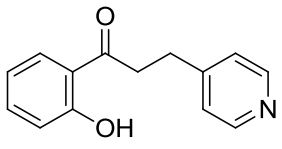

1-(2-Hydroxyphenyl)-3-(pyridin-4-yl)propan-1-one (3.13). Compound **3.13** was not formed in the reaction between **3.1k** and **2.2r**, but was

obtained instead from compound **3.14** by removal in a one-pot fashion of the silyl group.[11] In particular, the crude reaction mixture containing **3.14** (see below) was rotary evaporated to remove the solvent (MeCN) and then an excess of LiOH (100 mg, 4 mmol) in DMF (1 mL) was added. The solution was stirred overnight and then quenched with water (10 mL). The resulting mixture was extracted with ethyl acetate (3×10 mL), the organic phases were collected, dried and rotary evaporated to yield a reddish oil. Purification of the residue by column chromatography (cyclohexane/ethyl acetate 7:3 as the eluant) afforded 115 mg of 1-(2-hydroxyphenyl)-3-(pyridin-4-yl)propan-1-one (**3.13**, 34% yield over two steps) as an oil. ^{1}H NMR ($CDCl_3$, 300 MHz) δ: 12.14 (bs, 1H), 8.51 (bs, 2H), 7.71 (dd, *J* = 8 Hz, *J* = 1 Hz, 1H), 7.45 (ddd, *J* = 9 Hz, *J* = 3 Hz, *J* = 2 Hz, 1H), 7.17 (s, 2H), 6.96 (d, *J* = 8 Hz, 1H), 6.87 (dd, *J* = 8 Hz, *J* = 7 Hz, 1H), 3.33 (t, *J* = 7 Hz, 2H), 3.04 (t, *J* = 7 Hz, 2H). ^{13}C NMR ($CDCl_3$, 75 MHz) δ: 204.3, 162.5, 149.8, 136.6, 129.7, 124.0, 119.2, 119.1, 118.7, 38.4, 29.0. Anal. Calcd. for $C_{14}H_{13}NO_2$: C, 73.99; H, 5.77; N, 6.16;. Found: C, 74.0; H, 5.7; N, 6.2.

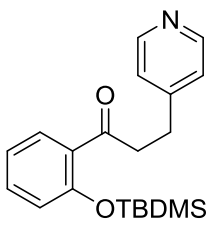

1-(2-((tert-Butyldimethylsilyl)oxy)phenyl)-3-(pyridin-4-yl)propan-1-one (3.14). From 355 mg (1.5 mmol, 0.1 M) of aldehyde (**3.1m)** and 161 μL (1.5 mmol, 0.1 M) of 4-vinylpyridine (**2.2r**). Purification of the residue by column chromatography (from cyclohexane/ethyl acetate 9:1 to 7:3 as the eluant) afforded 212 mg of 1-(2-((tert-butyldimethylsilyl)oxy)phenyl)-3-(pyridin-4-yl)propan-1-one (**3.14**, 42% yield) as an oil. ^{1}H NMR ($CDCl_3$, 300 MHz) δ: 8.46 (d, *J* = 4 Hz, 2H), 7.54 (dd, *J* = 8, *J* = 2 Hz, 1H), 7.42-7.24 (m, 1H), 7.12 (d, *J* =6 Hz, 2H), 7.01-6.92 (m, 1H), 6.85 (dd, *J* = 8, J = 1 Hz, 1H), 3.32 (t, *J* = 8 Hz, 2H), 2.99 (t, *J* = 8 Hz, 2H), 0.92 (s, 9H), 0.22 (s, 6H). ^{13}C NMR ($CDCl_3$, 75 MHz) δ: 201.3, 154.4, 150.5, 149.7, 132.9, 130.7, 129.9, 123.9, 121.3, 120.1, 43.9, 29.4, 25.8, 18.4, -4.0. Anal. Calcd. for $C_{20}H_{27}NO_2Si$: C, 70.34; H, 7.97; N, 4.10. Found: C, 70.3; H, 8.0; N, 4.1.

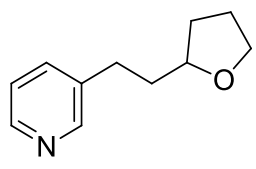

3-(2-(Tetrahydrofuran-2-yl)ethyl)pyridine (3.15). From 601 μL (7.5 mmol, 0.5 M) of THF (**3.1a**) and 161 μL (1.5 mmol, 0.1 M) of 3-vinylpyridine

(**3.2a**). Purification of the residue by column chromatography (ethyl acetate as the eluant) afforded 132 mg of 3-(2-(tetrahydrofuran-2-yl)ethyl)pyridine (**3.15**, 50% yield) as an oil. ^{1}H NMR ($CDCl_3$, 300 MHz) δ: 8.53-8.37 (m, 2H), 7.51 (dt, *J* = 8 Hz, *J* = 2 Hz, 1H), 7.19 (dd, *J* = 8 Hz, *J* = 5 Hz, 1H), 3.96-3.63 (m, 3H), 2.88-2.51 (m, 2H), 1.87 (m, 5H), 1.58-1.38 (m, 1H). ^{13}C NMR ($CDCl_3$, 75 MHz) δ: 150.0, 147.4, 137.5, 136.0, 123.4, 78.4, 67.9, 37.2, 31.5, 30.0, 25.9. Anal. Calcd. for $C_{11}H_{15}NO$: C, 74.54; H, 8.53; N, 7.90. Found: C, 74.5; H, 8.6; N, 7.9.

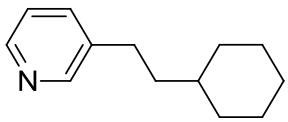

3-(2-Cyclohexylethyl)pyridine (3.16). From 808 μL (7.5 mmol, 0.5 M) of cyclohexane (**3.1g**) and 161 μL (1.5 mmol, 0.1 M) of 3-vinylpyridine (**3.2a**). Purification of the residue by column chromatography (cyclohexane/ethyl acetate 8:2 as the eluant) afforded 121 mg of 3-(2-cyclohexylethyl)pyridine (**3.16**, 42% yield) as an oil. ^{1}H NMR ($CDCl_3$, 300 MHz) δ: 8.43 (s, 2H), 7.48 (dd, *J* = 8 Hz, *J* = 2 Hz, 1H), 7.21-7.17 (m, 1H), 2.63-2.58 (m, 2H), 1.81-1.57 (m, 5H), 1.55-1.43 (m, 2H), 1.35-1.06 (m, 4H), 1.05-0.80 (m, 2H). ^{13}C NMR ($CDCl_3$, 75 MHz) δ: 150.1, 147.2, 138.4, 135.8, 123.4, 39.1, 37.3, 33.4, 30.8, 26.7, 26.4. Anal. Calcd. for $C_{13}H_{19}N$: C, 82.48; H, 10.12; N, 7.40. Found: C, 82.4; H, 10.2; N, 7.4.

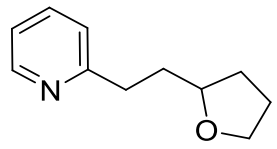

2-(2-(Tetrahydrofuran-2-yl)ethyl)pyridine (3.17). From 601 μL (7.5 mmol, 0.5 M) of THF (**3.1a**) and 161 μL (1.5 mmol, 0.1 M) of 2-vinylpyridine (**3.2b**). Purification of the residue by column chromatography (cyclohexane/ethyl acetate 7:3 as the eluant) afforded 185 mg of 2-(2-(tetrahydrofuran-2-yl)ethyl)pyridine (**3.17**, 70% yield) as an oil. ^{1}H NMR ($CDCl_3$, 300 MHz) δ: 8.51 (d, *J* = 5 Hz, 1H), 7.58 (td, *J* = 8 Hz, *J* = 2 Hz, 1H), 7.17 (d, *J* = 8 Hz, 1H), 7.13-6.99 (m, 1H), 3.94-3.78 (m, 2H), 3.73 (m, 1H), 3.00-2.75 (m, 2H), 2.08-1.81 (m, 5H), 1.60-1.43 (m, 1H). ^{13}C NMR ($CDCl_3$, 75 MHz) δ: 162.0, 149.4, 136.4, 123.0, 121.1, 78.8, 67.8, 35.8, 35.3, 31.5, 25.9. Anal. Calcd. for $C_{11}H_{15}NO$: C, 74.54; H, 8.53; N, 7.90. Found: C, 74.5; H, 8.6; N, 7.8.

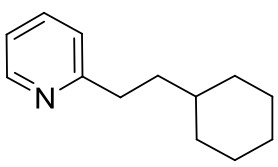

2-(2-Cyclohexylethyl)pyridine (3.18). From 808 μL (7.5 mmol, 0.5 M) of cyclohexane (**3.1g**) and 161 μL (1.5 mmol, 0.1 M) of 2-vinylpyridine

(**3.2b**). Purification of the residue by column chromatography (cyclohexane/ethyl acetate 8:2 as the eluant) afforded 177 mg of 2-(2-cyclohexylethyl)pyridine (**3.18**, 62% yield) as an oil. ^{1}H NMR ($CDCl_3$, 300 MHz) δ: 8.51 (d, *J* = 5 Hz, 1H), 7.56 (td, *J* = 8, *J* = 2 Hz, 1H), 7.18-7.02 (m, 2H), 2.89-2.64 (m, 2H), 1.88-1.48 (m, 7H), 1.41-1.05 (m, 4H), 1.04-0.79 (m, 2H). ^{13}C NMR ($CDCl_3$, 75 MHz) δ: 163.0, 149.3, 136.4, 122.8, 120.9, 37.8, 37.7, 36.0, 33.4, 26.8, 26.5. Anal. Calcd. for $C_{13}H_{19}N$: C, 82.48; H, 10.12; N, 7.40. Found: C, 82.6; H, 10.0; N, 7.4.

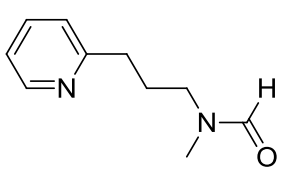

***N*-Methyl-*N*-(3-(pyridin-2-yl)propyl)formamide (3.19).** From 464 μL (6.0 mmol, 0.4 M) of *N*,*N*-dimethylformamide (**3.1d**) and 161 μL (1.5 mmol, 0.1 M) of 2-vinylpyridine (**3.2b**). Purification of the residue by column chromatography (acetone as the eluant) afforded 220 mg of *N*-methyl-*N*-(3-(pyridin-2-yl)propyl)formamide (**3.19**, 82% yield) as an oil. ^{1}H NMR (CD_3OD, 300 MHz, mixture of two rotamers) δ: 8.44 (t, *J* = 4 Hz, 2H), 8.01 (s, 2H), 7.76 (tt, *J* = 8, *J* = 2 Hz, 2H), 7.34 (dd, *J* = 8 Hz, *J* = 4 Hz, 2H), 7.29-7.22 (m, 2H), 3.42-3.36 (m, 4H), 2.99 (s, 3H, minor), 2.85 (s, 3H, major), 2.82-2.71 (m, 4H), 2.09-1.87 (m, 4H). ^{13}C NMR (CD_3OD, 75 MHz, mixture of two rotamers) δ: 165.1, 165.0, 162.3, 162.0, 149.8, 149.6, 138.9, 138.8, 124.7, 123.0, 122.9, 50.3, 44.8, 35.9, 35.4, 35.0, 29.7, 29.0, 27.9. Anal. Calcd. for $C_{10}H_{14}N_2O$: C, 67.39; H, 7.92; N, 15.72. Found: C, 67.3; H, 7.9; N, 15.7.

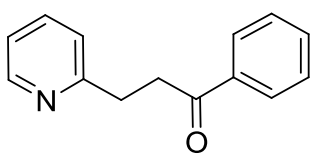

1-Phenyl-3-(pyridin-2-yl)propan-1-one (3.20). From 152 μL (1.5 mmol, 0.1 M) of benzaldehyde (**3.1j**) and 161 μL (1.5 mmol, 0.1 M) of 2-vinylpyridine (**3.2b**). Purification of the residue by column chromatography (cyclohexane/ethyl acetate 7:3 as the eluant) afforded 249 mg of 1-phenyl-3-(pyridin-2-yl)propan-1-one (**3.20**, 78% yield) as an oil. ^{1}H NMR ($CDCl_3$, 300 MHz) δ: 8.51 (d, *J* = 4 Hz, 1H), 7.99 (dd, *J* = 8 Hz, *J* =1 Hz, 2H), 7.64-7.50 (m, 2H), 7.44 (t, *J* = 8 Hz, 2H), 7.26 (d, *J* = 8 Hz, 1H), 7.15-7.07 (m, 1H), 3.51 (t, *J* = 7 Hz, 2H), 3.24 (t, *J* = 7 Hz, 2H). ^{13}C NMR ($CDCl_3$, 75 MHz) δ: 199.2, 160.6, 149.1, 136.8, 136.3, 132.9, 128.4, 128.0, 123.3, 121.1, 37.7, 32.0. Anal. Calcd. for $C_{14}H_{13}NO$: C, 79.59; H, 6.20; N, 6.63. Found: C, 79.6; H, 6.3; N, 6.6.

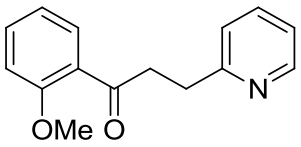

1-(2-Methoxyphenyl)-3-(pyridin-2-yl)propan-1-one (3.21). From 272 μL (1.5 mmol, 0.1 M) of 2-methoxybenzaldehyde (**3.1l**) and 161 μL (1.5 mmol, 0.1 M) of 2-vinylpyridine (**3.2b**). Purification of the residue by column chromatography (cyclohexane/ethyl acetate 8:2 as the eluant) afforded 244 mg of 1-(2-methoxyphenyl)-3-(pyridin-2-yl)propan-1-one (**3.21**, 67% yield) as an oil. The same reaction was carried out under flow conditions[10] (125 W medium pressure Hg vapors lamp; V_{tot}: 12 mL; Flow rate: 0.04 mL min^{-1}) to give **3.21** in 64% yield. ^{1}H NMR ($CDCl_3$, 300 MHz) δ: 8.50 (d, *J* = 4 Hz, 1H), 7.69 (dd, *J* = 8 Hz, *J* =2 Hz, 1H), 7.58 (td, *J* = 8 Hz, *J* = 2 Hz, 1H), 7.44 (td, *J* = 8 Hz, *J* = 2 Hz, 1H), 7.24 (d, *J* = 8 Hz, 1H), 7.09 (dd, *J* = 7 Hz, *J* = 5 Hz, 1H), 6.99 (d, *J* = 8 Hz, 1H), 6.95 (d, *J* = 8 Hz, 1H), 3.88 (s, 3H), 3.48 (t, *J* = 7 Hz, 2H), 3.19 (t, *J* = 7 Hz, 2H). ^{13}C NMR ($CDCl_3$, 75 MHz) δ: 201.6, 161.4, 158.8, 149.3, 136.4, 133.5, 130.4, 123.4, 121.2, 120.7, 111.6, 55.6, 43.3, 32.7. Anal. Calcd. for $C_{15}H_{15}NO_2$: C, 74.67; H, 6.27; N, 5.81. Found: C, 74.6; H, 6.3; N, 5.8.

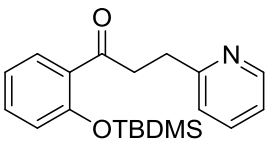

1-(2-((tert-Butyldimethylsilyl)oxy)phenyl)-3-(pyridin-2-yl)propan-1-one (3.22). From 355 mg (1.5 mmol, 0.1 M) of **3.1m** and 161 μL (1.5 mmol, 0.1 M) of 2-vinylpyridine (**3.2b**). Purification of the residue by column chromatography (cyclohexane/ethyl acetate 95:5 as the eluant) afforded 215 mg of 1-(2-((*tert*-butyldimethylsilyl)oxy)phenyl)-3-(pyridin-2-yl)propan-1-one (**3.22**, 42% yield) as an oil. ^{1}H NMR ($CDCl_3$, 300 MHz) δ: 8.39 (d, *J* = 4 Hz, 1H), 7.50-7.43 (m, 2H), 7.25-7.19 (m, 1H), 7.10 (d, *J* = 8 Hz, 1H), 7.00-6.94 (m, 1H), 6.90-6.84 (m, 1H), 6.76 (d, *J* = 8 Hz, 1H), 3.38 (t, *J* = 7 Hz, 2H), 3.10 (t, *J* = 7 Hz, 2H), 0.85 (s, 9H), 0.14 (s, 6H). ^{13}C NMR ($CDCl_3$, 75 MHz) δ: 202.3, 161.0, 154.3, 149.2, 136.2, 132.5, 131.3, 129.9, 123.1, 121.2, 121.1, 120.1, 43.0, 32.4, 25.8, 18.4, -4.0. Anal. Calcd. for $C_{20}H_{27}NO_2Si$: C, 70.34; H, 7.97; N, 4.10. Found: C, 70.4; H, 8.0; N, 4.0.

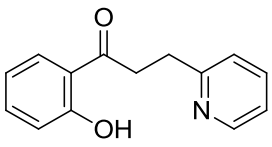

1-(2-Hydroxyphenyl)-3-(pyridin-2-yl)propan-1-one (3.23). Compound **3.23** was obtained from compound **3.22** by removal in a one-pot fashion of the silyl group.[11] In particular, the crude reaction mixture containing **3.22** (see above, for compound **3.13**) was rotary evaporated to remove the solvent (MeCN) and then an

excess of LiOH (100 mg, 4 mmol) in DMF (1 mL) was added. The solution was stirred overnight and then quenched with water (10 mL). The resulting mixture was extracted with ethyl acetate (3×10 mL), the organic phases were collected, dried and rotary evaporated to yield a brownish oil. Purification of the residue by column chromatography (cyclohexane/ethyl acetate 8:2 as the eluant) afforded 135 mg of 1-(2-hydroxyphenyl)-3-(pyridin-2-yl)propan-1-one (**3.23**, 39% yield over two steps) as an oil. ^{1}H NMR ($CDCl_3$, 300 MHz) δ: 12.24 (bs, 1H), 8.51 (d, *J* = 4 Hz, 1H), 7.83 (dd, *J* = 8 Hz, *J* = 2 Hz, 1H), 7.60 (td, *J* = 8 Hz, *J* = 2 Hz, 1H), 7.44 (ddd, *J* = 9 Hz, *J* = 7 Hz, *J* = 2 Hz, 1H), 7.25 (d, *J* = 8Hz, 1H), 7.11 (dd, *J* = 7 Hz, *J* = 5 Hz, 1H), 6.96 (dd, *J* = 8 Hz, *J* = 1 Hz, 1H), 6.91-6.83 (m, 1H), 3.54 (t, *J* = 7 Hz, 2H), 3.23 (t, *J* = 7 Hz, 2H). ^{13}C NMR ($CDCl_3$, 75 MHz) δ: 205.6, 162.4, 160.2, 149.4, 136.6, 136.3, 130.1, 123.4, 121.5, 119.6, 119.0, 118.5, 37.4, 31.9. Anal. Calcd. for $C_{14}H_{13}NO_2$: C, 73.99; H, 5.77; N, 6.16;. Found: C, 74.0; H, 5.8; N, 6.2.

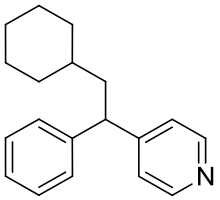

4-(2-Cyclohexyl-1-phenylethyl)pyridine (3.24). From 808 μL (7.5 mmol, 0.5 M) of cyclohexane (**3.1g**) and 272 mg (1.5 mmol, 0.1 M) of 4-(1-phenylvinyl)pyridine (**3.2c**). Purification of the residue by column chromatography (cyclohexane/ethyl acetate 7:3 as the eluant) afforded 283 mg of 4-(2-cyclohexyl-1-phenylethyl)pyridine (**3.24**, 71% yield) as a waxy solid. mp 62-64 °C. ^{1}H NMR ($CDCl_3$, 300 MHz) δ: 8.49 (bs, 2H), 7.42-7.06 (m, 7H), 4.03 (t, *J* = 8 Hz, 1H), 1.92 (dt, *J* = 14 Hz, *J* = 4 Hz, 2H), 1.81-1.59 (m, 6H), 1.19-0.87 (m, 5H). ^{13}C NMR ($CDCl_3$, 75 MHz) δ: 154.5, 149.9, 143.6, 128.8, 128.0, 126.7, 123.5, 47.6, 43.0, 35.0, 33.5, 33.4, 29.8, 26.7, 26.2. Anal. Calcd. for $C_{19}H_{23}N$: C, 85.99; H, 8.74; N, 5.28. Found: C, 85.9; H, 8.8; N, 5.3.

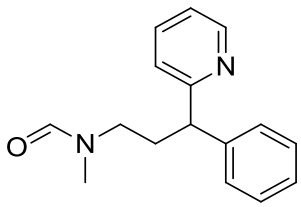

***N*-methyl-*N*-(3-phenyl-3-(pyridin-2-yl)propyl)formamide (3.25).** From 464 μL (6.0 mmol, 0.4 M) of *N*,*N*-dimethylformamide (**3.1d**) and 272 mg (1.5 mmol, 0.1 M) of 2-(1-phenylvinyl)pyridine (**3.2d**). Purification of the residue by column chromatography (pure ethyl acetate as the eluant) afforded 260 mg of *N*-methyl-*N*-(3-phenyl-3-(pyridin-2-yl)propyl)formamide (**3.25**, 68% yield) as a colorless oil. ^{1}H NMR (300 MHz, $CDCl_3$, mixture of two rotamers) δ: 8.69-8.49 (m, 2H), 7.95 (s, 1H, minor), 7.81 (s, 1H,

major), 7.56 (td, *J* = 8 Hz, *J* = 2 Hz, 2H), 7.37-7.06 (m, 14H), 4.07 (t, *J* = 8 Hz, 1H, minor), 3.99 (t, *J* = 8 Hz, 1H, major), 3.34-3.26 (m, 2H, minor), 3.20 (t, *J* = 7 Hz, 2H, major), 2.87 (s, 3H), 2.87 (s, 3H), 2.62 (m, 2H), 2.30 (m, 2H). ^{13}C NMR (75 MHz, $CDCl_3$, mixture of two rotamers) δ: 162.7, 162.3, 162.1, 149.3, 149.1, 143.0, 142.4, 136.5, 136.4, 128.7, 128.5, 127.8, 127.8, 126.8, 126.5, 123.1, 123.1, 121.6, 121.4, 51.1, 50.0, 47.7, 43.1, 34.4, 32.6, 31.6, 29.3. Anal. Calcd. for $C_{16}H_{18}N_2O$: C, 75.56; H, 7.13; N, 11.01. Found: C, 75.5; H, 7.2; N, 11.0.

*Photocatalyzed addition of cyclohexane (**3.1g**) onto (E)-ethyl 3-(pyridin-4-yl)acrylate (**3.2e**)*

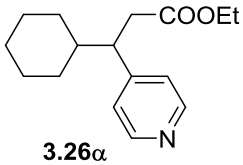

3.26α

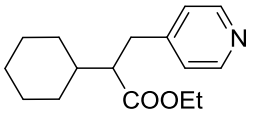

3.26β

From 808 μL (7.5 mmol, 0.5 M) of cyclohexane (**3.1g**) and 266 mg (1.5 mmol, 0.1 M) of (*E*)-ethyl 3-(pyridin-4-yl)acrylate (**3.2e**). Purification of the residue by column chromatography (ethyl acetate as the eluant) afforded 277 mg of a mixture of ethyl 3-cyclohexyl-3-(pyridin-4-yl)propanoate (**3.26α**) and of ethyl 2-cyclohexyl-3-(pyridin-4-yl)propanoate (**3.26β**) in a α/β ratio = 14:86 (determined by NMR analysis). Overall yield of **3.26**: 71%. ^{1}H NMR of the mixture ($CDCl_3$, 300 MHz): δ: 8.46 (d, *J* = 6 Hz, 4H), 7.07 (d, *J* = 6 Hz, 4H), 4.10-3.85 (m, 4H), 2.84-2.43 (m, 6H), 1.85-1.56 (m, 12H), 1.30-1.00 (m, 16H). ^{13}C NMR of the mixture ($CDCl_3$, 75 MHz) δ: 174.4, 149.8, 149.6, 149.3, 124.3 (β), 123.9 (α), 60.5, 60.3, 53.1, 47.7, 42.5, 40.6, 37.6, 35.0, 30.9, 30.8, 26.4, 26.3, 14.3 (β), 14.1 (α).

*Photocatalyzed addition of cyclohexane (**3.1g**) onto (E)-3-(pyridin-4-yl)acrylonitrile (**3.2g**)*

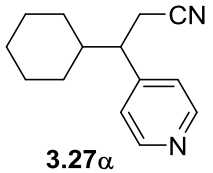

3.27α

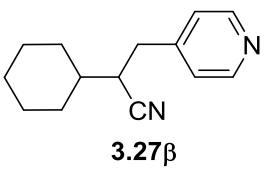

3.27β

From 807 μL (7.5 mmol, 0.5 M) of cyclohexane (**3.1g**) and 195 mg (1.5 mmol, 0.1 M) of (*E*)-3-(pyridin-4-yl)acrylonitrile (**3.2f**). Purification of the residue by column chromatography (ethyl acetate as the eluant) afforded 190 mg of a mixture of 3-cyclohexyl-3-(pyridin-4-yl)propanenitrile (**3.27α**) and 2-cyclohexyl-3-(pyridin-4-yl)propanenitrile (**3.27β**) in a α/β ratio = 34:66 (determined by NMR analysis). Overall yield of **3.27**: 60%. A further column purification allowed to isolate small amounts of pure (**3.27α**) and (**3.27β**). **3.27α** ^{1}H NMR ($CDCl_3$,

300 MHz) δ: 8.58 (d, *J* = 6 Hz, 2H), 7.13 (d, *J* = 6 Hz, 2H), 2.73-2.64 (m, 2H), 2.01-0.68 (m, 12H). **3.27β** ^{1}H NMR ($CDCl_3$, 300 MHz) δ: 8.56 (d, *J* = 6 Hz, 2H), 7.18 (d, *J* = 6 Hz, 2H), 2.99-2.78 (m, 2H), 2.75 -2.58 (m, 1H), 2.06-1.08 (m, 11H). ^{13}C NMR of the mixture ($CDCl_3$, 75 MHz): δ: 150.4, 150.1, 146.7, 124.3, 123.4, 120.3, 118.3, 47.7, 41.0, 39.8, 39.2, 35.3, 31.6, 30.8, 30.7, 29.2, 26.1, 26.0, 25.9, 25.8, 21.3.

UV-Vis Spectra

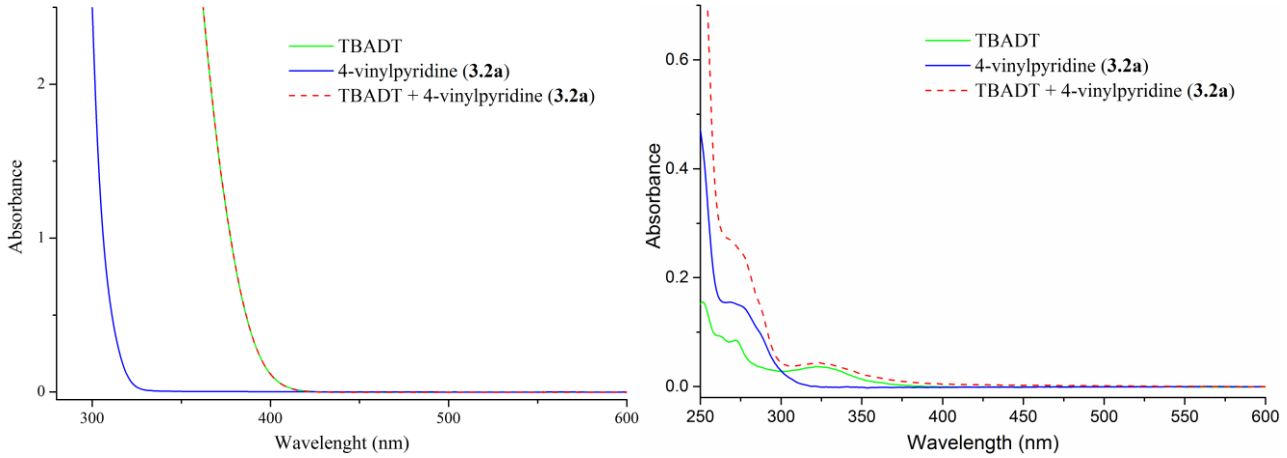

*Figure S.3.2 Left: UV-Vis absorption spectra of acetonitrile solutions containing: 2×10^{-3} M TBADT (green line); 0.1 M 4-vinylpyridine (**3.2a**, blue line); 2×10^{-3} M TBADT and 0.1 M 4-vinylpyridine (dashed red line). Right: UV-Vis absorption spectra of acetonitrile solutions containing: 2×10^{-6} M TBADT (green line); 10^{-4} M 4-vinylpyridine (**3.2a**, blue line); 2×10^{-6} M TBADT and 10^{-4} M 4-vinylpyridine (dashed red line).*

References

(1) Protti, S.; Ravelli, D.; Fagnoni, M.; Albini, A. *Chem. Commun.* **2009**, No. 47, 7351.

(2) Aizpurua, J. M.; Palomo, C. *Tetrahedron Lett.* **1985**.

(3) Lewis, R. S.; Garza, C. J.; Dang, A. T.; Pedro, T. K. A.; Chain, W. J. *Org. Lett.* **2015**, *17* (9), 2278–2281.

(4) Sada, M.; Komagawa, S.; Uchiyama, M.; Kobata, M.; Mizuno, T.; Utimoto, K.; Oshima, K.; Matsubara, S. *J. Am. Chem. Soc.* **2010**, *132* (49), 17452–17458.

(5) Tetsuhashi, M.; Ishikawa, M.; Hashimoto, M.; Hashimoto, Y.; Aoyama, H. *Bioorg. Med. Chem.* **2010**, *18* (14), 5323–5338.

(6) Clemo, G. R.; Popli, S. P. *J. Chem. Soc.* **1951**, *0* (0), 1406.

(7) Chandrasekhar, S.; Pavan Kumar Reddy, G.; Nagesh, C.; Raji Reddy, C. *Tetrahedron Lett.* **2007**, *48* (7), 1269–1271.

(8) Mei, K.; Wang, J.; Hu, X. *Synth. Commun.* **2006**, *36* (17), 2525–2532.

(9) Ravelli, D.; Protti, S.; Fagnoni, M. *Acc. Chem. Res.* **2016**, *49* (10), 2232–2242.

(10) Fagnoni, M.; Bonassi, F.; Palmieri, A.; Protti, S.; Ravelli, D.; Ballini, R. *Adv. Synth. Catal.* **2014**, *356* (4), 753–758.

(11) Ankala, S. V.; Fenteany, G. *Tetrahedron Lett.* **2002**, *43* (27), 4729–4732.

EXPERIMENTAL SECTION RELATIVE TO

CHAPTER 4

URANYL CATION: VISIBLE-LIGHT PHOTOCATALYZED HAT FOR C-C BOND FORMATION.

Optimization of Reaction Conditions

Reaction conditions were optimized for the photocatalyzed addition of cyclohexane (**3.1g**; 0.5 M) in the role of hydrogen donor onto 2-benzylidenemalononitrile (**2.2c**; 0.1 M) to give 2-(cyclohexyl(phenyl)methyl)malononitrile (**4.4**), see Tables 4.S.1-4.S.3.

The reaction was optimized in terms of solvent, catalyst loading, light source and time of irradiation. All solutions were prepared in a borosilicate glass vial, flushed with nitrogen if the case (1 min), closed with a screwed cap and then irradiated. After irradiation, dodecane was added as the standard and the mixture was filtered through a SiO_2 plug to remove U-based species. The outcome of the reaction was investigated via GC-FID analysis and yields were calculated by means of calibration curves with authentic samples.

Table 4.S.1 Solvent optimization.

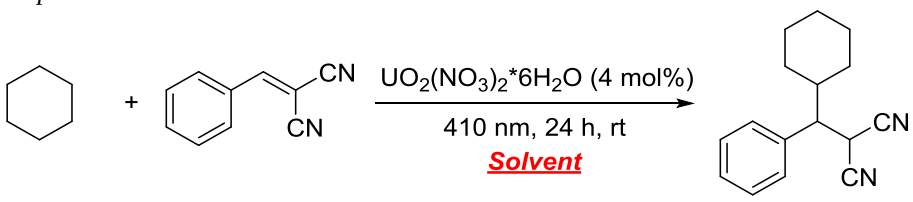

3.1g, 0.5 M **2.2c**, 0.1 M **4.4**

Entry	*Solvent*	*Consumption of 2.2c (%)*	*Yield of 4.4 (%)*[a]
1	*CH_2Cl_2*	*28*	*5*
2	*$CHCl_3$*	*46*	*3*
3	*$PhCF_3$*	*20*	*3*
4	*TFE*	*68*	*65*
5	*DMC*	*33*	*10*
6	*Ethyl acetate*	*39*	*15*
7	*MeCN*	*40*	*36*
8	*MeCN/H_2O 9:1*	*46*	*37*
9	*DMSO*	*57*	*8*
10	***Me_2CO***	***72***	***70***
11	*Me_2CO/H_2O 9:1*	*45*	*44*

TFE: 2,2,2-trifluoroethanol; DMC: dimethyl carbonate; DMSO: dimethyl sulfoxide
[a] GC yields by means of calibration curves, adopting dodecane as external standard.

Table 4.S.2 Catalyst loading optimization.

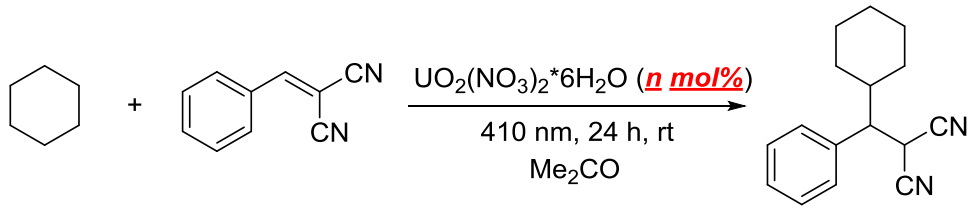

3.1g, 0.5 M **2.2c**, 0.1 M **4.4**

Entry	*Loading (n mol%)*	*Consumption of 2.2c (%)*	*Yield of 4.4(%)*[a]
1	*1*	*27*	*26*
2	*2*	*36*	*36*
3	*4*	*72*	*70*
4	*6*	*93*	*93*
5	***8***	***100***	***>95***

[a] *GC yields by means of calibration curves, adopting dodecane as external standard.*

We then decided to investigate the reaction depending on the wavelength of irradiation.

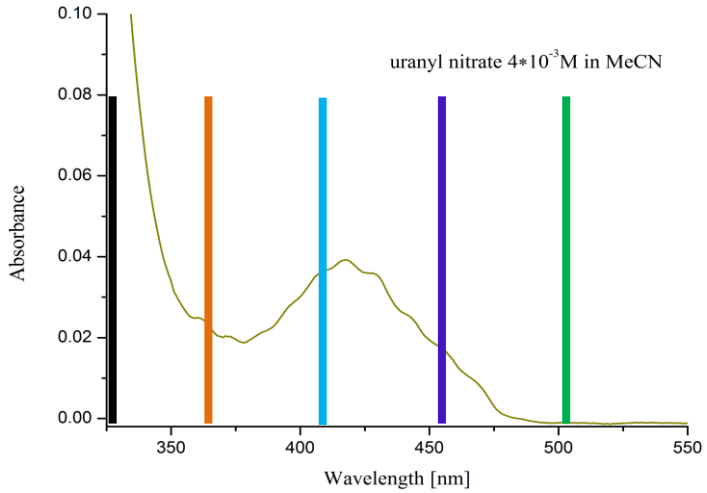

Figure 4.S.1 UV-Vis absorption spectrum with selected wavelength of irradiation.

Table 4.S.3 Wavelength optimization.

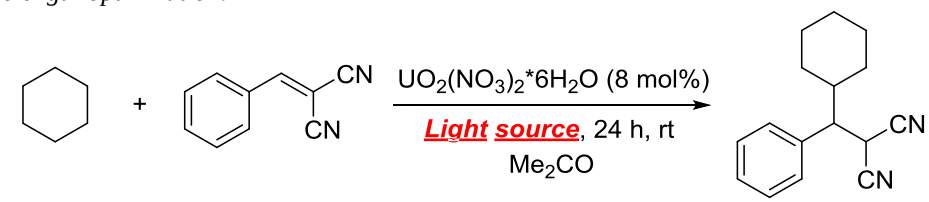

3.1g, 0.5 M **2.2c**, 0.1 M **4.4**

Entry	*Light source*	*Consumption of 2.2c (%)*	*Yield of 4.4 (%)*[a]
1	*310*[b]	*29*	*7*
2	*366*[c]	*17*	*3*
3	*410*[d]	*100*	*>95*
4	***456***[e]	***100***	***>95***
5	*505*[f]	*26*	*15*

[a] *GC yields by means of calibration curves, adopting dodecane as external standard.* [b] *multi-lamp apparatus fitted with 10×15 W phosphor-coated lamps (emission centered at 310 nm);* [c] *multi-lamp apparatus fitted with 12×15 W phosphor-coated lamps (emission centered at 366 nm);* [d] *1W LED, λ_{em} = 410 nm;* [e] *36 W Kessil Blue Lamp (456 nm, 50% intensity).* [f] *1W LED, λ_{em} = 505 nm.*

Reaction time optimization

A kinetic profile of the reaction was tracked in Figure 4.S.2 under optimized conditions (see Table 4.S.3, *entry 4*): small aliquots were subtracted from the reaction mixture at 1, 3, 4, 6, 12 and 23 hours, analysed via GC-FID and consumptions/yields were calculated by means of calibration curves with authentic samples (external standard: dodecane).

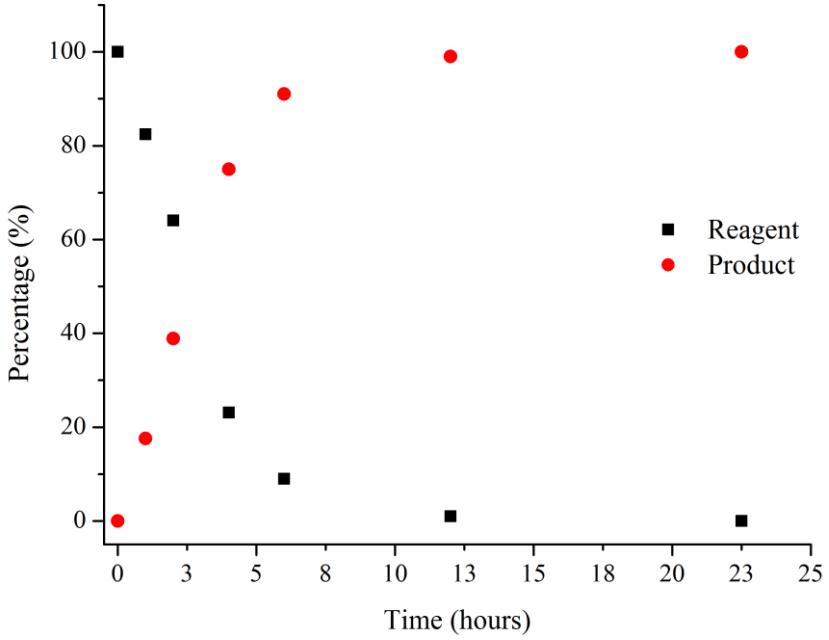

*Figure 4.S.2 Time profile for the consumption of **2.2c** (reagent) and formation of **4.4** (product).*

Synthetic procedures

Compounds **2.2d-2.2e**, **3.1a**, **3.1c**, **3.1d**, **3.1f**, **3.1g**, **3.1i**, **4.1a-4.1d** were commercially available and used as received, tetrahydrofuran (THF) and heptanal were distilled prior to use. Compounds **2.2c, 4.2a-4.2h** were synthesized following a procedure reported in the literature.[1,2] Acetonitrile (HPLC purity grade) employed for photochemical reactions was used as received. NMR spectra were recorded on a 300 (for ^{1}H) or 75 (for ^{13}C) MHz spectrometer; the attributions were made based on ^{1}H and ^{13}C NMR. Data for ^{1}H NMR are reported as follows: chemical shift referred to TMS (δ ppm), multiplicity (s = singlet, bs = broad singlet, d = doublet, t = triplet, q = quadruplet, quint = quintuplet, sext = sextuplet, sept = septuplet, m = multiplet), coupling constant (Hz) and integration. Data for ^{13}C NMR are reported in terms of chemical shift. Reactions were monitored by gas chromatographic (GC) analyses (HP-5 capillary column). Chromatographic purification of products

was accomplished using flash chromatography on 60 Å, 230-400 mesh silica gel. Thin-layer chromatography (TLC) was performed on silica gel 60 F-254 plates. Visualization of the developed plates was performed by fluorescence quenching or by $KMnO_4$ staining. UV-Vis spectra were recorded with a double beam spectrophotometer equipped with Deuterium lamp (190-350 nm) and Halogen lamp (330-900 nm) and a Photomultiplier R928.

*Synthesis of compounds **2.2c**, **4.2a-4.2d**, **4.2f-4.2h.*** Prepared on a 3 mmol scale following a procedure previously reported in the literature,[1] starting from the corresponding aromatic aldehyde (1.0 equiv., 1.0 M) and malononitrile or ethyl cyanoacetate (1.0 equiv., 1.0 M) in the presence of 10 mol% of 1,4-diazabicyclo[2.2.2]octane (DABCO). Solvent: water (3 mL); temperature: 20 °C. Reaction was monitored via TLC and products were purified via recrystallization in cyclohexane.

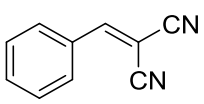

2-benzylidenemalononitrile (2.2c). Reaction time: 5 min. White solid, yield: 60%. mp: 83-85° C (lit. 83-84 °C).[1] Spectroscopic data of compound **2.2c** were in accordance with the literature.[1]

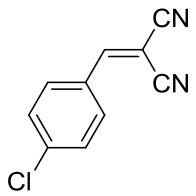

2-(4-chlorobenzylidene)malononitrile (4.2a). Reaction time: 2 min. White solid, yield: 80%. mp: 163-165 °C (lit.[1] 164-165 °C). Spectroscopic data of compound **4.2a** were in accordance with the literature.[1]

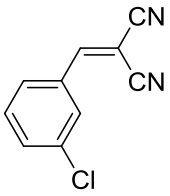

2-(3-chlorobenzylidene)malononitrile (4.2b). Reaction time: 2 min. White solid, yield: 90%. Spectroscopic data of compound **4.2b** were in accordance with the literature.[3]

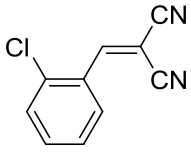

2-(2-chlorobenzylidene)malononitrile (4.2c). Reaction time: 2 min. White solid, yield: 99%. mp: 94-96 °C (lit.[4] 95 °C). Spectroscopic data of compound **4.4** were in accordance with the literature.[4]

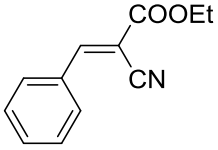

ethyl 2-cyano-3-phenylacrylate (4.2d). Reaction time: 3 h White solid, yield: 85%. mp: 48-49 °C (lit. 48-49 °C).[1] Spectroscopic data were in accordance with

the literature.[1]

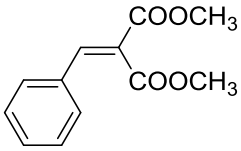

dimethyl 2-benzylidenemalonate (4.2e). Dimethyl 2-benzylidenemalonate was prepared according to a procedure reported in the literature.[2] Colorless oil. Spectroscopic data were in accordance with the literature.[3]

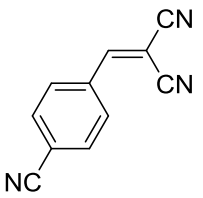

2-(4-cyanobenzylidene)malononitrile (4.2f). Reaction time: 2 min. White solid, yield: 88%. mp: 153-156 °C. Spectroscopic data were in accordance with the literature.[6]

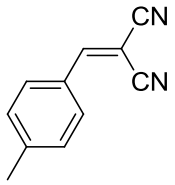

2-(4-methylbenzylidene)malononitrile (4.2g). Reaction time: 3 min. White solid, yield: 88%. mp: 132-134 °C (lit. 133-134 °C).[1] Spectroscopic data were in accordance with the literature.[1]

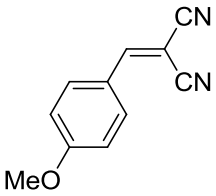

2-(4-methoxybenzylidene)malononitrile (4.2h). Reaction time: 10 min. White solid, yield: 88%. mp: 132-134 °C (lit.[4] 116-118 °C). Spectroscopic data were in accordance with the literature.[4]

General Procedure for the Uranyl Cation-Photocatalyzed Functionalization of styrenes: An acetone solution (10 mL) of the H-donor (1.0-5.0 mmol, 0.1-0.5 M, 1-5 equiv., except for **3.1f**, see below) and the electron-poor olefin (1.0 mmol, 0.1 M, 1 equiv.), in the presence of uranyl nitrate hexahydrate ($8 \cdot 10^{-3}$ M, 8 mol%) was poured in a borosilicate glass vessel (see Figure 4.S.1).

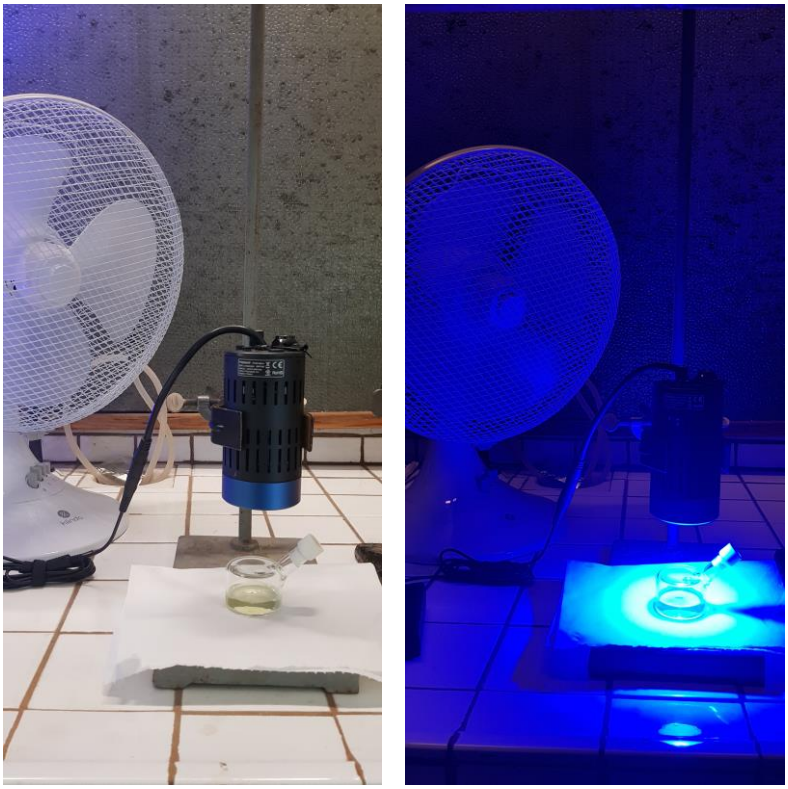

Figure 4.S.1 Picture of the irradiation system.

The solution was then purged for 3 min with nitrogen, capped with a septum, and irradiated for 24 h with a 36 W Kessil blue lamp (456 nm, 50% intensity). After completion, the solvent was removed under reduced pressure from the photolyzed solution and the product isolated by purification of the residue by flash column chromatography.

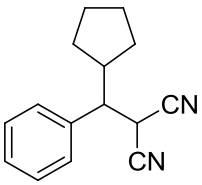

2-(cyclopentyl(phenyl)methylene)malononitrile (4.3). From cyclopentane **4.1a** (0.5 M, 5.0 equiv., 467 μL) and 2-benzylidenemalononitrile **2.2c** (0.1 M, 1.0 equiv., 154 mg). The crude mixture was purified through column chromatography (SiO_2: cyclohexane/ethyl acetate 8:2) to afford **4.3** as a colorless oil (150 mg), yield 67%.

^{1}H NMR (300 MHz, $CDCl_3$) δ 7.52 – 7.33 (m, 5H), 4.11 (d, J = 4.5 Hz, 1H), 2.95 (dd, J = 11.0, 4.5 Hz, 1H), 2.58 (dtd, J = 20.3, 9.8, 6.7 Hz, 1H), 2.07 (dtd, J = 11.1, 7.0, 3.5 Hz, 1H), 1.89 – 1.52 (m, 5H), 1.30 (dq, J = 11.7, 8.9 Hz, 1H), 1.19 – 0.97 (m, 1H).

^{13}C NMR (75 MHz, $CDCl_3$) δ 137.5, 129.1, 128.8, 128.3, 112.2, 112.0, 52.3, 42.5, 31.8, 31.7, 29.3, 25.6, 24.8.

Anal. Calcd for $C_{15}H_{16}N_2$: C, 80.32; H, 7.19; N, 12.49. Found: C, 80.2; H, 7.3; N, 12.5.

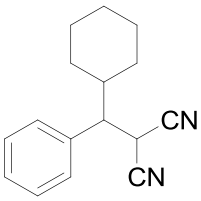

2-(cyclohexyl(phenyl)methylene)malononitrile (4.4). From cyclohexane **3.1g** (0.5 M, 5.0 equiv., 543 μL) and 2-benzylidenemalononitrile **2.2c** (0.1 M, 1.0 equiv., 154 mg). The crude mixture was purified through column chromatography (SiO_2: cyclohexane/ethyl acetate 8:2) to afford **4.4** as a colorless oil (229 mg), yield 96%. Spectroscopic data for **4.4** are in accordance with the literature.[7]

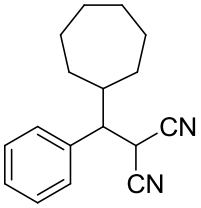

2-(cycloheptyl(phenyl)methyl)malononitrile (4.5). From cycloheptane **4.1b** (0.5 M, 5.0 equiv., 605 μL) and 2-benzylidenemalononitrile **2.2c** (0.1 M, 1.0 equiv., 154 mg). The crude mixture was purified through column chromatography (SiO_2: cyclohexane/ethyl acetate 8:2) to afford **4.5** as a colorless oil (192 mg), yield 76%.

^{1}H NMR (300 MHz, $CDCl_3$) δ 7.45 – 7.36 (m, 3H), 7.35 – 7.30 (m, 2H), 4.19 (d, J = 6 Hz, 1H), 3.00 (dd, J_1 = 10 Hz, J_2 = 6 Hz, 1H), 2.28 (m, 1H), 1.92 (m, 1H), 1.81 – 1.09 (m, 11H).

^{13}C NMR (75 MHz, $CDCl_3$) δ 137.0, 129.2, 128.8, 128.6, 112.4, 112.1, 52.3, 40.6, 32.8, 30.8, 28.7, 27.9, 27.9, 26.1, 26.0.

Anal. Calcd for $C_{17}H_{20}N_2$: C, 80.91; H, 7.99; N, 11.10. Found: C, 80.9; H, 8.0; N, 11.1

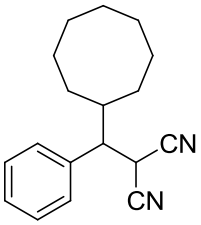

2-(cyclooctyl(phenyl)methyl)malononitrile (4.6). From cyclooctane **4.1c** (0.5 M, 5.0 equiv., 673 μL) and 2-benzylidenemalononitrile **2.2c** (0.1 M, 1.0 equiv., 154 mg). The crude mixture was purified through column chromatography (SiO_2: cyclohexane/ethyl acetate 8:2) to afford **4.6** as a colorless oil (208 mg), yield 78%.

^{1}H NMR (300 MHz, $CDCl_3$) δ 7.46 – 7.35 (m, 5H), 4.22 (d, J = 5 Hz, 1H), 2.98 (dd, J_1 = 10 Hz, J_2 = 5 Hz, 1H), 2.39 – 2.33 (m, 1H), 2.03 – 1.10 (m, 14H).

^{13}C NMR (75 MHz, $CDCl_3$) δ 137.1, 129.2, 128.9, 128.6, 112.4, 112.0, 52.3, 38.3, 30.7, 28.8, 27.9, 27.5, 26.8, 26.5, 25.9, 24.5.

Anal. Calcd for $C_{18}H_{22}N_2$: C, 81.16; H, 8.32; N, 10.52. Found: C, 81.2; H, 8.3; N, 10.5

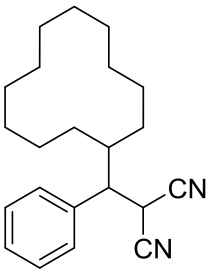

2-(cyclododecyl(phenyl)methyl)malononitrile (4.7). From cyclododecane **4.1d** (0.5 M, 5.0 equiv., 842 mg) and **2.2c** (0.1 M, 1.0 equiv., 154 mg). The crude mixture was purified through column chromatography (SiO_2: cyclohexane/ethyl acetate 8:2) to afford **4.7** as a colorless oil (136 mg), yield 42%. m.p.:106-107°C

^{1}H NMR (300 MHz, $CDCl_3$) δ 7.46 – 7.29 (m, 5H), 4.20 (d, J = 5.6 Hz, 1H), 3.03 (dd, J = 10.1, 5.6 Hz, 1H), 2.31 – 2.11 (m, 1H), 1.54 – 1.08 (m, 22H).

^{13}C NMR (75 MHz, $CDCl_3$) δ 136.7, 129.2, 128.9, 128.6, 112.4, 112.0, 49.3, 37.3, 28.0, 26.4, 25.6, 25.54, 25.5, 25.2, 23.3, 23.1, 22.5, 22.4, 21.1, 20.8.

Anal. Calcd for $C_{22}H_{30}N_2$: C, 81.94; H, 9.38; N, 8.69. Found: C, 82.0; H, 9.4; N, 8.7

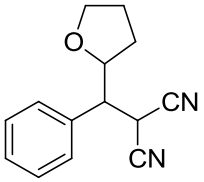

2-(phenyl(tetrahydrofuran-2-yl)methyl)malononitrile (4.8). From THF **3.1a** (0.5 M, 5 equiv., 401 μL) and **2.2c** (0.1 M, 1.0 equiv., 154 mg). The crude mixture was purified through column chromatography (SiO_2: cyclohexane/ethyl acetate 8:2) to afford **4.8** as a mixture of inseparable diastereomers as a yellowish oil (136 mg), yield 60%.

^{1}H NMR of the mixture (300 MHz, $CDCl_3$) δ 7.45 – 7.28 (m, 10H), 4.55 (d, J = 4.1 Hz, 1H, minor), 4.51 – 4.32 (m, 2H), 4.40 (d, J = 10.5 Hz, 1H), 4.02 – 3.81 (m, 2H), 3.74 (m, 2H, major), 3.29 (dd, J = 10.6, 3.2 Hz, 1H, major), 3.05 (dd, J = 10.3, 4.2 Hz, 1H, minor), 2.04 – 1.83 (m, 4H), 1.77 (m, 1H), 1.57 – 1.32 (m, 3H).

^{13}C NMR (75 MHz, $CDCl_3$) δ 134.6 (minor), 134.1 (major), 129.3 (major), 129.3 (minor), 129.2, 129.0, 129.0 (major), 128.6 (minor), 112.5, 112.4, 112.4, 111.9, 78.1, 77.6, 68.9 (major), 68.8 (minor), 51.9, 50.6, 30.4, 29.0, 27.4, 27.1, 25.8 (major), 25.8 (minor).

Anal. Calcd for $C_{14}H_{14}N_2O$: C, 74.31; H, 6.24; N, 12.38. Found: C, 74.3; H, 6.2; N, 12.4.

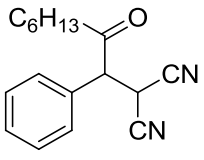

2-(2-oxo-1-phenyloctyl)malononitrile (4.9). From freshly distilled heptanal **3.1i** (0.15 M, 1.5 equiv., 212 μL) and **2.2c** (0.1 M, 1.0 equiv., 154 mg). The crude mixture was purified through column chromatography (SiO_2: cyclohexane/ethyl acetate 9:1) to afford **4.9** as a colorless oil (249 mg), yield 93%.

^{1}H NMR (300 MHz, $CDCl_3$) δ 7.52 – 7.43 (m, 3H), 7.28 (dt, J = 5.0, 1.9 Hz, 2H), 4.42 (dd, J = 8.6, 1.0 Hz, 1H), 4.29 (d, J = 8.6 Hz, 1H), 2.43 (t, J = 7.4 Hz, 2H), 1.57 (h, J = 6.1, 5.5 Hz, 2H), 1.31 – 1.12 (m, 6H), 0.85 (t, J = 6.8 Hz, 3H).

^{13}C NMR (75 MHz, $CDCl_3$) δ 204.2, 131.3, 130.1, 130.1, 128.8, 112.1, 111.6, 58.3, 41.1, 31.4, 28.53, 25.6, 23.6, 22.4, 14.0.

Anal. Calcd for $C_{17}H_{20}N_2O$: C, 76.09; H, 7.51; N, 10.44. Found: C, 76.1; H, 7.5; N, 10.4.

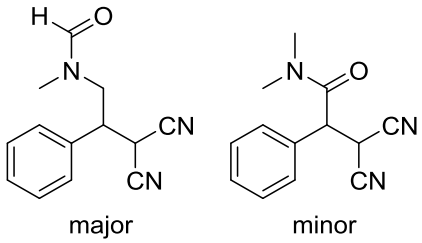

N-(3,3-dicyano-2-phenylpropyl)-N-methylformamide (4.10). From DMF **3.1d** (0.4 M, 4.0 equiv., 310 μL) and **2.2c** (0.1 M, 1.0 equiv., 154 mg). The crude mixture was purified through column chromatography (SiO_2: cyclohexane/ethyl acetate 8:2) to afford two constitutional isomers (ratio 2:1) of **4.10** as two colorless oils. Major isomer: 154 mg, 66% yield; minor isomer: 77 mg, 34% yield.

4.10 *Major (two conformers)*: ^{1}H NMR (300 MHz, $CDCl_3$) δ 8.02 (s, 1H), 7.95 (s, 1H), 7.51 – 7.29 (m, 10H), 4.26 (d, J = 5.1 Hz, 1H), 4.23 (dd, J = 6.0, 1.0 Hz, 1H), 4.09 (dd, J = 12.5, 6.3 Hz, 1H), 3.87 (dd, J = 14.4, 7.1 Hz, 1H), 3.77 – 3.48 (m, 4H), 2.84 (s, 3H), 2.82 (s, 3H).

^{13}C NMR (75 MHz, $CDCl_3$) δ 162.8, 134.6, 133.8, 129.8, 129.8, 129.5, 129.5, 128.1, 127.9, 112.0, 111.6, 111.6, 111.4, 51.4, 47.3, 44.3, 44.1, 35.8, 30.3, 27.8, 27.2.

Anal. Calcd for $C_{13}H_{13}N_3O$: C, 68.70; H, 5.77; N, 18.49. Found: C, 68.7; H, 5.8; N, 18.5.

4.10 *Minor*: ^{1}H NMR (300 MHz, $CDCl_3$) δ 7.43 (m, 3H), 7.35 (m, 2H), 4.51 (dd, J = 8.6, 0.9 Hz, 1H), 4.34 (d, J = 8.6 Hz, 1H), 3.00 (s, 3H), 2.82 (s, 3H).

^{13}C NMR (75 MHz, $CDCl_3$) δ 167.2, 132.2, 129.9, 129.8, 128.4, 112.7, 111.9, 51.0, 50.9, 37.1, 36.41, 28.1.

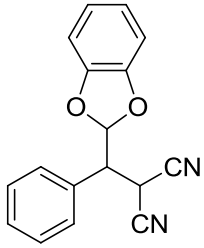

2-(benzo[d][1,3]dioxol-2-yl(phenyl)methyl)malononitrile (4.11). From freshly distilled 1,3-benzodioxole **3.1c** (0.11 M, 1.1 equiv., 126 μL) and **2.2c** (0.1 M, 1.0 equiv., 154 mg). The crude mixture was purified through column chromatography

(SiO_2: cyclohexane/ethyl acetate 8:2) to afford **4.11** as a colorless oil (160 mg), yield 58%.

^{1}H NMR (300 MHz, $CDCl_3$) δ 7.57 – 7.45 (m, 5H), 6.97 – 6.81 (m, 4H), 6.54 (d, J = 4.4 Hz, 1H), 4.44 (d, J = 5.8 Hz, 1H), 3.78 (dd, J = 5.9, 4.5 Hz, 1H).

^{13}C NMR (75 MHz, $CDCl_3$) δ 146.7, 146.5, 131.6, 130.0, 129.6, 129.1, 122.8, 122.7, 111.4, 111.2, 109.4, 109.4, 109.0, 50.0, 24.6.

Anal. Calcd for $C_{17}H_{12}N_2O_2$: C, 73.90; H, 4.38; N, 10.14. Found: C, 73.9; H, 4.4; N, 10.1.

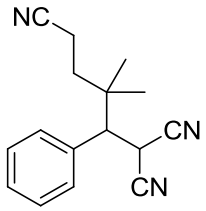

3,3-dimethyl-2-phenylpentane-1,1,5-tricarbonitrile (4.12). From freshly distilled isocapronitrile **3.1f** (1.0 M, 10.0 equiv., 1214 μL) and 2-benzylidenemalononitrile **2.2c** (0.1 M, 1.0 equiv., 154 mg). The crude mixture was purified through column chromatography (SiO_2: cyclohexane/ethyl acetate 9:1) to afford **4.12** as a colorless oil (171 mg), yield 68%.

^{1}H NMR (300 MHz, $CDCl_3$) δ 7.54 – 7.28 (m, 5H), 4.27 (d, J = 5.7 Hz, 1H), 3.05 (d, J = 5.7 Hz, 1H), 2.38 – 2.11 (m, 2H), 1.78 – 1.66 (m, 2H), 1.16 (s, 3H), 1.10 (s, 3H).

^{13}C NMR (75 MHz, $CDCl_3$) δ 135.1, 129.4, 129.2, 129.1, 119.7, 113.1, 112.9, 55.3, 37.3, 36.1, 25.0, 25.0, 23.8, 12.3.

Anal. Calcd for $C_{16}H_{17}N_3$: C, 76.46; H, 6.82; N, 16.72. Found: C, 74.5; H, 6.8; N, 16.7.

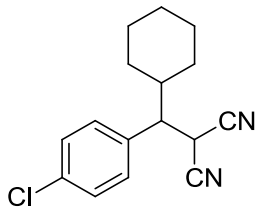

2-((4-chlorophenyl)(cyclohexyl)methyl)malononitrile (4.13). From cyclohexane **3.1g** (0.5 M, 5 equiv., 543 μL) and 2-(4-chlorobenzylidene)malononitrile **4.2a** (0.1 M, 189 mg). The crude mixture was purified through column chromatography (SiO_2: cyclohexane/ethyl acetate 9:1) to afford **4.13** as a yellowish oil (164 mg), yield 63%. Spectroscopic data for **4.13** are in accordance with the literature.[5]

^{1}H NMR (300 MHz, $CDCl_3$) δ 7.54 – 7.28 (m, 5H), 4.27 (d, J = 5.7 Hz, 1H), 3.05 (d, J = 5.7 Hz, 1H), 2.38 – 2.11 (m, 2H), 1.78 – 1.66 (m, 2H), 1.16 (s, 3H), 1.10 (s, 3H).

^{13}C NMR (75 MHz, $CDCl_3$) δ 135.1, 129.4, 129.2, 129.1, 119.7, 113.1, 112.9, 55.3, 37.3, 36.1, 25.0, 25.0, 23.8, 12.3.

Anal. Calcd for $C_{16}H_{17}N_3$: C, 76.46; H, 6.82; N, 16.72. Found: C, 74.5; H, 6.8; N, 16.7.

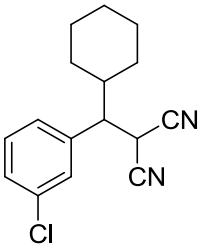

2-((3-chlorophenyl)(cyclohexyl)methyl)malononitrile (4.14). From cyclohexane **3.1g** (0.5 M, 5.0 equiv., 543 μL) and 2-(3-chlorobenzylidene)malononitrile **4.2b** (0.1 M, 1.0 equiv., 189 mg). The crude mixture was purified through column chromatography (SiO_2: cyclohexane/ethyl acetate 8:2) to afford **4.14** as a yellowish oil (199 mg), yield 73%.

^{1}H NMR (300 MHz, $CDCl_3$) δ 7.55 – 7.12 (m, 5H), 4.21 (d, J = 5.6 Hz, 1H), 2.88 (dd, J = 9.7, 5.5 Hz, 1H), 2.11 – 1.78 (m, 3H), 1.69 (dq, J = 15.1, 7.2, 5.6 Hz, 2H), 1.58 – 0.97 (m, 4H), 0.84 (qd, J = 12.1, 3.4 Hz, 1H).

^{13}C NMR (75 MHz, $CDCl_3$) δ 138.8, 135.1, 130.6, 129.2, 128.6, 126.5, 112.0, 111.7, 52.0, 39.3, 31.2, 30.7, 27.0, 25.87, 25.84, 25.76.

Anal. Calcd for $C_{16}H_{17}ClN_2$: C, 70.45; H, 6.28; N, 10.27. Found: C, 70.5; H, 6.3; N, 10.3

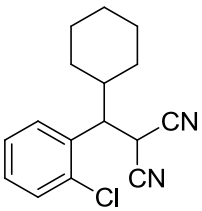

2-((2-chlorophenyl)(cyclohexyl)methyl)malononitrile (4.15). From cyclohexane **3.1g** (0.5 M, 5.0 equiv., 543 μL) and 2-(2-chlorobenzylidene)malononitrile **4.2c** (0.1 M, 189 mg). The crude mixture was purified through column chromatography (SiO_2: cyclohexane/ethyl acetate 8:2) to afford **4.15** as an orange oil (224 mg), yield 82%.

^{1}H NMR (300 MHz, $CDCl_3$) δ 7.57 (d, J = 8 Hz, 1H), 7.49 (dd, J_1 = 8 Hz, J_2 = 1 Hz, 1H), 7.42 – 7.28 (m, 2H), 4.19 (d, J = 5 Hz, 1H), 3.81 (dd, J_1 = 10 Hz, J_2 = 5 Hz, 1H), 2.11 – 1.98 (m, 2H), 1.96 – 1.83 (m, 1H), 1.80 – 1.59 (m, 2H), 1.49 – 1.33 (m, 2H), 1.27 – 1.08 (m, 3H), 1.06 – 0.85 (m, 1H).

^{13}C NMR (75 MHz, $CDCl_3$) δ 138.8, 135.1, 130.6, 129.2, 128.6, 126.5, 112.0, 111.7, 52.0, 39.3, 31.2, 30.7, 27.0, 25.9, 25.8, 25.8.

Anal. Calcd for $C_{16}H_{17}ClN_2$: C, 70.45; H, 6.28; N, 10.27. Found: C, 70.4; H, 6.3; N, 10.3.

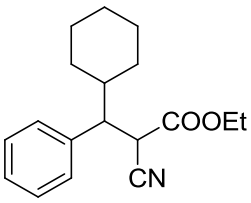

ethyl 2-cyano-3-cyclohexyl-3-phenylpropanoate (4.16). From cyclohexane **3.1g** (0.5 M, 5.0 equiv., 543 μL) and 2-(2-chlorobenzylidene)malononitrile

4.2d (0.1 M, 1.0 equiv., 187 mg). The crude mixture was purified through column chromatography (SiO_2: cyclohexane/ethyl acetate 9:1) to afford **4.16** as a mixture of inseparable diastereomers (ratio 1:1) as a yellowish oil (209 mg), yield 77%.

^{1}H NMR (300 MHz, $CDCl_3$) δ 7.42 – 7.11 (m, 10H), 4.17 – 4.08 (m, 2H), 4.03 (d, J = 5.5 Hz, 1H), 4.00 – 3.90 (m, 2H), 3.82 (d, J = 6.3 Hz, 1H), 3.27 – 3.15 (m, 1H), 2.97 (dd, J = 10.4, 5.6 Hz, 1H), 2.17 – 0.72 (m, 28H).

^{13}C NMR (75 MHz, $CDCl_3$) δ 166.0, 165.8, 139.2, 138.2, 128.7, 128.7, 128.6, 128.5, 127.9, 127.7, 116.3, 115.8, 62.8, 62.5, 52.0, 51.7, 42.2, 41.7, 40.3, 39.7, 31.7, 31.5, 31.3, 31.2, 30.0, 26.5, 26.3, 26.3, 26.2, 26.2, 26.1, 26.0, 13.9, 13.8.

Anal. Calcd for $C_{18}H_{23}NO_2$: C, 75.76; H, 8.12; N, 4.91. Found: C, 75.7; H, 8.2; N, 4.9.

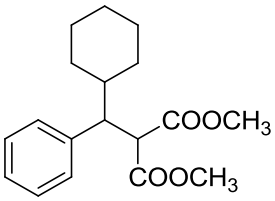

dimethyl 2-(cyclohexyl(phenyl)methyl)malonate (4.17). From cyclohexane **3.1g** (0.5 M, 5.0 equiv., 543 μL) and 2-(2-chlorobenzylidene)malononitrile **4.2e** (0.1 M, 1.0 equiv., 220 mg). The crude mixture was purified through column chromatography (SiO_2: cyclohexane/ethyl acetate 9:1) to afford **4.17** as a yellowish oil (225 mg), yield 74%. Spectroscopic data for **4.17** are in accordance with the literature.[1] m.p.: 60-62 °C

ANTIMONY-OXO PORPHYRINS AS PROMISING PHOTOCATALYSTS FOR VISIBLE-LIGHT INDUCED H-ATOM ABSTRACTION.

Experimental Data

Dimethyl maleate (**2.2e**) and dimethyl fumarate (**2.2d**) were commercially available and used as received, while tetrahydrofuran (THF, **3.1a**) was distilled prior to use. 2-Cyclohexylidenemalononitrile (**4.2k**) was synthesized according to a published procedure.[1] Complex **I** was synthesized as previously reported.[8] Acetonitrile and water (HPLC purity grade) employed for photochemical reactions were used as received. A NaOH stock solution in HPLC-grade water ($4 \cdot 10^{-3}$ M) was prepared and, when required, the proper amount of solution was added to the reaction mixture, as detailed in the main text.

NMR spectra were recorded on a 300 (for ^{1}H) or 75 (for ^{13}C) MHz spectrometer; the attributions were made on the basis of ^{1}H and ^{13}C NMR.

Reactions were monitored by gas chromatographic (GC-FID) analyses (HP-5 capillary column). The GC oven temperature was held at 80 °C for 2 min, increased to 250 °C by a temperature ramp of 10 °C min^{-1} and held for 5 min. Products **4.18** and **4.19** were quantified via calibration curves in the presence of *n*-dodecane (1 $\mu L \cdot mL^{-1}$) as internal standard by comparison with authentic samples. The conversion degree of the employed olefin was determined in the same way.

GC-MS analyses were carried out using a Thermo Scientific DSQII single quadrupole GC-MS system. A Restek Rtx-5MS (30 m × 0.25 mm × 0.25 μm) capillary column was used for analytes separation with helium as carrier gas at 1 mL min^{-1}. The injection in the GC system was performed in split mode and the injector temperature was 250 °C. The GC oven temperature was held at 80 °C for 2 min, increased to 220 °C by a temperature ramp of 10 °C min^{-1} and held for 10 min. The transfer line temperature was 250 °C and the ion source temperature 250 °C. Mass spectral analyses were carried out in full scan mode.

Irradiation was carried out with the following apparatuses:

- At 310 nm: 10×15 W phosphor-coated lamps Hg-lamps (emission centered at λ_{em}=310 nm);
- At 366 nm: 12×15 W phosphor-coated lamps Hg-lamps (emission centered at λ_{em}=366 nm);
- At 410 nm: 1 W LEDs;
- At 455 nm: 1 W LEDs;
- Medium-pressure Na lamp (emission centered at at λ_{em}=589 nm);
- Solar simulator: 1.5 kW Xe lamp, 500 W/m^2.

General Procedure for the Antimony-Oxo Porphyrin-Photocatalyzed Functionalization of Electrophilic Olefins. In a typical experiment, a 1 mm-thin cuvette was used as a reaction vessel (see Figure 4.S.3). Dimethyl fumarate (7.2 mg, 0.05 M, 1 equiv.) and tetrahydrofuran (40.5 μL, 0.5 M, 10 equiv.) were dissolved in 1 mL of a MeCN/H_2O 95:5 solution $5\cdot10^{-4}$ M both in complex **I** and NaOH. 300 μL of the freshly prepared solution were transferred into a 1 mm cuvette, flushed with N_2 and finally irradiated 48 hours with the selected irradiation system. Before irradiation a t_0 aliquot was removed to track the consumption of the olefin.

External std: *n*-dodecane (1 μl/mL)

Figure 4.S.3 Cuvette containing the reaction mixture before irradiation

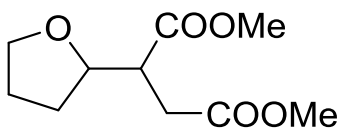

dimethyl 2-(tetrahydrofuran-2-yl)succinate. The identity of the product was confirmed by GC-MS analysis and yield (67% from dimethyl maleate and 77% from dimethyl fumarate as the olefin) was calculated via calibration curve with authentic sample.

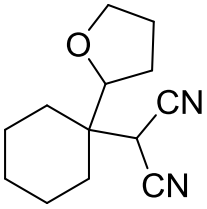

2-(1-(tetrahydrofuran-2-yl)cyclohexyl)malononitrile. The identity of the product was confirmed by GC-MS analysis and yield (77%, based on 39% conversion of olefin **4.2k**) was calculated via calibration curve with authentic sample.

Chemical quenching experiments

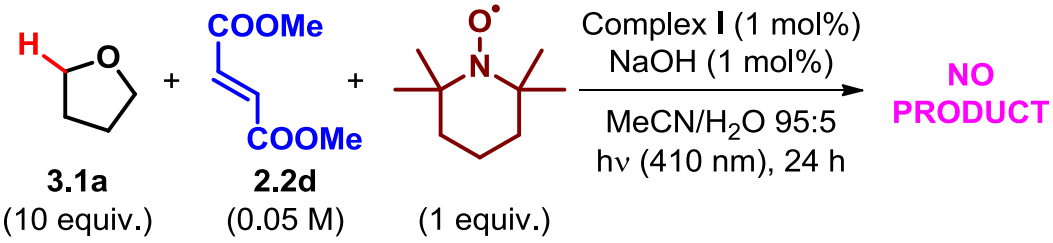

Figure 4.S.4 Trapping experiment with TEMPO

To the solution prepared according to the procedure already described above, TEMPO (7.8 mg, 0.05 M, 1 equiv.) was added. 300 µL of the freshly prepared solution were transferred into a 1 mm cuvette, flushed with N_2 and finally irradiated 24 hours with the selected irradiation system. GC analysis revealed the reaction was completely inhibited.

Deuteration experiments

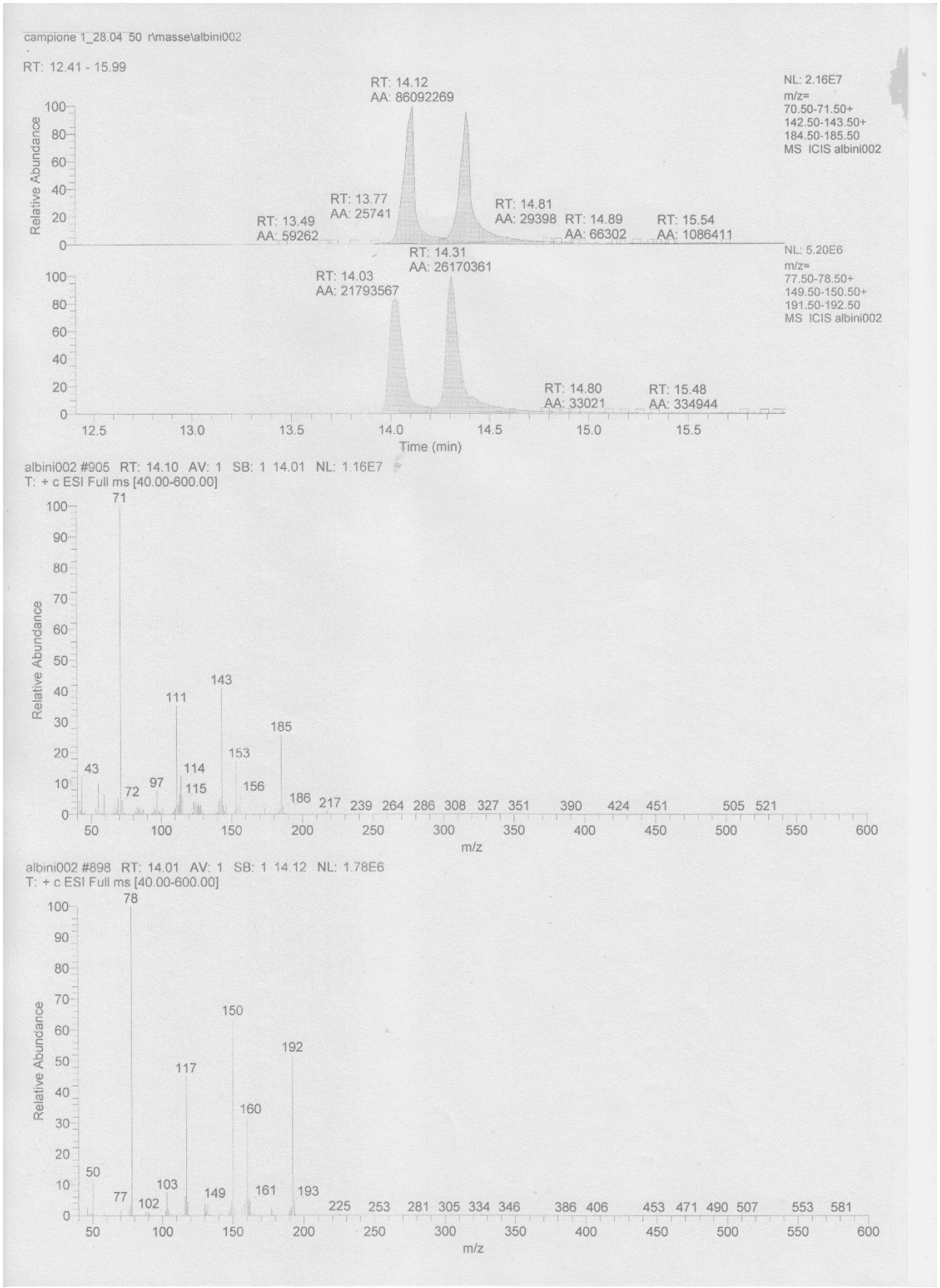

Figure 4.S.5 GC-MS spectrum of Experiment a) reported in Scheme 4.1.

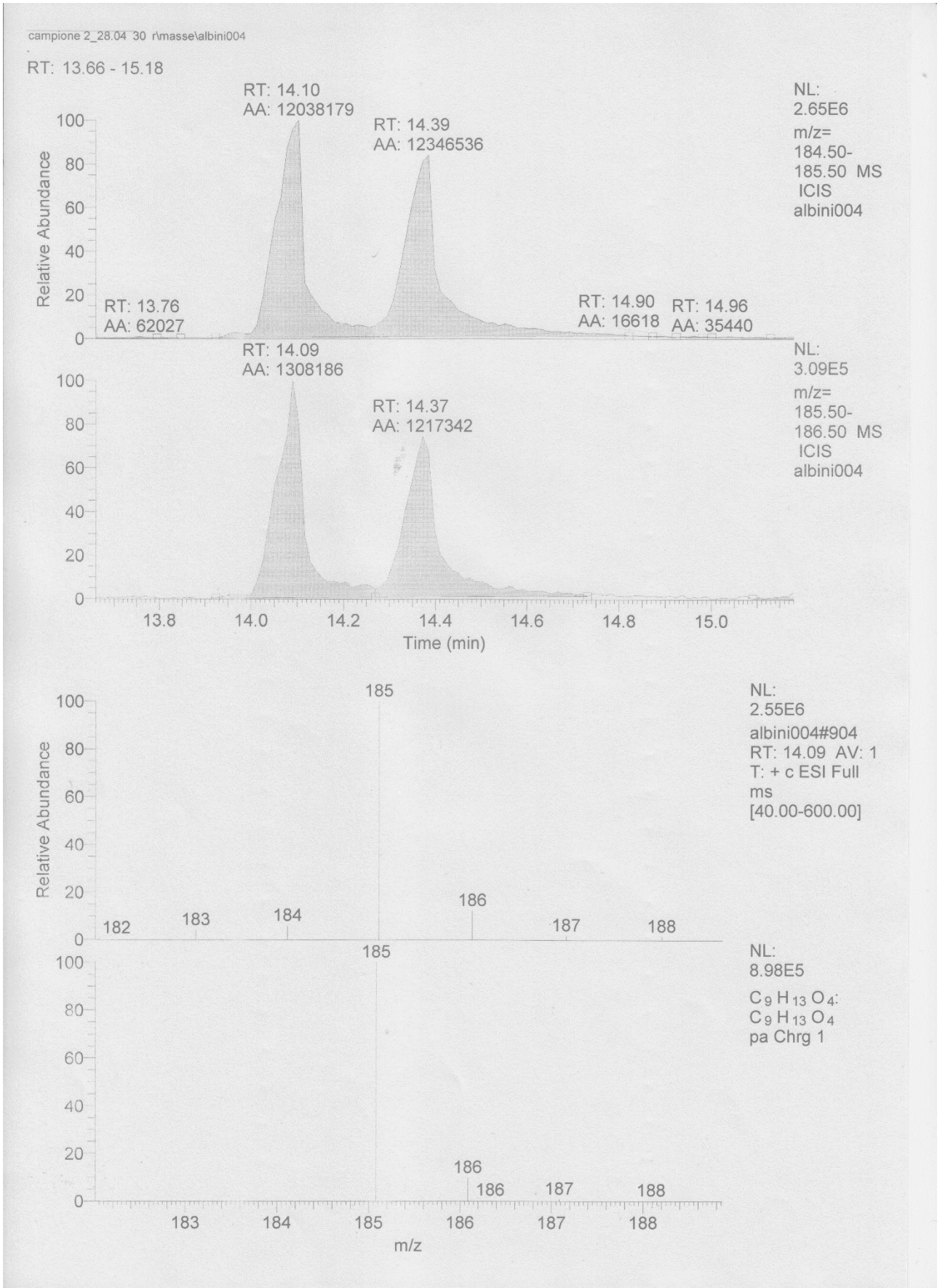

Figure 4.S.6 GC-MS spectrum of Experiment b) reported in Scheme 4.1.

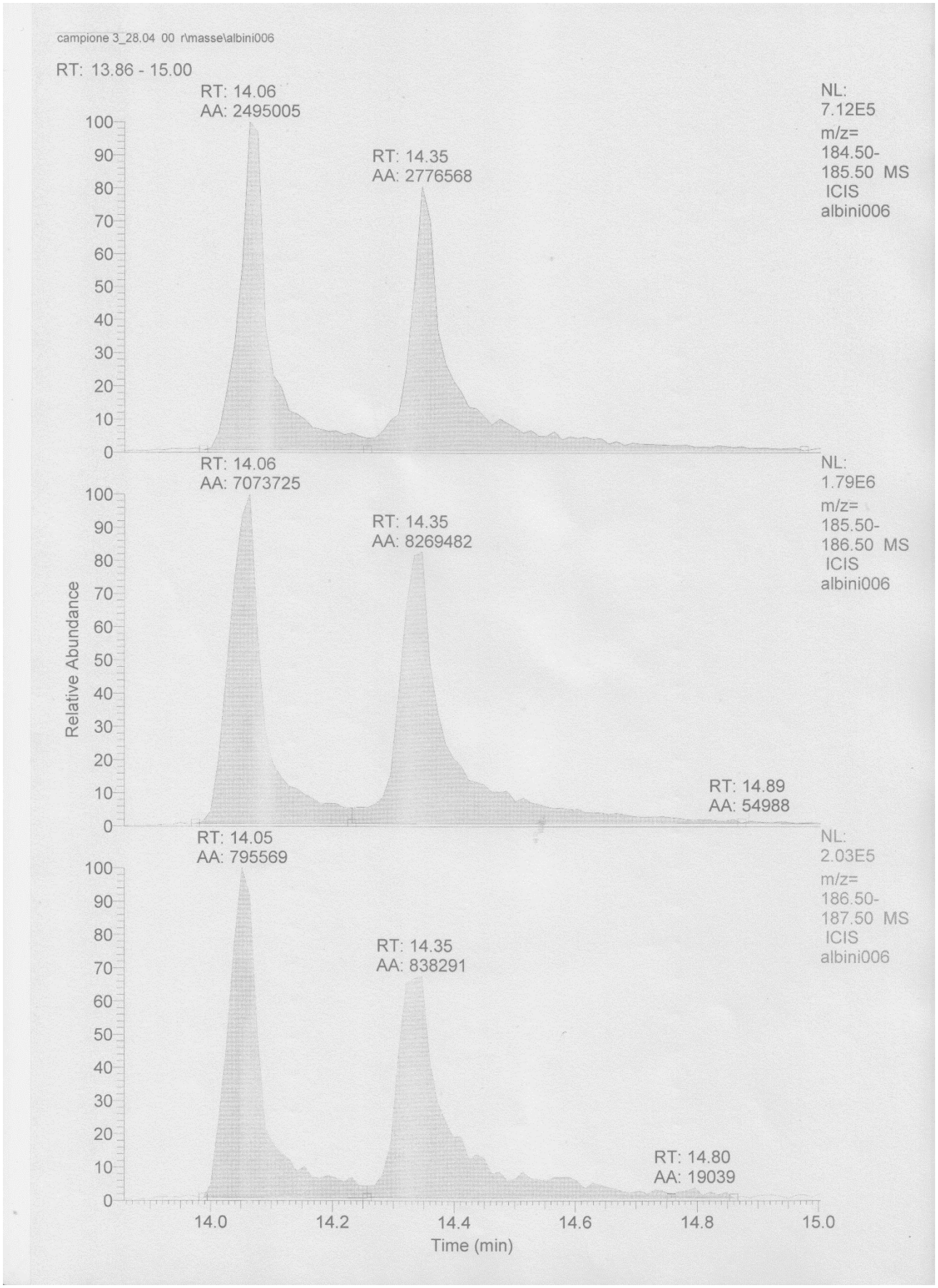

Figure 4.S.7 GC-MS spectrum of Experiment c) reported in Scheme 4.1.

References

(1) Yu, Y.-Q.; Wang, Z.-L. *J. Chi. Chem. Soc.* **2013**, *60* (3), 288–292.

(2) Goldberg, A. F. G.; O'Connor, N. R.; Craig II, R. A.; Stoltz, B. M. *Org. Lett.* **2012**, *14* (20), 5314-5317.

(3) Sturz, H.; Noller, C. *J. Am. Chem. Soc.* **2013**, *60* (3), 288-292.

(4) Hosseini-Sarvari, M.; Sharghi, H.; Etemad, S. *Chin, J. Chem.* **2007**, *25* (10), 1563-1567.

(5) Smith, Amos B., III; *Org. Lett.* **2008**, *10* (19), 4363-4365.

(6) Berryman, O. B. *Angew. Chem. Int. Ed.* **2011**, *50* (40), 9400-9403.

(7) Liu, J.-T. J.-Y.; Jang, Y.-J.; Lin, W.-W.; Liu, J.-T. J.-Y.; Yao, C.-F. *J. Org. Chem.* **2003**, *68* (10), 4030–4038.

(8) Ertl, M.; Wöβ, E.; Knör, G. *Photochem. Photobiol. Sci.* **2015**, *14* (10), 1826–1830.

EXPERIMENTAL SECTION RELATIVE TO

CHAPTER 5

VISIBLE LIGHT PROMOTED [2+2] CYCLOADDITIONS OF VINYL BORONATE ESTERS

Synthetic Procedures

Dichloromethane, tetrahydrofuran, diethyl ether, and acetonitrile were dried by elution through alumina as described by Grubbs.[1] 36 W H150 Blue from Kessil Lights was used for irradiations. Flash chromatography was performed with Sigma Aldrich 60 Å silica gel (230–400 mesh) and thin layer chromatography (TLC) was performed utilizing pre-coated silica gel F_{254} plates from SiliCycle Inc. containing a fluorescent indicator. Plates were visualized using either $KMnO_4$ or iodine/sand stain. ^{1}H and ^{13}C NMR data for all previously uncharacterized compounds were obtained using a Bruker Avance III 500 MHz spectrometer and are referenced to TMS (0.0 ppm) and $CDCl_3$ (77.16 ppm), respectively. ^{11}B data were obtained using a Bruker Avance III 400 MHz spectrometer. The following instruments in the Paul Bender Chemical Instrumentation Center at UW-Madison are supported by: Bruker Advance III 500 MHz by a generous gift from Paul J. and Margaret M. Bender; Bruker Advance III 400 MHz by NSF (CHE-1048642). Mass spectrometry was performed with Thermo Q Exactive Plus™ whose purchase was funded by NIH Award 1S10 OD020022-1 to the Department of Chemistry and Bruker Impact II™ whose purchase was funded by a generous gift from Paul J. and Margaret Bender. The photocatalyst $[Ir(dF(CF_3)ppy)_2(dtbbpy)](PF_6)$ utilized in this study was synthesized as previously reported.[2]

*Synthetic Procedure for the Synthesis of Ether-Tethered Alkynes (**5.12a-5.14a**, **5.20a**)*

A round-bottom flask was charged with NaH 60% w/w (1.5-2.0 equiv.) and purged with nitrogen, then a solution of the alcohol (1 equiv.) in 10 mL of THF was added dropwise and the suspension was stirred and cooled at 0°C with an ice bath. The solution was let stir at room temperature for 15 minutes. The solution was cooled again at 0°C and propargyl bromide (80% solution in toluene, 1.0-3.0 equiv.) was added dropwise over a period of 10 minutes. The solution was allowed to warm to room temperature and stirred for 24 h, before the addition of NH_4Cl (sat. aq. solution). The

solution was extracted with Ethyl acetate, dried over Na_2SO_4, and concentrated in vacuo to give the crude product that was further purified by flash column chromatography.

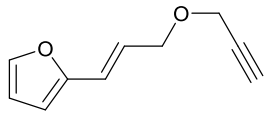

(E)-2-(3-(prop-2-yn-1-yloxy)prop-1-en-1-yl)furan (5.12a). From 573 mg of (E)-3-(furan-2-yl)prop-2-en-1-ol (4.6 mmol, 1.0 equiv.), 300 mg of NaH 60% w/w (7.5 mmol, 1.6 equiv.) and 1.4 mL of propargyl bromide (80% solution in toluene, 13.8 mmol, 3.0 equiv.). Purified via flash column chromatography (SiO_2, hexane/ethyl acetate 10:1). Yellow oil, 49%.

^{1}H NMR (500 MHz, $CDCl_3$) δ 7.35 (d, J = 1.7 Hz, 1H), 6.46 (d, J = 15.9 Hz, 1H), 6.37 (dd, J = 3.3, 1.8 Hz, 1H), 6.26 (d, J = 3.3 Hz, 1H), 6.20 (dt, J = 15.9, 6.1 Hz, 1H), 4.22 (dd, J = 6.1, 1.5 Hz, 2H), 4.19 (d, J = 2.3 Hz, 2H), 2.45 (t, J = 2.4 Hz, 1H).

^{13}C NMR (125.8 MHz, $CDCl_3$) δ 152.2, 142.1, 123.6, 121.4, 111.3, 108.3, 79.6, 74.5, 69.7, 57.0.

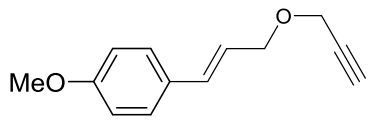

(E)-1-methoxy-4-(3-(prop-2-yn-1-yloxy)prop-1-en-1-yl)benzene (5.13a). From 1.91 g of (E)-3-(4-methoxyphenyl)prop-2-en-1-ol (11.6 mmol, 1.0 equiv.), 0.92 g of NaH 60% w/w (23.2 mmol, 2.0 equiv.) and 2.0 mL of propargyl bromide (80% solution in toluene, 17.4 mmol, 1.5 equiv.). Purified via flash column chromatography (SiO_2, hexane/Ethyl acetate 9:1). Yellow liquid, 91%. Spectroscopic data for **5.14a** are in accordance with those reported in the literature.[3]

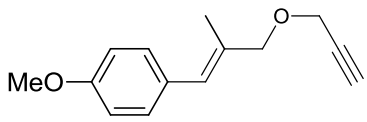

(E)-1-methoxy-4-(2-methyl-3-(prop-2-yn-1-yloxy)prop-1-en-1-yl)benzene (5.14a). From 377 mg of (E)-3-(4-methoxyphenyl)prop-2-en-1-ol (2.1 mmol, 1.0 equiv.), 127 mg of NaH 60% w/w (3.2 mmol, 1.5 equiv.) and 353 μL of propargyl bromide (80% solution in toluene, 3.2 mmol, 1.5 equiv.). Purified via flash column chromatography (SiO_2, hexane/Ethyl acetate 8:2). Yellowish oil, 67%.

^{1}H NMR (500 MHz, $CDCl_3$) δ 7.24 (d, J = 8.7 Hz, 2H), 6.88 (d, J = 8.7 Hz, 2H), 6.47 (s, 1H), 4.17 (d, J = 2.3 Hz, 2H), 4.11 (d, J = 1.2 Hz, 2H), 3.82 (s, 3H), 2.45 (t, J = 2.4 Hz, 1H), 1.91 (d, J = 1.3 Hz, 3H).

^{13}C NMR (125.8 MHz, $CDCl_3$) δ 158.4, 132.7, 130.3, 130.06, 127.9, 113.8, 80.0, 76.4, 74.5, 56.9, 55.4, 15.7.

*Synthetic Procedure for the Synthesis of **5.16a-5.19a**.*

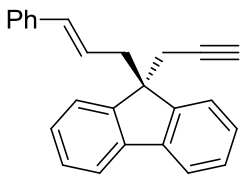

9-cinnamyl-9-(prop-2-yn-1-yl)-9H-fluorene (5.16a). In a 250 mL 3-necks round bottom flask 1.5 g of 9-cinnamyl-9H-fluorene (5.0 mmol, 1.0 equiv.) were dissolved in 100 mL of dry tetrahydrofuran under nitrogen atmosphere. The solution was cooled at -78°C and 2.6 mL of BuLi 2.5 M (6.4 mmol, 1.2 equiv.) were added slowly to afford a dark red solution. Solution was allowed to warm up at room temperature for 15 mins. Afterwards, 768 μL of propargyl bromide (80% solution in toluene, 6.9 mmol, 1.3 equiv.) were added dropwise. After 4 hours reaction was completed and was quenched with 20 mL of water at 0°C. Product was extracted with diethyl ether (3 x 50 mL), organic phases were collected, dried over $MgSO_4$ and solvent was removed under reduced pressure. Product was further purified via flash column chromatography (SiO_2, hexane/Ethyl acetate 99:1). Colorless oil, 94%.

^{1}H NMR (500 MHz, $CDCl_3$) δ 7.72 (dt, J = 7.6, 0.9 Hz, 2H), 7.65 – 7.61 (m, 2H), 7.37 (td, J = 7.5, 1.2 Hz, 2H), 7.32 (td, J = 7.5, 1.3 Hz, 2H), 7.21 (dd, J = 8.3, 6.4 Hz, 2H), 7.17 – 7.13 (m, 3H), 6.31 (d, J = 15.7 Hz, 1H), 5.89 – 5.77 (m, 1H), 2.98 (dd, J = 7.5, 1.4 Hz, 2H), 2.71 (d, J = 2.6 Hz, 2H), 2.07 (t, J = 2.6 Hz, 1H).

^{13}C NMR (125.8 MHz, $CDCl_3$) δ 149.0, 140.2, 137.4, 133.2, 128.4, 127.6, 127.1, 127.0, 126.1, 125.5, 123.8, 119.9, 81.4, 70.8, 52.2, 40.7, 28.7.

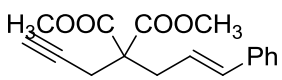

*dimethyl 2-cinnamyl-2-(prop-2-yn-1-yl)malonate (**5.17a**)*. A procedure reported in the literature was used.[4] Spectroscopic data for **5.17a** are in accordance with those reported in the literature.[4]

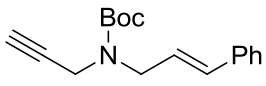

*tert-butyl cinnamyl(prop-2-yn-1-yl)carbamate (**5.18a**)*. A procedure reported in the literature was used.[5] Spectroscopic data for **5.18a** are in accordance with those reported in the literature.[5]

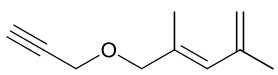

(E)-2,4-dimethyl-5-(prop-2-yn-1-yloxy)penta-1,3-diene (5.19a). From 0.5 g of (E)-2,4-dimethylpenta-2,4-dien-1-ol (4.4 mmol, 1.0 equiv.), 161 mg of NaH 60% w/w (6.7 mmol, 1.5 equiv.) and 746 μL of propargyl bromide (80% solution in toluene, 6.7 mmol, 1.5 equiv.). Purified via flash column chromatography (SiO_2, hexane/Ethyl acetate 9:1). Yellowish oil, 58%.

^{1}H NMR (500 MHz, $CDCl_3$) δ 6.01 – 5.82 (m, 1H), 5.01 (t, J = 1.8 Hz, 1H), 4.93 – 4.80 (m, 1H), 4.13 (d, J = 2.3 Hz, 2H), 3.99 (d, J = 1.1 Hz, 2H), 2.43 (t, J = 2.4 Hz, 1H), 1.87 (s, 3H), 1.84 (d, J = 1.3 Hz, 3H).

^{13}C NMR (125.8 MHz, $CDCl_3$) δ 141.5, 133.0, 130.1, 115.7, 80.0, 76.3, 74.4, 56.9, 23.6, 15.7.

*Compounds **5.15a** and **5.20a** were synthesized by Dr. Spencer O. Scholz.*

*Synthesis of vinyl boronate esters **5.12b-5.20b**.*

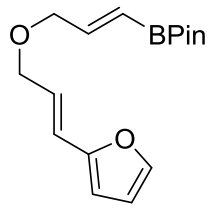

2-((E)-3-(((E)-3-(furan-2-yl)allyl)oxy)prop-1-en-1-yl)-4,4,5,5-tetramethyl-1,3,2-dioxaborolane (5.12b). Synthesized according to the general procedure using 195 mg (E)-2-(3-(prop-2-yn-1-yloxy)prop-1-en-1-yl)furan (**5.12a**) (1.20 mmol, 1.00 equiv.), 0.261 mL 4,4,5,5-tetramethyl-1,3,2-dioxaborolane (2.16 mmol, 1.8 equiv.) and 16 mg bis(cyclopentadienyl)zirconium chloride hydride (0.060 mmol, 0.05 equiv.). Purified using boric acid-doped silica gel and a gradient 94:6 hex/Ethyl acetate to yield 268mg (77% yield) of the desired product as a yellowish oil.

^{1}H NMR: (500.2 MHz, $CDCl_3$) δ 7.31 (d, J = 1.7 Hz, 1H), 6.64 (dt, J = 18.1, 4.6 Hz, 1H), 6.45 – 6.39 (m, 1H), 6.33 (dd, J = 3.3, 1.8 Hz, 1H), 6.23 – 6.14 (m, 2H), 5.72 (dt, J = 18.1, 1.8 Hz, 1H), 4.10 (dd, J = 5.8, 1.6 Hz, 2H), 4.08 (dd, J = 4.7, 1.9 Hz, 2H), 1.24 (s, 12H);

^{13}C NMR: (125.8 MHz, $CDCl_3$) δ 152.5, 149.2, 142.0, 124.7, 120.3, 111.3, 107.9, 83.3, 71.7, 70.4, 24.8. The signal for the carbon attached to boron was not observed due to quadrupolar relaxation of the boron nucleus.

^{11}B NMR (128.4 MHz, $CDCl_3$) δ 29.4.

HRMS (ESI) calculated for $[C_{23}H_{31}BO_6+NH_4]^+$ requires 431.2588 m/z, found 431.2590 m/z.

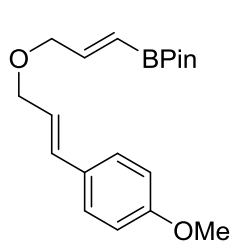

2-((E)-3-(((E)-3-(4-Methoxyphenyl)allyl)oxy)prop-1-en-1-yl)-4,4,5,5-tetramethyl-1,3,2-dioxaborolane (5.13b). Synthesized according to the general procedure using 0.746 g (E)-1-methoxy-4-(3-(prop-2-yn-1-yloxy)prop-1-en-1-yl)benzene (**5.13a**) (3.58 mmol, 1.00 equiv.), 0.571 mL 4,4,5,5-tetramethyl-1,3,2-dioxaborolane (3.94 mmol, 1.1 equiv.) and 63.2 mg bis(cyclopentadienyl)zirconium chloride hydride (0.179 mmol, 0.05 equiv.). Purified using boric acid-doped silica gel and a gradient 94:6 hex/Ethyl acetate to yield 851 mg (70% yield) of the desired product as a yellowish oil.

^{1}H NMR: (500.2 MHz, $CDCl_3$) δ 7.32 (d, J = 8.7 Hz, 2H), 6.85 (d, J = 8.7 Hz, 2H), 6.67 (dt, J = 18.2, 4.7 Hz, 1H), 6.55 (dd, J = 15.9, 1.5 Hz, 1H), 6.15 (dt, J = 15.9, 6.1 Hz, 1H) 5.74 (dt, J = 18.2, 1.8 Hz, 1H), 4.14 (dd, J = 6.1, 1.5 Hz, 2H), 4.11 (dd, J = 4.8, 1.8 Hz, 2H), 3.81 (s, 3H), 1.27 (s, 12H).

^{13}C NMR: (125.8 MHz, $CDCl_3$) δ 159.4, 149.4, 132.2, 129.7, 127.8, 123.9, 114.1, 83.4, 71.7, 71.2, 55.4, 24.9. The signal for the carbon attached to boron was not observed due to quadrupolar relaxation of the boron nucleus.

^{11}B NMR (128.4 MHz, $CDCl_3$) δ 29.9.

HRMS (ESI) calculated for $[C_{19}H_{27}BO_4+NH_4]^+$ requires 347.2377 m/z, found 347.2371 m/z.

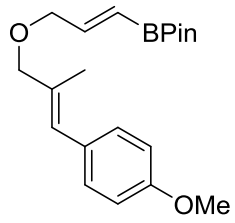

2-((E)-3-(((E)-3-(4-methoxyphenyl)-2-methylallyl)oxy)prop-1-en-1-yl)-4,4,5,5-tetramethyl-1,3,2-dioxaborolane (5.14b). Synthesized according to the general procedure using 285 mg (E)-1-methoxy-4-(2-methyl-3-(prop-2-yn-1-yloxy)prop-1-en-1-yl)benzene (**5.14a**) (1.41 mmol, 1.00 equiv.), 0.241 mL 4,4,5,5-tetramethyl-1,3,2-dioxaborolane (1.69 mmol, 1.2 equiv.) and 18 mg bis(cyclopentadienyl)zirconium chloride hydride (0.07 mmol, 0.05 equiv.). Purified using boric acid-doped silica gel and a gradient 85:15 hex/Ethyl acetate to yield 318 mg (100% yield) of the desired product as a yellowish oil.

^{1}H NMR: (500.2 MHz, $CDCl_3$) δ 7.22 (d, J = 8.7 Hz, 2H), 6.87 (d, J = 8.7 Hz, 2H), 6.68 (dt, J = 18.1, 4.7 Hz, 1H), 6.44 (s, 1H), 5.75 (dt, J = 18.2, 1.8 Hz, 1H), 4.08 (dd, J = 4.7, 1.8 Hz, 2H), 4.02 (d, J = 1.2 Hz, 2H), 3.81 (s, 3H), 1.88 (d, J = 1.3 Hz, 3H), 1.27 (s, 12H).

^{13}C NMR: (125.8 MHz, $CDCl_3$) δ 158.2, 149.5, 133.6, 130.3, 130.2, 126.6, 113.6, 83.4, 76.8, 71.4, 55.4, 24.9, 15.6. The signal for the carbon attached to boron was not observed due to quadrupolar relaxation of the boron nucleus.

^{11}B NMR (128.4 MHz, $CDCl_3$) δ 29.8.

HRMS (ESI) calculated for $[C_{20}H_{29}BO_4+Na]^+$ requires 366.2087 m/z, found 366.2086 m/z.

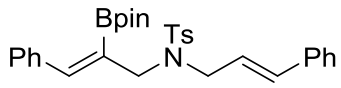

N-cinnamyl-4-methyl-N-((E)-3-phenyl-2-(4,4,5,5-tetramethyl-1,3,2-dioxaborolan-2-yl)allyl)benzenesulfonamide (5.15b). Synthesized adopting a procedure reported in the literature.[6] A flame-dried 10 mL round-bottom flask was charged with 240 mg of N-cinnamyl-4-methyl-N-(3-phenylprop-2-yn-1-yl)benzenesulfonamide (**5.15a**) (1 equiv., 0.6 mmol), 6 mg of CuCl (0.1 equiv., 0.06 mmol), 167 mg of bis(pinacolato)diboron (1.1 equiv., 0.66 mmol) and 8.6 mg of NaOtBu (0.15 equiv., 0.9 mmol). The flask was sealed and purged with nitrogen for 5 minutes. A degassed solution of 24.2 mg of tri-*tert*-butylphosphine (0.12 equiv., 0.072 mmol) in dry toluene (1.6 mL) was added to the reaction vessel. Finally, 48.5 μL of MeOH were added and the mixture was stirred at rt for 2 hours. The reaction is quenched with MeOH, filtered through a silica plug washed with DCM. The crude was purified through column chromatography using hexane/Ethyl acetate 8:2 as the eluent mixture to get 301 mg (95%) of a white solid.

^{1}H NMR (500.2 MHz, $CDCl_3$) δ 7.62 (d, J = 8.2 Hz, 2H), 7.39 (s, 1H), 7.31 – 7.15 (m, 10H), 7.08 – 7.01 (m, 2H), 6.18 (d, J = 15.8 Hz, 1H), 5.81 (dt, J = 15.9, 6.8 Hz, 1H), 4.13 (d, J = 1.5 Hz, 2H), 3.85 (dd, J = 6.8, 1.4 Hz, 2H), 2.36 (s, 3H), 1.28 (s, 12H).

^{13}C NMR (125.8 MHz, $CDCl_3$) δ 145.2, 143.0, 137.0, 136.8, 136.6, 133.6, 129.5, 129.4, 128.4, 128.3, 127.8, 127.6, 126.5, 124.4, 83.9, 50.1, 45.6, 24.9, 21.6.

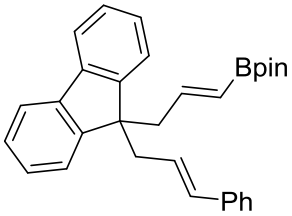

2-((E)-3-(9-cinnamyl-9H-fluoren-9-yl)prop-1-en-1-yl)-4,4,5,5-tetramethyl-1,3,2-dioxaborolane (5.16b). Prepared according to the general procedure using 1.00 g 9-cinnamyl-9-(prop-2-yn-1-yl)-9H-fluorene (**5.16a**) (3.10 mmol, 1.00 equiv.), 0.540 mL 4,4,5,5-tetramethyl-1,3,2-dioxaborolane (3.72 mmol, 1.2 equiv.) and 40 mg bis(cyclopentadienyl)zirconium chloride hydride (0.155 mmol). Purified by recrystallization in 94:6 hex/Ethyl acetate to yield 819 mg (56% yield) of the desired product as a white solid.

^{1}H NMR: (500.2 MHz, $CDCl_3$) δ 7.70 – 7.67 (m, 1H), 7.43 – 7.40 (m, 2H), 7.35 – 7.24 (m, 4H), 7.21 – 7.15 (m, 2H), 7.14 – 7.10 (m, 1H), 7.10 – 7.06 (m, 2H), 6.31 (dt, J = 17.7, 7.1 Hz, 1H), 6.19 (d, J = 15.7 Hz, 1H), 5.73 (dt, J = 15.3, 7.4 Hz, 1H), 5.36 (d, J = 17.8 Hz, 1H), 2.85 – 2.76 (m, 4H), 1.19 (s, 12H).

^{13}C NMR: (125.8 MHz, $CDCl_3$) δ 149.4, 140.6, 137.7, 132.9, 128.4, 127.3, 127.1, 127.0, 126.1, 125.9, 124.0, 120.0, 83.1, 54.3, 45.6, 42.6, 24.8. The signal for the carbon attached to boron was not observed due to quadrupolar relaxation of the boron nucleus.

^{11}B NMR (128.4 MHz, $CDCl_3$) δ 29.4.

HRMS (ESI) calculated for $[C_{31}H_{33}BO_2 + NH_4]^+$ requires 466.2912 *m/z*, found 466.2919 *m/z*.

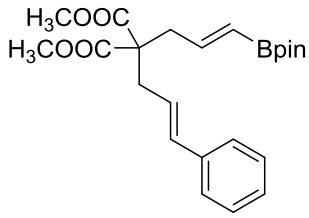

dimethyl 2-cinnamyl-2-((E)-3-(4,4,5,5-tetramethyl-1,3,2-dioxaborolan-2-yl)allyl)malonatedioxaborolane (5.17b). Synthesized according to the general procedure using 1.00 g dimethyl 2-cinnamyl-2-(prop-2-yn-1-yl)malonate (**5.17a**) (3.50 mmol, 1.00 equiv.), 1.12 mL 4,4,5,5-tetramethyl-1,3,2-dioxaborolane (7.7 mmol, 2.2 equiv.) and 45 mg bis(cyclopentadienyl)zirconium chloride hydride (0.175 mmol, 0.05 equiv.). Purified using boric acid-doped silica gel and a gradient 80:20 hexane/Ethyl acetate to yield 1.1 g (76% yield) of the desired product as a thick oil.

^{1}H NMR: (500.2 MHz, $CDCl_3$) δ 7.33 – 7.18 (m, 5H), 6.49 – 6.38 (m, 2H), 6.03 (dt, J = 15.4, 7.6 Hz, 1H), 5.55 (dt, J = 17.6, 1.3 Hz, 1H), 3.72 (s, 6H), 2.80 (m, 4H), 1.26 (s, 12H).

^{13}C NMR: (125.8 MHz, $CDCl_3$) δ 171.2, 147.0, 137.2, 134.3, 128.6, 127.5, 126.4, 123.9, 83.4, 58.0, 52.7, 39.4, 36.5, 24.9. The signal for the carbon attached to boron was not observed due to quadrupolar relaxation of the boron nucleus.

^{11}B NMR (128.4 MHz, $CDCl_3$) δ 29.9.

HRMS (ESI) calculated for $[C_{23}H_{31}BO_6+NH_4]^+$ requires 431.2588 m/z, found 431.2590 m/z.

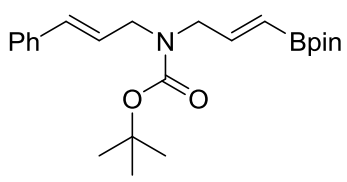

tert-butyl cinnamyl((E)-3-(4,4,5,5-tetramethyl-1,3,2-dioxaborolan-2-yl)allyl)carbamate (5.18b). Synthesized according to the general procedure using 543 mg dimethyl 2-cinnamyl-2-(prop-2-yn-1-yl)malonate (**5.18a**) (2.00 mmol, 1.00 equiv.), 290 μL 4,4,5,5-tetramethyl-1,3,2-dioxaborolane (2.0 mmol, 1.0 equiv.) and 26 mg bis(cyclopentadienyl)zirconium chloride hydride (0.1 mmol, 0.05 equiv.). Purified using boric acid-doped silica gel and a gradient 90:10 hexane/Ethyl acetate to yield 535 mg (67% yield) of the desired product as a very thick oil.

^{1}H NMR (400 MHz, DMSO at 80°C) δ 7.38 (d, J = 6.9 Hz, 2H), 7.32 (t, J = 7.5 Hz, 2H), 7.27 – 7.20 (m, 1H), 6.48 (d, J = 16.4 Hz, 1H), 6.43 (dt, J = 5.1 Hz, 1H), 6.17 (dt, J = 15.9, 6.1 Hz, 1H), 5.43 (d, J = 18 Hz, 1H), 3.93 (d, J = 6.2 Hz, 2H), 3.91 – 3.88 (m, 2H), 1.42 (s, 6H), 1.21 (s, 9H).

^{13}C NMR (101 MHz, DMSO at 80°C) δ 155.1, 149.3, 137.1, 132.0, 128.9, 127.9, 126.6, 126.3, 83.4, 79.4, 50.6, 49.2, 28.6, 25.0.

^{11}B NMR (128.4 MHz, $CDCl_3$) δ 29.9.

HRMS (ESI) calculated for $[C_{23}H_{34}BNO_4+H]^+$ requires 399.2690 m/z, found 399.2686 m/z

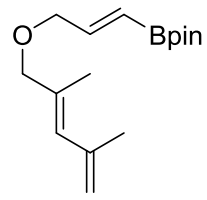

4,4,5,5-tetramethyl-2-((E)-3-(((E)-4-methylpenta-2,4-dien-1-yl)oxy)prop-1-en-1-yl)-1,3,2-dioxaborolane (5.19b). Prepared according to the general procedure using 0.300 g (E)-2-methyl-5-(prop-2-yn-1-yloxy)penta-1,3-diene (**5.19a**) (2.00 mmol, 1.00 equiv.), 0.290 mL 4,4,5,5-tetramethyl-1,3,2-dioxaborolane (2.00 mmol, 1.0 equiv.) and 26 mg bis(cyclopentadienyl)zirconium chloride hydride (0.100 mmol). Purified using boric acid-doped silica gel and a gradient of 96:4 hexane/Ethyl acetate to yield 254 mg (46% yield) of the desired product as a colorless oil.

^{1}H NMR: (500.2 MHz, $CDCl_3$) δ 6.66 (dt, J = 18.1, 4.6 Hz, 1H), 5.90 (s, 1H), 5.72 (dt, J = 18.2, 1.8 Hz, 1H), 5.04 – 4.94 (m, 1H), 4.86 – 4.81 (m, 1H), 4.04 (dd, J = 4.6, 1.8 Hz, 2H), 3.91 (s, 2H), 1.86 (s, 3H), 1.84 – 1.80 (m, 3H), 1.27 (s, 12H). ^{13}C NMR: (125.8 MHz, $CDCl_3$) δ 149.3, 141.4, 133.7, 128.8, 115.2, 83.2, 76.6, 71.3, 24.8, 23.5, 15.5. The signal for the carbon attached to boron was not observed due to quadrupolar relaxation of the boron nucleus.

^{11}B NMR (128.4 MHz, $CDCl_3$) δ 29.9.

HRMS (ESI) calculated for $[C_{16}H_{27}BO_3+H]^+$ requires 279.2126 *m/z*, found 279.2125 *m/z*.

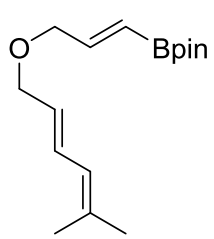

4,4,5,5-tetramethyl-2-((E)-3-(((E)-5-methylhexa-2,4-dien-1-yl)oxy)prop-1-en-1-yl)-1,3,2-dioxaborolane (5.20b). Prepared according to the general procedure using 0.300 g (E)-5-methyl-1-(prop-2-yn-1-yloxy)hexa-2,4-diene (previously synthesized in our lab by Rowen Littlefield) (2.00 mmol, 1.00 equiv.), 0.316 mL 4,4,5,5-tetramethyl-1,3,2-dioxaborolane (2.60 mmol, 1.2 equiv.) and 26 mg bis(cyclopentadienyl)zirconium chloride hydride (0.100 mmol). Purified using boric acid-doped silica gel and a gradient of 94:6 hexane/Ethyl acetate to yield 260 mg (47% yield) of the desired product as a clear oil.

^{1}H NMR: (500.2 MHz, $CDCl_3$) δ 6.65 (dt, *J* = 18.1, 4.7 Hz, 1H), 6.44 (ddt, *J* = 15.1, 11.1 1.4, 1H), 5.83 (d, *J* = 10.8, 1H), 5.70 (dt, *J* = 18.2, 1.8 Hz, 1H), 5.62 (dt, *J* = 15.1, 6.3 Hz, 1H), 4.06 (dd, *J* = 4.7, 1.8 Hz, 2H), 4.03 (d, *J* = 6.3 Hz, 2H), 1.78 (s, 3H), 1.76 (s, 3H), 1.27 (s, 12H).

^{13}C NMR: (125.8 MHz, $CDCl_3$) δ 149.5, 136.2, 129.8, 126.5, 124.5, 83.4, 71.6, 71.2, 26.1, 24.9, 18.5. The signal for the carbon attached to boron was not observed due to quadrupolar relaxation of the boron nucleus.

^{11}B NMR (128.4 MHz, $CDCl_3$) δ 29.9.

HRMS (ESI) calculated for $[C_{16}H_{27}BO_3+Na]^+$ requires 300.1982 *m/z*, found 300.1978 *m/z*.

*Synthesis of cycloadducts **5.13c-5.20c**.*

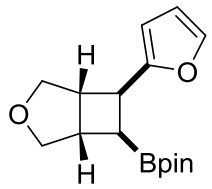

2-((1S,5S,6S,7S)-7-(furan-2-yl)-3-oxabicyclo[3.2.0]heptan-6-yl)-4,4,5,5-tetramethyl-1,3,2-dioxaborolane (5.12c). Synthesized according to the general procedure using 87 mg 2-((E)-3-(((E)-3-(furan-2-yl)allyl)oxy)prop-1-en-1-yl)-4,4,5,5-tetramethyl-1,3,2-dioxaborolane **5.12b** (0.3 mmol, 1.00 equiv.), 3.3 mg $Ir(df(CF_3ppy)_2dtbbpy)PF_6$ and 6 mL CH_3CN (0.05 M) yielding 77 mg (89% yield) of the desired product in 4:1:1 d.r.

^1H NMR (500.2 MHz, $CDCl_3$) δ 7.33 (d, J = 1.7 Hz, 1H), 6.29 (dd, J = 3.2, 1.8 Hz, 1H), 6.03 (d, J = 3.1 Hz, 1H), 4.19 (d, J = 9.5 Hz, 1H), 3.97 (d, J = 9.4 Hz, 1H), 3.45 (dd, J = 9.4, 5.2 Hz, 1H), 3.41 (dd, J = 9.6, 5.3 Hz, 1H), 3.29 (dd, J = 8.2, 5.0 Hz, 1H), 3.16 – 3.09 (m, 1H), 3.09 – 3.04 (m, 1H), 2.22 (dd, J = 9.9, 8.2 Hz, 1H), 1.26 (d, J = 3.2 Hz, 12H).

^{13}C NMR (125.8 MHz, $CDCl_3$) δ 159.3, 141.2, 110.2, 110.1, 103.9, 83.6, 73.5, 71.92, 45.2, 37.7, 37.0, 25.1.

^{11}B NMR (128.4 MHz, $CDCl_3$) δ 33.5.

HRMS (ESI) calculated for $[C_{16}H_{23}BO_4+H]^+$ requires 291.1762 m/z, found 291.1761 m/z.

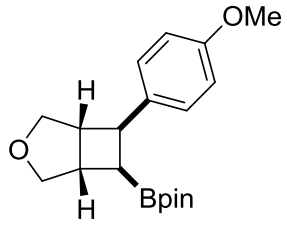

2-((1R,5S,6R,7S)-7-(4-methoxyphenyl)-3-oxabicyclo[3.2.0]heptan-6-yl)-4,4,5,5-tetramethyl-1,3,2-dioxaborolane (5.13c). Synthesized according to the general procedure using 100 mg 2-((E)-3-(((E)-3-(4-Methoxyphenyl)allyl)oxy)prop-1-en-1-yl)-4,4,5,5-tetramethyl-1,3,2-dioxaborolane **5.13b** (0.3 mmol, 1.00 equiv.), 3.3 mg $Ir(df(CF_3ppy)_2dtbbpy)PF_6$ and 6 mL CH_3CN (0.05 M) yielding 80 mg (80% yield) of the desired product in 4:1:1 d.r. after flash column chromatography on boric acid-doped silica gel in hexanes:Ethyl acetate 95:5.

^1H NMR: (500.2 MHz, $CDCl_3$) δ 7.24 (d, J = 8.6 Hz, 2H), 6.83 (d, J = 8.6 Hz, 2H), 3.95 (d, J = 9.3 Hz, 1H), 3.91 (d, J = 9.2 Hz, 1H), 3.61 (dd, J = 9.2, 5.5 Hz, 1H), 3.55 (dd, J = 9.3, 5.3 Hz, 1H), 3.40 (dd, J = 11.2, 5.3 Hz, 1H), 3.19 (m, 1H), 3.08 (m, 1H), 2.08 (dd, J = 11.3, 5.6 Hz, 1H), 1.02 (s, 6H), 0.89 (s, 6H).

^{13}C NMR (125.8 MHz, $CDCl_3$) δ 158.1, 137.0, 128.6, 113.7, 83.2, 75.2, 74.3, 55.6, 44.8, 42.8, 36.8, 25.2, 24.8. The signal for the carbon attached to boron was not observed due to quadrupolar relaxation of the boron nucleus.

^{11}B NMR (128.4 MHz, $CDCl_3$) δ 32.9.

HRMS (ESI) calculated for $[C_{19}H_{27}BO_4+H]^+$ requires 330.2111 *m/z*, found 330.2106 *m/z*.

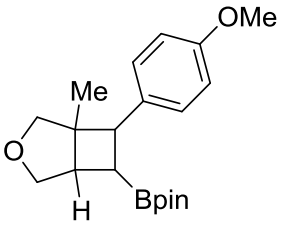

2-(7-(4-methoxyphenyl)-1-methyl-3-oxabicyclo[3.2.0]heptan-6-yl)-4,4,5,5-tetramethyl-1,3,2-dioxaborolane (5.14c). Synthesized according to the general procedure using 103 mg 2-((E)-3-(((E)-3-(4-methoxyphenyl)-2-methylallyl)oxy)prop-1-en-1-yl)-4,4,5,5-tetramethyl-1,3,2-dioxaborolane **5.14b** (0.3 mmol, 1.00 equiv.), 3.3 mg Ir(df(CF_3ppy)$_2$dtbbpy)PF_6 and 6 mL CH_3CN (0.05 M) yielding 83 mg (81% yield) of the desired product in 3:1.3:1 d.r. In order to isolate the major and the prevalent minor diastereomer, the mixture was oxidized[7] to afford the correspondent alcohol mixture and purified via a preparative TLC (hexanes/Ethyl acetate 6:4).

Major: ^{1}H NMR: (500.2 MHz, $CDCl_3$) δ 7.13 (d, J = 8.6 Hz, 2H), 6.88 (d, J = 8.7 Hz, 2H), 4.31 (q, J = 5.0 Hz, 1H), 4.02 (d, J = 9.2 Hz, 1H), 3.80 (s, 3H), 3.60 (d, J = 9.8 Hz, 1H), 3.57 (dd, J = 9.3, 4.2 Hz, 1H), 3.17 (d, J = 7.1 Hz, 1H), 2.98 (d, J = 9.7 Hz, 1H), 2.42 (t, J = 4.3 Hz, 1H), 1.93 – 1.87 (m, 1H), 1.41 (s, 3H).

^{13}C NMR (125.8 MHz, $CDCl_3$) δ 158.4, 130.6, 128.8, 113.9, 73.5, 71.7, 71.5, 57.1, 55.3, 53.3, 44.1, 29.7. The signal for the carbon attached to boron was not observed due to quadrupolar relaxation of the boron nucleus.

^{11}B NMR (128.4 MHz, $CDCl_3$) δ 33.8.

HRMS (ESI) calculated for $[C_{16}H_{27}BO_3+H]^+$ requires 278.2162 *m/z*, found 278.2163 *m/z*. Characterization to be completed (NOE experiment).

Prevalent minor: ^{1}H NMR: (500.2 MHz, $CDCl_3$) δ 7.13 (d, J = 8.6 Hz, 2H), 6.88 (d, J = 8.7 Hz, 2H), 4.31 (q, J = 5.0 Hz, 1H), 4.02 (d, J = 9.2 Hz, 1H), 3.80 (s, 3H), 3.60 (d, J = 9.8 Hz, 1H), 3.57

(dd, J = 9.3, 4.2 Hz, 1H), 3.17 (d, J = 7.1 Hz, 1H), 2.98 (d, J = 9.7 Hz, 1H), 2.42 (t, J = 4.3 Hz, 1H), 1.93 – 1.87 (m, 1H), 1.41 (s, 3H).

^{13}C NMR (125.8 MHz, $CDCl_3$) δ 158.5, 130.8, 129.0, 114.1, 73.6, 71.8, 71.7, 57.3, 55.4, 53.5, 44.3, 29.9.

^{11}B NMR (128.4 MHz, $CDCl_3$) δ 33.5.

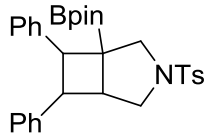

6,7-diphenyl-1-(4,4,5,5-tetramethyl-1,3,2-dioxaborolan-2-yl)-3-tosyl-3-azabicyclo[3.2.0]heptane (5.15c). Synthesized according to the general procedure using 159 mg N-cinnamyl-4-methyl-N-((Z)-3-phenyl-2-(4,4,5,5-tetramethyl-1,3,2-dioxaborolan-2-yl)allyl)benzenesulfonamide (**5.15b**) (0.3 mmol, 1.00 equiv.), 3.3 mg Ir(df(CF_3ppy)$_2$dtbbpy)PF_6 and 6 mL CH_3CN (0.05 M) yielding 146 mg (92% yield) of the desired product in 2:1.4:1 d.r.

^{1}H NMR (500.2 MHz, $CDCl_3$) δ 7.77 (d, J = 8.3 Hz, 2H), 7.34 (d, J = 8.0 Hz, 2H), 7.10 (t, J = 7.6 Hz, 2H), 7.07 – 6.93 (m, 4H), 6.93 – 6.87 (m, 4H), 4.13 (dd, J = 10.1, 7.5 Hz, 1H), 3.84 (d, J = 10.7 Hz, 1H), 3.80 (d, J = 10.2 Hz, 1H), 3.63 (d, J = 9.6 Hz, 1H), 3.57 (dd, J = 7.4, 5.4 Hz, 1H), 2.98 (d, J = 10.6 Hz, 1H), 2.93 (dd, J = 9.6, 5.4 Hz, 1H), 2.43 (s, 3H), 0.97 (s, 6H), 0.78 (s, 6H).

^{13}C NMR (125.8 MHz, $CDCl_3$) δ 143.5, 140.4, 140.0, 132.6, 129.5, 129.3, 128.0, 127.7, 127.5, 127.5, 125.9, 125.4, 83.5, 57.0, 54.7, 51.4, 44.8, 42.6, 24.6, 24.4, 21.5.

^{11}B NMR (128.4 MHz, $CDCl_3$) δ 32.7.

HRMS (ESI) calculated for $[C_{31}H_{36}BNO_4S+Na]^+$ requires 551.2387 m/z, found 551.2388 m/z. Characterization to be completed (NOE experiment).

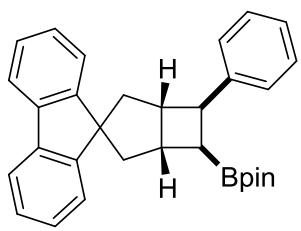

4,4,5,5-tetramethyl-2-((1S,5S,6S,7S)-6-phenylspiro[bicyclo[3.2.0]heptane-3,9'-fluoren]-7-yl)-1,3,2-dioxaborolane (5.16c). Synthesized according to the general procedure using 134 mg 4,4,5,5-tetramethyl-2-((E)-3-(((E)-5-methylhexa-2,4-dien-1-yl)oxy)prop-1-en-1-yl)-1,3,2-dioxaborolane **5.16b** (0.3 mmol, 1.00 equiv.), 3.3 mg Ir(df(CF_3ppy)$_2$dtbbpy)PF_6 and 6 mL CH_3CN (0.05 M) yielding 129 mg (97% yield) of the desired product in 4:2:1 d.r. In order to isolate the

major diastereomer, the mixture was oxidized to afford the correspondent alcohol mixture[7] and purified via flash chromatography on silica gel, using hexanes:MTBE 80:20 as the eluent mixture. ^{1}H NMR: (500.2 MHz, $CDCl_3$) δ 7.75 – 7.70 (m, 2H), 7.64 – 7.53 (m, 1H), 7.47 – 7.39 (m, 4H), 7.39 – 7.27 (m, 6H), 4.58 (td, J = 6.7, 3.4 Hz, 1H), 3.75 (dd, J = 7.0, 5.2 Hz, 1H), 3.52 (qd, J = 8.3, 4.8 Hz, 1H), 3.29 – 3.17 (m, 1H), 2.49 (dd, J = 13.8, 7.2 Hz, 1H), 2.38 (dd, J = 13.6, 7.6 Hz, 1H), 2.32 – 2.24 (m, 2H).

^{13}C NMR (125.8 MHz, $CDCl_3$) δ 153.9, 149.9, 140.3, 139.0, 138.5, 129.0, 128.9, 127.6, 127.6, 127.4, 127.1, 127.1, 123.1, 122.8, 120.0, 119.9, 74.6, 63.7, 51.3, 50.0, 46.9, 44.3, 41.6. The signal for the carbon attached to boron was not observed due to quadrupolar relaxation of the boron nucleus.

HRMS (ESI) calculated for $[C_{31}H_{33}BO_2+NH_4]^+$ requires 466.2912 *m/z*, found 466.2918 *m/z*.

HRMS (ESI) calculated for $[C_{25}H_{25}O+Na]^+$ requires 339.1743 *m/z*, found 339.1742 *m/z*.

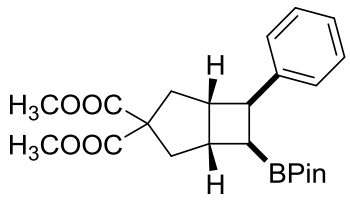

(1S,5S,6S,7S)-dimethyl 6-phenyl-7-(4,4,5,5-tetramethyl-1,3,2-dioxaborolan-2-yl)bicyclo[3.2.0]heptane-3,3-dicarboxylate (5.17c). Synthesized according to the general procedure using 128 mg dimethyl 2-cinnamyl-2-((E)-3-(4,4,5,5-tetramethyl-1,3,2-dioxaborolan-2-yl)allyl)malonatedioxaborolane **5.17b** (0.3 mmol, 1.00 equiv.), 3.3 mg $Ir(df(CF_3ppy)_2dtbbpy)PF_6$ and 6 mL CH_3CN (0.05 M) yielding 102 mg (80% yield) of the desired product in 4:1.4:1 d.r.. In order to isolate the major diastereomer, the mixture was oxidized to afford the correspondent alcohol mixture[7] and purified via flash chromatography on silica gel, using hexanes:Ethyl acetate 80:20 as the eluent mixture.

Major: ^{1}H NMR: (500.2 MHz, $CDCl_3$) δ 7.37 (m, 2H), 7.26 (m, 3H), 4.23 (td, J = 7.0, 3.7 Hz, 1H), 3.80 (s, 3H), 3.74 (s, 3H), 3.45 (dd, J = 7.2, 5.5 Hz, 1H), 3.09 (tt, J = 9.2, 4.8 Hz, 1H), 2.82 (dq, J = 9.5, 4.9 Hz, 1H), 2.62 – 2.55 (m, 2H), 2.50 (dd, J = 14.2, 4.2 Hz, 1H), 2.41 (dd, J = 14.0, 4.7 Hz, 1H), 1.34 (d, J = 6.6 Hz, 1H).

Further characterization to be completed.

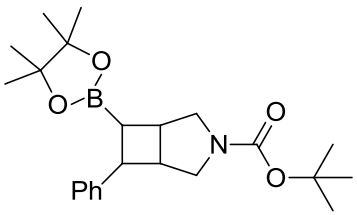

tert-butyl 6-phenyl-7-(4,4,5,5-tetramethyl-1,3,2-dioxaborolan-2-yl)-3-azabicyclo[3.2.0]heptane-3-carboxylate (5.18b): Synthesized according to the general procedure using 128 mg tert-butyl cinnamyl((E)-3-(4,4,5,5-tetramethyl-1,3,2-dioxaborolan-2-yl)allyl)carbamate (**5.18b**) (0.3 mmol, 1.00 equiv.), 3.3 mg $Ir(df(CF_3ppy)_2dtbbpy)PF_6$ and 6 mL CH_3CN (0.05 M) yielding 109 mg (91% yield) of the desired product in 8:1 d.r.

^1H NMR: (500 MHz, $CDCl_3$ at room temperature) δ 7.28 – 7.25 (m, 4H), 7.17 – 7.12 (m, 1H), 3.76 – 3.19 (m, 6H), 3.12 – 2.97 (m, 1H), 2.19 – 2.09 (m, 1H), 1.49 (s, 9H), 0.97 (s, 6H), 0.89 (s, 6H).

Further characterization to be completed.

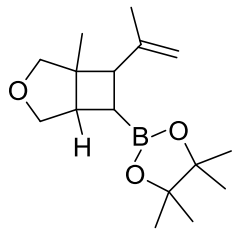

4,4,5,5-tetramethyl-2-((1R,5S,6R,7R)-1-methyl-7-(prop-1-en-2-yl)-3-oxabicyclo[3.2.0]heptan-6-yl)-1,3,2-dioxaborolane (5.19c): Synthesized according to the general procedure using 86 mg 2-((E)-3-(((E)-2,4-dimethylpenta-2,4-dien-1-yl)oxy)prop-1-en-1-yl)-4,4,5,5-tetramethyl-1,3,2-dioxaborolane **5.19b** (0.3 mmol, 1.00 equiv.), 3.3 mg $Ir(df(CF_3ppy)_2dtbbpy)PF_6$ and 6 mL CH_3CN (0.05 M) yielding 65 mg (76% yield) of the desired product in 4:2:1 d.r. after flash column chromatography on boric acid-doped silica gel in hexanes:Ethyl acetate 80:20 to isolate the prevalent minor diastereomer and another column in pure DCM to isolate the major diastereomer.

Major: ^1H NMR: (500.2 MHz, $CDCl_3$) δ 4.85 (q, J = 1.3 Hz, 1H), 4.82 – 4.79 (m, 1H), 3.84 (dd, J = 9.4, 1.2 Hz, 1H), 3.80 (d, J = 8.9 Hz, 1H), 3.73 (dd, J = 9.4, 5.9 Hz, 1H), 3.23 (d, J = 8.9 Hz, 1H), 3.07 (d, J = 10.6 Hz, 1H), 2.37 (t, J = 5.5 Hz, 1H), 1.74 (dd, J = 10.7, 5.0 Hz, 1H), 1.66 (s, 3H), 1.25 (s, 6H), 1.25 (s, 6H), 1.19 (s, 3H).

^{13}C NMR (125.8 MHz, $CDCl_3$) δ 145.9, 110.8, 83.4, 80.6, 75.4, 49.8, 47.4, 43.9, 25.1, 23.5, 16.8. The signal for the carbon attached to boron was not observed due to quadrupolar relaxation of the boron nucleus.

^{11}B NMR (128.4 MHz, $CDCl_3$) δ 33.8.

HRMS (ESI) calculated for $[C_{16}H_{27}BO_3+H]^+$ requires 278.2162 *m/z*, found 278.2163 *m/z*.

Prevalent minor: ^{1}H NMR: (500.2 MHz, $CDCl_3$) δ 4.90 (q, J = 1.6 Hz, 1H), 4.68 (s, 1H), 3.85 (d, J = 9.3 Hz, 1H), 3.65 (d, J = 9.1 Hz, 1H), 3.55 (dd, J = 9.0, 4.3 Hz, 1H), 3.19 (d, J = 9.3 Hz, 1H), 2.64 (d, J = 10.2 Hz, 1H), 2.37 (dd, J = 7.5, 4.3 Hz, 1H), 1.62 (s, 3H), 1.60 (m, 1H), 1.28 (s, 3H),1.24 (s, 12H);

^{13}C NMR (125.8 MHz, $CDCl_3$) δ 144.3, 110.7, 83.2, 75.2, 73.2, 49.2, 48.0, 44.4, 25.3, 25.1, 24.9, 24.8, 22.2. The signal for the carbon attached to boron was not observed due to quadrupolar relaxation of the boron nucleus.

^{11}B NMR (128.4 MHz, $CDCl_3$) δ 33.6

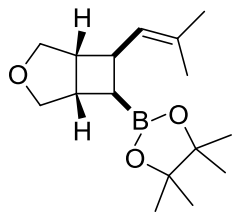

4,4,5,5-tetramethyl-2-((1R,5S,6R,7R)-7-(2-methylprop-1-en-1-yl)-3-oxabicyclo[3.2.0]heptan-6-yl)-1,3,2-dioxaborolane (5.20c): Synthesized according to the general procedure using 84 mg 4,4,5,5-tetramethyl-2-((E)-3-(((E)-5-methylhexa-2,4-dien-1-yl)oxy)prop-1-en-1-yl)-1,3,2-dioxaborolane **5.20b** (0.3 mmol, 1.00 equiv.), 3.3 mg $Ir(df(CF_3ppy)_2dtbbpy)PF_6$ and 6 mL CH_3CN (0.05 M) yielding 34.5 mg (41% yield) of the desired product in 4:1 d.r. In order to isolate the major diastereomer, the mixture was oxidized to afford the correspondent alcohol mixture[7] and purified via flash chromatography on silica gel, using dichloromethane:methanol 94:6 as the eluent mixture. ^{1}H NMR: (500.2 MHz, $CDCl_3$) δ 5.26 (dp, J = 8.4, 1.4 Hz, 1H), 4.06 (m, 1H), 4.02 (d, J = 9.5 Hz, 1H), 3.89 (d, J = 9.3 Hz, 1H), 3.50 (dd, J = 9.4, 5.6 Hz, 1H), 3.45 (dd, J = 9.4, 5.5 Hz, 1H), 2.99-2.95 (m, 1H), 2.78-2.75 (m, 1H), 2.70-2.66 (m, 1H), 1.80 (s, 3H=, 1.59 (s, 3H); ^{13}C NMR (125.8 MHz, $CDCl_3$) δ 121.7, 73.3, 72.3, 71.4, 48.3, 42.8, 42.3, 29.9, 25.9, 18.8. The signal for the carbon attached to boron was not observed due to quadrupolar relaxation of the boron nucleus. ^{11}B NMR (128.4 MHz, $CDCl_3$) δ 33.1. HRMS (ESI) calculated for $[C_{16}H_{27}BO_3+Na]^+$ requires 301.1946 *m/z*, found 301.1940 *m/z*. HRMS (ESI) calculated for $[C_{10}H_{16}O_2+H]^+$ requires 169.1223 *m/z*, found 169.1221 *m/z*.

References

(1) Pangborn, A. B.; Giardello, M. A.; Grubbs, R. H.; Rosen, R. K.; Timmers, F. J. *Organometallics* **1996**, *15* (5), 1518–1520.

(2) Lowry, M. S.; Goldsmith, J. I.; Slinker, J. D.; Rohl, R.; Robert A. Pascal, J.; Malliaras, G. G.; Bernhard, S. *Chem. Mater.* **2005**, *17* (23), 5712–5719.

(3) Pal, S.; Lucarini, F.; Ruggi, A.; Kilbinger, A. F. M. *J. Am. Chem. Soc.* **2018**, *140* (9), 3181–3185.

(4) Vaghi, L.; Benincori, T.; Cirilli, R.; Alberico, E.; Mussini, P. R.; Pierini, M.; Pilati, T.; Rizzo, S.; Sannicolò, F. *Eur. J. Org. Chem.* **2013**, *2013* (36), 8174–8184.

(5) Nishimura, T.; Takiguchi, Y.; Maeda, Y.; Hayashi, T. *Adv. Synth. Catal.* **2013**, *355* (7), 1374–1382.

(6) Moure, A. L.; Mauleón, P.; Arrayás, R. G.; Carretero, J. C. *Org. Lett.* **2013**, *15* (8), 2054–2057.

(7) Ito, H.; Toyoda, T.; Sawamura, M. *J. Am. Chem. Soc.* **2010**, *132* (17), 5990–5992.

APPENDIX I

CHART OF MOLECULES

MOLECULES OF CHAPTER 2

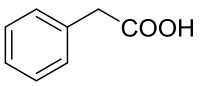

2.1a

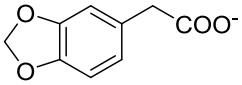

2.1k-

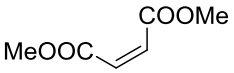

2.2e

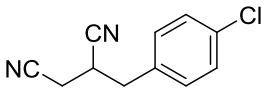

2.13

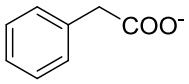

2.1a-

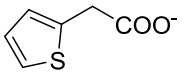

2.1l-

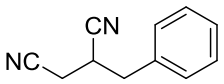

2.3

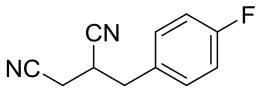

2.14

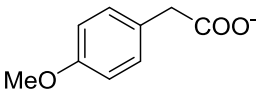

2.1b-

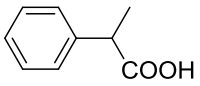

2.1m

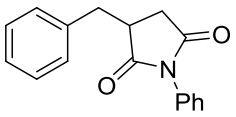

2.4

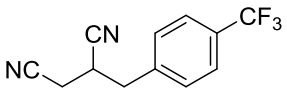

2.15

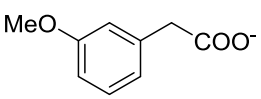

2.1c-

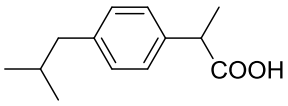

2.1n

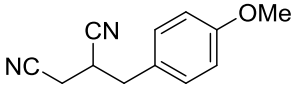

2.5

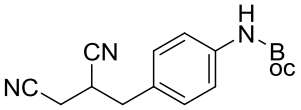

2.16

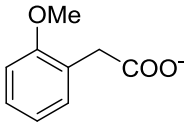

2.1d-

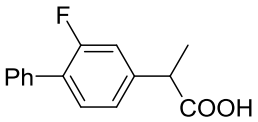

2.1o

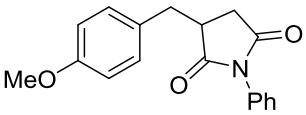

2.6

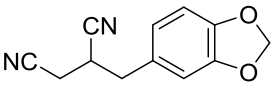

2.17

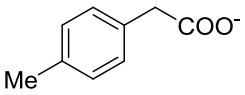

2.1e-

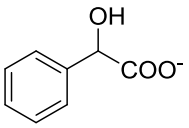

2.1p-

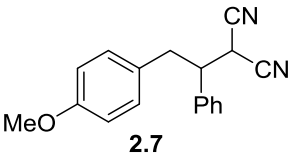

2.7

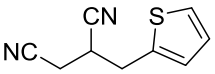

2.18

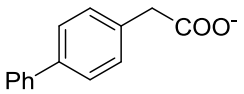

2.1f-

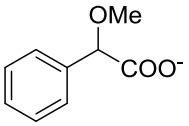

2.1q-

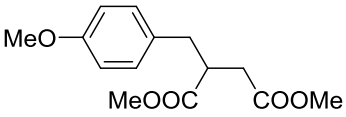

2.8

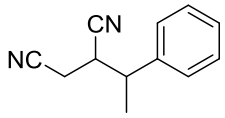

2.19

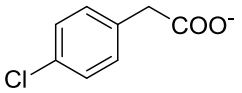

2.1g-

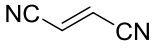

2.2a

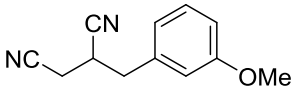

2.9

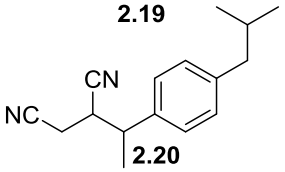

2.20

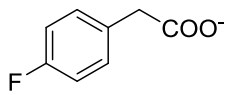

2.1h-

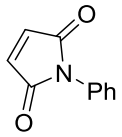

2.2b

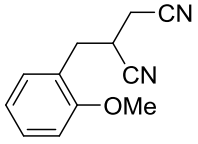

2.10

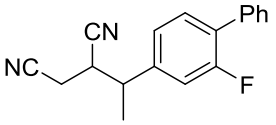

2.21

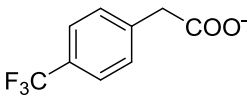

2.1i-

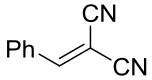

2.2c

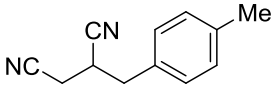

2.11

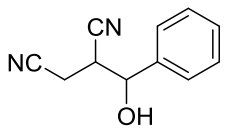

2.22

2.1j-

2.2d

2.12

2.23

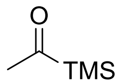
2.24a

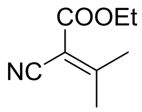
2.2m

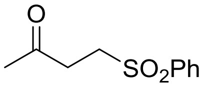
2.30

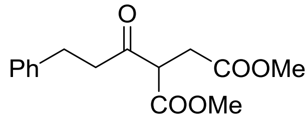
2.42

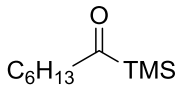
2.24b

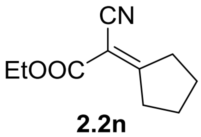
2.2n

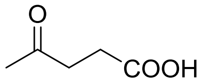
2.31

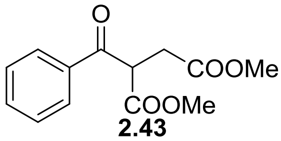
2.43

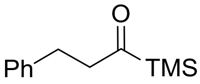
2.24c

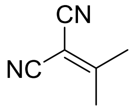
2.2o

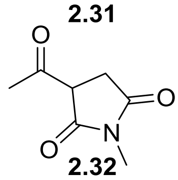
2.32

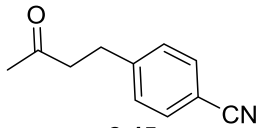
2.45

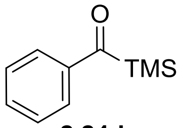
2.24d

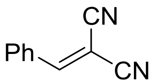
2.2c

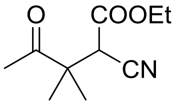
2.33

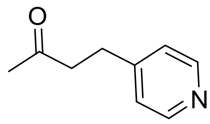
2.46

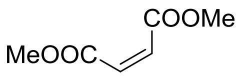
2.2e

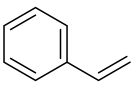
2.2p

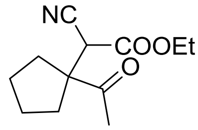
2.34

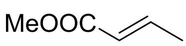
2.2f

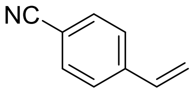
2.2q

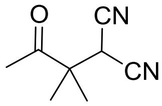
2.35

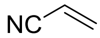
2.2g

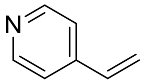
2.2r

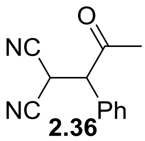
2.36

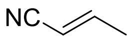
2.2h

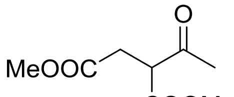
2.25

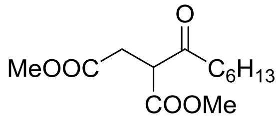
2.37

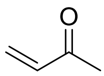
2.2i

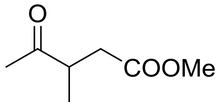
2.26

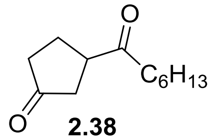
2.38

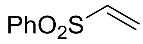
2.2j

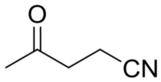
2.27

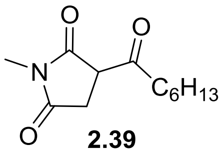
2.39

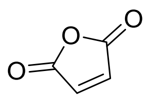
2.2k

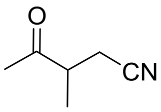
2.28

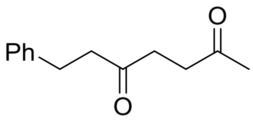
2.40

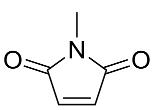
2.2l

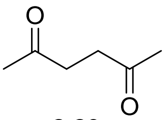
2.29

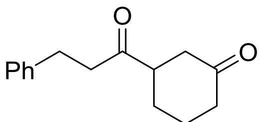
2.41

MOLECULES OF CHAPTER 3


3.1a

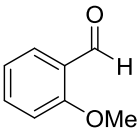
3.1l

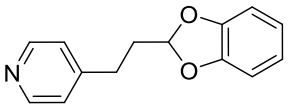
3.5

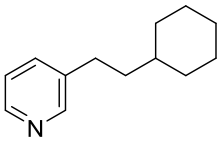
3.16

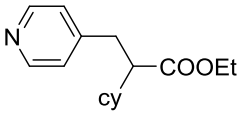
3.26b


3.1b

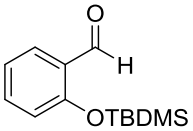
3.1m

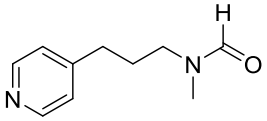
3.6

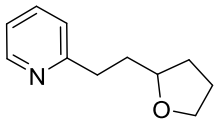
3.17

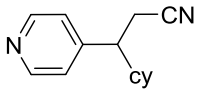
3.27a

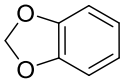
3.1c

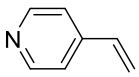
2.2r

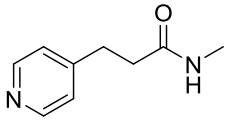
3.7

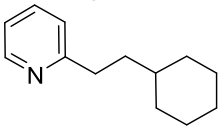
3.18

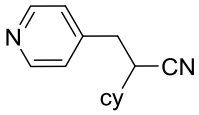
3.27b


3.1d

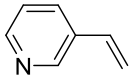
3.2a

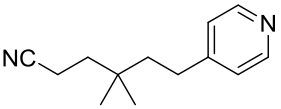
3.8

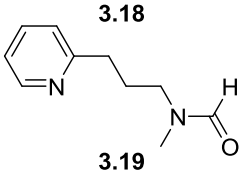
3.19

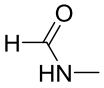
3.1e

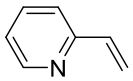
3.2b

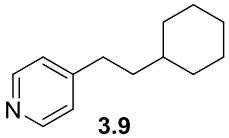
3.9

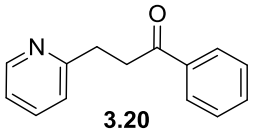
3.20

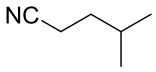
3.1f

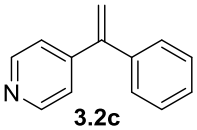
3.2c

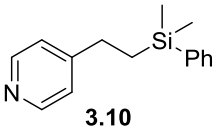
3.10

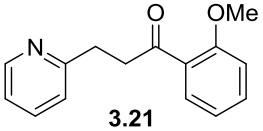
3.21


3.1g

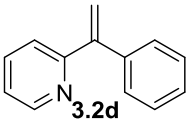
3.2d

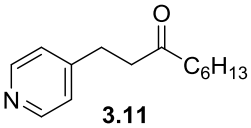
3.11

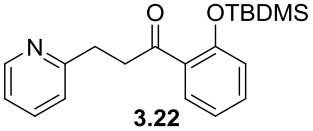
3.22


3.1h

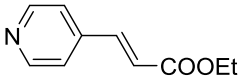
3.2e

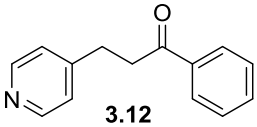
3.12

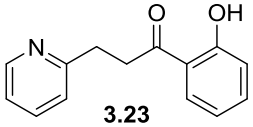
3.23

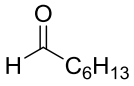
3.1i

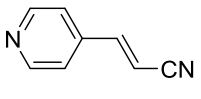
3.2f

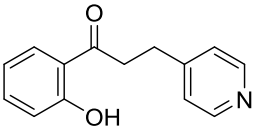
3.13

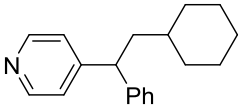
3.24

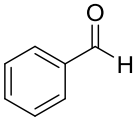
3.1j

3.3

3.14

3.25

3.1k

3.4

3.15

3.26a

MOLECULES OF CHAPTER 4

4.1a

3.1g

4.1b

4.1c

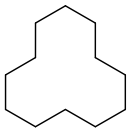

4.1d

3.1a

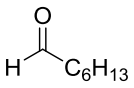

3.1i

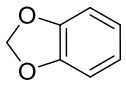

3.1c

3.1d

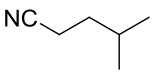

3.1f

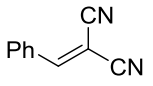

2.2c

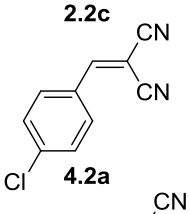

4.2a

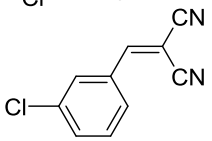

4.2b

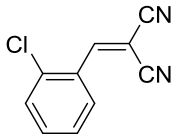

4.2c

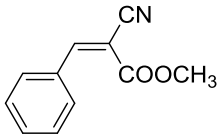

4.2d

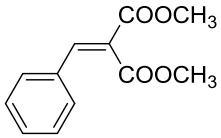

4.2e

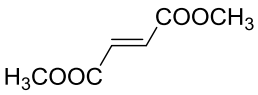

2.2d

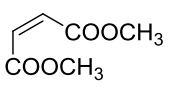

2.2e

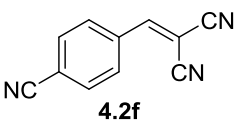

4.2f

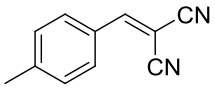

4.2g

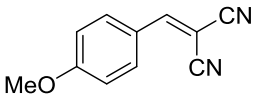

4.2h

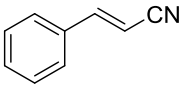

4.2i

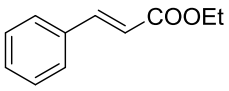

4.2j

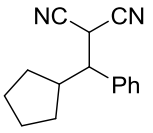

4.3

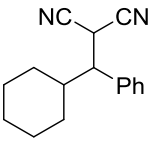

4.4

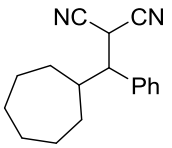

4.5

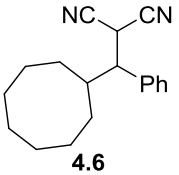

4.6

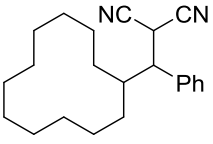

4.7

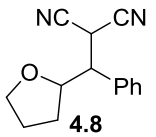

4.8

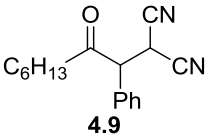

4.9

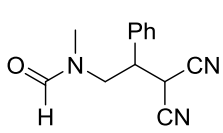

4.10

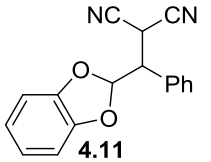

4.11

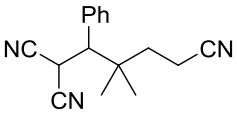

4.12

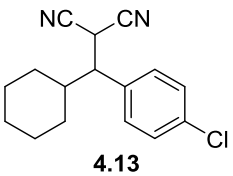

4.13

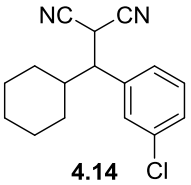

4.14

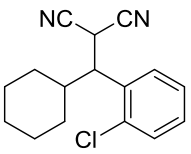

4.15

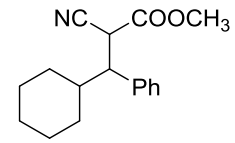

4.16

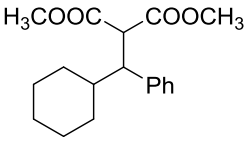

4.17

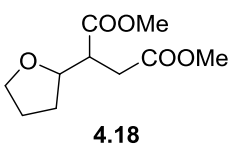

4.18

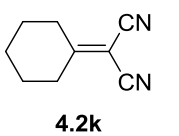

4.2k

4.19

MOLECULES OF CHAPTER 5

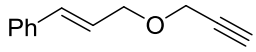

5.1a

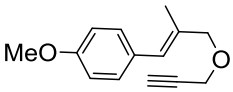

5.14a

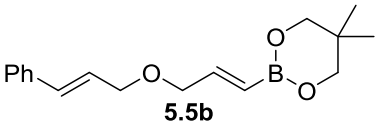

5.5b

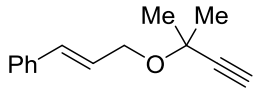

5.6a

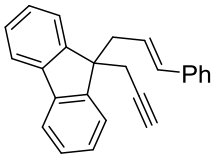

5.16a

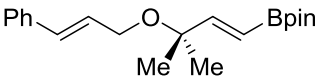

5.6b

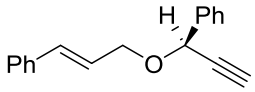

5.7a

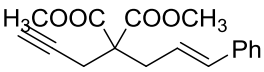

5.17a

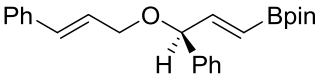

5.7b

5.8a

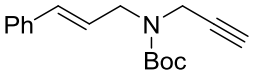

5.18a

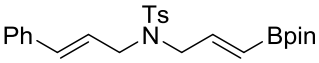

5.8b

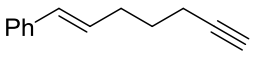

5.9a

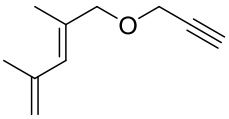

5.19a

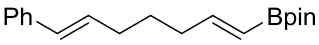

5.9b

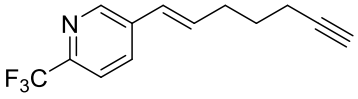

5.10a

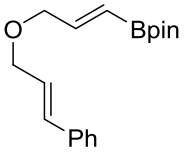

5.1b

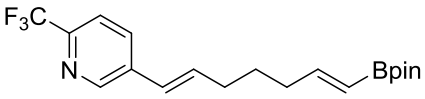

5.10b

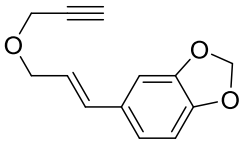

5.11a

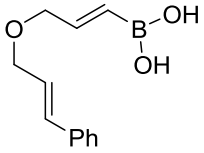

5.2b

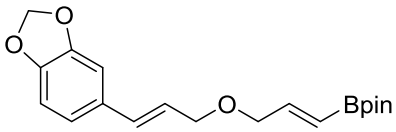

5.11b

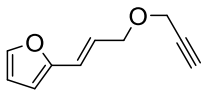

5.12a

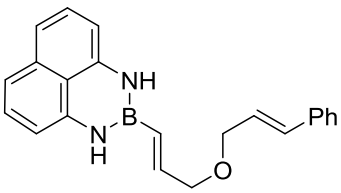

5.3b

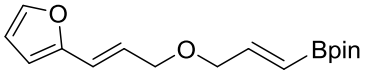

5.12b

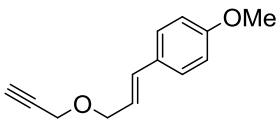

5.13a

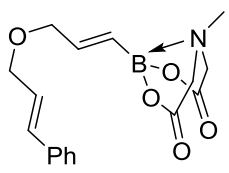

5.4b

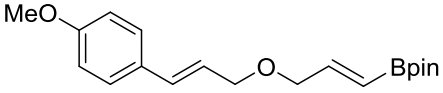

5.13b

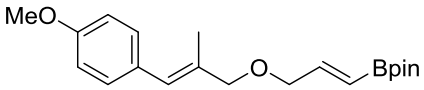

5.14b

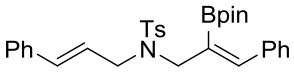

5.15b

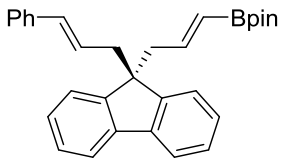

5.16b

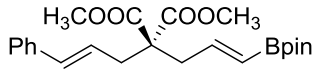

5.17b

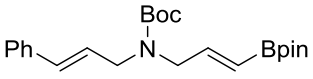

5.18b

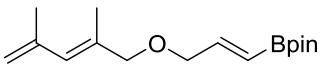

5.19b

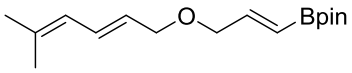

5.20b

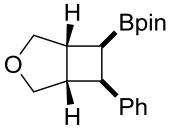

5.1c

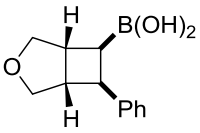

5.2c

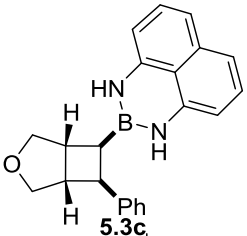

5.3c

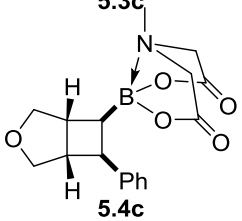

5.4c

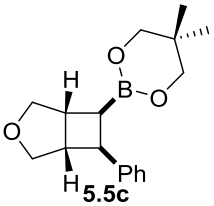

5.5c

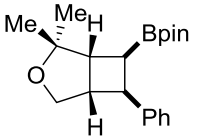

5.6c

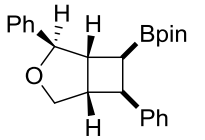

5.7c

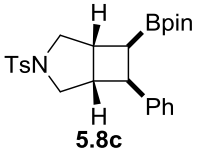

5.8c

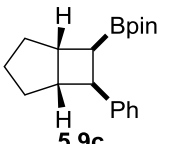

5.9c

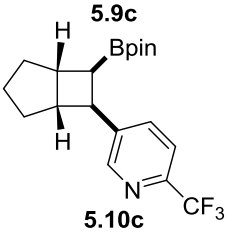

5.10c

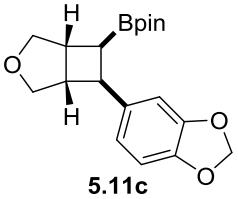

5.11c

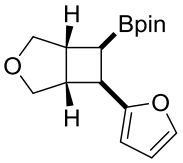

5.12c

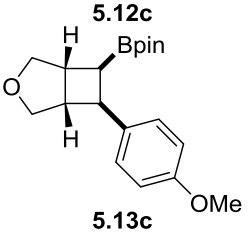

5.13c

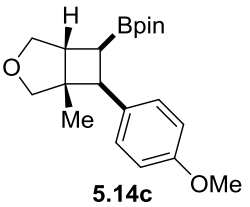

5.14c

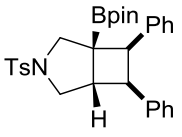

5.15c

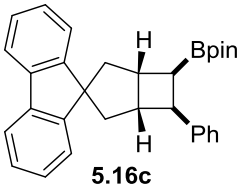

5.16c

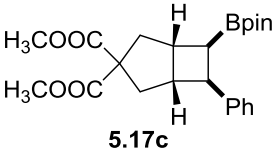

5.17c

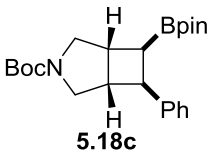

5.18c

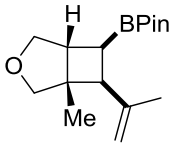

5.19c

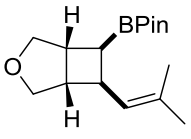

5.20c

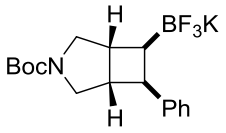

5.18d

APPENDIX II

OPTIMIZATION OF GEOMETRIES

DFT calculations were carried out with the Gaussian16 (rev. B.01) software. The ground state and the lowest lying triplet state of cinnamonitrile and ethyl cinnamate have been initially optimized having recourse to the standard ωB97XD functional (with the Unrestricted – U – formalism for the triplets) with the def2TZVP basis set in the gas phase. The optimized structures were characterized through vibrational frequencies calculation at the same level of theory as geometry optimizations, to verify that they had only real frequencies. Indeed, the reported triplet energies have been calculated by taking the difference between the Gibbs free energy value of the triplet and that of the corresponding ground state.

2-benzylidenemalononitrile

C	3.44640300	0.18832700	-0.00003100
C	2.51062300	1.21345200	0.00021100
C	1.15802800	0.92923900	0.00026200
C	0.71796500	-0.39951300	0.00007200
C	1.67441000	-1.42173600	-0.00014000
C	3.02581400	-1.13279300	-0.00020300
H	4.50368600	0.42065500	-0.00007400
H	2.83709700	2.24510000	0.00036500
H	0.45216800	1.74608100	0.00046800
H	1.34699100	-2.45462900	-0.00026500
H	3.75001700	-1.93672300	-0.00038000
C	-0.67512900	-0.81390500	0.00009600
C	-1.81877400	-0.09755800	0.00001000
H	-0.82116900	-1.88894300	0.00016900
C	-3.07361900	-0.78957000	0.00005900
N	-4.07289500	-1.35551300	0.00010100
C	-1.90354100	1.32953100	-0.00015800
N	-1.99022900	2.47488500	-0.00029300

2-benzylidenemalononitrile_triplet

C	3.28192200	-0.00009900	0.65248500
C	2.15851300	-0.00035600	1.47440900
C	0.89422000	-0.00040700	0.92853700
C	0.71491100	-0.00013700	-0.47495500
C	1.87139800	0.00005400	-1.29140700
C	3.12845200	0.00009000	-0.73206500
H	4.27234400	-0.00004700	1.08828700
H	2.27709200	-0.00052700	2.55022100
H	0.02815500	-0.00062100	1.57891500
H	1.75388200	0.00025000	-2.36822000
H	4.00137800	0.00027400	-1.37202800
C	-0.55880200	-0.00018600	-1.06952900

C	-1.81427300	0.00004600	-0.30179300
H	-0.65181900	0.00001300	-2.15012800
C	-2.42781800	-1.20898500	0.06121900
N	-2.90129400	-2.22491800	0.34435700
C	-2.42720600	1.20937100	0.06128200
N	-2.89998000	2.22553400	0.34476800

Cinnamonitrile

C	0.36299200	-0.18455600	-0.00000100
C	1.23137400	-1.27590300	-0.00000200
C	2.60441600	-1.09377800	0.00000100
C	3.13145600	0.18713600	0.00000000
C	2.27849500	1.28359100	-0.00000100
C	0.90886700	1.10103200	0.00000000
H	0.82194800	-2.27924700	0.00000000
H	3.26200500	-1.95341400	0.00000300
H	4.20383300	0.33439400	0.00000200
H	2.68608300	2.28633700	0.00000000
H	0.26254400	1.96935500	0.00000000
C	-1.07730000	-0.44145000	0.00000000
C	-2.05197400	0.47150400	0.00000000
H	-1.36513400	-1.48789100	0.00000000
H	-1.85368700	1.53579300	0.00000000
C	-3.42666400	0.09935100	0.00000000
N	-4.54108000	-0.18384000	0.00000000

Cinnamonitrile_triplet

C	0.29822700	-0.48549200	0.15653400
C	1.41545100	-1.26312600	-0.23143700
C	2.65558200	-0.68813600	-0.39347600
C	2.83235100	0.67660600	-0.17768600
C	1.74754000	1.46151300	0.20235400
C	0.50096800	0.89849300	0.36803800
H	1.28149900	-2.32473100	-0.40168100
H	3.49698800	-1.30079100	-0.69147200
H	3.80855500	1.12520700	-0.30737800
H	1.88177900	2.52314300	0.36670300
H	-0.33867900	1.51905000	0.65653000
C	-0.96247800	-1.09102300	0.31909000
C	-2.16770600	-0.37902200	0.74392300
H	-1.05710100	-2.15706600	0.13370800
H	-2.43145100	-0.30839700	1.79507900
C	-3.03828500	0.20740100	-0.16443100
N	-3.76164100	0.70004300	-0.92699200

Ethyl cinnamate

C	1.67501000	0.09951800	-0.00000200
C	2.30242700	1.34507600	-0.00000700

C	3.68378700	1.44980300	-0.00000400
C	4.46347900	0.30491900	0.00000400
C	3.85308700	-0.94284800	0.00000800
C	2.47479700	-1.04555000	0.00000600
H	1.69486700	2.24256500	-0.00001500
H	4.15053000	2.42651600	-0.00001000
H	5.54332800	0.38114900	0.00000500
H	4.45778800	-1.84081100	0.00001500
H	2.01839500	-2.02687900	0.00001000
C	0.21048400	0.05297400	-0.00000400
C	-0.55635900	-1.03638000	-0.00000400
H	-0.28616300	1.01768900	-0.00000500
H	-0.14928700	-2.03892200	-0.00000200
C	-2.03135200	-1.00933500	-0.00000500
O	-2.70867900	-2.00605700	-0.00000600
O	-2.54356800	0.22894900	0.00000100
C	-3.97128300	0.32285500	0.00000400
C	-4.33542600	1.78729400	0.00000700
H	-4.36045400	-0.19145600	0.88060300
H	-4.36045700	-0.19145400	-0.88059400
H	-5.42092300	1.89485200	0.00000100
H	-3.94077900	2.28682600	0.88544700
H	-3.94076900	2.28683000	-0.88542600

Ethyl cinnamate_triplet

C	-1.41453500	-0.47358900	-0.47721400
C	-2.42979500	0.13528800	-1.25137500
C	-3.51804100	0.72941400	-0.65206600
C	-3.63908800	0.74158800	0.73543300
C	-2.65184600	0.14931100	1.51769800
C	-1.55791300	-0.44789700	0.92962500
H	-2.33957900	0.12957600	-2.33117900
H	-4.28327600	1.19001600	-1.26424200
H	-4.49572600	1.20955100	1.20271900
H	-2.74195800	0.15789500	2.59673900
H	-0.79322600	-0.90446000	1.54681200
C	-0.30272100	-1.07494100	-1.10083700
C	0.78460300	-1.72526600	-0.38821600
H	-0.24345100	-1.04326300	-2.18580600
H	0.75877800	-2.78898600	-0.17546400
C	1.97970300	-1.04439300	0.08370500
O	2.87276100	-1.59438200	0.68942800
O	1.97991900	0.26326400	-0.21892200
C	3.10895900	1.01688000	0.23076000
C	2.89985500	2.45056900	-0.19072100
H	4.01598700	0.59317500	-0.20521000
H	3.19003600	0.92107500	1.31536700
H	3.74375700	3.05717900	0.14064900
H	2.82348100	2.52984100	-1.27556000
H	1.98865700	2.85555400	0.25037200

APPENDIX III

LIST OF ABBREVIATIONS

Acr^+-Mes:	9-mesityl-10-methylacridinium
BA:	benzoic acid
BDE:	bond dissociation energy
BP:	biphenyl
BPO:	benzoyl peroxide
bpz:	2,2'-bipyrazine
COSY:	correlation spectroscopy
DABCO:	1,4-diazabicyclo[2.2.2]octane
DBU:	1,8-diazabiciclo[5.4.0]undec-7-ene
DCA:	dicyanoanthracene
DEPT:	distortionless enhancement by polarization transfer
DHT:	α,n-didehydrotoluenes
DMF:	N,N-dimethylformamide
DMSO:	dimethylsulfoxide
e.g.:	exempli gratia
ET:	energy transfer
EWG:	electron withdrawing
GC:	gas chromatography
GC-MS:	gas chromatography mass spectrometry
HAT:	hydrogen atom transfer
HMPA:	hexamethylphosphoramide
HOMO:	highest occupied molecular orbital
HPLC:	high performance liquid chromatography
i.e.	id est
ISC:	inter-system crossing
KIE:	kinetic isotope effect
LED:	light emitting diode
LMCT:	ligand-to-metal charge transfer
LUMO:	lowest unoccupied molecular orbital
m.p.:	melting point
mCPBA:	m-chloroperoxybenzoic acid
MSA:	methanesulfonic acid
NBS:	N-bromosuccinimide
NHC:	N-heterocyclic carbenes
NHP:	N-hydroxyphthalimide
NMR:	nuclear magnetic resonance
NOE:	nuclear overhauser effect
Nphth:	see phth
NSAIDS:	non-steroidal anti-inflammatory drugs
OAc:	acetate
PC:*	photocatalyst in the excited state
PC:	photocatalyst
PC_{HAT}:	photocatalyst operating via HAT
PC_{SET}:	photocatalyst operating via SET
phth:	phthalimide
PPE:	personal protection equipment
ppm:	part per milion
PT:	5,7,12,14-pentacenetetrone
PTFE:	polytetrafluoroethylene
PTSA:	paratoluensulfonic acid
SCE	saturated calomel electrode
SET:	single-electron transfer
S_n:	singlet state
TBADT	tetrabutylammonium decatungstate
TBDMS:	tert-butyldimethylsilyl
TEA:	triethylamine
TEMPO:	(2,2,6,6-tetramethylpiperid-1-yl)oxyl
THF:	tetrahydrofuran
TLC:	thin layer chromatography
TMCs:	transition metal complexes
TMS:	trimethylsilyl
T_n:	triplet state
TPP:	tetraphenylporphyrin
TPT:	2,4,6-triphenylpyrylium tetrafluoroborate
UV:	ultraviolet
Vis:	visible
wO:	excited state of TBADT
λ_{em}:	emission wavelength
λ_{exc}:	excitation wavelength
λ_{IRR}:	irradiation wavelength